Deutsches Institut für Ernährungsforschung

Potsdam-Rehbrücke

Arbeitsgruppe Intestinale Mikrobiologie
(Abteilung Molekulare Toxikologie)

Role of intestinal bacteria in the conversion of dietary sulfonates

Dissertation

zur Erlangung des akademischen Grades

„doctor rerum naturalium“

(Dr. rer. nat.)

in der Wissenschaftsdisziplin „Gastrointestinale Mikrobiologie“

eingereicht an der

Mathematisch-Naturwissenschaftlichen Fakultät

der Universität Potsdam

und dem Deutschen Institut für Ernährungsforschung Potsdam-Rehbrücke

von

Master of Biomedical Sciences

Theresa Rausch

Eingereicht im März 2022

Disputation am 01.12.2022

Hauptbetreuer: Prof. Dr. Michael Blaut
Betreuer: Prof. Dr. Burkhard Kleuser
Gutachter: Prof. Dr. med. Karl-Herbert Schäfer

Published online on the
Publication Server of the University of Potsdam:
https://doi.org/10.25932/publishup-57403
https://nbn-resolving.org/urn:nbn:de:kobv:517-opus4-574036

`There's more to see than can ever be seen […].

More to find than can ever be found´

Tim Rice and Elton John, 1994

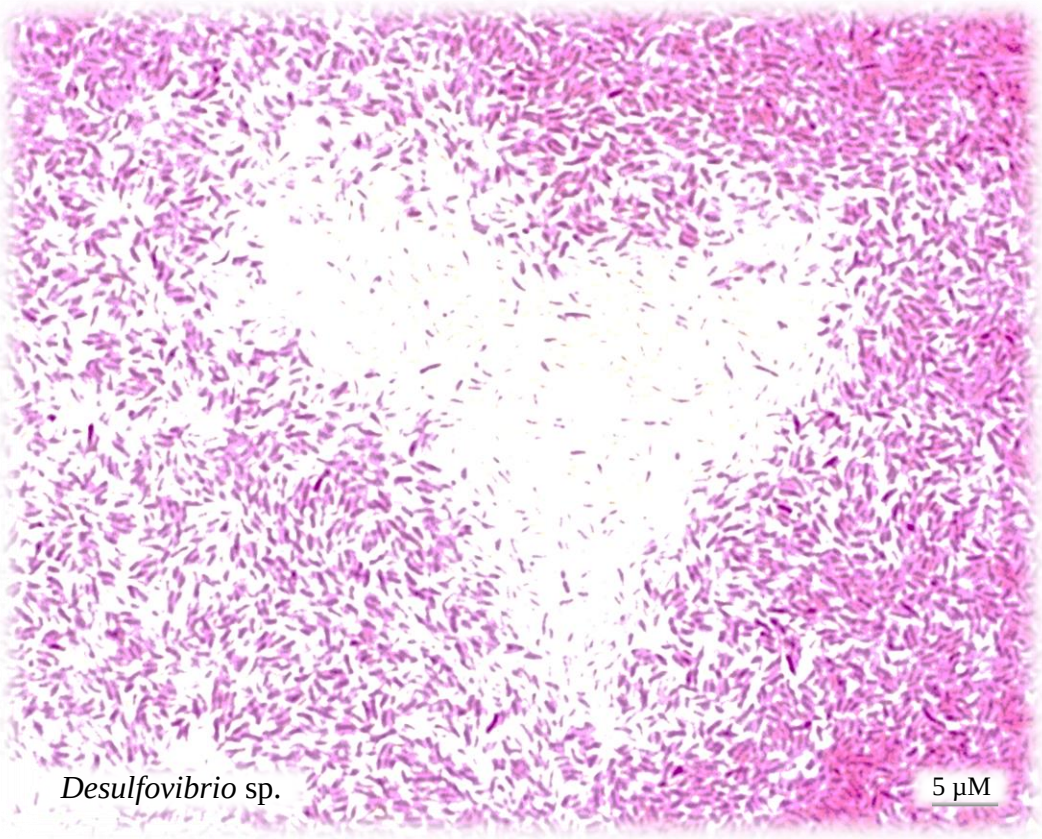

Desulfovibrio sp.

SUMMARY

Over the last decades, interest in the impact of the intestinal microbiota on host health has steadily increased. Diet is a major factor that influences the gut microbiota and thereby indirectly affects human health. For example, a high-fat diet rich in saturated fatty acids led to an intestinal proliferation of the colitogenic bacterium *Bilophila* (*B.*) *wadsworthia* by stimulating the release of the bile acid taurocholate (TC). TC contains the sulfonated head group taurine, which undergoes conversion to sulfide (H_2S) by *B. wadsworthia*. In a colitis-prone murine animal model ($IL10^{-/-}$ mice), the bloom of *B. wadsworthia* was accompanied by an exacerbation of intestinal inflammation. *B. wadsworthia* is able to convert taurine and also other sulfonates to H_2S, indicating the potential association of sulfonate utilization and the stimulation of colitogenic bacteria.

This potential link raised the question, whether dietary sulfonates or their sulfonated metabolites stimulate the growth of colitogenic bacteria such as *B. wadsworthia* and whether these bacteria convert sulfonates to H_2S. Besides taurine, which is present in meat, fish and lifestyle beverages, other dietary sulfonates are part of daily human nutrition. Sulfolipids such as sulfoquinovosyldiacylglycerols (SQDG) are highly abundant in salad, parsley and the cyanobacterium *Arthrospira platensis* (Spirulina). Based on previous findings, *Escherichia* (*E.*) *coli* releases the polar headgroup sulfoquinovose (SQ) from SQDG. Moreover, *E. coli* is able to convert SQ to 2,3-dihydroxypropane-1-sulfonate (DHPS) under anoxic conditions. DHPS is also converted to H_2S by *B. wadsworthia* or by other potentially harmful gut bacteria such as members of the genus *Desulfovibrio*. However, only few studies report the conversion of sulfonates to H_2S by bacteria directly isolated from the human intestinal tract. Most sulfonate-utilizing bacteria were obtained from environmental sources such as soil or lake sediment or from potentially intestinal sources such as sewage.

In the present study, fecal slurries from healthy human subjects were incubated with sulfonates under strictly anoxic conditions, using formate and lactate as electron donors. Fecal slurries that converted sulfonates to H_2S, were used as a source for the isolation of H_2S-forming bacteria. Isolates were identified based on their *16S ribosomal RNA* (*16S rRNA*) gene sequence. In addition, conventional C57BL/6 mice were fed a semisynthetic diet supplemented with the SQDG-rich Spirulina (SD) or a Spirulina-free control diet (CD). During the intervention, body weight, water and food intake were monitored and fecal samples were collected. After three weeks, mice were killed and organ weight and size were measured, intestinal sulfonate concentrations were quantified, gut microbiota composition was determined and parameters of intestinal and hepatic fat metabolism were analyzed.

Human fecal slurries converted taurine, isethionate, cysteate, 3-sulfolacate, SQ and DHPS to H_2S. However, inter-individual differences in the degradation of these sulfonates were observed. Taurine, isethionate, and 3-sulfolactate were utilized by fecal microbiota of all donors, while SQ, DHPS and cysteate were converted to H_2S only by microbiota from certain individuals. Bacterial isolates from human feces able to convert sulfonates to H_2S were

identified as taurine-utilizing *Desulfovibrio* strains, taurine- and isethionate-utilizing *B. wadsworthia*, or as SQ- and 3-sulfolactate- utilizing *E. coli*. In addition, a co-culture of *E. coli* and *B. wadsworthia* led to complete degradation of SQ to H_2S, with DHPS as an intermediate. Of the human fecal isolates, *B. wadsworthia* and *Desulfovibrio* are potentially harmful. *E. coli* strains might be also pathogenic, but isolated *E. coli* strains from human feces were identified as commensal gut bacteria.

Feeding SD to mice increased the cecal and fecal SQ-concentration and altered the microbiota composition, but the relative abundance of SQDG- or SQ-converting bacteria and colitogenic bacteria was not enriched in mice fed SD for 21 days. SD did not affect the relative abundance of *Enterobacteriaceae*, to which the SQDG- and SQ-utilizing *E. coli* strain belong to. Furthermore, the abundance of *B. wadsworthia* decreased from day 2 to day 9 in feces, but recovered afterwards in the same mice. In cecum, the family *Desulfovibrionaceae*, to which *B. wadsworthia* and *Desulfovibrio* belong to, were reduced. No changes in the number of *B. wadsworthia* in cecal contents or of *Desulfovibrionaceae* in feces were observed. SD led to a mild activation of the immune system, which was not observed in control mice fed CD. Mice fed SD had an increased body weight, a higher adipose-tissue weight, and a decreased liver weight compared to the control mice, suggesting an impact of Spirulina supplementation on fat metabolism. However, expression levels of genes involved in intestinal and hepatic intracellular lipid uptake and availability were reduced. Further investigations on the lipid metabolism at protein level could help to clarify these discrepancies.

In summary, humans differ in the ability of their fecal microbiota to utilize dietary sulfonates. While sulfonates stimulated the proliferation of potentially colitogenic isolates from human fecal slurries, the increased availability of SQ in Spirulina-fed conventional mice did not lead to an enrichment of such bacteria. Presence or absence of these bacteria may explain the inter-individual differences in sulfonate conversion observed for fecal slurries. This work provides new insights in the ability of intestinal bacteria to utilize sulfonates and thus, contributes to a better understanding of microbiota-mediated effects on dietary sulfonate utilization. Interestingly, feeding of the Spirulina-supplemented diet led to body-weight gain in mice in the first two days of intervention, the reasons for which are unknown.

ZUSAMMENFASSUNG

Die Darmmikrobiota hat auf die Gesundheit des Menschen einen wesentlichen Einfluss. Hierbei spielen Nahrungskomponenten eine wichtige Rolle, da sie die Hauptquelle für bakterielle Substrate darstellen und somit für das Wachstum der Darmbakterien sind. Unverdaute Nahrungsmittelbestandteile gelangen in den Dickdarm und können hier von der Mikrobiota verwertet werden. In einer Studie mit Mäusen wurde der Einfluss einer fettreichen Diät auf die Darmmikrobiota-Zusammensetzung untersucht. Die Hochfettdiät führte zur Proliferation des kolitogenen Bakteriums *Bilophila* (*B.*) *wadsworthia*, indem sie die Freisetzung der Gallensäure Taurocholat (TC) stimulierte. TC enthält den sulfonierten Taurin-Rest, der von *B. wadsworthia* als Elektronenakzeptor für das Wachstum genutzt werden kann. In dem Interleukin (IL)-10-defizienten Maus-Model für Kolitis, führte eine erhöhte intestinale Verfügbarkeit von TC zu Darmentzündungen. *B. wadsworthia* ist in der Lage, Taurin und auch andere Sulfonate in H_2S umzuwandeln, was auf einen möglichen Zusammenhang zwischen der Nutzung von Sulfonaten und der Stimulierung kolitogener Bakterien hinweist.

Aus diesen Literaturdaten resultierten die Fragen, ob Sulfonate die in Nahrungsmitteln enthalten sind, oder deren sulfonierte Metabolite, das Wachstum von kolitogenen Bakterien wie *B. wadsworthia* stimulieren und ob diese Bakterien Sulfonate zu H_2S umsetzen können. Neben Taurin, enthalten in Fleisch, Fisch und Energy-Getränken, gibt es noch weitere Nahrungsmittel-Sulfonate, die Menschen über ihre tägliche Nahrung aufnehmen. So enthalten z.B. Salat, Petersilie und das Cyanobakterium *Arthrospira platensis* (Spirulina) die Sulfolipide Sulfoquinovosyldiacylglycerole (SQDG). *Escherichia* (*E.*) *coli* kann die polare Kopfgruppe Sulfoquinovose (SQ) aus SQDG freisetzen und SQ in 2,3-Dihydroxypropan-1-sulfonat (DHPS) und Dihydroxyacetonphosphat spalten. DHPS kann wiederum von *B. wadsworthia* oder einem anderen potenziell kolitogenen Darmbakterium, nämlich einem *Desulfovibrio*-Stamm, verwendet und zu H_2S reduziert werden. Bisher gibt es jedoch nur wenige Studien, welche die Umwandlung von Sulfonaten in H_2S durch Bakterien belegen, die direkt aus dem humanen Darmtrakt isoliert wurden. Die meisten sulfonatverwertenden Bakterien wurden aus Umweltquellen wie Komposterde oder Seesedimenten oder aus potenziellen Darmquellen wie Abwasser gewonnen.

In der vorliegenden Arbeit wurden Fäzes-Suspensionen von gesunden Menschen unter strikt anoxischen Bedingungen mit Sulfonaten inkubiert, wobei Formiat und Laktat als Elektronendonoren verwendet wurden. Aus diesen Fäzes-Suspensionen wurden H_2S-bildende Bakterienstämme isoliert und anhand ihrer *16S ribosomalen RNA* (*16S rRNA*)-Gensequenz identifiziert. Zusätzlich wurden konventionelle C57BL/6-Mäuse entweder mit einer semisynthetischen Diät, welche mit SQDG-reicher Spirulina supplementiert war (SD), oder mit einer Spirulina-freien Kontrolldiät (CD) gefüttert. Während des Versuchs wurde das Körpergewicht der Mäuse und deren Wasser- und Nahrungsaufnahme bestimmt und Fäzesproben gesammelt. Nach drei Wochen wurden das Masse und die Größe der Organe gemessen, die Sulfonatkonzentration im Darm quantifiziert, die Zusammensetzung der Mikrobiota bestimmt und Parameter des hepatischen und intestinalen Fettstoffwechsels analysiert.

Die Ergebnisse zeigen, dass humane Fäzes-Suspensionen Taurin, Isethionat, Cysteat, 3-Sulfolaktat, SQ und DHPS mit interindividuellen Unterschieden in H_2S umwandeln. Taurin, Isethionat und 3-Sulfolaktat wurden von der Mikrobiota aller Donoren genutzt, während SQ, DHPS und Cysteat von der Mikrobiota von nur einzelnen Personen zu H_2S umgewandelt wurden. Als Sulfonat-umsetzende Bakterien wurden Stämme der Gattung *Desulfovibrio*, *B. wadsworthia* oder *E. coli* isoliert, wobei die *Desulfovibrio*-Stämme Taurin, *B. wadsworthia* Taurin und Isethionat und *E. coli* SQ und 3-Sulfolaktat zu H_2S reduzieren konnten. Des Weiteren zeigte die Kokultivierung von *E. coli* und *B. wadsworthia* den vollständigen Abbau von SQ über DHPS zu H_2S. Von den isolierten Bakterien werden *B. wadsworthia* und *Desulfovibrio* sp. mit Darmentzündungen assoziiert. *E. coli*-Stämme können auch pathogene Bakterien sein, jedoch wurden aus der humanen Fäzes isolierte *E. coli*-Stämme in dieser Arbeit als kommensale Darmbakterien identifiziert.

Die Gabe von SD an Mäuse erhöhte die SQ-Konzentration im Zäkum und Fäzes und veränderte die Zusammensetzung der intestinalen Mikrobiota, jedoch war die Zellzahl von SQDG- oder SQ-umwandelnden Bakterien und kolitogenen Bakterien nach 21 Tagen der Intervention nicht erhöht. Die Zellzahl von *Enterobacteriaceae*, zu denen die SQDG- und SQ-verwertenden *E. coli*-Stämme gehören, waren im Zäkum und der Fäzes unverändert. Außerdem nahm die Zellzahl von *B. wadsworthia* in denselben Mäusen von Tag 2 bis 9 ab, normalisierte sich danach aber wieder. Im Zäkum war die Familie der *Desulfovibrionaceae* reduziert, zu welcher *B. wadsworthia* und *Desulfovibrio*-Stämme gehören. Es wurden keine Veränderungen in der Anzahl von *B. wadsworthia* im Zäkuminhalt oder von *Desulfovibrionaceae* im Fäzes der Mäuse beobachtet. SD führte des Weiteren zu einer schwachen Aktivierung des Immunsystems, die bei Mäusen, die mit CD gefüttert wurden, nicht beobachtet wurde. Mäuse, die mit SD gefüttert wurden, wiesen im Vergleich zu den Kontrollmäusen ein höheres Körpergewicht, eine größere Ansammlung von Fettgewebe und ein geringeres Lebergewicht auf, was auf eine Veränderung des gesamten Fettstoffwechsels schließen ließ. Allerdings war die Genexpression von Genen, die an der intestinalen und hepatischen intrazellulären Lipidaufnahme und -verfügbarkeit beteiligt sind, vermindert. Weitere Untersuchungen des Lipidstoffwechsels auf Proteinebene könnten zur Klärung dieser Diskrepanzen beitragen.

Zusammenfassend lässt sich sagen, dass Darmbakterien des Menschen in der Lage sind, Sulfonate aus der Nahrung zu verwerten, wobei interindividuelle Unterschiede zu beobachten waren. Während Sulfonate die Vermehrung von potenziell kolitogenen Bakterien aus humaner Fäzes stimulierten, führte die erhöhte SQ-Verfügbarkeit bei mit Spirulina gefütterten Mäusen nicht zu einer Anreicherung solcher Bakterien in Darminhalten. Das Vorkommen oder Fehlen dieser Bakterien könnte die interindividuellen Unterschiede erklären, die bei der Umsetzung von Sulfonaten durch humane Fäzes festgestellt wurden. Diese Studie ermöglicht es uns, die biologische Rolle der mit der Nahrung aufgenommenen Sulfonate zu verstehen, und könnte neue Erkenntnisse über die Fähigkeit der Darmbakterien zur Verwertung von Sulfonaten liefern. Interessanterweise führte die Einnahme einer Spirulina-supplementierten Diät in den ersten zwei Tagen der Fütterung zu einem erhöhten Körpergewicht, die Gründe hierfür konnten nicht erklärt werden.

TABLE OF CONTENTS

SUMMARY IV
ZUSAMMENFASSUNG VI
TABLE OF CONTENTS VIII
ABBREVIATIONS XII
LIST OF FIGURES XVII
LIST OF TABLES XX
1 INTRODUCTION 1
1.1 Organization of the human gastrointestinal tract 1
1.1.1 Gut microbiota composition 2
1.1.2 Gut microbiota function and factors influencing the microbiota composition 2
1.2 The role of sulfur in the human body 3
1.2.1 Intestinal sulfate metabolism 3
1.2.2 Sulfonate utilization by the colitogenic bacterium *B. wadsworthia* 4
1.3 Microbial sulfonate metabolism 5
1.3.1 Taurine 7
1.3.2 Isethionate 9
1.3.3 Cysteate 10
1.3.4 Coenzyme M 11
1.3.5 SQDG, SQ, DHPS and 3-sulfolactate 12
1.4 Aim of the study 15
2 MATERIAL AND METHODS 17
2.1 Materials and bacterial strains 17
2.1.1 Sulfonates 17
2.1.2 Bacterial strains and growth conditions 17
2.2 Human study 17
2.2.1 Study design and study participants 17
2.2.2 Collection of fecal samples 17
2.2.3 Processing of fecal samples 18
2.2.4 Incubation of fecal slurries with sulfonates 18
2.2.5 Enrichment and isolation of sulfonate-utilizing gut bacteria 19
2.2.6 Testing the ability of obtained bacterial isolates and relevant gut bacteria to convert sulfonates 20

2.2.7 Examination of the metabolism of taurine-converting isolates 21
2.2.8 Test for bacterial motility 21
2.2.9 Flagella staining 22
2.2.10 Catalase test 22
2.2.11 Quantification of bacteria with the Thoma cell counting chamber 22
2.2.12 Enumeration of bacterial colony-forming units 22
2.3 Biochemical and analytical methods 22
2.3.1 Quantification of sulfonates based on LC-MS/MS analysis 22
2.3.2 Quantification of sulfoquinovose and glucose based on colorimetric determination 23
2.3.3 Taurine quantification with fluorometric determination 23
2.3.4 Analysis of taurocholate deconjugation with thin-layer chromatography 24
2.3.5 Quantification of H_2S using the methylene-blue method 24
2.3.6 Calculation of the growth rate and the doubling time of bacterial cultures 25
2.4 Molecular methods 25
2.4.1 DNA extraction from bacterial cells, PCR and gel electrophoresis 25
2.4.2 Visualization of the RAPD fingerprint 26
2.4.3 Identification of bacteria based on *16S rRNA* and *dsrAB* gene sequencing 26
2.4.4 Quantification of bacteria with real-time PCR 26
2.5 Animal study 27
2.5.1 Housing conditions 27
2.5.2 Experimental design 27
2.5.3 Preparation of gut contents for sulfonate quantification 29
2.5.4 Analysis of microbiota composition in cecal contents and feces based on *16S rRNA* gene sequencing 29
2.5.5 Enumeration of sulfonate-converting bacteria in cecal contents and feces 29
2.5.6 Quantification of gene copy numbers in feces and cecal contents 29
2.5.7 Macronutrient analysis (Weender analysis) of diets 30
2.5.8 Analysis of diet digestibility 30
2.5.9 Histological analysis of hepatic and mesenteric white adipose tissues 30
2.5.10 Analysis of hepatic triglyceride contents 30
2.5.11 Analysis of hepatic glycogen content 31
2.5.12 Analysis of hepatic protein content 32
2.5.13 RNA and protein extraction from liver and intestinal mucosa 32

2.6 Statistical analysis 36
3 RESULTS 37
3.1 *In vitro* testing of human fecal slurries for their ability to convert sulfonates and 37
3.1.1 Human fecal microbiota degraded taurine, isethionate, SQ and DHPS 37
3.1.2 The ability of human fecal microbiota to convert SQ to DHPS and / or H_2S was donor-dependent 39
3.1.3 Isethionate was not detected as an intermediate in taurine degradation by human fecal slurries 41
3.1.4 Human fecal bacteria converted taurine, isethionate, 3-sulfolacate, SQ, DHPS and cysteate to H_2S with inter-individual differences 41
3.2 Identification and sulfonate utilization of human fecal bacteria 43
3.2.1 Taurine-utilizing bacteria from human fecal slurries were identified as *B. wadsworthia* and members of *Desulfovibrio* sp. 43
3.2.2 Characteristics of human fecal taurine-converting *Desulfovibrio* isolates were further identified 44
3.2.3 Human fecal taurine-converting isolate Tau1 was identified as *Desulfovibrio desulfuricans* ATCC 27774 46
3.2.4 The fecal isolate Tau1 converted taurine and isethionate to H_2S 47
3.2.5 *Desulfovibrio simplex* DSM 4141^T utilized the sulfite moiety of taurine 49
3.2.6 SQ-converting human fecal isolates were identified as *E. coli* 51
3.2.7 SQ utilization by human fecal isolates was dependent on the presence or absence of oxygen 52
3.2.8 Human fecal bacteria able to convert isethionate- or 3-sulfolactate were identified as *B. wadsworthia* or *E. coli* respectively 55
3.2.9 *In vitro* cultures of *B. wadsworthia* converted TC, taurine, isethionate, and DHPS to H_2S 57
3.2.10 Anoxic co-culturing of the *E. coli* isolate SQ6 and *B. wadsworthia* led to the conversion of sulfoquinovose to H_2S 59
3.3 Spirulina feeding experiment in conventional mice 61
3.3.1 Spirulina diet feeding initially increased body weight and led to fat tissue accumulation, a decreased liver weight and a smaller stomach surface 61
3.3.2 SQDG of Spirulina were converted to SQ during small intestinal transit 62
3.3.3 SQDG-containing diet influenced the expression of SQ- and DHPS-degrading enzymes of bacteria in intestinal contents and tissues. 64
3.3.4 Spirulina feeding evoked a mild immune response in the ileum 65
3.3.5 The fecal and cecal microbiota diversity were altered due to Spirulina diet 66

3.3.6 Energy intake and food efficiency of SD-fed mice were elevated 73
3.3.7 Spirulina diet feeding did not affect the glucose metabolism 74
3.3.8 Spirulina feeding led to hypertrophic obesity 75
3.3.9 SD feeding reduced the intracellular lipid availability in jejunal tissue 76
3.3.10 SD reduced gene-expression levels of key enzymes for hepatic lipid uptake and synthesis 77
4 DISCUSSION 80
4.1 Sulfonate conversion by human gut microbiota 80
4.1.1 Human gut microbiota converted sulfonates to H_2S with inter-individual differences 80
4.1.2 Human fecal *Desulfovibrio* spp. converted taurine and isethionate to H_2S 81
4.1.3 SQ utilization differed among fecal *E. coli* strains 82
4.1.4 Human fecal *E. coli* strains converted 3-sulfolactate to H_2S 84
4.1.5 A co-culture of *B. wadsworthia* with *E. coli* enhanced H_2S formation 84
4.2 The effects of a SQDG-rich Spirulina supplemented diet in mice 85
4.2.1 Spirulina reduced the stomach surface in mice 86
4.2.2 Spirulina increased the quantity of intestinal SQ 86
4.2.3 Spirulina stimulated the gene expression of pro-inflammatory cytokines in ileal sections 88
4.2.4 Spirulina modulated the α- and β-diversity of the cecal and fecal microbiota 89
4.2.5 Spirulina did not stimulate the growth of SQDG- or SQ-converting bacteria 91
4.2.6 Sulfonates stimulated the growth of potentially colitogenic bacteria *in vitro*, while Spirulina did not do so *in vivo* 91
4.2.7 Spirulina increased body- and fat-tissue weight in mice 93
4.2.8 Spirulina enhanced the expression of key enzymes for lipid uptake and synthesis 94
5 CONCLUSIONS AND PERSPECTIVES 97
APPENDIX XXII
REFERENCES XXXI
ACKNOWLEDGEMENT LXII
LIST OF ORIGINAL COMMUNICATIONS LXIII
DECLARATION OF ACADEMIC HONESTY LXIV

ABBREVIATIONS

16S rRNA	*16S ribosomal RNA*
ACLY (*Acly*)	ATP-citrate synthase (*gene*)
ADIPOR1 (*Adipor1*)	Adiponectin receptor protein 1 (*gene*)
ADIPOR2 (*Adipor2*)	Adiponectin receptor protein 2 (*gene*)
ADIPOQ (*Adipoq*)	Adiponectin (*gene*)
α-diversity	Alpha-diversity
AGS	Amyloglucosidase
aPBS	Anoxic phosphate buffered saline
APS	Adenosine 5′ phosphosulfate
ATP	Adenosine triphosphate
B. wadsworthia	*Bilophila wadsworthia*
ß-diversity	Beta-diversity
BMI	Body mass index
C57BL/6J	Inbred C57 Black *6 mouse strain from Jackson laboratory, bred at DIfE*
CD	Semisynthetic control diet
CD36 (*Cd36*)	Fatty acid translocase (*gene*)
cDNA	Complementary DNA
CFU	Colony-forming units
CoM	Coenzyme M, 2-mercaptoethanesulfonate
CPT1a (*Cpt1a*)	Carnitine *O*-palmitoyltransfe rase 1 (*gene*)
CSA	Cysteine sulfinate
CuyA	Sulfo-lyase
CuyZ	Sulfite Exporter

d	Day, days
D.	*Desulfovibrio*
D0 - D10	Human fecal donors
DEPC-treated water	Diethylpyrocarbonate-treated water
DGAT2 (*Dgat2*)	Diacylglycerol acyltransferase 2 (*gene*)
DHAP	Dihydroxyacetone phosphate
DHPS	2,3-Dihydroxypropane-1-sulfonate
DIfE	German Institute of Human Nutrition Potsdam-Rehbruecke
DNS	Dinitrosalicylic acid
dNTPs	Deoxynucleoside triphosphates
Dsr (*dsrABC*)	Dissimilatory sulfite reductase (*genetical subunits*)
E. coli	*Escherichia coli*
ELOVL5 (*Elovl5*)	Elongation of very long chain fatty acids protein 5 (*gene*)
ELOVL6 (*Elovl6*)	Elongation of very long chain fatty acids protein 6 (*gene*)
E. rectale	*Eubacterium rectale*
ESPA	Sodium *N*-ethyl-*N*-(3-sulfopropyl) *m*-aniside
eWAT	Epididymal white adipose tissue
F	Feces
FABP1 (*Fabp1*)	Fatty acid-binding protein 1 (*gene*)
FABP2 (*Fabp2*)	Fatty acid-binding protein 2 (*gene*)
FASN (*Fasn*)	Fatty acid synthase (*gene*)
FeS	Iron sulfide
FFA	Free fatty acids
Fig.	Figure
GAPDH (*Gapdh)*	*G*lyceraldehyde-3-phosphate dehydrogenase (*gene*)

GLUT2 (*Glut2*)	Glucose transporter type 2 (*gene*)
GYS2 (*Gys2*)	Glycogen synthase (*gene*)
h	Hour, hours
H_2	Hydrogen
H_2O_2	Hydrogen peroxide
H_2S	Hydrogen sulfide
HIV	Human immunodeficiency virus
HMGCR (*Hmgcr*)	3-Hydroxy-3-methylglutaryl-coenzyme A reductase (*gene*)
HPLC	High performance liquid chromatography
HSO_3^-	Hydrogen sulfite
IBD	Inflammatory bowel disease
IL-6 (*Il-6*)	Interleukin-6 (*gene*)
IL-$10^{-/-}$	Interleukin-10 knockout, used as colitis prone mouse model
Ise	Isethionate
Ise2 and Ise3	Isethionate-converting human fecal isolates
LC-MS/MS	Liquid chromatography-tandem mass spectrometry
LIPE (*Lipe*)	Hormone-sensitive lipase (*gene*)
LLOQ	Detection limit
min	Minute, minutes
MSM	Mineral salts medium
mWAT	Mesenteric white adipose tissue
NADP	Nicotinamide adenine dinucleotide phosphate
NADPH	Reduced nicotinamide adenine dinucleotide phosphate
Na_2S	Sodium sulfide
NBD-F	4-Fluoro-7-nitrobenzofurazan

NMDS	Non-metric Multidimensional Scaling
NTA	Titanium(III) nitrilotriacetate
OD_{600}	Optical density measurements at a wavelength of 600 nm
OTUs	Number of observed species
PAPS	Phosphoadenosine-5′-phosphosulfate
PAT1	Na^+ / Cl^- independent proton-coupled amino acid transporter
PCR	Polymerase chain reaction
PLIN2 (*Plin2*)	Perilipin 2 (*gene*)
PLIN5 (*Plin5*)	Perilipin 5 (*gene*)
PNPLA2 (*Pnpla2*)	Patatin-like phospholipase domain-containing protein 2 (*gene*)
PPARα (Ppar*α*)	Peroxisome proliferator-activated receptor alpha (*gene*)
pWAT	Perirenal white adipose tissue
qPCR	Quantitative real-time PCR
RAPD	Random amplification of polymorphic DNA
RT	Room temperature
S.	*Shigella*
SCD1 (*Scd1*)	Acyl-CoA desaturase 1 (*gene*)
SD	CD supplemented with 20% Spirulina powder
SEM	Standard error of the mean
3-SL1 and 3-SL2	3-Sulfolactate-converting human fecal isolates
SLC27A2 (*Slc27a2*)	Very long-chain acyl-CoA synthetase (*gene*)
SLC27A4 (*Slc27a4*)	Long-chain fatty acid transport protein 4 (*gene*)
sp.	One specie
spp.	Multiple species
SQ	Sulfoquinovose

SQ6, SQ10 - SQ13	SQ-utilizing human fecal isolates
SQDG	Sulfoquinovosyldiacylglycerols
SQ-ED	SQ Entner-Doudoroff
SQ-EMP	SQ Embden-Meyerhof-Parnas
SQG	Sulfoquinovosylglycerol
SRB	Sulfate-reducing bacteria
sWAT	Subcutaneous white adipose tissue
TAE buffer	TRIS-acetate-EDTA buffer
Tau	Taurine
Tau1	Taurine-converting human fecal isolate
TauABC	ATP binding cassette transporters
TauT	Na^+ / Cl^- dependent taurine transporter
TC	Taurocholate
t_d	Doubling time
TEA	Terminal electron acceptor
TNF- α (*Tnf-α)*	Tumor necrosis factor (*gene*)
UC	Ulcerative colitis
YihQ (*yihq*)	Sulfoquinovosidase (*gene*)
YihS (*yihS*)	SQ-isomerase (*gene*)

LIST OF FIGURES

Figure 1: Chemical structure of sulfated compounds (A) and sulfonates (B), where R is an inorganic or an organic group.

Figure 2: Naturally occurring sulfonates and their microbial metabolism in a simplified model.

Figure 3: Biosynthesis of taurine.

Figure 4: Experimental set-up of anoxic incubation of human fecal slurries (1%) with sulfonates.

Figure 5: Degradation of taurine (Tau, 20 mM), isethionate (Ise, 20 mM), sulfoquinovose (SQ, 4 mM) and 2,3-dihydroxypropane-1-sulfonate (DHPS, 4 mM) during 72 h of anoxic incubation with human fecal slurries (F, 1%).

Figure 6: Sulfonate content after 72 h of anoxic incubation with human fecal slurries (F, 1%, n = 10).

Figure 7: Patterns of sulfoquinovose (SQ, 4 mM) conversion by human fecal slurries (1%) from various donors (D1 - D10) under anoxic conditions.

Figure 8: Time-course of H_2S formation in anoxic incubations of sulfonates with human fecal slurries (F, 1%) from different donors (D1 - D10).

Figure 9: Phenotypic and genotypic characterization of *Desulfovibrio* isolates.

Figure 10: Sulfide and nitrite formation within 48 h by the taurine-converting isolate Tau1 under anoxic conditions with one electron donor and one acceptor (20 mM both) in basal freshwater medium (Appendix, Table A1).

Figure 11: Taurine-converting isolate Tau1 utilized taurine and isethionate (both 20 mM) during anoxic incubation while releasing H_2S.

Figure 12: *D. simplex* converted taurine to H_2S under anoxic conditions.

Figure 13: Sulfide concentrations measured by the methylene blue method in anoxic ($-O_2$) and oxic ($+O_2$) enrichment subcultures with human fecal slurries from D1 (1%) and SQ (4 mM) during three sequential culture transfers.

Figure 14: Phenotypic and genotypic identification of sulfoquinovose (SQ)-converting isolates SQ6, SQ10, SQ11, SQ12 and SQ13.

Figure 15: Glucose (4 mM) degradation and conversion of sulfoquinovose (SQ, 4mM) to 2,3-dihydroxypropane-1-sulfonate (DHPS) by *E. coli* isolates (SQ6, SQ10 - SQ13) in comparison to *E. coli* MG1655.

Figure 16: Isethionate- and 3-sulfolactate-utilizing bacteria able to convert both sulfonates to H_2S during anoxic incubation were identified as Gram-negative rods.

Figure 17: RAPD-PCR profiles of the isolates 3-SL2, SQ6 and *E. coli* MG1655 using M13-core primer and a 2% agarose gel in 1 x TAE buffer (Appendix, Table A1).

Figure 18: Growth (OD_{600}) and H_2S formation during anoxic incubation of the isolates 3-SL2, SQ6 or strain *E. coli* MG1655 with 3-sulfolactate (4 mM) or 2,3-dihydroxypropane-1-sulfonate (DHPS, 4 mM) in comparison to cultures without sulfonates.

Figure 19: *B. wadsworthia* converted taurocholate, taurine, isethionate and 2,3-dihydroxy-propane-1-sulfonate (DHPS) to H_2S during anoxic respiration within 96 h.

Figure 20: A co-culture of *Bilophila wadsworthia* (*B.w.*) and a fecal *E. coli* isolate completely degraded sulfoquinovose (SQ) to sulfide (H_2S).

Figure 21: Body-weight increase, liver weight, stomach surface reduction and fat tissue accumulation in conventional C57BL/6J mice after intake of an SQDG-containing diet.

Figure 22: Cell wall breakdown and gastrointestinal release of sulfoquinovose (SQ) in conventional C57BL/6J mice fed a semisynthetic diet supplemented with 20% Spirulina.

Figure 23: Fold change in the expression of bacterial genes involved in SQ degradation in feces and cecal contents and relative gene expression of inflammatory markers in intestinal mucosa of mice fed a semisynthetic diet supplemented with 20% Spirulina (SD) versus mice fed a semisynthetic control diet (CD) for 21 days.

Figure 24: Alpha (α)-diversity, species richness and evenness of fecal (A - E) and cecal (F, G) microbiota of mice fed a semisynthetic diet supplemented with 20% Spirulina (SD) compared to mice fed a semisynthetic control diet (CD).

Figure 25: NMDS plots of generalized Unifrac distances visualizing the spatial distribution of fecal (A - D, CD- and SD-Feces) and cecal (E, CD- and SD-Cecum) microbiota of mice fed a semisynthetic diet supplemented with 20% Spirulina (SD) and mice fed a semisynthetic control diet (CD).

Figure 26: Relative abundance of bacterial phyla in feces (A - D) and cecal contents (E) of mice fed a semisynthetic diet supplemented with 20% Spirulina (SD) and mice fed a semisynthetic control diet (CD) at different times of the experiment.

Figure 27: Family-level differences in fecal (A) and cecal (B) microbiota composition between mice fed semisynthetic diet supplemented with 20% Spirulina (SD) and mice fed semisynthetic control diet (CD).

Figure 28: Genus-level differences in fecal (A) and cecal (B) microbiota composition between mice fed semisynthetic diet supplemented with 20% Spirulina (SD) and mice fed semisynthetic control diet (CD).

Figure 29: Abundance of *B. wadsworthia* in (A) feces and (B) cecal contents of mice fed semisynthetic diet supplemented with 20% Spirulina (SD) and mice fed semisynthetic control diet (CD).

Figure 30: Blood-glucose levels and storage as glycogen of mice fed semisynthetic diet supplemented with 20% Spirulina (SD) and mice fed semisynthetic control diet (CD).

Figure 31: Adipocyte analysis of the mesenteric white adipose tissue (mWAT) of mice fed semisynthetic diet supplemented with 20% Spirulina (SD) and mice fed semisynthetic control diet (CD).

Figure 32: Gene-expression levels of enzymes of the intestinal lipid metabolism in (A) jejunal, (B) ileal and (C) colonic mucosa of mice fed semisynthetic diet supplemented with 20% Spirulina (SD) and mice fed semisynthetic control diet (CD).

Figure 33: Representative images of hepatic tissue of mice fed semisynthetic diet supplemented with 20% Spirulina (SD) and mice fed semisynthetic control diet (CD).

Figure 34: (A) Hepatic triglycerides and (B) gene expression levels of tumor necrosis factor (*Tnf*)-α of mice fed semisynthetic diet supplemented with 20% Spirulina (SD) and mice fed semisynthetic control diet (CD).

Figure 35: Gene-expression levels of key enzymes of the hepatic lipid metabolism of mice fed semisynthetic diet supplemented with 20% Spirulina (SD) and mice fed semisynthetic control diet (CD).

LIST OF TABLES

Table 1: Primer sequences used for PCR.

Table 2: Composition of diets used for the animal experiment.

Table 3: Primer sequences used for gene-expression analyses in mouse tissues.

Table 4: Characteristics of human fecal donors.

Table 5: Quantified sulfonate content (%) after 72 h of anoxic incubation with human fecal slurries (F, 1%) from different donors (D1 - D10).

Table 6: Enrichment conditions, origin, and assignment (*16S rRNA* gene sequence) of obtained taurine-converting isolates.

Table 7: Similarity of *16S rRNA* gene sequence of fecal taurine-converting *B. wadsworthia* (A) and *Desulfovibrio* (B) isolates, related type strains and relevant sulfonate-utilizing bacteria.

Table 8: Ability of *Desulfovibrio* strains to degrade an electron acceptor in the presence of an appropriate electron donor (both 20 mM).

Table 9: Comparison of sequence identity (*16S rRNA* and partial *dsrAB* gene sequence), growth behavior and catalase activity of *Desulfovibrio* (*D.*) isolates and *D. desulfuricans* ATCC 27774, *D. desulfuricans* DSM 642^{T}, *D. intestinalis DSM* 11275^{T} and *D. simplex* DSM 4141^{T}.

Table 10: Doubling time during incubation of strain Tau1 with taurine or isethionate.

Table 11: H_2S formation (mM) measured with the methylene blue method in anoxic incubations of SRB with taurine (Tau) or sulfate (SO_4^{2-}) (both 20 mM).

Table 12: Identification and alignment of SQ-converting isolates SQ6, SQ10, SQ11, SQ12 and SQ13 with *E. coli* DSM30083^{T} (type strain) and *E. coli* MG1655 (able to degrade SQ to DHPS) based on their *16S rRNA* gene sequence using BLASTn.

Table 13: Growth (doubling time) of isolated *E. coli* strains (SQ6, SQ10 - SQ13) in comparison to *E. coli* MG1655 incubated with glucose (g, 4 mM) or sulfoquinovose (SQ, 4 mM) under oxic (+ O_2) or anoxic (- O_2) conditions.

Table 14: (A) Identification and alignment of isethionate- and (B) 3-sulfolac-tate-converting isolates based on their *16S rRNA* gene sequence using BLASTn.

Table 15: Growth (doubling time) during anoxic incubation of *E. coli* MG1655, the isolate 3-SL2 or the isolate SQ6 with 3-sulfolactate (3-SL, 4 mM).

Table 16: Growth (doubling time) of *Bilophila wadsworthia* (*B.w.*) and the *E. coli* isolate SQ6 during anoxic co-culturing with sulfoquinovose (SQ, 4 mM) in comparison to individual incubations with SQ or 2,3-dihydroxypropane-1-sulfonate (DHPS, 4 mM) or SQ (4mM).

Table 17: Macronutrient composition of control diet (CD) and semisynthetic diet supplemented with 20% Spirulina (SD) according to Weender analysis (also known as proximate analysis).

Table 18: Biometric parameters of mice fed a semisynthetic diet supplemented with 20% Spirulina (SD) or a semisynthetic control diet (CD) for three weeks.

Table A1: Media and solutions used.

Table A2: Sulfonate utilization by bacteria under oxic conditions.

Table A3: Sulfonate utilization by bacteria under anoxic conditions.

Table A4: Used conditions for PCR.

Table A5: Difference of bacterial relative abundance in feces (F) and cecal contents (C) after respectively 16 or 21 days of intake of semisynthetic diet supplemented with 20% Spirulina in comparison to semisynthetic control diet in conventional mice.

1 INTRODUCTION

Sulfonates are widespread in both oxic and anoxic ecosystems occurring naturally or as xenobiotics, and are available for a variety of bacteria. Bacteria utilize sulfonates as sole source of carbon or sulfur, or as terminal electron acceptor (TEA) [1-3]. Detailed pathways are described in chapter 1.3 and Appendix Table A2 and A3. Sulfonates are also present in dietary components and therefore are potentially available for intestinal bacteria in humans [4-7]. As an example, the sulfonate taurine is present in meat, fish and live style beverages.

Taurine stimulates the growth of the colitogenic bacterium *Bilophila* (*B.*) *wadsworthia*, a bacterium that is linked to intra- and extra-abdominal infections. The colitogenic effect of *B. wadsworthia* was associated with its ability to convert the sulfite moiety of taurine to hydrogen sulfide (H_2S) [8, 9]. Furthermore, an increased intestinal availability of taurine could contribute to colitis, as demonstrated by Devkota *et al.* (2012), inducing intestinal inflammation in a colitis-prone murine model (IL-$10^{-/-}$ mice) [9]. To investigate whether sulfonate utilization is common to pro-inflammatory gut bacteria, human fecal bacteria were tested for their ability to convert sulfonates to H_2S and identified in this study. This helps to clarify the factors contributing to colitis. Additionally, the fate of diet-derived sulfonates throughout the whole gastrointestinal tract was investigated in conventional mice to unravel the metabolic pathway of sulfonates in correlation to the growth of pro-inflammatory bacteria that so far has been hardly investigated.

1.1 Organization of the human gastrointestinal tract

The human gastrointestinal tract extends from the mouth to the anus throughout the human body. As an organ with one of the largest surfaces (250 - 400 m^2) and an average length of five meters, it represents a huge interface separating the luminal content from the body's internal milieu. The intestine can be divided in the upper gastrointestinal (esophagus to proximal ileum) and the lower gastrointestinal tract (distal ileum to rectum). Its primary function is the absorption of nutrients, water, and electrolytes to ensure crucial body functions for a good health state. As a luminal interface between the internal and external environment, it also acts as a physiological barrier to protect the body from harmful agents, such as pathogens, luminal foodborne pathogenic antigens, chemicals and/or potentially detrimental agents. Additional functions include the secretion of digestive enzymes and mucus and the transition and digestion of luminal content [10-14]. The integrity of the intestinal wall is ensured by a single layer of epithelial cells, additionally protected by a mucosal layer and by a complex population of intestinal microbiota [15]. Only the esophagus harbors a multi-cell layer [15].

1.1.1 Gut microbiota composition

The human gut harbors a complex microbial community, the number of which has been estimated to be the same order of magnitude as human cells [16]. The components of the gastrointestinal microbiota include a variety of microorganisms, including bacteria, eukarya (fungi and yeasts), archaea, and viruses [17, 18]. Bacteria make up the vast majority of these microorganisms. To date, approximately 2000 different bacterial species have been isolated from human beings [19, 20]. These bacterial strains show remarkably varying concentrations in the digestive tract. Starting with a low bacterial number in the oral cavity, which contains less than 1% of the total colonic bacterial number: From here, the microbial concentration gradually increases throughout the alimentary tract, depending on gut motility and present pH. Stomach, duodenum and jejunum harbor a relatively small number of bacteria, namely 10^3 - 10^4 bacteria/ml, due to the relatively low pH in the stomach and the rapid progress of luminal content through stomach and small intestine. The colon harbors the highest number of bacterial communities at 10^{11} cells/ml, not only of the total alimentary tract but also within the entire human body [16, 21].

The majority of the representative gut bacteria belong to the phyla *Firmicutes* and *Bacteroidetes*, representing over 90% of the total intestinal bacterial cell number [22, 23]. Bacteria with a lower abundance in the intestinal tract are members of the phyla *Actinobacteria, Proteobacteria, Fusobacteria,* and *Verrucomicrobia* [22, 24, 25]. Bacteria undergo a taxonomical division on genus, family, order, class and phylum level. Some of them might be even not identified yet. However, difficulties in culturing bacteria under laboratory conditions have promoted metagenomic analysis as a means of identifying a large number of previously uncultured intestinal bacteria [26, 27].

1.1.2 Gut microbiota function and factors influencing the microbiota composition

The gut microbiota has been linked to health and disease state of its host in different ways [21]. Increasing knowledge indicates this dynamic community to play a role in immunological, defensive, and metabolic processes [28]. Inflammatory bowel disease (IBD) and metabolic disorders, including obesity and type 2 diabetes, are linked to alterations of the gut microbiota composition [11, 19]. Unravelling the factors influencing the intestinal microbiota composition and its growth is important for understanding the correlation between this microbial community and disease. Therefore, the interest in the intestinal microbiota has markedly increased. Bacteria play a crucial role in intestinal homeostasis by providing a barrier function against pathogens, maintaining the immune system and forming metabolites and nutrients preserving the body's needs [18, 21, 29, 30]. Metabolites formed by intestinal bacteria may have beneficial and detrimental effects on host health [31-34].

The individual human gut microbiota composition is shaped by host genetics and environmental factors including antibiotics and diet [31-34]. Dietary components are considered as main driver shaping the intestinal microbiota composition, as they are the main source of bacterial substrates [35]. During digestion, dietary substances pass from the mouth to the anus through alimentary sections in which milieus and therefore also microbial colonization vary considerably. Nondigestible food components, such as fibers, reach the colon, and serve as carbon, sulfur and energy source for residential bacteria. Only bacteria that are able to

ferment these undigested constituents, survive and proliferate. Important modulators released by bacteria include short-chain fatty acids and amino acids which affect the host health [36, 37]. Hence, diet directly shapes the gut microbiota and hereby affects human health [38].

1.2 The role of sulfur in the human body

With ~0.3% of the total body mass, sulfur is a highly abundant element in the human body and present in all intra- and extracellular compartments [39-42]. Sulfur is essential in maintaining cellular homeostasis through influencing the detoxification of reactive oxygen species and free radicals. The major sulfur-containing amino acids in the human body are methionine and cysteine [43, 44]. Sulfhydryl groups form the tertiary structure of proteins by disulfide bridges which is necessary for the cellular function of these proteins. Sulfur is also present in components of the blood (heparin) and in bones, such as in chondroitin and cartilage [39]. Defects in regulatory processes of the body's sulfur pool have been linked to multiple disorders, including cystinuria, homocystinuria, and neurodevelopmental disorders [45-47].

Colonic sulfur compounds are either inorganic, such as sulfates (Fig. 1A) and sulfites, or organic, including dietary amino acids and host mucins [48]. Other potential organic sulfur sources for the gut are sulfonates containing a covalent carbon-sulfur bond, with the oxidation state of sulfur +5 (Fig. 1B) [49]. Sulfonates are found in the environment (such as marine sediments and soils), in mammalian tissue (such as bile acids) and in diet (such as salad and meat), all of which might influence the intestinal sulfonate availability in human beings. While the microbial sulfate-sulfur metabolism within the intestine is well understood (1.2.1), only little is known about the intestinal sulfonate-sulfur metabolism.

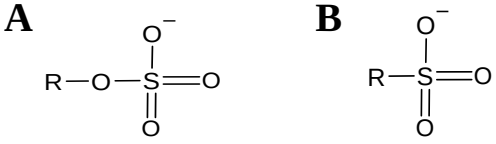

Figure 1: Chemical structure of sulfated compounds (A) and sulfonates (B), where R is an inorganic or an organic group.

1.2.1 Intestinal sulfate metabolism

Diets containing inorganic sulfate enhance the H_2S production in the colon [50, 51]. Intestinal sulfate is either reduced to H_2S by assimilatory sulfate reduction to satisfy sulfur requirements of biochemical reactions, such as the synthesis of cysteine and methionine. Or, intestinal sulfate is used by archaea and sulfate-reducing bacteria (SRB) as TEA, referred to as dissimilatory sulfate reduction. Herein, H_2S is released as end product and energy is conserved [52, 53]. Assimilatory sulfate reduction is found in a high proportion of bacteria, whereas dissimilatory sulfate reduction is restricted to a minority of bacteria [48, 52, 54]. For both pathways an activation of the relatively inert sulfate by adenosine triphosphate (ATP) is necessary, because the reduction of sulfate to sulfite is energetically unfavorable ($E^{0\prime}$ = −516 mV) [55]. Sulfate activation to adenosine 5′ phosphosulfate (APS) is mediated by ATP sulfurylase at the expense of two ATP, increasing the redox potential (APS / hydrogen sulfite (HSO_3^-)) to -60 mV [53]. APS is further reduced by APS

reductase to sulfite and adenosine monophosphate, using electrons from a specific electron donor, such as lactate, formate, or hydrogen (H_2), followed by a six-electron reduction of sulfite to H_2S, reaching a redox potential of $E^{0\prime} = -116$ mV [55, 56]. In dissimilatory sulfate reduction, H_2S is finally released from the bacterial cell by diffusion [53]. Assimilatory sulfate reduction needs another activation step in which APS is converted to sulfite via phosphoadenosine-5′-phosphosulfate (PAPS) by the membrane-bound enzymes CysC and PAPS reductases [48].

SRB are the most extensively studied intestinal bacteria participating in the colonic sulfur metabolism, colonizing the gut of approximately 50% of humans [48, 57]. SRB are able to reduce sulfate to H_2S and are obligate anaerobic bacteria being motile by means of flagella [58, 59]. The predominant SRB found in the human gut are members of the genus *Desulfovibrio* belonging to the *Deltaproteobacteria*, of which *D. piger* is the most abundant species [54, 56, 57, 60]. Other SRB present in the human gut are *Desulfobacter*, *Desulfobulbus* (*Deltaproteobacteria*) and *Desulfotomaculum* (*Firmicutes*) spp. [56].

1.2.2 Sulfonate utilization by the colitogenic bacterium *B. wadsworthia*

A closely related bacterium to the SRB is the sulfite-reducing *B. wadsworthia*, which was named for its ability to grow with bile acids [9, 61]. *B. wadsworthia* is an anaerobic Gram-negative bacterium, which was first isolated from patients with appendicitis [62, 63]. Interestingly, *B. wadsworthia* could be also recovered from feces of healthy human individuals, but was mostly found in regions of intra- and extra-abdominal infections [61]. For example, the organism has been observed in necrotizing ulcerative stomatitis, excess fluid between pleural layers of the lung, osteomyelitis, and in blood of a patient with abdominal distension and diarrhea, indicating its immense role in inflammatory processes [62]. In mice, a diet rich in saturated fatty acids enhanced the availability of intestinal taurocholate (TC) and thereby stimulated the growth of the colitogenic bacterium *B. wadsworthia*. The bloom of *B. wadsworthia* was linked to an exacerbated colitis in IL-$10^{-/-}$ mice, which was even more enhanced, when TC was orally applied to mice fed a low-fat diet [9].

In contrast to SRB, *B. wadsworthia* is not capable of utilizing sulfate as TEA but gains energy from the reduction of the sulfite moiety of sulfonated compounds including TC, taurine, isethionate, cysteate, and 2,3-dihydroxypropane-1-sulfonate (DHPS) to H_2S [8]. This might be due to the differences in the functional groups of sulfonated and sulfated compounds (Fig. 1). In this way, *B. wadsworthia* releases H_2S from sulfonates by sulfite reduction and circumvents in comparison to the dissimilatory sulfate reduction by SRB the energy-dependent activation of sulfate, conserving energy for its growth and gaining a growth advantage towards SRB [9].

H_2S is an important gaseous signaling molecule participating in a wide range of physiological and pathological processes in human beings. H_2S is a potent genotoxin, playing an important role in the intestine. It has been linked to IBD and colorectal cancer [64-68]. However, more recently observations describe H_2S as a protective agent for vascular and cardiac tissues with anti-inflammatory, antioxidant and cytoprotective functions, preventing from intestinal inflammation. For example, in mice with dextran sulfate sodium (DSS)-induced colitis, H_2S led to a downregulation of pro-inflammatory colonic cytokines (tumor necrosis

factor (TNF)-α, interleukin (IL)-1β, and IL-6) and a decreased colonic pathogenesis in these mice [69]. However, the effect of H_2S seems to be concentration-dependent [70-72].

Despite the biological relevance of H_2S formation, only few studies report the conversion of sulfonates to H_2S by human intestinal bacteria. Most sulfonate-utilizing bacteria were obtained from environmental such as compost soil or lake sediment or only potential intestinal sources such as sewage (Appendix, Tables A2, A3). Hence, little is known about H_2S formation from sulfonated compounds by gut bacteria, despite their biological relevance.

1.3 Microbial sulfonate metabolism

Sulfonates are synthesized chemically by industrial processes, or biologically by plants and microorganisms, among others [73, 74]. Organic sulfonates, also referred to as organosulfonates or C-sulfonates, occur naturally or as xenobiotics [2, 3]. Environmental sulfonated compounds are found in marine sediments, soils and are released into the environment from industrially produced sulfonate dyes and surfactants. Surfactants are poorly biodegradable and thereby pollute the environment [73, 74]. Synthetic sulfonates enter sewage and rivers where they accumulate and may have toxic effects on algae and living organisms. Degradation by microorganisms reduces but does not resolve the environmental pollution [1, 75]. Sulfonated compounds are therefore widespread in oxic and anoxic ecosystems and available for a variety of bacteria [76]. The microbial role in sulfonate degradation has been investigated over the last 30 years and is a quite new scientific field. Despite their occurrence in dietary components and biologically important processes, naturally occurring sulfonates were earlier thought to have a minimal relevance in the biological sulfur cycle [1, 3]. However, in the last years the interest in microbial sulfonate degradation has increased. Yet it is known that sulfonates can be used by a variety of bacteria as sole source of carbon or sulfur, but also as TEA [1, 2, 77]. Until now, most studies were performed with environmental bacteria (Appendix, Tables A2, A3). Only little is known about sulfonate degradation by human gut bacteria, despite the presence of sulfonates in the daily human nutrition. Dietary sulfonates that may serve as potential substrate for human gut bacteria include taurine, isethionate (2-hydroxyethanesulfonate), cysteate, coenzyme M (2-mercaptoethanesulfonate, CoM), sulfoquinovosyldiacylglycerols (SQDG), sulfoquinovose (SQ), DHPS, and 3-sulfolactate (2-hydroxy-3-sulfopropanoic acid). The known microbial catabolic pathways of these sulfonates are illustrated in a simplified model (Fig. 2). The state of knowledge regarding intestinal sulfonate availability (biosynthesis and transport) and microbial sulfonate metabolism is described below (1.3.1 – 1.3.5).

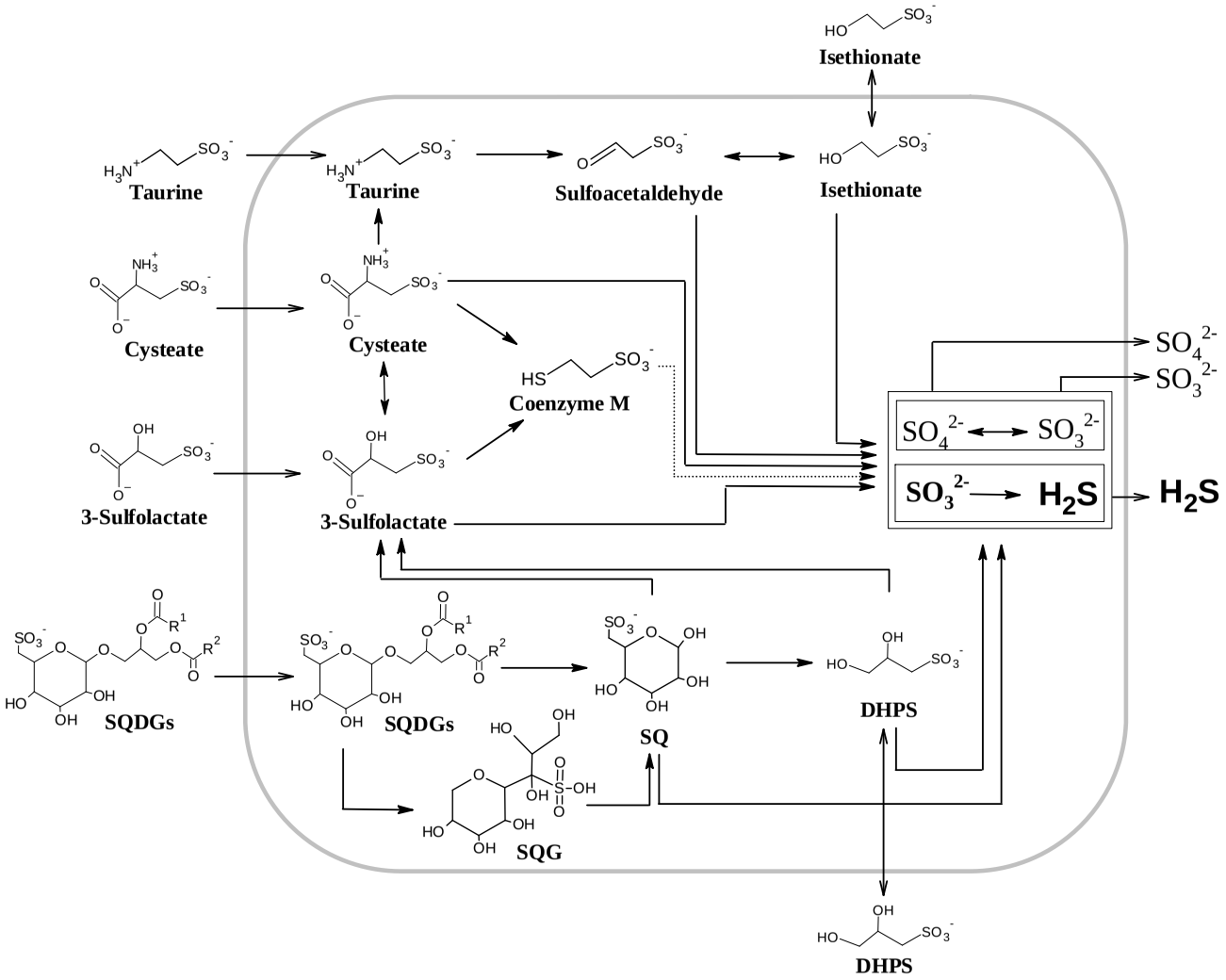

Figure 2: Naturally occurring sulfonates and their microbial metabolism in a simplified model. The dashed line indicates the hypothesis that Coenzyme M might be converted to sulfate, sulfite or sulfide by bacteria. → = transport; → = conversion. Graph elements were depicted with ACD/ChemSketch 2.0.

1.3.1 Taurine

First isolated in 1872 from ox bile, taurine plays a major role in numerous biological and physiological processes, such as during transmission in the nervous system, in calcium homeostasis, and in the formation of hepatic TC [78-84]. In humans, taurine is the most abundant free amino acid in the body and occurs mainly in liver and brain tissues, but can also be found in blood, heart tissue, as well as in skeletal muscles and kidney tissue [85-87].

Taurine is an essential amino acid in human infants and conditionally essential in human adults [84]. In human embryos and neonates, taurine deficiency has been linked to several disorders including retinal degeneration and growth retardation. Here, taurine biosynthesis is limited due to enzymatic immaturity [88-92]. In children and in adults, long-term parenteral nutrition is linked to taurine deficiency and a variety of clinical abnormalities, such as cancer [93-96].

Biosynthesis of taurine

The primary site of taurine synthesis is the liver. However, extrahepatic tissues such as adipose tissue, brain tissue and kidney tissue, expresses also enzymes catalyzing for taurine synthesis [78, 97-100]. The *de novo* biosynthesis in mammalian hepatocytes from methionine turned out to be the main pathway (Fig. 3) [101-103]. Methionine undergoes first a methylation and transsulfuration to form cysteine, followed by a reaction with O_2 to cysteine sulfinate (CSA) [100, 102-107]. The main pathway for taurine synthesis is the decarboxylation of CSA to hypotaurine, which is then oxidized [102, 103, 105-107]. Alternatively, taurine synthesis takes place via the bypass of CSA to cysteate and further to taurine [103, 105]. Hypotaurine can also be produced from cysteamine, a degradation product of coenzyme A [106].

Despite the fact that taurine can be synthesized endogenously (50 - 125 mg/d), the main source of taurine for human adults are dietary products, such as meat (such as chicken: 169 mg/100 g or beef: 43 mg/100 g), fish (mussels: 655 mg/100 g or tuna: 42 mg/100 g) and life style beverages (4 - 8 g/l) [4, 5]. This may be due to the fact that CSA decarboxylase levels in humans are extremely low, resulting in low hypotaurine synthesis [102, 108]. Since taurine is not present in fruits and vegetables, vegetarians and vegans have a lower taurine plasma concentration [5, 109].

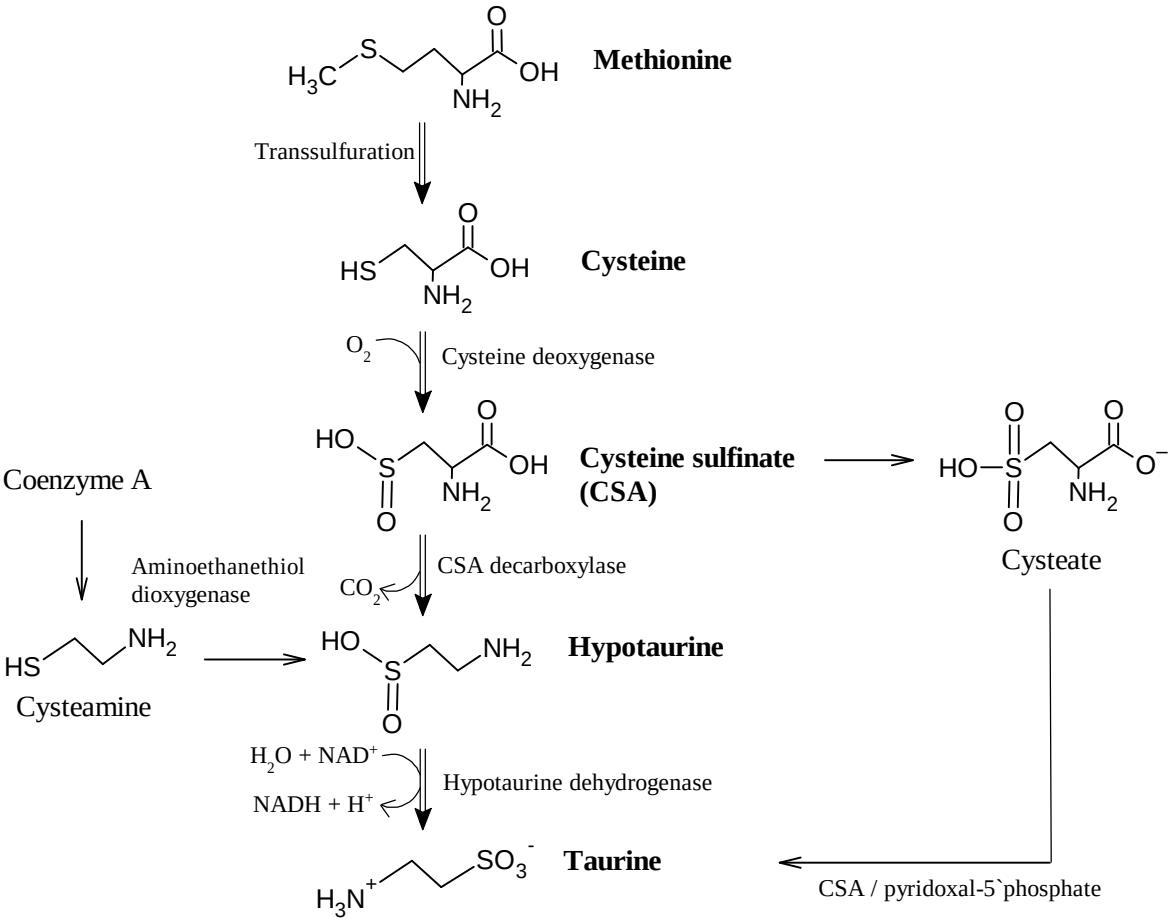

Figure 3: Biosynthesis of taurine. Graph elements were depicted with ACD/ChemSketch 2.0.

Fate of dietary taurine

Only little is known about the pharmacokinetics of taurine in man after administration [107]. Ingested taurine is absorbed from the enterocytes in the small intestinal tract via a carrier-mediated active transport system of the brush border membrane [110]. Responsible taurine transporters are the Na^+ / Cl^- dependent TauT (SLC6A6) and the Na^+ / Cl^- independent proton-coupled amino acid transporter PAT1 (SLC36A1), which vary in expression from stomach to colon. Especially in the stomach and the jejunum expression levels are high, suggesting there the main taurine uptake. However, TauT seems to be responsible for the transport of the endogenously produced taurine, while PAT1 regulates taurine concentrations after ingestion of taurine-rich meals (above 10 µM) [111-113]. After transport to the enterocytes, taurine is carried via the portal vein to the liver where it is used for primary bile salt conjugation with cholic acid to form TC. Otherwise taurine is released into the circulation via TauT [107, 110]. Similarly, glycine is conjugated to cholic acid to the bile salt glycocholate. With each meal, 4 - 6 g bile salts cycle repeatedly from the gall bladder through the small intestine to the ileal section. Here, they predominantly enter the enterohepatic circulation to return to the liver (95%). The residual 5% are released to the distal ileum and colon where they undergo bacterial conversion including deconjugation, dehydroxylation, and epimerization, releasing taurine or glycine from the secondary bile acid (deoxycholic acid) [114-116].

Despite the low proportion of bile acids reaching the colon, taurine is the second most abundant amino acid of colonic mucosa after glutamate (2.5 mmol/kg tissue weight) [117]. The higher the intake of dietary taurine, the higher the hepatic taurine conjugation and the higher the availability of taurine for intestinal bacteria [118]. Excess of taurine is excreted with urine (average taurine concentration, 0.5-2.0 mM) [115, 119, 120].

Microbial taurine utilization

Taurine is the most intensely studied sulfonate that can be utilized by bacteria and yeasts [3]. The most investigated pathways for microbial taurine degradation are sulfur assimilation, sulfur dissimilation, deamination, and the utilization as sole source of carbon (Fig. 2 and Appendix, Tables A2, A3).

For its further utilization taurine needs to be taken up into the bacterial cytoplasm which is brought about by the ATP binding cassette transporters (TauABC) or TRAP (TauKLM) transporters. The TauABC-encoding genes have been detected in both environmental and commensal gut bacteria, such as *Clostridium butyricum* and *Escherichia (E.) coli*, indicating that TauABC may be the main transport system for microbial taurine uptake [3, 119, 121-126].

Microbial taurine dissimilation, which involves the desulfonication of sulfoacetaldehyde, has been first described in 1973 [127, 128]. Subsequently, the sulfur moiety is reduced to sulfite by sulfoacetaldehyde acetyltransferase (Xsc) and directly exported by sulfite exporters (OrfX). Alternatively, sulfite is first oxidized to sulfate and then exported (TauZ) [122, 124, 129]. Yet, the microbial taurine degradation pathways are diverse, but most of them still involve sulfoacetaldehyde as an intermediate. [122, 124, 130, 131].

Sulfoacetaldehyde also serves as an intermediate in bacterial taurine-fermentation to H_2S. While both gut and environmental bacteria release sulfite or sulfate from taurine, H_2S formation from taurine was observed especially in intestinal bacteria (Appendix, Tables A2, A3). Exceptions are marine bacteria, which are also able to convert taurine to H_2S [132, 133]. Gut bacteria convert sulfoacetaldehyde, arising from taurine degradation, to isethionate as catalyzed by the glycal radical enzyme IseG / IslA, resulting in either a direct release of isethionate as in *Bifidobacterium kashiwanohense* PV20-2 or a further reduction to H_2S by dissimilatory sulfite reductase (Dsr) [9, 134-137]. A common isethionate transporter in bacteria is IsfE [132]. Alternatively, H_2S is released as end product of taurine fermentation, as described for *Veillonellaceae* 2C or *B. wadsworthia* 3.1.6 [9, 136-138]. The same pathway, resulting in H_2S formation has been detected in the intestinal bacteria *Desulfovibrio* sp. RZACYSA and *B. wadsworthia* RZATAU (DSM 11045) [8, 137, 139, 140]. More details about isethionate formation from taurine will be given in chapter 1.3.2.

1.3.2 Isethionate

Isethionate, the deaminated derivative of taurine, is present in squid axoplasm and red algae (200 mM) in strikingly high concentrations, while mammalian tissues (1.5 - 4.8 mM) and urine (0.05 mM) contain much lower levels [141-145]. Intestinal bacteria, such as *Klebsiella oxytoca* and *B. wadsworthia*, (Appendix Tables A2, A3), are responsible for the conversion of taurine to isethionate, whereas mammalian tissues are not able to synthesize

isethionate by their own [9, 119, 132, 134, 136, 146-148]. Therefore, the concentration of intestinal isethionate seems to be linked to the intestinal taurine concentration and the presence of bacteria, able to convert taurine to isethionate.

Another source of intestinal isethionate may be diet. For example, lentils (0.35 µmol/g), ginger (< 0.005 µmol/g), onion (< 0.005 µmol/g) and garlic (0.13 µmol/g) contain isethionate. However, the fate of isethionate after ingestion is not known yet [146]. Moreover, isethionate can be found in hair shampoos, soap or in pharmaceuticals [149-151].

Microbial isethionate utilization

A high diversity of bacteria dissimilate isethionate to obtain energy for their growth. These include environmental and intestinal bacteria, both releasing the sulfite moiety of isethionate either as sulfate, sulfite or H_2S (Figure 2, Appendix, Tables A2, A3). While the ability of sulfate and sulfite formation from isethionate seems to be evenly distributed among environmental and intestinal bacteria, H_2S formation is almost completely restricted to gut bacteria, such as *B. wadsworthia* and *Desulfovibrio* spp. [3, 9, 119, 121, 131, 132, 134, 136, 137, 139, 152-166].

There are two main pathways of microbial isethionate utilization. Firstly, released isethionate is directly internalized and then reduced to sulfoacetaldehyde [131, 167]. Sulfoacteldehyde is converted to sulfate, which is reduced to sulfite and released by the TauE exporter [167]. The enzyme responsible for the conversion of isethionate to sulfoacetaldehyde (isethionate dehydrogenase) is present in *Paracoccus* spp. and *Ralstonia* spp., indicating the importance of this pathway especially in such environmental bacteria [131].

Secondly, intestinal bacteria gain isethionate from internalized taurine (such as *Klebsiella oxytoca* TauN1 and *B. wadsworthia*) [148]. The sulfite moiety of isethionate is subsequently either released as sulfite, as described for *Clostridium* spp., or reduced to H_2S by Dsr as found in *B. wadsworthia* and then released [3, 8, 119, 134, 136, 160].

1.3.3 Cysteate

L-Cysteate has first been recognized as a natural product in 1946, namely as component of weathering wool and spiders' webs. However, since 1992 it is better known as an intermediate in the taurine biosynthetic pathway or as precursor and product of 3-sulfolactate, present in bacterial spores (Fig. 2 and 3) [168-172].

Biosynthesis of cysteate

In mammals, L-cysteate is a common component of urine, plasma, and in the brain [173-175]. Though this sulfonate is a neurotransmitter in the central nervous system, its synthesis in mammalians remains unclear [176, 177]. In the yolk sac of developing chicken, cysteate biosynthesis from L-cysteine and sulfite is catalyzed by cysteine lyase (EC 4.4.1.1) and coupled to the release of H_2S, but this pathway does not seem to exist in mammalian tissue [178]. Similarly, its synthesis from PAPS and aminoacrylate was only identified *in vitro*, not *in vivo* [179, 180].

More recent studies indicate that cysteate is not a mammalian product, but synthesized exclusively by bacteria. In the phototroph *Rhodospirillum rubrum*, cysteate is a product of bacterial sulfate metabolism [181]. A biosynthetic pathway of cysteate from CSA as part of

taurine synthesis has been described for *Proteus vulgaris* OX19 (Fig. 3) [182]. Interestingly, cysteate has also been observed in *Staphylococcus aureus* and *Bacillus subtilis*, indicating its relevance in microbial metabolism [170, 183].

The fate of dietary cysteate

Dietary products, such as milk protein, contain cysteate. Therefore, diet may be a potential source of mammalian cysteate. However, the fate of ingested cysteate is not known yet [173, 174, 184-187].

Microbial cysteate utilization

Cysteate can be utilized as sole source of carbon and energy, as electron acceptor (both by SRB), electron donor (by nitrate-reducing bacteria) or as substrate for fermentation (by SRB) [9, 139, 161-163, 165, 166, 188, 189]. Environmental and intestinal bacteria release the sulfite moiety of cysteate as sulfite, sulfate or H_2S. The main product of environmental bacteria resulting from cysteate degradation is sulfate, while intestinal bacteria release H_2S, indicating that cysteate contributes to the intestinal H_2S pool.

Environmental bacteria deaminate cysteate, which is subsequently desulfonated to 3-sulfolactate and followed by a transient release of sulfite by the sulfite exporter CuyZ. However, most bacteria convert sulfite to sulfate before it is released by the sulfate exporter SuyZ [129, 165, 172, 190-192].

The use of cysteate as growth substrate is also widespread among *E. coli* strains. For example, an *E. coli* K-12 derivative contains an ABC-type uptake system (SsuABC) for cysteate and a monooxygenase system (SsuDE) for sulfite release [154, 193, 194]. Also, other *Enterobacteriaceae* (such as *Klebsiella aerogenes, Desulfovibrio* spp., *B. wadsworthia*) are able to utilize cysteate as the sole source of sulfur [9, 139, 156, 161-163, 195]. Interestingly, most of these bacteria finally released the sulfonate sulfur as H_2S. [9, 139, 161-163, 195]. However, the majority of investigated intestinal strains were isolated from environmental or indirect sources originating from the intestine, similarly to taurine and isethionate utilizing bacteria (Appendix, Tables A2, A3).

1.3.4 Coenzyme M

CoM is present in all methanogenic archaea, acting as the terminal methyl carrier in methanogenesis. [196].

In humans, methanogens are present in the oral cavity, vagina, and the human gut [197-201]. As commensal human gut microorganisms, they are the main representatives of all intestinal archaea [202]. In the gut, methanogens colonize the small intestine, as well as the colon from the cecum to the rectum [24, 60, 203, 204]. Methanogens have been linked to disorders of the gastrointestinal tract, including IBD, colon cancer, and metabolic disorders linked to microbiota dysfunctions, such as anorexia and obesity and therefore make them an interesting topic in gastrointestinal research [205-210]

Biosynthesis of CoM

Studies indicate two different pathways for CoM biosynthesis in methanogens, involving either sulfolactate or cysteate as precursors [211]. Both reactions include sulfopyruvate as an intermediate. Sulfolactate is oxidized to the product by a sulfolactate dehydrogenase,

while cysteate is transaminated by L-aspartate and L-phosphoserine aminotransferases [212-214]. Subsequently, sulfopyruvate decarboxylase catalyzes the decarboxylation of sulfopyruvate to produce sulfoacetaldehyde [214]. Finally, CoM is predicted to be formed by a reductive thiolation reaction [211].

Microbial CoM utilization

CoM is required for intestinal methanogenesis and therefore may play a major role in the gut microbial sulfonate metabolism. However, previous studies indicate that intestinal microorganisms other than methanogens do not utilize CoM. Although bacteria, such as *B. wadsworthia*, were able to grow with sulfonates other than CoM [9, 161, 162, 164-166, 216, 217]. The role of CoM in the gastrointestinal tract besides its role in methanogens remains unclear until now.

1.3.5 SQDG, SQ, DHPS and 3-sulfolactate

SQDG

SQDG were first isolated from a green alga, *Chlorella vulgaris*, and structurally identified in 1959 [217, 218]. The sulfolipids are characterized by the polar head group SQ containing a carbon-sulfur bond between its hexose and the sulfone group [218]. The sulfur-containing lipid is localized in the thylakoid membranes of chloroplasts, maintaining the integrity of the photosynthetic structures and the function of the thylakoid membrane [219, 220]. The total mass of biosynthesized SQDG has been estimated to be in the range of ten billion tons per year [219]. SQDG make up 4 - 7% of total leaf lipids and up to 66% of all polar lipids in marine plants and algae [221, 222]. Therefore, SQDG represent a large fraction of organic sulfur in the biosphere, indicating their crucial role in the global biogeochemical sulfur cycle [219]. Together with other sulfolipids, SQDG serve as a sulfur and carbon source for photosynthetic organisms, and for terrestrial and aquatic bacteria [220]. Besides SQDG, additional three types of lipids are present in the thylakoid membranes: monogalactosyl diacylglycerol, digalactosyl diacylglycerol, and phosphatidylglycerol [223, 224]. However, SQDG are the only sulfur-containing lipids [225].

Biosynthesis of SQDG

The metabolism of SQDG comprises complex biosynthetic and catabolic pathways. Whereas the sulfolipid synthesis has been extensively investigated in the last 60 years, the catabolism has been elucidated only in the last years. Synthesis of SQDG is a common process in photosynthetic organisms, such as mosses, ferns and algae, but is also found in diatoms, dinoflagellates and in photosynthetic bacteria and proceeds in two reactions [218, 227-229]. First, UDP-SQ synthase (SQD1) catalyzes the formation of UDP-SQ from UDP-glucose and sulfite and second, sulfoquinovosyltransferase (SQD2) transfers SQ to diacylglycerol, forming SQDG [230-232].

The fate of dietary SQDG

SQDG are not only a common component of photosynthetic organisms, but are also present in the human diet. High levels are found in green leafy vegetables, such as spinach (824 µg/g dry weight) and parsley (450 µg/g dry weight), while lower levels are present in other vegetables, including potato (17 µg/g dry weight) and garlic (46 µg/g dry weight) [6, 7, 232]. The cyanobacterium *Athrospira platensis*, commercially known as Spirulina, contains a total

lipid fraction that varies from 3.4 to 29.5% dry weight, which in turn consists of 11.4 ± 0.71% of SQDG [234-238].

To investigate the fate of ingested SQDG, [^{35}S]SQDG was orally administered to guinea pigs and its degradation was monitored throughout the gut. Three hours after administration, 1 - 5% of the radioactivity was detected as SQDG in the intestinal mucosa, while 60% was identified as sulfoquinovosylglycerol (SQG). Hence, it was concluded that a stepwise deacetylation of SQDG to SQG occurs in animal tissue [238].

Microbial SQDG degradation

Intestinal bacterial cultures are able to degrade SQDG *in vitro*. A bacterial sulfoquinovosidase of *E. coli* (YihQ) hydrolyzes SQDG resulting in the release of its headgroup SQ [239]. Furthermore, the cleavage of fatty acids from SQDG by plant acylhydrolases leads to SQG, which in turn can undergo bacterial degradation to SQ by YihQ in *E. coli* [239, 240].

SQ

As the polar headgroup of SQDG, SQ is also a major component of the global sulfur cycle [241]. Half of all organosulfur in nature is estimated to be located in SQ [220, 242]. SQ is usually present in SQDG or is incorporated in *N*-linked glycans of some archaea, whereas its abundance as free sugar is scarce [244-247]. SQ is a derivative of D-glucose, in which the hydroxyl group at C-6 is replaced by a sulfonate group [220, 247]. Two catabolic pathways of SQ considered as variants of well-known glucose-degradation pathways have been identified in bacteria: The SQ Embden-Meyerhof-Parnas (SQ-EMP) pathway in *E. coli* K-12 and the SQ Entner-Doudoroff (SQ-ED) pathway in *Pseudomonas putida* SQ1 [248, 249]. The first resembles the glycolytic EMP pathway and is therefore referred to as sulfoglycolysis [249]. Interestingly, the SQ-ED pathway mainly proceeds in environmental bacteria, while the majority of commensal gut bacteria use the SQ-EMP pathway.

Microbial SQ degradation

Sulfoglycolysis enables *E. coli* to utilize SQ as sole source of carbon and energy. The first step is the isomerization of SQ to 6-deoxy-6-sulfo-D-fructose (SF) catalyzed by SQ isomerase (YihS). SF is subsequently phosphorylated to 6-deoxy-6-sulfo-D-fructose 1-phosphate (SFP) by 6-deoxy-6-sulfofructose kinase (YihV), which is cleaved to dihydroxyacetone phosphate (DHAP) and (2*R*)-3-sulfolactaldehyde by 6-deoxy-6-sulfofructose-1-phosphate aldolase (YihT). Finally, (2R)-3-sulfolactaldehyde is reduced to DHPS by 3-sulfolactaldehyde reductase (YihU). While DHAP enters the carbon metabolism for energy conservation, DHPS is excreted and utilized by other bacteria [249]. Sulfoglycolysis is controlled by a transcriptional regulator (CsqR) that inhibits the expression of sulfoglycolytic enzymes at low SQ concentrations [250]. Another member of *Enterobacteriaceae*, namely *Citrobacter* sp., is able to convert SQ to DHPS. It was assumed that the degradative pathway is most likely the SQ-EMP sulfoglycolytic pathway, as in *E. coli* [251].

The alternative SQ-ED pathway, in *Pseudomonas putida* SQ1, includes the following five enzymatic reaction steps: SQ is oxidized to 6-deoxy-6-sulfogluconolactone (SGL) by SQ dehydrogenase and afterwards hydrolyzed to 6-deoxy-6-sulfogluconate (SG) by 6-deoxy-6-sulfogluconolactone (SGL) lactonase. In the next step, SG is dehydrated to 2-keto-3,6-dideoxy-6-sulfogluconate (KDSG) by SG dehydratase and then pyruvate and

3-sulfolactaldehyde (SLA) are formed by 2-keto-3,6-dideoxy-6-sulfogluconate (KDSG) aldolase. Finally, SLA is oxidized to 3-sulfolactate by SLA dehydrogenase, which is then exported [248]. Besides *Pseudomonas putida*, the nitrogen-fixing bacterium *Rhizobium leguminosarum* SRDI565 takes advantage of the SQ-ED pathway for the degradation of SQ, but DHPS was detected in addition to 3-sulfolactate [252]. Several other *Pseudomonas* strains utilize SQ as a substrate, but release sulfate or an undefined metabolite. No DHPS and / or 3-sulfolactate were detected [241, 253]. Another bacterium, isolated from forest leaf mould (*Agrobacterium* sp. ABR2), releases the sulfite moiety of SQ as sulfate [241, 253].

DHPS and 3-SL

Besides as an intermediate in microbial SQ degradation, DHPS has been linked to osmoregulatory functions in *Sulfurimonas denitrificans* and as metabolite of dinoflagellates and diatoms, such as in *Thalassiosira pseudonana* and *Chaetoceros* strains [250, 255-261]. Similarly, 3-sulfolactate is a widespread natural product, which for instance is present in bacterial spores (5% of dry weight), indicating the importance of both sulfonates in bacterial metabolism [261, 262]. 3-Sulfolactate plays a role as an intermediate in CoM and cysteate biosynthesis, and in cysteate degradation, which enables such bacteria to utilize the latter as sole source of carbon and energy (see above, 1.3.3 and 1.3.4, Fig. 2).

Microbial degradation of DHPS and 3-sulfolactate by environmental bacteria

The enzymatic pathway of DHPS degradation encoded in the *hps* gene cluster has been described in *Ruegeria pomeroyi*, which was isolated from seawater: DHPS uptake (HpsKLM) and reduction to sulfite is catalyzed by sulfo-lyase (CuyA) [172, 263]. Another bacterial DHPS catabolic pathway is present in *Cupriavidus pinatubonensis* JMP134, isolated from soil [263]. This organism oxidizes internalized DHPS to 3-sulfolactate, which is subsequently cleaved to sulfite by CuyA. Subsequently sulfate release is presumed [251, 263].

Bacteria isolated from the environment degrade the 3-sulfolactate to sulfite and / or sulfate. The marine bacterium *Roseovarius nubinhibens* ISM degrades 3-sulfolactate by a bifurcated pathway, in which the sulfonate is taken up by a tripartite sulfolactate uptake system (SlcHFG) and subsequently oxidized to 3-sulfopyruvate by a membrane-bound sulfolactate dehydrogenase (SlcD). Sulfopyruvate is then transaminated to (*S*)-cysteate, which is desulfonated by CuyA, yielding sulfite. Sulfite is presumably exported by CuyZ [130, 172, 251]. A similar pathway has been detected in the marine bacterium *Silicibacter pomeroyi* DSS-3 [190, 264]. The aerobe *Chromohalobacter salexigens* DSM 3043, isolated from a solar salt facility, also contains an SlcHFG uptake system, but sulfate and sulfite are released as end products [212, 266-268]. Furthermore, sulfolactate serves as an intermediate in anoxic cysteate degradation in *Paracoccus pantotrophus* NKNCYSA (DSM 12449) resulting in the release of sulfate [129, 165, 166].

Microbial degradation of DHPS and 3- sulfolactate by intestinal bacteria

Commensal gut bacteria release H_2S from DHPS and / or 3-sulfolacate. For example, incubation of DHPS with *B. wadsworthia* leads to H_2S formation [140]. In a co-culture of *Eubacterium* (*E.*) *rectale* DSM 17629 and *B. wadsworthia* 3.1.6 DHPS was formed as an intermediate in SQ conversion to H_2S. First, *E. rectale* converts SQ to DHPS, which is then utilized by *B. wadsworthia* 3.1.6 and the sulfite moiety of DHPS is released as H_2S. In addition,

a co-culture of *E. coli* and *Desulfovibrio* sp. DF1 degraded SQ via DHPS and 3-sulfolactate to H_2S [1]. First *E. coli* converted SQ to DHPS taking advantage of the sulfoglycolytic SQ-EMP pathway, while *D.* sp. DF1 formed H_2S from DHPS [251]. The latter reaction involves 3-sulfolactate as an intermediate, which is formed after oxidation of DHPS by two NAD^+-dependent dehydrogenases (DhpA, SlaB). 3-Sulfolactate is then cleaved to pyruvate and sulfite by a sulfolactate sulfite lyase (SuyAB). After reduction of sulfite by Dsr, H_2S is released as end product [251].

Other gut bacteria, such as *Clostridium* spp. and *Klebsiella* sp. also degrade 3-sulfolactate, but the underlying enzymatic reactions and the released end products have not yet been investigated [3, 119, 129, 160]. However it can be summarized that environmental bacteria release either sulfite or sulfate from DHPS and / or 3-sulfolactate, while gut bacteria form H_2S as an end product (Appendix, Tables A2, A3).

1.4 Aim of the study

This study aimed to clarify to which extent dietary sulfonates and their sulfonic metabolites can be utilized by intestinal bacteria enabling H_2S production. Furthermore, it was investigated whether sulfonates stimulate the growth of colitogenic bacteria, such as *B. wadsworthia*.

Sulfonates, such as taurine, isethionate, cysteate and or SQDG, are part of the daily human diet by ingestion of meat, fish and leafy green vegetables and therefore might potentially reach the human gut. Evidence illustrates the ability of bacteria to degrade these sulfonates to other sulfonic metabolites, including CoM, SQ, DHPS, and / or 3-sulfolactate and further to H_2S, indicating an important role of gut bacteria in intestinal sulfonate degradation. In addition, these sulfonates may contribute to the intestinal H_2S pool. A bloom of the colitogenic bacterium *B. wadsworthia* was associated to exacerbated colitis in IL-$10^{-/-}$ mice and H_2S formation from taurine [8, 9]. However, the association of sulfonate conversion to H_2S and growth of colitogenic gut bacteria is not well understood. Instead, most of the bacteria studied were isolated exclusively from either environmental source such as river sediment, soil or compost, or from indirect intestinal sources, including sewage sludge. Therefore, no direct link between sulfonate utilization by colitogenic bacteria and H_2S formation in the human intestinal tract can be drawn yet.

This thesis aims to demonstrate the ability of human intestinal bacteria to convert sulfonates to H_2S using *in vitro* cultures of human fecal slurries and sulfonates under anoxic conditions. To assess inter-individual differences in H_2S formation among the donors, human fecal slurries were individually incubated with each one of the following seven sulfonates: taurine, isethionate, cysteate, CoM, SQ, DHPS, or 3-sulfolactate. To further unravel the intestinal sulfonate cycle and its link to the stimulation of pro-inflammatory bacteria such as *B. wadsworthia* (colitogenic effect), bacteria capable of H_2S formation from sulfonates were isolated and identified. In addition, the impact of a SQDG-rich diet was assessed in conventional mice fed a semisynthetic diet supplemented with 20% Spirulina, which is rich in SQDG. The fate of ingested SQDG was monitored along the whole gastrointestinal tract and

the overall impact on the murine health status and on the intestinal microbiota composition were investigated.

The experiments were performed to address the following research objectives:

- To identify human intestinal bacteria that contribute to the formation of H_2S from dietary sulfonates and their sulfonic metabolites
- To investigate the biochemical pathways that enable such bacteria to gain sulfite from dietary sulfonates and their sulfonic metabolites
- To investigate the fate of sulfonates, such as SDQGs, after ingestion
- To examine whether growth of colitogenic bacteria is stimulated by dietary SQDG, SQ and DHPS by contributing to the pool of endogenous sulfonated compounds such as taurine

2 MATERIAL AND METHODS

Distilled water cleaned with the pure water system Ultra Clear (Siemens Water Technologies, Günsburg, Germany) was used as solvent, if not otherwise indicated. Sterile autoclaved solutions (120 °C, 15 min) were used for microbial and molecular biological experiments and analyses to prevent contamination, if not otherwise stated.

2.1 Materials and bacterial strains

2.1.1 Sulfonates

Isethionate, CoM and cysteate were purchased from Sigma-Aldrich (Darmstadt, Germany), taurine and TC from Roth (Karlsruhe, Germany), SQ from MCAT (Donaueschingen Germany), and DHPS and 3-sulfolactate from Enamine (Kyiv, Ukraine) or Chemspace (Riga, Latvia).

2.1.2 Bacterial strains and growth conditions

B. wadsworthia DSM 11045, *Escherichia* (*E.*) *coli* MG1655 (DSM 18039), *Desulfovibrio* (*D.*) *desulfuricans* DSM 642^{T}, *D. piger* DSM 749^{T}, *D. simplex* DSM 4141^{T} and *D. intestinalis* DSM 11275^{T} were purchased from the Leibniz Institute DSMZ-German Collection of Microorganisms and Cell Cultures (Braunschweig, Germany).

The purity of the cultures was tested based on their phenotype after streaking on Columbia blood agar plates (Biomérieux, Marcy-l'Étoile, France), and on cell morphology after Gram staining. The Columbia blood agar plates were incubated under anoxic conditions in an Anaerocult anaerobic jar (Merck, Darmstadt, Germany) containing an AnaeroGen sachet (Thermo Fisher Scientific, Schwerte, Germany), or under oxic conditions, both at 37 °C. The identity of bacterial species was verified based on *16S ribosomal RNA* (*16S rRNA*) gene sequencing (2.4.3).

2.2 Human study

2.2.1 Study design and study participants

The human observational study was approved by the ethics committee of the University of Potsdam, Germany (no. 11/2016). The study comprised a one-time human fecal collection of approximately 20 ml. Healthy human subjects, who did not use antibiotics in the six months prior to the fecal sample collection were included. Exclusion criteria were intestinal diseases, intake of probiotics in the past 6 months, food intolerances, allergies, lactation and / or pregnancy. The participants were recruited at the German Institute of Human Nutrition Potsdam-Rehbruecke (DIfE, Germany).

2.2.2 Collection of fecal samples

The participants collected the first fecal sample of the day using a feces catcher (Servoprax, Wesel, Germany) and immediately transferred three partial quantities of the sample to a feces tube containing a previous perforated lid (Sarstedt, Nürnbrecht, Germany). The feces-containing tube was immediately stored in a plastic container with an anaerobic sachet (Thermo Fisher Scientific) to create anoxic conditions. Fecal samples were transported

within a maximum of 45 min to the DIfE by the participants, immediately stored at 4 °C upon arrival and processed within 2 h after sample collection.

2.2.3 Processing of fecal samples

To process the sample, the entire plastic container with the feces tube was transferred into an anaerobic chamber (Meintrup-Don Whitley Scientific, West Yorkshire, UK). Using a spatula, the fecal sample was suspended in sterile anoxic phosphate buffered saline (aPBS, pH 7.0, Appendix, Table A1) to a final concentration of 10% (w / v). Following the addition of 10 glass beads (2.85 - 3.45 mM, Roth), the suspension was homogenized by vortexing. The fecal slurries were transferred into Hungate tubes fitted with butyl rubber septa screw caps and further processed [269-271]. The residual fecal sample was stored in the fecal tube at -20 °C for short-term and -80 °C for long-term storage.

2.2.4 Incubation of fecal slurries with sulfonates

Fecal slurries (1%) from ten donors (D1 - D10) were individually incubated with sterile filtered (syringe filter, 0.2 µM pore size, Sarstedt) taurine (20 mM), isethionate (20 mM), CoM (20 mM), cysteate (20 mM), SQ (4 mM), DHPS (4 mM), or 3-sulfolactate (4 mM) in aPBS (Appendix, Table A1) under anoxic conditions for 96 h at 37 °C. For this purpose, 500 µl 10% prepared fecal slurries (2.2.3) and a single sulfonate were added to Hungate tubes containing 4.0 ml aPBS (Fig. 4A). Sterile filtered titanium(III) nitrilotriacetate (NTA, Appendix, Table A1, 3.18 mM) was added as reducing agent [271] and afterwards the final volume in the Hungate tubes was adjusted to 5 ml using aPBS. Two control incubations were included in each experimental series (Fig. 4B): First, 1% fecal slurries without sulfonates and second, each sulfonate without fecal slurries. Samples were taken at different points in time for the analysis of sulfonates with liquid chromatography-tandem mass spectrometry (LC-MS/MS) analysis (2.3.1) and for H_2S quantification using the methylene blue method (2.3.5). SQ was also quantified with the dinitrosalicylic acid (DNS) method (2.3.2) and taurine with the 4-fluoro-7-nitrobenzofurazan (NBD-F) assay (2.3.3). Injection of additives into and collection of samples from the Hungate tubes were performed with sterile injection needles (Henry Schein, Berlin, Germany) flushed three times with N_2/CO_2 (80/20, v/v, %) to ensure anoxic conditions [269-271].

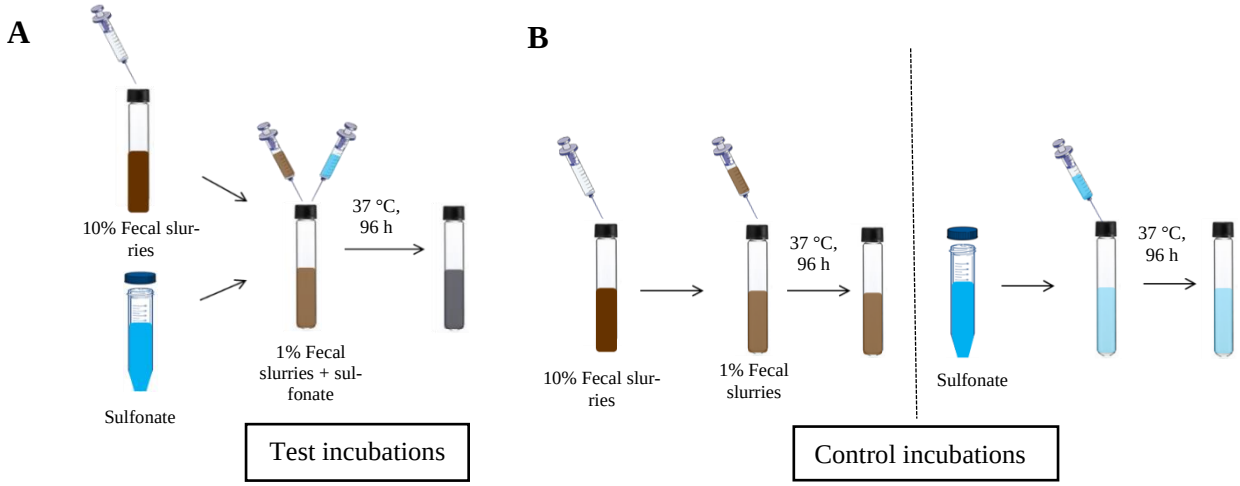

Figure 4: Experimental set-up of anoxic incubation of human fecal slurries (1%) with sulfonates. (A) Test incubations: Anoxic incubation of human fecal slurries from each donor (n = 10) for 96 h at 37 °C with one of these sulfonates: taurine, isethionate, cysteate, coenzyme M (20 mM each), sulfoquinovose, 2,3-dihydroxypropane-1-sulfonate, or 3-sulfolactate (4 mM each). (**B**) Control incubations: Anoxic incubation of human fecal slurries without sulfonate or of each sulfonate without fecal slurries. All incubations were stored at 37 °C for 96 h. Graph elements were depicted with PowerPoint2019.

2.2.5 Enrichment and isolation of sulfonate-utilizing gut bacteria

Enrichment cultures of sulfonate-converting bacteria from human feces were set up with fecal slurries from one donor with one sulfonate with the aim to isolate and identify human fecal bacteria able to convert sulfonates to H_2S. For the enrichment of taurine-, isethionate- and 3-sulfolactate-utilizing bacteria, a 1% fecal suspension was prepared as described above (2.2.4). Instead of aPBS, a previously described base medium was used, which was modified (Appendix, Table A1) [272].

Taurine-converting bacteria were enriched in parallel starting with fecal slurries from two donors (D0 or D1) containing one electron donor, either DL-lactate (L) or formate (F) (both 40 mM), and taurine (20 mM) as electron acceptor. Furthermore, yeast extract (YE, 3.5 mg/l) was added or excluded and a gas phase of either of N_2/CO_2 or H_2/CO_2 (80/20, v/v, %) was used. Enrichment cultures were incubated at 37°C and tested for H_2S formation after 48 h of incubation using the methylene blue method (2.3.5). Subcultures prepared with a 1% inoculum of H_2S-releasing cultures were defined as positive for sulfonate conversion. Seven transfers were performed, until taurine-converting bacteria were isolated from final enrichment cultures by streaking.

The enrichment of isethionate- and 3-sulfolactate-converting bacteria started with fecal slurries obtained from D10, two electron donors (formate and DL-lactate, 40 mM each), isethionate (20 mM) or 3-sulfolactate (4 mM) as electron acceptor and a gas phase of N_2/CO_2 (80/20, v/v, %). Enrichment cultures were incubated at 37°C. Subcultures were prepared from enrichment cultures positive for H_2S formation. After three transfers, isethionate- and 3-sulfolactate-converting isolates were obtained by streaking.

To obtain SQ-converting isolates, a 10% fecal suspension obtained from feces of D1 was prepared in aPBS as described above (2.2.3) and subsequently centrifuged to eliminate fecal debris (500 x *g*, 4 °C, 5 min). The supernatant was pelleted (14,000 x *g*, 5 min, 4 °C) and the

pellet was washed twice (14,000 x *g*, 4 °C, 5 min) using a modified mineral salts medium (MSM, Appendix, Table A1) [273]. A 2% fecal suspension in MSM supplemented with 4 mM SQ was incubated either under oxic conditions in test tubes closed with a loose-fitting cap while shaking (175 rpm) or under anoxic conditions in Hungate tubes with a gas phase of N_2/CO_2 (80/20, v/v, %). Control cultures contained fecal suspensions without SQ. Following three transfers to fresh medium and incubations, isolates were obtained by streaking.

Pure cultures of sulfonate-converting bacteria were obtained by streaking diluted subcultures (10^{-1} - 10^{-8}) on Columbia blood agar plates (Biomérieux). The agar plates were incubated anoxically in gas-tight jars containing sachets and / or oxically, both at 37 °C. Purity of cultures and morphology of bacterial cells were examined with Gram staining. Phylogenetic analysis of bacterial isolates was done based on *16S rRNA* gene sequencing (2.4.3). Phenotypic characteristics including motility and presence of flagella were examined (2.2.9).

2.2.6 Testing the ability of obtained bacterial isolates and relevant gut bacteria to convert sulfonates

Testing taurine- or 3-sulfolacate-utilizing isolates

Pure cultures of fecal isolates capable of converting taurine or 3-sulfolactate to H_2S, were grown for 4 d (taurine converter) or 24 h (3-sulfolactate converter) on Columbia blood agar plates under anoxic conditions at 37 °C. Afterwards modified base medium (Appendix, Table A1) was inoculated with cells and supplemented with lactate (taurine converter) or formate (3-sulfolactate converter) as electron donor (both 40 mM) and one sulfonate as electron acceptor and adjusted to an optical density at 600 nm (OD_{600}) of 0.04. Cultures were incubated at 37°C for 96 h under strictly anoxic conditions with N_2/CO_2 (80/20, v/v, %) as a gas phase. Samples were taken every 24 h for the analysis of bacterial growth based on OD_{600} measurements and / or determination of the number of colony-forming units (CFU, 2.2.12), for sulfonate conversion using LC-MS/MS analysis (2.3.1) and for H_2S quantification (2.3.5). Base medium solely containing the inoculum, without the addition of the tested sulfonate and vice versa were included as controls.

Investigating sulfoquinovose conversion by fecal isolates

SQ utilization under oxic and anoxic conditions by human fecal isolates was tested. Bacterial cells were harvested from cultures grown on Columbia blood agar plates (Biomérieux) (24 h, 37°C, oxic conditions) and suspended in MSM (Appendix, Table A1). MSM with or without NTA, respective for anoxic or oxic incubation, was supplemented with SQ (4 mM) and inoculated with 100 µl bacterial suspension to an OD_{600} of 0.1. Glucose (4 mM) instead of SQ was used in parallel as positive control. Medium supplemented with SQ served as negative control. Cultures were grown at 37 °C for 70 h. Samples were taken at appropriate points in time for analysis of bacterial growth (OD_{600}) and SQ conversion (DNS method, 2.3.2 and LC-MS/MS analysis, 2.3.1).

Testing growth of relevant gut bacteria with sulfonates

The capability of *B. wadsworthia* or SRB (*D. simplex*^{T}, *D. intestinalis*^{T}, *D. desulfuricans*^{T} and *D. piger*^{T}) to convert sulfonates was tested. Bacterial growth conditions and the experimental set-up were equal to those used for the taurine-utilizing isolates, as described above (2.2.6). Formate (40 mM) was used as electron donor for incubations with *B. wadsworthia*, and lactate (40 mM) for incubations with SRB. Modified basal medium (Appendix, Table A1) containing sulfate (20 mM) instead of the taurine was used as a positive control in SRB-culturing experiments. *B. wadsworthia* cells were additionally enumerated using the Thoma chamber (2.2.11).

Testing 3-sulfolactate and DHPS conversion by *Escherichia coli* strains

To examine whether *E. coli* utilizes 3-sulfolactate or DHPS, *E. coli* MG1655 and human fecal isolated *E. coli* strains were individually cultivated with each sulfonate in modified base medium (Appendix, Table A1). Growth conditions and the experimental set-up were the same as used 3-sulfolactate-converting isolates, as described above (2.2.6).

Co-culturing of a sulfoquinovose-converting isolate with *B. wadsworthia*

The human fecal isolate SQ6, found to convert SQ to DHPS, and *B. wadsworthia* capable of degrading DHPS to H_2S were co-cultured to investigate whether SQ is completely converted to H_2S. The co-culture was compared to single cultures. The experiment was done in Hungate tubes as described above for incubation of *B. wadsworthia* as single culture (2.2.6). Bacterial cell numbers were determined with quantitative real-time polymerase chain reaction (qPCR) (2.4.4).

2.2.7 Examination of the metabolism of taurine-converting isolates

The following three growth conditions were tested for the taurine-converting isolate Tau1: Na_2SO_4 (Riedel de Häen, Seelze, Germany) with succinate (Fluka), Na_2SO_3 (Merck) with lactate or $NaNO_3$ (Sigma-Aldrich) with lactate (20 mM each). Bacteria were grown under anoxic conditions at 37 °C in a previously described basal freshwater medium (pH 7.0) [195], which was modified due to unexpected precipitation (Appendix, Table A1). The inoculum was obtained by streaking on Columbia blood agar plates (Biomérieux) as described in 2.2.5. Samples were taken at 0 h and 48 h for the analysis of bacterial growth (OD_{600} and the CFU number, 2.2.12), and of the metabolites H_2S and nitrite. H_2S formation was examined using the methylene blue method (2.3.5) and nitrite formation using the Griess Reagent System (Promega, Walldorf, Germany) according to the manufacturer's instructions. The Griess reaction is based on a colorimetric reaction using sulfanilamide and *N*-(1-naphthyl)ethylenediamine forming a pink-magenta azo compound in an acidic environment, which was determined at 540 nm.

2.2.8 Test for bacterial motility

Cultures grown on Columbia blood agar plates (24 - 48 h, Biomérieux) were gently touched with a loopful of sterile 0.15 M NaCl and transferred to a drop of NaCl on a slide. The preparation was sealed with a coverslip and microscopically examined for motility at a 1000 x magnification (Eclipse E600, Nikon, Düsseldorf, Germany).

2.2.9 Flagella staining

Motile bacterial preparations (2.2.8) were kept for 10 - 20 min at room temperature (RT) until approximately 30% of the cells attached to the cover slip. Subsequently, two drops RYU flagella stain (Appendix, Table A1) [274] were gently applied to the edge of the coverslip, allowing it to mix with the cell suspension. The cultures were immediately examined for the presence of flagella at a 1000 x magnification.

2.2.10 Catalase test

Catalase positive bacteria catalyze the depletion of hydrogen peroxide (H_2O_2) to O_2 and H_2O. Catalase activity was tested from bacterial cells grown for 24 - 48 h on Columbia blood agar plates (Biomérieux). Grown bacterial cells were transferred with a sterile loop to a microscopic slide and covered with a H_2O_2 (3%) solution (Biomerieux). Development of bubbles confirmed catalase activity.

2.2.11 Quantification of bacteria with the Thoma cell counting chamber

Bacterial cells were enumerated using a Thoma cell counting chamber (hemocytometer, per large square a depth of 0.1 mm, surface of 4.0×10^{-2} mm^2, and a volume of 4.0×10^{-3} mm^3). A volume of 3 µl cell suspension was drawn under a coverslip by capillary action and cells present in four of the large squares were microscopically enumerated (Eclipse E600, Nikon, Germany) at a 400 x magnification. Cell suspensions were diluted or concentrated if required. Cell number per ml was calculated with the following equation:

$$\text{Cell number/ml} = [(\text{cell number of four large squares} \times \text{dilution factor}) \times 625] \times 10^3 \quad \text{(Eq. 1)}$$

2.2.12 Enumeration of bacterial colony-forming units

Enumeration of viable bacteria was performed based on the quantification of CFU using the drop plate technique [275]. For this, serial dilutions (10^{-1} to 10^{-8}) of the samples were prepared in aPBS (Appendix, Table A1) containing 2.5% agar. Afterwards, 50 µl diluted suspension was plated on Columbia blood agar plates (Biomérieux) and incubated for 4 d at 37 °C under anoxic conditions in an anaerobic chamber. The number of colonies was determined using a binocular and the cell number is expressed as $\log_{10}$ CFU ml^{-1}.

2.3 Biochemical and analytical methods

2.3.1 Quantification of sulfonates based on LC-MS/MS analysis

For sulfonate quantification, samples were diluted in acetonitrile as follows: Samples collected in the experiments described under 2.2.7 (Investigating sulfoquinovose conversion by fecal isolates) were diluted 1:5,000. All other samples were diluted 1:10,000. The four sulfonates taurine, isethionate, SQ and DHPS were determined simultaneously with LC-MS/MS analysis and multiple reaction monitoring (MRM) at the Helmholtz-Zentrum Umweltforschung (UFZ, Leipzig), as previously described [276]. Sulfonates were analyzed in negative ionization mode with chosen transition mass of 124 Da to 81 Da for taurine, 125.3 Da to 107 Da for isethionate, 243 Da to 123 Da for SQ and 155 Da to 95 Da for DHPS. Diluted samples were injected into an Ultimate 3000 high performance liquid chromatography (HPLC) (Dionex, Sunnyvale, USA) and separated on a BEH amide column (2.1 × 100 mM, 1.7 µM; Waters, Milford, USA). The column temperature was set at 60 °C and the

flow rate was 0.5 ml/min. The elution solvents used were (A) 0.1% formic acid in water and (B) 50% acetonitrile/0.1% formic acid in water. The following gradients were used: 2 min at 80%, linear gradient of 3 min to 50%, which was held for 2 min, and increased to 80%, which was held for 3 min. The eluted sulfonates were analyzed inline on a QTRAP 5500 (AB Sciex, Framingham, USA). Data acquisition and peak picking were performed using the Analyst software (Version 1.6.2, AB Sciex). For quantification, a calibration curve was generated for each sulfonate by spiking a human fecal matrix solution with the sulfonate at nine concentrations ranging from 1 ng/ml to 600 ng/ml. The fecal matrix solution was prepared from 1% fecal slurries (2.2.4) containing 3.18 mM NTA (Appendix, Table A1). Subsequently, fecal slurries were centrifuged (14,000 x *g*, 4 °C, 5 min) and the supernatant serially diluted with 50% acetonitrile and 0.1% formic acid in water to obtain a final dilution of either 1:5000 or 1:10,000. Calibration curves gave a linear response for isethionate ($R^2 = 0.9985$) and SQ ($R^2 = 0.9989$), while DHPS ($R^2 = 0.9997$) and taurine ($R^2 = 0.9994$) were characterized by a non-linear response. The regression equations and concentrations of sulfonates were determined using inhouse-written R-scripts [277].

Limits of sulfonate quantification in LC-MS/MS analysis

All samples were diluted 1:10.000 or 1:5000 with 50% acetonitrile in water before analysis due to a reduced reliability of measurements for samples with a lower or higher dilution. Dilutions lower than 1:5.000 indicated interference of a medium constituent, which could not be identified. Higher sample-dilutions ranged outside of the generated calibration curves.

Accuracy of the method was assessed as described in Haange *et al.* [276]. Mean recovery of the sulfonates was tested and acceptable at 25, 50 or 100 ng/ml for all sulfonates, except isethionate whose recovery was slightly outside the acceptable values for 100 ng/ml. Intra- and inter-day precision was assessed with multiple measurements.

Relative standard deviations were < 5%, except for cysteate at 25 ng/ml, indicating a very high precision of the measurements (Haange *et al.*, [276]). The collected samples were analyzed within 2 - 3 weeks. Sulfonates diluted in 50% acetonitrile and stored at -80°C were stable for one month. Accuracy of sulfonate quantification was largely decreased when diluted samples were stored for extended time periods before analysis.

2.3.2 Quantification of sulfoquinovose and glucose based on colorimetric determination

SQ and glucose were quantified with the DNS method as previously described [279-281]. DNS reacts with reducing sugars under influence of heat (100 °C) to 3-amino-5-nitrosalicylic acid, which strongly absorbs light at 540 nm. Samples were centrifuged (14,000 x *g*, 5 min, 4 °C) and 100 µl supernatant was stored at -20 °C until further analysis. For analysis, 50 µl supernatant was mixed with 50 µl reagent, subsequently incubated for 15 min at 100 °C and afterwards cooled down to RT. Absorbance was determined at 540 nm. SQ and glucose standard solutions were applied in the linear range of 1 to 10 mM.

2.3.3 Taurine quantification with fluorometric determination

Taurine was quantified based on its derivatization with the fluorescent reagent NBD-F [281]. Supernatant of centrifuged samples (14,000 x *g*, 5 min, 4 °C) was stored at -20 °C for further analysis. For quantification, the supernatant was thawed, centrifuged (20,800 x *g* for 10 min

at RT), and diluted 1:40 with the respective medium. Ten µl were transferred into brown plastic tubes, mixed with 20 µl acetonitrile, 70 µl borate buffer (0.05 M sodium tetraborate, pH 9.5) and 100 µl NBD-F (Merck, 1 mM). After incubating the samples for 3 min at 70 °C, they were analyzed at an excitation wavelength of 470 nm and an emission wavelength of 530 nm. Taurine standard solutions were prepared in the linear range of 0.1 to 1 mM with an absorbance ranging from 6×10^3 to 9×10^3 AU.

2.3.4 Analysis of taurocholate deconjugation with thin-layer chromatography

The deconjugation of TC by bacteria was analyzed with thin-layer chromatography [282]. Silica gel coated aluminium sheets (TLC Silica gel 60, Merck) were used as stationary phase. Supernatants (14,000 x *g*, 5 min, 4 °C) of bacterial cultures incubated with TC were stored at -20 °C for further analysis. For analysis, 50 µl thawed samples was lyophilized (Christ alpha 1-4, Loc-1m), dissolved in methanol and centrifuged (4,000 x *g*, 10 min, RT). Afterwards, 3 µl supernatant was analyzed using 1-butanol/acetic acid/water as mobile phase (100:10:10, v/v/v). Subsequently, the plate was soaked in 5% sulfuric acid in ethanol and heated for 10 min at 110 °C. Sodium taurocholate (Roth) and sodium cholate (Sigma-Aldrich) (both 20 mM) were used as standards.

2.3.5 Quantification of H_2S using the methylene-blue method

H_2S was determined with the methylene blue method [283]. The analysis is based on the formation of methylene blue by the reaction of stabilized H_2S (zinc sulfide, ZnS) with *N*,*N*-dimethyl-*p*-phenylenediamine and a Fe^{3+} solution in an acidic environment [283, 284]. A volume of 250 µl sample was immediately added to a mixture of 5 µl zinc acetate (0.27 M) and 25 µl NaOH (100 mM). If required, samples were diluted (1:2 to 1:200) in water. Twenty µl reagent containing *N*,*N*-dimethyl-1,4-phenylenediamine hydrochloric acid (Fluka, 0.017 M), and $FeCl_3$ (Riedel-de Haën, 0.022 M) dissolved in 18.5% hydrochloric acid was added. Samples were vortexed, incubated for 20 min at RT, and centrifuged (12,000 x *g*, 3 min, RT) to limit interference by bacterial or fecal material with the colorimetric detection [285]. Formed methylene blue was detected at 670 nm. Standards were prepared in a range of 40 to 200 µM with sodium sulfide (Na_2S) from a stock of anoxic 500 µM Na_2S stored in a rubber septum bottle (N_2/CO_2, 80/20, v/v).

Limits of detection for H_2S measurement

Since Fischer *et al.* introduced the methylene blue method for determination of H_2S, the method has been widely used and modified depending on the sample type [285, 286]. The method has also been used to study H_2S formation in fecal samples [285]. However, in the present study the amount of H_2S observed during incubation of 3-sulfolactate with human fecal slurries were higher than the concentration of the initially added sulfonate (Fig. 8C). Interference of the human gut microbiota or the sulfonate itself with the medium could be excluded, as the addition of both as separate control incubations did not reveal H_2S formation during control incubations in any of the tested donors. Therefore, the reasons for the high H_2S concentrations observed in incubations with 3-sulfolactate could not be clarified. It may be concluded that the methylene blue method rather allows qualitative than quantitative H_2S measurements.

2.3.6 Calculation of the growth rate and the doubling time of bacterial cultures

The growth rate (r) and the doubling time (t_d) were both calculated using growth curves of bacterial cultures and plotting the growth (OD_{600}) vs. time:

$$r = 2.303 (lgOD_2 - lgOD_1) / (t_2 - t_1) \quad \text{(Eq. 2)}$$

$$t_d = ln2 / r \quad \text{(Eq. 3)}$$

OD_1, OD_2, t_1, and t_2 represent the OD_{600} values and points in time, respectively, of the beginning (OD_1, t_1) and the end (OD_2, t_2) of the exponential growth phase.

2.4 Molecular methods

2.4.1 DNA extraction from bacterial cells, PCR and gel electrophoresis

Bacterial cell pellets were obtained by centrifugation (9,300 x *g*, 3 min, RT) of bacterial liquid cultures collected at the end of the exponential growth phase. To avoid interference during DNA extraction, cultures were filtered (filter paper, 150 mM diameter, Macherey-Nagel). Genomic DNA was isolated from bacteria with the RTP Bacteria DNA Mini Kit (Stratec, Berlin, Germany) according to the manufacturer's instructions and was eluted with 50 µl elution buffer. The DNA concentration was determined photometrically at 260 nm (NanoDrop ND-1000, Peqlab, Germany) before storage at 4 °C. Genomic DNA was amplified with polymerase chain reaction (PCR) using a peqSTAR Thermocycler (Peqlab, Germany) (Table 1, Appendix Table A4).

For visualization, PCR products were diluted 1:5 with indicated loading buffer and separated electrophoretically on an agarose gel (Serva, Germany) prepared with 1 x TRIS-acetate-EDTA buffer (TAE buffer, Appendix, Table A1) at 80 - 95 V for 25 - 40 min in a horizontal electrophoresis chamber (Biometra). Gel imaging was done with the G:BOX F3 gel doc system and the GeneSys software version 1.5.2.0 (Syngene, UK).

Table 1: Primer sequences used for PCR. All primers were synthesized by Eurofins genomics.

Target (amplicon size in bp)	Primer sequence	References
16S rRNA (1465)	27-F: 5'-AGA GTT TGA TCC TGG CTC AG-3'*	1492-R (modified)[287]
	338-R: 5'-GCT GCC TCC CGT AGG AGT-3'**	[288], also referred as 355-R[289]
	968-F: 5'-AAC GCG AAG AAC CTT AC-3'***	[290]
	1401-R: 5'-CGG TGT GTA CAA GAC CC-3'****	[291]
	1492-R: 5'-TAC CTT GTT ACG ACT T-3'*	1492-R (modified) [287]
dsrAB (649)	F: 5'-CCA ACA TGC ACG GYT CCA-3' R: 5'-ACG AGC AGC GAA CCC ATC-3'	[9, 292] and self-designed
yihS (332)	F: 5'-ACG CGG TGG AAG CTT TCT TGA T-3'; R: 5'-CAC GGT GGC GTT AAA CAG ACC TT-3'	[249]
yihQ (2032)	F: 5'-AGC GGC TCT TCA ATG GAT ACG CCA CGT CCA CAGT-3'; R: 5'-AGC GGC TCT TCT CCC GAT GCT TTT TAA CGA CGC GAA-3'	Self-designed
RAPD M13-core	F: 5'-GAG GGT GGC GGT TCT-3'	[293]
E. coli K12 strains (970)	F: 5'-CGC GAT GGA AGA TGC TCT GTA-3' R: 5'-ATC CTG CGC ACC AAT CAA CAA-3'	[294]
E. coli (212)	F: 5'-CCA GGC AAA GAG TTT ATG TTG-3' R: 5'-GCT ATT TCC TGC CGA TAA GAG A-3'	[295]
E. albertii (393)	F: 5'-GTA AAT AAT GCT GGT CAG ACG TTA-3' R: 5'-AGT GTA GAG TAT ATT GGC AAC TTC -3'	[295]
E. fergusonii (575)	F: 5'-AGA TTC ACG TAA GCT GTT ACC TT-3' R: 5'-CGT CTG ATG AAA GAT TTG GGA AG-3'	[295]
16S rRNA *B. wadsworthia* (239)	F: 5'-AAG TCC TTC GGG GCG AGT AA-3' R: 5'-ATC CTC TCA GAC CGG CTAC-3'	[296]

2.4.2 Visualization of the RAPD fingerprint

Random amplification of polymorphic DNA (RAPD) uses short PCR primers (8 - 15 nucleotides), annealing to random regions of the microorganism's genome. This results in strain-specific heterogeneous DNA products and generates complex band patterns [297]. Characterization of bacterial isolates at strain level was assessed with RAPD using the *M13*-core primer. PCR was performed as described in 2.4.1.

2.4.3 Identification of bacteria based on *16S rRNA* and *dsrAB* gene sequencing

For identification of bacterial isolates, DNA was extracted and PCR performed as described in 2.4.1 targeting the sequences of the *16S rRNA* gene and *dsr* gene subunits (*dsrAB*).

PCR products were purified with the Wizard SV gel and PCR Clean-Up System as described in instructions, but DNA was eluted with 30 µl water. PCR products were sequenced by Eurofins genomics (Ebersberg, Germany). Obtained *16S rRNA* gene amplicons were assembled with SnapGene 5.1.4.1 (GSL Biotech, San Diego, CA, U.S.A.) and subsequently aligned to sequences of the *16S rRNA* sequences database using the Basic Local Alignment Search Tool algorithm of Nucleotides (BLASTn) [298]. For the identification of the bacteria, the first ten results of BLASTn were included.

2.4.4 Quantification of bacteria with real-time PCR

In single bacterial incubation and co-culturing experiments investigating the conversion of sulfonates, cell numbers of *B. wadsworthia* were determined with qPCR. For that purpose, the DNA of *B. wadsworthia* from the incubation experiments was extracted with the RTP

Bacteria DNA mini Kit (Stratec), as described in 2.4.1. From cells collected during co-culturing, DNA was extracted with the RTP pathogen Kit (Stratec) using a modified protocol. Briefly, bacterial cell pellets were obtained through centrifugation (14,000 x *g*, 5 min, 4 °C) and resuspended in 400 µl resuspension buffer. After agitating the sample twice, the protocol of the manual was followed to the DNA binding step by centrifugation at 13,400 x *g* for 8 min at RT. The filter was washed (first wash: 14,000 x *g*, RT, 5 min; second wash: 14,000 x *g*, RT, 5 min) and the DNA was eluted in 50 µl elution buffer.

Cell numbers were determined using primers specifically targeting the *16S rRNA* gene sequence of *B. wadsworthia* (F: 5'-AAG TCC TTC GGG GCG AGT AA-3'; R: 5'-ATC CTC TCA GAC CGG CTAC-3', [292]). For the qPCR reaction, 0.33 µM of each primer, 0.475 µl DEPC (diethylpyrocarbonate)-treated water (Merck), 2.5 µl QuantiNova SYBR green master mix, and 0.025 µl ROX reference dye (Qiagen, Hilden, Germany) were mixed with 100 ng/µl extracted DNA. For qPCR run and analysis, the Viia™ 7 -Real-Time PCR System (Applied Biosystems, Waltham, Massachusetts, USA) with the QuantStudio™ Real-Time PCR Software v1.3 (Thermo Fisher Scientific) was used. The qPCR program was performed as follows: heating at 50 °C for 2 min, polymerase activation at 94 °C for 4 min, 35 cycles of denaturation at 94 °C for 15 s and annealing and elongation at 53.5 °C for 30 s, followed by 95 °C for 15 s and a melting curve analysis from 60 to 95 °C. Bacterial cells were determined using standards of extracted DNA ranging from 10^3 to 10^8 cells. The volume of a bacterial culture containing 10^8 cells was determined based on the cell concentration determined with a Thoma cell counting chamber (2.2.11) and pelleted by centrifugation (14,000 x *g*, 5 min, 4 °C). The DNA was extracted from cell pellets (2.4.1) and the calibration curves were prepared using serial dilutions. Specificity of amplicons was analyzed by melting curve comparison.

2.5 Animal study

2.5.1 Housing conditions

The animal experiment was approved by the Animal Welfare Committee of the State of Brandenburg (approval no. 2347-10-2016 and G-01-16-GAMI). Conventional male, 10 – 12 - weeks old C57BL/6J mice bred under specific pathogen-free (SPF) conditions in the animal facility of the DIfE were used. Mice were kept in a 12 h light-dark cycle at 22 ± 2 °C and 55 ± 5% air humidity in individually ventilated cages.

2.5.2 Experimental design

In order to acclimatize to the housing conditions, 8 - 10-week old mice were single-housed two weeks prior to study start (points in time: -14 to 0 d). At the same time, diet was switched from a standard chow diet (complete diet for rats and mice V1534, 10 mM pellets, Ssniff, Soest, Germany) to a semisynthetic diet (control diet, CD) (Table 2), which was irradiated (50 kGy, Synergy Health Radeberg, Radeberg, Germany). At the start of the experiment (point in time: day 0), mice were randomly allocated into two groups (n = 18 per group): the intervention group was fed CD supplemented with 20% Spirulina powder (Spirulina diet, SD) (Table 2), whereas the control group continued to receive CD. The diets were isocaloric and administered *ad libitum* for three weeks. Drinking water was autoclaved twice and applied *ad libitum*. Twice a week, water and dietary intake were measured, body

weight was determined and fecal samples were collected. After three weeks of intervention, mice were killed subsequently to exposure to isoflurane. Blood was collected from the portal vein into sterile microvettes (Sarstedt) rinsed with dipeptidyl peptidase-IV inhibitor/EDTA (1:1), and from heart blood into sterile EDTA-coated monovettes (Sarstedt). The blood was centrifuged (2,000 x *g*, 10 min, 4 °C), the plasma snap frozen in liquid nitrogen and stored at -80 °C until further analysis. Blood-glucose concentrations were determined in thawed samples with a blood glucose meter (Contour XT device, Bayer, Leverkusen, Germany) using Contour NEXT test sensors (Bayer) according to the manufacturer's instructions. Liver, mesenteric lymph nodes, kidney, heart, spleen, gallbladder, epididymal white adipose tissue (eWAT), mesenteric white adipose tissue (mWAT), subcutaneous white adipose tissue (sWAT), perirenal white adipose tissue (pWAT), and the quadriceps femoris muscle were collected, weighted, frozen in liquid nitrogen and stored at -80 °C. The apex of the hepatic left lateral lobe and a part of the mWAT were fixed in 4% paraformaldehyde (Roth) for 20 - 24 h (liver) or 16 h (mWAT) at RT and embedded in paraffin for histological analysis (2.5.9). Small intestinal, colonic and cecal contents were collected and stored at -20 °C. Mucosa was scraped from the small intestine and from the colon. Small intestinal samples were separated in duodenal (7 cm distal from the pyloric sphincter), jejunal (residual part) and ileal (7 cm proximal from the ileocecal valve) sections. The mucosa was snap-frozen in liquid nitrogen and stored at -80 °C. The surface of stomach and caecum as well as the lengths of small intestine and colon were determined.

For the analysis of cell wall integrity of Spirulina before and after digestion, samples of freeze-dried Spirulina powder, SD or feces of SD-fed mice collected at day 20 were homogenized with water by vortexing. The suspensions were microscopically examined at a 1000 x magnification (Eclipse E600, Nikon, Düsseldorf, Germany) and microscopic pictures were taken using Lucia G software version 4.51 (Laboratory Imaging, Praha, Czech Republic).

Table 2: Composition of diets used for the animal experiment.

Ingredient (Supplier)	**Control diet (CD) (g/kg)**	**Spirulina diet (SD) (g/kg)**
Casein (Bayerische Milchindustrie, Landshut, Germany)	200.0	71.2
Wheat starch (Kröner, Ibbenbüren, Germany)	564.0	527.0
Sunflower oil (Gut & Günstig, Edeka, Hamburg, Germany)	35.0	24.7
Palm kernel fat (Palmin, Peter Kölln, Elmshorn, Germany)	9.0	6.4
Linseed oil (Kunella, Cottbus, Germany)	6.0	4.2
Cellulose (J. Rettenmeier und Söhne, Rosenberg, Germany)	50.0	43.0
Vitamin mixture (C1000, Altromin, Lage, Germany)	20.0	20.0
Mineral mixture (C1000, Altromin)	60.0	48.0
Choline bitartrate (Altromin)	2.5	2.5
L-Cysteine (Altromin)	3.0	3.0
Maltodextrin (Altromin)	50.0	50.0
Spirulina Premium + powder (Institute for Food and Environmental Research, ILU, Nuthetal, Germany)	0	200.0

2.5.3 Preparation of gut contents for sulfonate quantification

Murine gut contents and feces were homogenized in 50% acetonitrile (1:20, w/v) by shaking (Uniprep Gyrator-24, UniEquip, Martinsried, Germany) and centrifuged (14,000 x *g*, 5 min, 4 °C). The supernatant was diluted with 50% acetonitrile (1:10,000), transferred to HPLC vials and frozen at -80 °C. Vials were send on dry ice to the Helmholtz-Zentrum Umweltforschung (UFZ, Leipzig) for sulfonate quantification with LC-MS/MS analysis (2.3.1).

2.5.4 Analysis of microbiota composition in cecal contents and feces based on *16S rRNA* gene sequencing

A total of 1 - 3 mouse droppings collected at day 0 or 16, or a maximum of 250 µl cecal content was transferred to DNAse-free tubes containing 600 µl stool DNA stabilizer (Stratec). Samples were frozen at -20 °C and send on dry ice for DNA extraction and *16S rRNA* gene sequencing to the ZIEL Core Facility Microbiome/NGS at the Technical University of Munich, Germany. The V3 and V4 regions of the *16S rRNA* gene were sequenced using the Illumina technology as previously described [299]. Sequences were analyzed using the Integrated Microbial Next Generation Sequencing (IMNGS) platform [300] and the Rhea software [301]. Alpha-diversity (α-diversity) was estimated using the Shannon-Wiener index, the Simpson index, the number of observed species (OTUs), the richness and the evenness of each sample. It refers to the species richness and evenness within one habitat, which is in this case one murine sample [302, 303]. The Beta-diversity (ß-diversity) was visualized with Non-metric Multidimensional Scaling (NMDS) plots and with a Generalized UniFrac approach. [304, 305]. It describes the spatial differences of microbiota composition among the animals [306].

2.5.5 Enumeration of sulfonate-converting bacteria in cecal contents and feces

DNA of murine feces and of cecal contents was extracted with the PSP Spin Stool DNA Kit (Invitek Molecular, Berlin, Germany) as described by the manufacturer. Cells were quantified with qPCR as described in 2.4.4 using standards of extracted DNA based on feces of germfree mice spiked with cell pellets containing 10^3 - 10^8 cells of *B. wadsworthia* or 10^5 - 10^9 cells of *E. coli*. Therefore, aliquots of bacterial cultures containing 10^8 *B. wadsworthia* or 10^9 *E. coli* cells were centrifuged (14,000 x *g*, 4 °C, 5 min) and pellets were spiked with 50 mg feces from germfree mice. Calibration curves were then prepared by serial dilutions.

2.5.6 Quantification of gene copy numbers in feces and cecal contents

DNA from murine feces and cecal contents was extracted (2.5.5). Gene-expression levels of *dsrA* and *yihS* were quantified with qPCR as described in 2.4.4 using *dsrA* primer (expected amplicon 270 bp; F: 5'-CCA ACA TGC ACG GYT CCA-3'; R: 5'-CGT CGA ACT TGA ACT TGA ACT TGT AGG-3'[9, 292], Eurofins Genomics) and *yihS* primer (expected amplicon 332 bp; F: 5'-ACG CGG TGG AAG CTT TCT TGA T-3'; R: 5'-CAC GGT GGC GTT AAA CAG ACC TT-3', [249], Eurofins Genomics).

2.5.7 Macronutrient analysis (Weender analysis) of diets

Aliquots of 250 g CD and SD were quantified for their water content, crude ash, raw fibers, raw protein, raw fat, and N-free substances at the Agrolab LUFA (Kiel, Germany). The water content was determined by weighing samples before and after heating them at 103 °C for 4 h. To examine the inorganic compounds of the diet (crude ash consisting of trace elements), the samples were afterwards heated at 550 °C. At this high temperature all organic compounds are burned, while inorganic compounds remain. Raw protein, lipids and fibers and N-free substances were obtained from the organic fraction.

2.5.8 Analysis of diet digestibility

Fecal samples collected at day -5, 2, 6, and 13 were pooled per group for each point in time and freeze dried (Alpha 1-4, Christ, Osterode, Germany). The amount of consumed diet and excreted feces per day was calculated. The energy content of the diet and feces was determined with bomb calorimetry (IKA-Kalorimetriesystem C5003, IKA-Werke, Staufen, Germany). Diet digestibility and digestible energy were calculated using the following equations:

$$\text{Diet digestibility (\%)} = [(\text{energy intake} - \text{energy loss}) / \text{energy intake}] \times 100 \quad \text{(Eq. 4)}$$

$$\text{Digestible energy (kJ/d)} = \text{energy intake} \times \text{diet digestibility (\%)} \quad \text{(Eq. 5)}$$

2.5.9 Histological analysis of hepatic and mesenteric white adipose tissues

Fixed and embedded left lateral hepatic lobe and the mWAT (2.5.2) were stained with hematoxylin and eosin (HE). Afterwards, tissue sections were examined microscopically (Axioplan 2, Carl Zeiss, Jena, Germany) at a 100 x and 400 x magnification. The size and number of adipocytes of mWAT were assessed using the software ImageJ 1.52g (Wayne Rasband, National Institutes of Health, Bethesda, Maryland, USA) and the Adiposoft plugin (version 1.16, CIMA University of Navarre, Pamplona, Navarra, Spain). The mean area and number of adipocytes and their ratio (mean area to number) were determined for each section.

2.5.10 Analysis of hepatic triglyceride contents

Grounded liver tissue (40 mg) was homogenized in 800 µl HB buffer (Appendix, Table A1) with ten zirconium beads using a tissue lyser (LT, Qiagen, 50 Hz, 10 min, 24 °C). After centrifugation (23,100 x *g*, 30 min, 4 °C), the supernatant was transferred to cooled reaction tubes. The tubes were shaken at 600 rpm for 5 min at 70 °C (Thermomixer 5436, Eppendorf, Hamburg, Germany) and afterwards kept on ice for 5 min. Samples were centrifuged at 23,100 x *g* for 30 min at 4 °C and the obtained supernatant containing the tissue extract was stored at -20 °C until further analysis.

Triglycerides (TG) in the extracts were quantified by a cascade of enzymatic reactions using the TG and the free-glycerol (G) reagents (Sigma-Aldrich). The lipase of the TG reagent hydrolyzes TG to free fatty acids (FFA) and G (Eq. 6). The free-G reagent enables the quantification of glycerol based on a colorimetric reaction as follows. Glycerol kinase catalyzes the phosphorylation of G to glycerol-1-phosphate using ATP (Eq. 7). Glycerol-1-phosphate is oxidized to DHAP and H_2O_2 by glycerol phosphate oxidase (Eq. 8). H_2O_2, 4-aminoantipyrine (4-AAP) and sodium *N*-ethyl-*N*-(3-sulfopropyl) *m*-aniside (ESPA) are converted by a

peroxidase to a quinoneimine dye (Eq. 9). Absorbance of the formed quinoneimine dye is measured spectrophotometrically at 540 nm. The increase in absorbance at 540 nm is directly proportional to the G concentration of the sample. G-standards were prepared with concentrations ranging from 0.075 - 2.5 mg/ml triolein equivalents (stock 2.5 mg/ml, Sigma-Aldrich). TG concentrations (mM) were determined by dividing calculated G concentrations through the molar mass of triolein.

$$\mathrm{TG} + 3\,\mathrm{H_2O} \xrightarrow{\text{Lipase}} \mathrm{G} + 3\,\mathrm{FFA} \qquad \text{(Eq. 6)}$$

$$\mathrm{G} + \mathrm{ATP} \xrightarrow{\text{Glycerol kinase}} \mathrm{Glycerol-1-phosphate} + \mathrm{ADP} \qquad \text{(Eq. 7)}$$

$$\mathrm{Glycerol-1-phophate} + \mathrm{O_2} \xrightarrow{\text{Glycerol phosphate oxidase}} \mathrm{Dihydroxyacteone\ phosphate} + \mathrm{H_2O_2} \qquad \text{(Eq. 8)}$$

$$\mathrm{H_2O_2} + 4-\mathrm{AAP} + \mathrm{ESPA} \xrightarrow{\text{Peroxidase}} \mathrm{Quinoneimine\ dye} + \mathrm{H_2O} \qquad \text{(Eq. 9)}$$

Tissue extracts, standard solutions and blanks (HB buffer) (5 µl each) were transferred to 96-well plates and 100 µl diluted glycerol reagent (125 mU glycerol kinase, 250 mU glycerol phosphate oxidase, 75 nmol ATP) was added, followed by an incubation for 5 min at 37 °C while shaking (Microplate Genie™, Scientific Industries). Subsequently, the initial absorbance (A1) at 540 nm was determined. After adding 25 µl diluted TG reagent (6250 mU lipase) to each well, the plate was shortly vortexed and incubated at 37 °C for 15 min while shaking. Afterwards, the absorbance (A2) was measured. TG concentrations were calculated according to Eq. 10, with "m" as slope of the calibration curve.

$$[\mathrm{TG}] = \frac{(\mathrm{A2_{sample}} - \mathrm{A1_{sample}}) - (\mathrm{A2_{blank}} - \mathrm{A1_{blank}})}{\mathrm{m}} \qquad \text{(Eq. 10)}$$

2.5.11 Analysis of hepatic glycogen content

Hepatic extracts were obtained as described above (2.5.10). Hepatic tissue (35 mg) was extracted with 800 µl 0.1 M NaOH. Glycogen concentrations were determined with the Starch Kit (R-Biopharm, Pfungstadt, Germany) based on enzymatic glycogen degradation steps. First, glycogen is hydrolyzed to D-glucose by glycogen amyloglucosidase (AGS, Eq. 11), followed by phosphorylation of D-glucose to D-glucose-6-phosphate (G-6-P) by hexokinase (Eq. 12). Subsequently, G-6-P is oxidized by dehydrogenase to D-gluconate-6-phosphate with the formation of reduced nicotinamide adenine dinucleotide phosphate (NADPH) from nicotinamide adenine dinucleotide phosphate (NADP) (Eq. 13). NADPH correlates with the initial glycogen concentration and is measured at 340 nm. Glycogen from bovine liver (85%, Sigma-Aldrich) was used for the preparation of standards in 0.1 M NaOH ranging from 0.01 - 3 µg/µl.

$$\mathrm{Glycogen} \xrightarrow{\text{AGS}} \mathrm{D-glucose} \qquad \text{(Eq. 11)}$$

$$\mathrm{D-glucose} + \mathrm{ATP} \xrightarrow{\text{Hexokinase}} \mathrm{G-6-P} + \mathrm{ADP} \qquad \text{(Eq. 12)}$$

$$\mathrm{G-6-P} + \mathrm{NADP^+} \xrightarrow{\text{G-6-P-DH}} \mathrm{D-gluconate-6-phophate} + \mathrm{NADPH} + \mathrm{H^+} \qquad \text{(Eq. 13)}$$

For assays, 50 µl tissue extract or glycogen standard, 1 µl 100% acetic acid, and 100 µl solution 1 (1400 mU AGS) were combined in tubes, and incubated at 60 °C for 15 min while shaking. After incubation, samples were centrifuged at 23,100 x *g* for 10 min at 20 °C and 30 µl supernatant was transferred in triplicates (samples) or duplicates (standards, blank control) to 96-well plates. A volume of 100 µl each of ultrapure water and solution 2 (373 nmol $NADP^+$, 1387 nmol ATP) was added and the plate was briefly centrifuged (1000 rpm, 1 min, 24 °C) and incubated at RT for 3 min while shaking. Afterwards, the initial absorbance (A1) was measured at 340 nm. Next, 12 µl aqueously diluted (1:6) solution 3 (571 mU hexokinase, 286 mU glucose-6-phosphate dehydrogenase) was added to each well, and the plate was incubated while shaking for 15 min at RT and shortly centrifuged (1000 rpm, 1 min, 24 °C). The final absorbance (A2) was measured at 340 nm. In order to determine the concentration of free glucose present in the sample, the procedure was repeated by replacing solution 1 with ultrapure water. Glycogen concentration was calculated by subtraction of A1 from A2 (ΔA) of measurements with and without solution 1, using Eq. 14, with "m" as slope of the calibration curve.

$$[\text{Glycogen}] = \frac{[(\Delta A_{AGS+}(\text{sample}) - \Delta A_{AGS-}(\text{sample})) - (\Delta A_{AGS+}(\text{blank}) - \Delta A_{AGS-}(\text{blank}))]}{m} \quad \text{(Eq. 14)}$$

2.5.12 Analysis of hepatic protein content

The protein content of the liver was determined with the DC Protein Kit (Bio-Rad) based on the Lowry principle [307]. A volume of 15 µl diluted tissue extracts (1:4, in ultrapure water, v/v), standards and blank samples was transferred to a 96-well plate. A volume of 2.8 ml reagent A (alkaline copper tartrate solution) was gently mixed with 56 µl reagent S and 25 µl of the mixture was added to each well. The plate was shaken and subsequently 200 µl reagent B (diluted folin reagent) was added and shaken again. After an incubation period of 15 min at RT, the absorbance was measured at 750 nm. Protein concentrations were determined based on a calibration curve prepared with bovine serum albumin in HB buffer ranging from 0.1 - 1 µg/µl.

2.5.13 RNA and protein extraction from liver and intestinal mucosa

Extraction of total RNA

Murine hepatic and mucosal RNA were isolated using the peqGOLD TriFast reagent (Peqlab, Erlangen, Germany) and the guanidinium thiocyanate-phenol-chloroform method [308]. In detail, 20 mg grounded liver or intestinal mucosa was combined with 1 ml peqGOLD TriFast solution and ten sterile ceramic beads (2.4 - 2.6 mM, Analytik Jena, Jena, Germany). The tissue was homogenized and lyzed twice for 1.5 min at 50 Hz (tissue lyzer, LT, Qiagen) and subsequently stored on ice. Samples were centrifuged (18,400 x *g*, 10 s, 4 °C), and the supernatants were transferred to new tubes. For RNA extraction, the beads were washed with 0.1 ml peqGOLD TriFast, centrifuged, and supernatants were combined. Samples were stored at RT for 5 min and afterwards shortly centrifuged again. The supernatant was combined with 0.2 ml chloroform, vortexed for 15 s and afterwards vortexed every 2.5 min while incubating at RT for 10 min. Samples were again centrifuged (18,400 x *g*, 20 min, 4 °C) and the aqueous phase was transferred into RNase-free

tubes containing 500 µl isopropanol, which were six times inverted. The remaining phenol phase was stored at -20 °C for subsequent protein isolation.

The isopropanol mixture was stored for 10 min on ice and centrifuged at 18,400 x *g* for 20 min at 4 °C. The supernatant was discarded and the pellet containing the RNA was washed with 1 ml of 75% ethanol and afterwards with 1 ml of 100% ethanol. The upper ethanol phase was removed, and the pellet was air-dried for 15 min and afterwards resuspended in DEPC-treated water (100 µl for mucosa, 150 µl for liver). Samples were incubated for 5 min at 60 °C at 900 rpm in a thermocycler to increase solubility. After determination of RNA concentrations (EON Microplate Spectrophotometer and Gen5 software, BioTeK, Winooski, VT, USA), samples were stored at -80 °C until further analysis.

Elimination of DNA

Potential genomic DNA contamination was eliminated from RNA samples by treatment with DNase I (Thermo Fisher Scientific). The reaction mixture (30 µl) contained 8 µg RNA, 2 µl DNase I (1 U/µl), 0.75 µl RiboLock RNase-Inhibitor (40 U/µl), 0.25 µl DEPC-treated water and 3 µl 10 x reaction buffer with Mg_2Cl. Mixtures were incubated for 30 min at 37 °C in a thermocycler and afterwards 1 µl 50 mM ethylenediaminetetraacetic acid (EDTA, Thermo Fisher Scientific) was added to each sample to stop the reaction followed by another incubation step for 10 min at 65 °C. RNA samples were stored at -80 °C until further use.

RNA quality controls

The absence of genomic DNA from the extracted RNA was confirmed with qPCR using a Taqman probe (5'-6-FAM-AGG CGC GCA AAT TAC CCA CTC CC-TAMRA-3', Eurofins Genomics). Each reaction mixture contained 5 ng RNA, 0.5 µl *18S rRNA* forward and reverse primer (both 3 µM, 18S-fwd, 5'-ACC ACA TCC AAG GAA GGC AG-3'; 18S-rev, 5'-TTT TCG TCA CTA CCT CCC C-3'), 0.5 µl *18S rRNA* probe (2 µM) and 2.5 µl Taqman gene expression master mix (Life Technologies). The qPCR was run using ViiA™ 7 Real-Time PCR System as follows: incubation of uracil-*N*-glycosylase incubation at 50 °C for 2 min, activation of DNA polymerase at 95 °C for 10 min, and 40 cycles of denaturation (95 °C, 15 s) and annealing/elongation (60 °C, 1 min). Negative controls (n = 6) containing DEPC-treated water instead of RNA were included. Their mean cycle threshold (C_t) value (number of cycles at which the amplification signal reaches above the background noise) was determined. The mean C_t value subtracted by six was considered as the threshold for all RNA samples. C_t values below the determined number indicated the presence of DNA remainders and DNA degradation was repeated.

RNA integrity was controlled with horizontal gel electrophoresis. A 1% gel was prepared using 3 g agarose (Biozym, Hessisch Oldendorf, Germany), 30 ml 10 x 3-morpholino-propane-sulfonic acid buffer (MOPS buffer, Appendix, Table A1), 9 ml 37% formaldehyde, and 270 ml autoclaved water. Purified RNA (0.5 µg) was mixed with 2 µl 2 x RNA loading dye containing ethidium bromide (Thermo Scientific), followed by RNA denaturation at 70 °C for 10 min using a thermocycler. Samples were subsequently stored on ice for 5 min, and loaded on the gel. Electrophoresis was run for 20 min at 120 V in MOPS buffer. RNA bands were visualized with ultraviolet trans-illumination (UVIprochemie, Biometra, Göttingen, Germany).

Reverse Transcription of RNA into cDNA

Complementary DNA (cDNA) synthesis was conducted using the RevertAid H Minus first strand cDNA synthesis Kit (Thermo Fisher Scientific). First, 1 µg purified RNA, diluted to a total volume of 10 µl with DEPC-treated water, was combined with 1 µl random hexamer primer solution and incubated in a thermocycler (70 °C, 5 min) for RNA denaturation. Samples were afterwards stored on ice for 3 min, shortly centrifuged. Afterwards, a mixture of 4 µl 5 x reaction buffer, 1 µl RiboLock™ RNase inhibitor (20 U/µl), 2 µl deoxynucleoside triphosphates (dNTPs, 10 mM) and 1 µl DEPC-water was added for each reaction, followed by a short centrifugation (10,000 rpm, 10, RT). Samples were incubated for another 5 min at RT and subsequently 1 µl reverse transcriptase (200 U) was added, followed by incubation steps of 10 min at 25 °C, for 60 min at 42 °C and for 10 min at 60 °C. Finally, the samples were diluted 1:9 (v/v) with DEPC-water and stored at - 80 °C until qPCR analysis.

Gene-expression analyses in murine tissue with quantitative real-time PCR

The qPCR was carried out using a Viia 7- Realtime PCR System as described in 2.4.4, with individual adjustments regarding master mix composition, annealing and elongation temperature. In detail, SYBR™ green fluorescence dye was used, which intercalates double-stranded DNA followed by a fluorescent emission when DNA is amplified. Each qPCR reaction was prepared in a total volume of 5 µl with 2.5 µl Power SYBR™ Green PCR Master Mix (Applied Biosystems), 0.3 µM forward and reverse primer (Table 3), 0.5 µl DEPC-treated water and 1 µl cDNA. DEPC-treated water instead of cDNA was used as negative control. During processing, samples and master mix were stored in the dark and on ice. The following PCR program was used: incubation at 50 °C for 2 min, polymerase activation at 95 °C for 10 min, 40 cycles of denaturation at 95 °C for 15 s, annealing and elongation at 60 °C for 1 min, and a melting curve analysis from 60 to 95 °C. C_T values were determined using the Viia 7 Software version 1.3 as described above (2.4.4) and relative gene expression was determined with the threshold cycle ($\Delta\Delta C_T$) method [309]. *Gapdh* was used as reference gene for evaluation of changes in gene expression (Table 3).

Table 3: Primer sequences used for gene-expression analyses in mouse tissues. Primers were synthesized by Eurofins Genomics.

Target (amplicon size in bp)	Accession No.	Sequence (5' to 3') forward primer	Sequence (5' to 3') reverse primer
Tumor necrosis factor alpha (*Tnf-α*)	NM_013693.3	GAC CCT CAC ACT CAG ATC ATC TTC T	CCA CTT GGT GGT TTG CTA CGA
Interleukin-6 (*Il-6*)	NM_031168.2	TAG TCC TTC CTA CCC CAA TTT CC	TTG GTC CTT AGC CAC TCC TTC
Glucose transporter member 2 (*Glut2*)	NM_031197.2	CTG TTC CTA ACC GGG ATG AT	ATC CAG GCG AAT TTA TCC AG
Glycogen synthase (*Gys2*)	NM_145572.2	GGA CTG GGC TGA TCC TTT CTC	GCA GTG TGG CAT GGG TTG TA
Fatty acid translocase (*Cd36*)	NM_007643.4	CCA AGC TAT TGC GAC ATG AT	ACA GCG TAG ATA GAC CTG CAA A
Fatty acid-binding protein 1 (*Fabp1*)	NM_017399.5	TCA CCA TCA CCT ATG GAC CCA	GCT TGA CGA CTG CCT TGA CTT T
Fatty acid-binding protein 2 (*Fabp2*)	NM_007980.3	GTT GTG TTT GAG CTC GGT GT	AGC AAT CAG CTC CTT TCC AT
Very long-chain acyl-CoA synthetase (*Fatp2, Slc27a2*)	NM_011978.2	CCA GTT ACG CGA GGC CTC GGT TCC TGA G	GTC TAT CGA GTT TCT TTC TGG
Long-chain fatty acid transport protein 4 (*Fatp4, Slc27a4*)	NM_011989.4	TTC ATC AAG ACG GTC AGG AG	ACC ATT GAA GCA AAC AGC AG
Fatty acid synthase (*Fasn*)	NM_007988.3	TTG ATG ATT CAG GGA GTG GA	TTA CAC CTT GCT CCT TGC TG
Elongation of very long chain fatty acids protein 5 (*Elovl5*)	NM_134255.3	GGT GGC TGT TCT TCC AGA TT	CCC TTC AGG TGG TCT TTC C
Elongation of very long chain fatty acids protein 6 (*Elovl6*)	NM_130450.2	TGC AGG AAA ACT GGA AGA AGT CT	AGC GGC TTC CGA AGT TCA A
Acyl-coenzyme A desaturase 1 (*Scd1*)	NM_009127.4	TTC TTC TCT CAC GTG GGT TG	CGG GCT TGT AGT ACC TCC TC
Diacylglycerol O-acyltransferase 2 (*Dgat2*)	NM_026384.3	TGC TAG GAG TGG CCT GCA GTG T	CAC TGC GAT CTC CTG CCA CCT T
Patatin-like phospholipase domain-containing protein (*Atgl, Pnpla2*)	NM_025802.3	AAC ACC AGC ATC CAG TTC AA	GGT TCA GTA GGC CAT TCC TC
Hormone-sensitive lipase (*Hsl, Lipe*)	NM_010719.5	GCT TGG TTC AAC TGG AGA GC	TGC CTC TGT CCC TGA ATA GG
3-Hydroxy-3-methylglutaryl-coenzyme A reductase (*Hmgcr*)	NM_008255.2	GGC CAA CTA CTT TGT GTT CAT GAC	CCT CAC GGC TTT CAC GAG AA
ATP-citrate synthase (*Acly*)	NM_134037.3	TAT GCC AAG ACC ATC CTC TCA CT	TCT CAC AAT GCC CTT GAA GGT
Carnitine O-palmitoyltransferase 1 (*Cpt1a*)	NM_013495.2	CCA AAC CCA CCA GGC TAC A	GCA CTG CTT AGG GAT GTC TCT ATG
Peroxisome proliferator-activated receptor alpha (*Pparα*)	NM_001113418.1	TGG CAA AGT CTT AGT GCC AGA	TCA CTA GGT CAC ACA GCC TCT
Adiponectin (*Adipoq*)	NM_009605.5	GCA GAG ATG GCA CTC CTG GA	CCC TTC AGC TCC TGT TCC CAT
Adiponectin receptor protein 1 (*Adipor1*)	NM_028320.4	ACG TTG GAG AGT CAT CCC GTA T	CTC TGT GTG GAT GCG GAA GAT
Adiponectin receptor protein 2 (*Adipor2*)	NM_197985.4	TCC CAG GAA GAT GAA GGG TTT AT	TTC CAT TCG TTC GAT AGC ATG A
Perilipin 2 (*Plin2*)	NM_007408.3	GTG TGT GAG ATG GCC GAG AA	AAC AAT CTC GGA CGT TGG CT
Perilipin 5 (*Plin5*)	NM_025874.3	TGT CCA GTG CTT ACA ACT CGG	CAG GGC ACA GGT AGT CAC AC
Glyceraldehyde-3-phosphate dehydrogenase (*Gapdh*)	NM_008084.3	ACC ACC CAC CCC AGC AA	GAA ATT GTG AGG GAG ATG CTC AGT

2.6 Statistical analysis

For statistical analysis and graphical presentation of data, the software Graph Pad Prism 8.2.1 (GraphPad Software, La Jolla, CA, USA) was used. Outliers were detected using the ROUT test with an average False Discovery Rate of less than 1% (Q = 1%) and excluded [310]. Normality of the distribution of data was tested using the Kolmogorov-Smirnov test. In case of normal distribution, the hypothesis was tested based on the difference between sample means with Student's *t*-test and presented as mean ± standard error of the mean (SEM). Normally distributed data were analyzed with the Mann-Whitney *U* test and are shown as median ± 95% CI. For comparison of data with more than two sample means, ordinary one-way ANOVA was used with normal distribution (post-hoc test: Bonferroni's multiple comparisons test). Non-normally distributed data were analyzed with a Kruskal-Wallis test (post-hoc test: Dunn's multiple comparison test). Data sets were assessed as significantly different at $*P < 0.05$, $**P < 0.01$, $***P < 0.001$ and **** $P < 0.0001$. Phylogenetic β-diversity analysis of *16S rRNA* gene sequencing data was performed with generalized UniFrac distances using *P* values from the PERMANOVA test. The Bonferroni-Hochberg test was used to correct for multiple testing.

3 RESULTS

3.1 *In vitro* testing of human fecal slurries for their ability to convert sulfonates and

To elucidate the role of human gut bacteria in the intestinal sulfonate catabolism, human fecal slurries were first tested for their capability to convert dietary and endogenous sulfonates under anoxic conditions. Sulfonate-converting strains were then isolated from fecal slurries and identified after repeated enrichment and plating. Selected strains were, individually or in co-cultures, tested for their ability to convert sulfonates and to produce H_2S as end product of sulfonate degradation.

3.1.1 Human fecal microbiota degraded taurine, isethionate, SQ and DHPS

Taurine, isethionate, SQ, and DHPS conversion by bacteria present in the human gut such as *E. coli* has previously been described [8, 154, 249, 251, 311]. To investigate whether sulfonate conversion is a common feature of the human gut microbiota, fecal slurries from ten healthy donors (Table 4, all omnivores) were individually incubated under anoxic conditions with one of the various sulfonates under a gas phase of N_2/CO_2 (80/20, v/v, %). Sodium DL-lactate and formate (40 mM) were used as electron donors.

Table 4: Characteristics of human fecal donors.

Donor-Identity	Sex	Age (years)
D0	Female	27
D1	Female	39
D2	Female	57
D3	Female	27
D4	Female	31
D5	Female	30
D6	Male	28
D7	Female	50
D8	Female	35
D9	Female	28
D10	Male	29

The time course of taurine, isethionate, SQ and DHPS utilization by human fecal slurries under anoxic conditions was monitored. Individual donors were chosen depending on the ability of their fecal microbiota to convert these sulfonates to H_2S (Fig. 8). Fecal microbiota of different donors utilized taurine, isethionate, SQ, and DHPS within 72 h (Tau + F, Ise + F, SQ + F, DHPS + F) (Fig. 5). No conversion was observed in the control incubations (Tau, Ise, SQ, DHPS). Degradation of all sulfonates occurred from 24 h to 72 h of incubation, but there were differences in the kinetics. After 24 h of incubation, SQ was almost completely degraded (95%), while only 58% of taurine, 19% of isethionate, and 40% of DHPS were degraded (Fig. 5). This was in line with the results after 72 h, where partial degradation of taurine, isethionate and DHPS, but complete depletion of SQ was observed, indicating a higher degradation rate of SQ compared to taurine, isethionate, or DHPS. However, a direct

comparison has to be drawn with caution because different fecal donors were used. The observed slight increase in taurine and SQ concentrations at 48 h and 72 h may be due to increased bacterial cellular lysis leading to the release of the corresponding sulfonate. These results demonstrate that human fecal microbiota is capable of utilizing various sulfonates but that conversion rates differ.

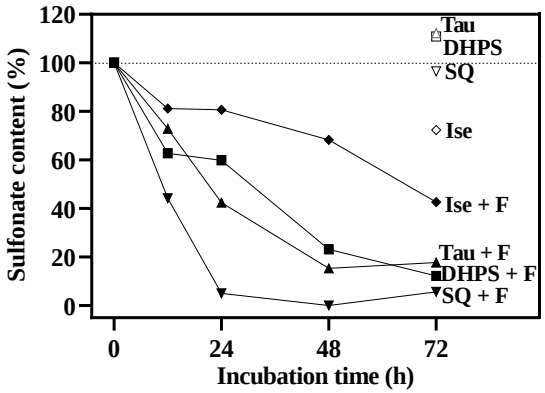

Figure 5: Degradation of taurine (Tau, 20 mM), isethionate (Ise, 20 mM), sulfoquinovose (SQ, 4 mM) and 2,3-dihydroxypropane-1-sulfonate (DHPS, 4 mM) during 72 h of anoxic incubation with human fecal slurries (F, 1%). Fecal microbiota from human donors capable of converting sulfonates to H_2S were selected (Fig. 8). The sulfonate content was quantified with LC-MS/MS analysis. The sulfonate content is given as percentage with the initial sulfonate concentration set to 100%. Fecal donors (D) are indicated by different numbers: Tau + F (D5), Ise + F (D4), SQ + F (D1), DHPS + F (D5). Data presented as mean (n = 2 - 3).

The residual concentrations of taurine, isethionate, DHPS or SQ after an incubation time of 72 h with fecal slurries from ten donors were compared. While SQ (9/10 individuals) and DHPS (6/10 individuals) in most cases were completely degraded, taurine and isethionate most often (7/10 or 8/10 individuals) were only partially degraded (Fig. 6, Table 5). This indicates inter-individual differences in sulfonate degradation by human fecal microbiota. Mean values representing all donors showed a significantly reduced sulfonate concentration compared to control without fecal slurries (Table 5).

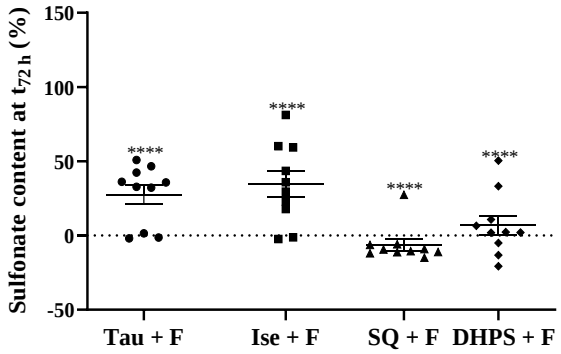

Figure 6: Sulfonate content after 72 h of anoxic incubation with human fecal slurries (F, 1%, n = 10). The sulfonate content was quantified with LC-MS/MS analysis and is given as percentage with the initial sulfonate concentration set to 100%. Initial sulfonate concentrations were: taurine (Tau, 20 mM), isethionate (Ise 20 mM), sulfoquinovose (SQ, 4 mM) or 2,3-dihydroxypropane-1-sulfonate (DHPS, 4 mM). Data presented as individual values with mean ± SEM (n = 3). Mean control (No feces, data in Table 5) vs. corresponding Tau + F, Ise + F, SQ + F or DHPS + F: **** $P < 0.0001$.

Table 5: Quantified sulfonate content (%) after 72 h of anoxic incubation with human fecal slurries (F, 1%) from different donors (D1 - D10). Sulfonate concentration measured with LC-MS/MS analysis in fecal incubation with taurine (20 mM), isethionate (20 mM), sulfoquinovose (SQ, 4 mM) or 2,3-dihydroxypropane-1-sulfonate (DHPS, 4 mM) (test incubation) or without feces (No feces, control incubation). The sulfonate content is given as percentage with the initial sulfonate concentration set to 100%. Data presented as mean (n = 2 - 3). Control vs. test incubations: **P* < 0.05, ***P* < 0.01.

Fecal slurries (from donor) or control (No feces)	Taurine	Isethionate	SQ	DHPS
+ F (D1)	42.4	81.2	-15.0	-13.2**
+ F (D2)	50.8	29.6	-11.2	-20.7**
+ F (D3)	32.8	-1.3	-9.1	-5.0**
+ F (D4)	46.7	60.2	-6.0	10.7**
+ F (D5)	35.7	59.3	27.3	6.6*
+ F (D6)	36.2	43.4	-6.3	2.3**
+ F (D7)	-1.3*	-2.4*	-10.5	1.9*
+ F (D8)	1.5*	35.9	-12.0	2.0*
+ F (D9)	-1.9	22.9	-11.2	33.2*
+ F (D10)	32.2	17.8	-9.5	50.4
No feces	112.3	87.5	95.6	110.9

3.1.2 The ability of human fecal microbiota to convert SQ to DHPS and / or H_2S was donor-dependent

Human gut bacteria, such as *E. coli* convert SQ to DHPS by sulfoglycolysis [241, 251]. The DHPS thereby formed can be converted to H_2S during anaerobic respiration by other gut bacteria, such as *Desulfovibrio* sp. [251]. In the present investigation, human fecal microbiota was tested for the ability to convert SQ to DHPS and further to H_2S.

Fecal microbiota from all tested donors degraded SQ completely and four main SQ-degradation types were observed (Fig. 7): (1) SQ was degraded, but DHPS (at 24 h and 72 h) and H_2S (until 72 h) were not detected (D5, D8 and D9) (Fig. 7A). (2) DHPS formation from SQ was observed at 24 h, followed by complete DHPS degradation until 72 h. H_2S was produced from 24 to 72 h with non-equimolar concentrations of DHPS formed (D2, D3 and D4) (Fig. 7B). (3) and (4) Either DHPS (D6 and D10, Fig. 7C, 24 h) or H_2S (D1 and D7, Fig. 7D, within 72 h) was released from SQ. DHPS was not detected in control incubations without fecal slurries containing only SQ (Fig. 7E).

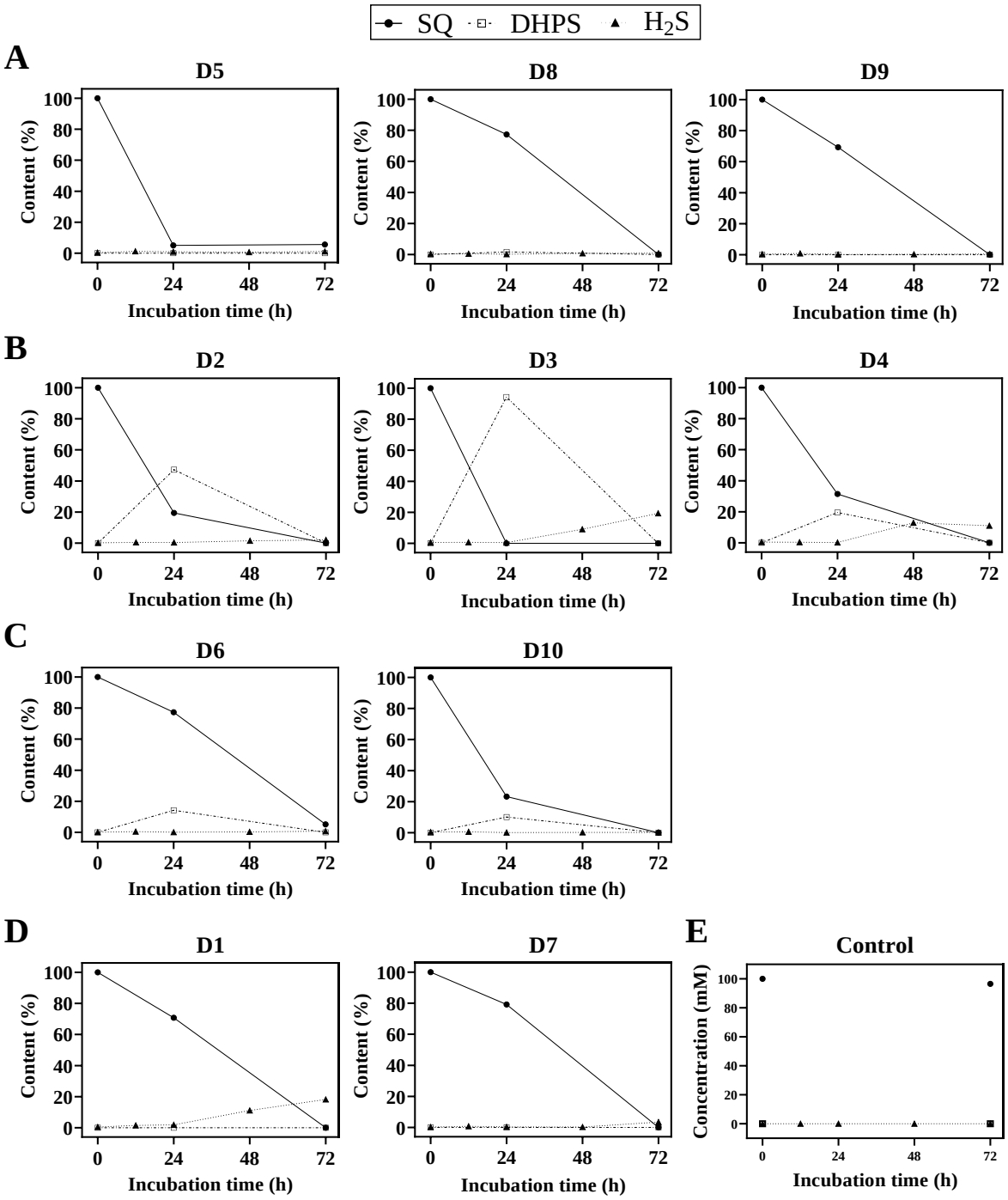

Figure 7: Patterns of sulfoquinovose (SQ, 4 mM) conversion by human fecal slurries (1%) from various donors (D1 - D10) under anoxic conditions. (A) Complete degradation of SQ, without formation of 2,3-dihydroxypropane-1-sulfonate (DHPS, at 24 h and 72 h) or H_2S (within 72 h). (**B)** DHPS formation from SQ (at 24 h) which was partially converted to H_2S (from 24 to 72 h). (**C, D**) Release of either DHPS (**C**) or H_2S (**D**) as end product from SQ. (**E**) SQ-incubation without fecal inoculum. Sulfonates were quantified with LC-MS/MS analysis and H_2S with the methylene blue method. Data presented as mean (n = 2 - 3).

3.1.3 Isethionate was not detected as an intermediate in taurine degradation by human fecal slurries

Isethionate is highly abundant in mammalian tissues and has been observed as a byproduct of taurine-derived nitrogen assimilation by bacteria residing in the mammalian gut [132, 134, 147, 148]. The ability of human gut bacteria to convert taurine to isethionate was examined. Therefore, human fecal slurries from ten donors were incubated with taurine and samples taken at the time of 72 h were analyzed for their isethionate concentration. No isethionate formation from taurine was observed, all values quantified were below the detection limit (<LLOQ) of LC-MS/MS analysis (data not shown).

3.1.4 Human fecal bacteria converted taurine, isethionate, 3-sulfolacate, SQ, DHPS and cysteate to H_2S with inter-individual differences

Formation by intestinal bacteria of H_2S as end product of microbial sulfonate degradation has been described for taurine, isethionate, 3-sulfolacate, SQ, DHPS, cysteate, but not for CoM [189, 251, 312, 313]. H_2S has been identified as an important gaseous signaling molecule potentially linked to IBD and colorectal cancer [64, 67, 68]. However, more recently H_2S has been recognized as a protective agent with anti-inflammatory and antioxidant properties, counteracting intestinal inflammation [69]. However, this effect of H_2S seems to be concentration-dependent [70-72]. To elucidate the role of sulfonates in intestinal H_2S formation, the time course was analyzed in incubation experiments with human fecal slurries as described above (3.1.1).

Amount and kinetics of the released H_2S formed depended on the amount of sulfonate utilized. H_2S formation from taurine, isethionate, 3-sulfolactate, SQ and DHPS started at 0 - 12 h and increased to 72 h only (Fig. 8A - E), while H_2S formation from cysteate started at 72 h (Fig. 8F). H_2S formation from CoM was not observed (Fig. 8G). Remarkably, bacterial H_2S release from sulfonates showed high inter-individual differences. While the fecal microbiota from all donors (D1 - D10) converted taurine, isethionate and 3-sulfolactate to H_2S (Fig. 6 and Fig. 8A - C), H_2S from SQ, DHPS, and cysteate was only formed by the fecal microbiota from some donors (Fig. 6 and Fig. 8D - F; SQ: D1, D3, D4, DHPS: D1 - D4, cysteate: D1). Donor identity of fecal microbiota that converted SQ and DHPS to H_2S were identical (D1, D3, D4). Control incubations of fecal slurries without sulfonates released 0.01 - 0.06 mM H_2S within 96 h (Fig. 8H). In comparison, the lowest H_2S concentration measured during incubation of fecal slurries (D4) with a sulfonate was considerably higher (0.3 mM) when incubated with DHPS (Fig. 8E).

These experiments revealed high inter-individual differences in the conversion of sulfonates to H_2S by the fecal microbiota of human subjects indicating differences in the presence or absence of sulfonate-converting bacteria among the donors. Bacterial strains able to convert taurine, isethionate, 3-sulfolactate, or SQ were therefore isolated from those human fecal slurries with the highest conversion activity and the isolates were subsequently identified.

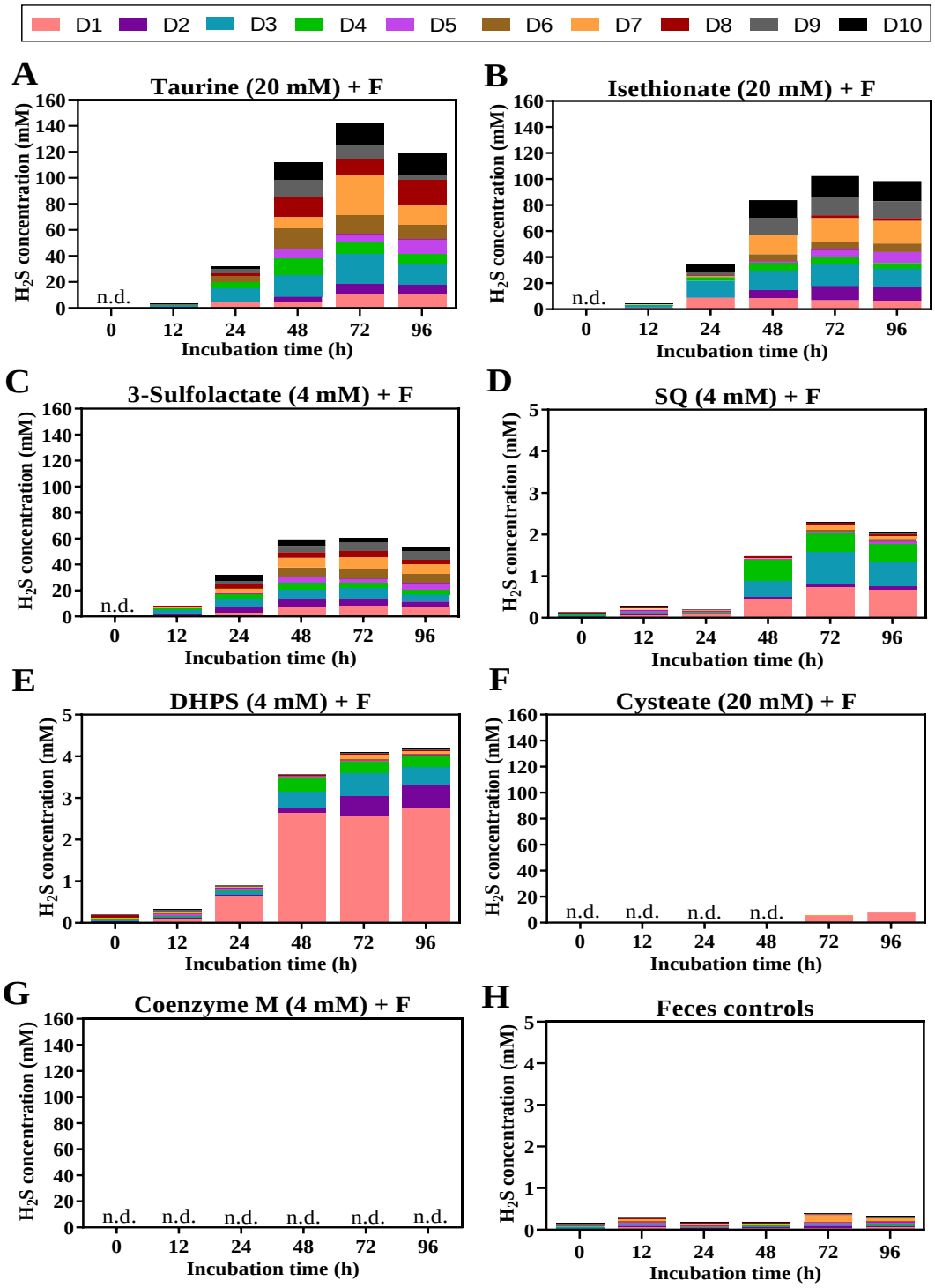

Figure 8: Time-course of H_2S formation in anoxic incubations of sulfonates with human fecal slurries (F, 1%) from different donors (D1 - D10). (A - G) H_2S concentrations measured with the methylene blue method of fecal incubations with sulfonate using the indicated initial concentrations or (**H)** without sulfonate. Sulfoquinovose = SQ, 2.3-dihydroxypropane-1-sulfonate = DHPS, n.d. = not detected. Data presented as mean (n = 2 - 3).

3.2 Identification and sulfonate utilization of human fecal bacteria

Human fecal donors for the isolation of sulfonate-degrading bacteria were chosen depending on the amount of H_2S formed in previous experiments (Fig. 8). Taurine-converting bacteria were isolated from human fecal slurries from D1 and D0, SQ-converting isolates from fecal slurries from D1 and D2, and 3-sulfolactate- and isethionate-converting isolates from fecal slurries from D10. D0 was excluded from the above-described experiments, because of the intake of antibiotics during the course of the experiments described in 3.1.

3.2.1 Taurine-utilizing bacteria from human fecal slurries were identified as *B. wadsworthia* and members of *Desulfovibrio* sp.

For the enrichment of taurine-converting bacteria from human fecal slurries from D0 and D1, various growth conditions were tested: taurine as electron acceptor, DL-lactate (L) or formate (F) as electron donor, the addition or exclusion of yeast extract (YE), and a gas phase of either N_2/CO_2 or H_2/CO_2 (80/20, v/v, %). A total of eight enrichment cultures were set up per donor (Table 6).

A total number of 42 bacteria, able to convert taurine to H_2S were isolated from fecal enrichment cultures of both donors using the following media combinations (Table 6): (1) Lactate or formate as electron donor and a gas phase of N_2/CO_2, or (2) formate as electron donor, the addition of yeast extract and a gas phase of H_2/CO_2. Isolates were also obtained from D0 using the following media (Table 6): (1) Lactate or formate as electron donor, the addition of yeast extract and N_2/CO_2 as gas phase, or (2) lactate as electron donor, the addition of yeast extract and a gas phase of H_2/CO_2. No H_2S was formed in enrichments without yeast extract with a gas phase of H_2/CO_2.

All 42 taurine-converting isolates were Gram-negative rods. Of these, 22 isolates were identified as strains of *B. wadsworthia* (98 - 100% identity, 95 - 1427 bp) and the residual 20 isolates as members of *Desulfovibrio* spp. (410 - 1472 bp) based on *16S rRNA* gene sequencing (Table 6 and 7). All *B. wadsworthia* isolates had an identity of 98 - 100% among each other, indicating that they are identical, despite their origin from two different donors (≥ 97% identity, Table 7A). They had a 98 - 100% identity compared to the *B. wadsworthia* type strain CCUG 32349^T, and 98 - 99% identity compared to *B. wadsworthia* DSM11045, which has been described to convert taurine to H_2S under anoxic conditions [8]. Similarly, *Desulfovibrio* isolates had an identity of 99 - 100% to each other, indicating identity. *Desulfovibrio* isolates were only obtained from one donor (D0, Table 6). Furthermore, they had the highest similarity to the type strains *Desulfovibrio intestinalis* DSM 11275T (98 - 99% identity), *D. simplex* DSM 4141^T (96 - 98% identity), and *D. desulfuricans* DSM 642^T (95 - 97% identity) (Table 7B). However, the *16S rRNA* gene sequence of *D. intestinalis*, *D. simplex*, and *D. desulfuricans* (*D. intestinalis*: Y12254, *D. simplex*: FR733678, and *D. desulfuricans*: AF192153) showing 97% to 99% identity may be considered as highly identical (≥ 97%) (Table 7B). Therefore, the *Desulfovibrio* isolates could not be assigned unequivocally to one of these species and additional tests were required (see below, 3.2.2).

Table 6: Enrichment conditions, origin, and assignment (*16S rRNA* gene sequence) of obtained taurine-converting isolates. Enrichment cultures with human fecal slurries (1%) from donor 0 or donor 1 were set up with taurine (20 mM) in the indicated media. Isolates were obtained after seven transfers involving streaking of diluted cultures (10^{-1} - 10^{-8}) and anoxic incubation. DNA was extracted, PCR performed and PCR products sequenced as described in 2.4.3. *16S rRNA* gene amplicons were assembled with SnapGene 5.1.4.1 and aligned to sequences of the *16S rRNA* gene-sequence database using BLASTn.

Medium components for enrichment			Numbers of obtained taurine-converting isolates	Isolate identity and origin (donor identity: number of obtained isolates)	
Electron donor (40 mM)	Yeast extract (3.5 mg/l)	Gas phase (80/20, v/v, %)		*B. wadsworthia*	*Desulfovibrio* spp.
Formate	No	N_2/CO_2	9	0:3 and 1:5	0:1
	No	H_2/CO_2	0	-	-
	Yes	N_2/CO_2	9	0:1	0:8
	Yes	H_2/CO_2	2	0:1 and 1:1	-
Lactate	No	N_2/CO_2	12	0:1 and 1:6	0:5
	No	H_2/CO_2	0	-	-
	Yes	N_2/CO_2	6	-	0:6
	Yes	H_2/CO_2	4	0:4	-

Table 7: Similarity of *16S rRNA* gene sequence of fecal taurine-converting *B. wadsworthia* (A) and *Desulfovibrio* (B) isolates, related type strains and relevant sulfonate-utilizing bacteria. *B.w. = Bilophila wadsworthia, D. = Desulfovibrio.*

A

	B.w. isolates	*B. w.* CCUG 3234^T	*B. w.* DSM11045
B. w. isolates	98 - 100%	98 - 100%	98 - 99%

B

	D. spp. isolates	*D. intestinalis* DSM 11275^T	*D. simplex* DSM 4141^T	*D. desulfuricans* DSM 642^T
D. spp. isolates	99 - 100%	98 - 99%	96 - 98%	95 - 97%
D. intestinalis DSM 11275^T	98 - 99%	97% - 99%		
D. simplex DSM 4141^T	96 - 98%			
D. desulfuricans DSM 642^T	95 - 97%			

The ability of *B. wadsworthia* to convert taurine to H_2S has been well studied in the last decades, but knowledge about taurine degradation by *Desulfovibrio* sp. is scarce. Therefore, the obtained *Desulfovibrio*-isolates were first subjected to their further identification and their ability to convert sulfonates. The role of *B. wadsworthia* in sulfonate conversion was also further investigated (3.2.9 and 3.2.10).

3.2.2 Characteristics of human fecal taurine-converting *Desulfovibrio* isolates were further identified

Because of the high degree of *16S rRNA g*ene-sequence similarity among the *Desulfovibrio* isolates, only those with a nearly completely determined *16S rRNA g*ene sequence (≥ 1400 bp) were studied further. All of these 13 *Desulfovibrio* isolates were Gram-negative rods (Fig. 9A) and grew on blood agar plates within 2 - 4 days under

strict anoxic conditions at 37°C. Colonies had a diameter of 1 mM after two days and up to 4 mM after four days. *Desulfovibrio* spp. are known to be motile using a single polar flagellum [58]. The motility of all 13 isolates was confirmed as being mediated by a polar monotrichous flagellum (Fig. 9B).

Differences at strain level were analyzed using RAPD PCR. RAPD revealed similar patterns of genomic DNA amplicons for the isolates 1-13 (Fig. 9C), indicating strain similarity among the isolates. Furthermore, Dsr is a key enzyme of sulfate reduction, catalyzing the six-electron reduction of sulfite to H_2S [137]. It is encoded by the *dsrAB* genes which all SRB, including the *Desulfovibrio* family, do have in common [314]. The presence of the partial *dsrA* and *dsrB* gene subunits was investigated and detected in all 13 isolates (Fig. 9D). *D. intestinalis*, *D. simplex*, and *D. desulfuricans* vary in their *dsrAB* gene sequence, which made further identification of the isolates possible. The partial *dsrAB* gene sequence was compared for distinction among *D. intestinalis* (AF418183), *D. simplex* (AB061541), and *D. desulfuricans* (AF273034). Alignment of the corresponding sequences (580 - 606 bp) of all 13 isolates showed a 95% identity to the partial *dsrAB* gene sequence of *D. intestinalis* and *D. simplex* and a 92% identity to partial *dsrAB* gene sequence of *D. desulfuricans* (Table 9), indicating that the isolates likely differ from the type strains (< 97% identity).

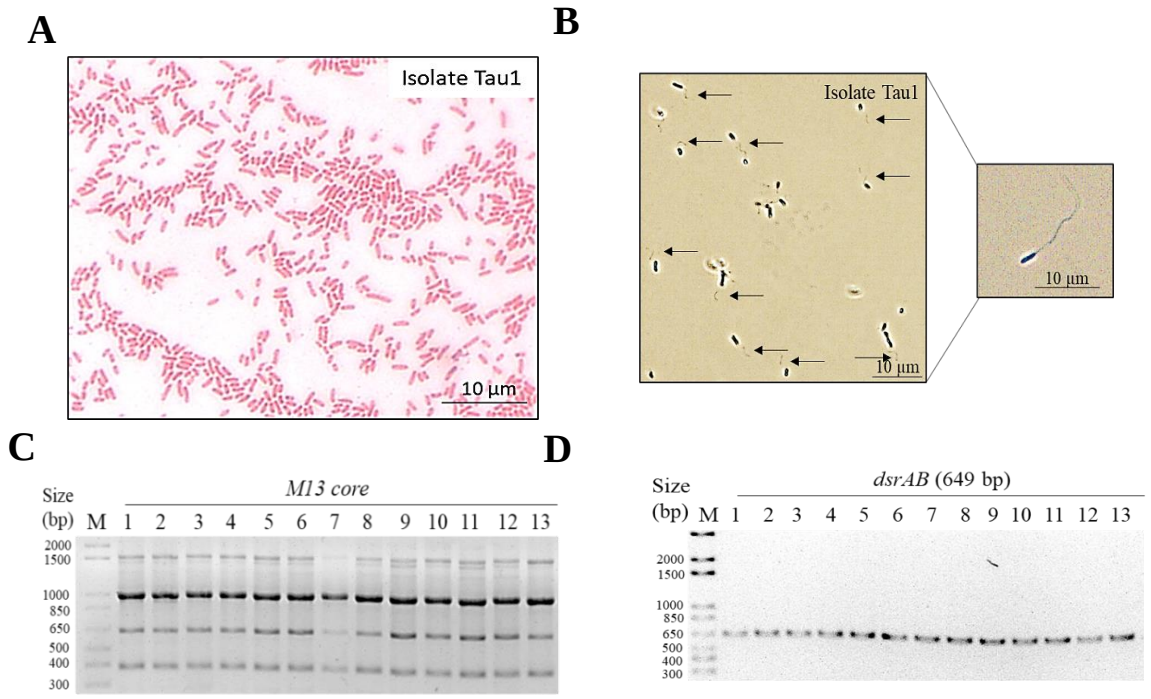

Figure 9: Phenotypic and genotypic characterization of *Desulfovibrio* isolates. (A) Gram staining and (**B)** visualization of the flagellum of the *Desulfovibrio* isolate Tau1 with RYU staining. (**C**) RAPD-PCR profiles of 13 selected *Desulfovibrio* isolates (M13-core primer, 2% agarose gel in 1 x TAE buffer (Appendix, Table A1)). **(D)** PCR profiles targeting *dsrAB* gene subunit in 13 selected *Desulfovibrio* isolates (1% agarose gel in 1 x TAE buffer (Appendix, Table A1)).

Because of the great similarities of the 13 *Desulfovibrio* isolates among each other (Fig. 9), additional tests for further identification were performed with only one *Desulfovibrio* isolate, strain Tau1. *Desulfovibrio* spp. grow under strictly anoxic conditions in the presence of an electron acceptor, such as sulfate, sulfite or nitrate, and an appropriate electron donor, such

as DL-lactate or succinate (Table 8) [316-323]. *D. desulfuricans* obtains energy from the reduction of sulfite or nitrate in the presence of DL-lactate [318, 320]. *D. intestinalis* obtains energy from an alternative electron acceptor, sulfate, when combined with succinate or from sulfite with DL-lactate [318]. *D. simplex* grows with nitrate in the presence of DL-lactate (Table 8) [317]. The following three growth conditions were tested to compare the growth behavior of isolate Tau1 with those of the type strains: 1) Succinate with sulfate, 2) DL-lactate with sulfite or 3) DL-lactate with nitrate (Table 8).

The ability of the isolate to convert sulfite to H_2S and nitrate to nitrite in the presence of DL-lactate was identical to that described for *D. desulfuricans* (Table 8) [318, 320]. This was indicated by a release of ca. 0.5 mM H_2S from DL-lactate incubated with sulfite or ca. 0.4 mM nitrite from DL-lactate incubated with nitrate (Fig. 10). In contrast, incubation with succinate and sulfate did not result in the formation of H_2S (Fig. 10).

Table 8: Ability of *Desulfovibrio* strains to degrade an electron acceptor in the presence of an appropriate electron donor (both 20 mM). Bacterial cultures of strain Tau1 were incubated in basal freshwater medium (Appendix, Table A1) for 48 h under anoxic conditions. Growth response was scored when H_2S or nitrite formation was detected (+) or when formation was not observed (-), respectively with the methylene blue method and the Griess Reagent (Fig. 10). SO_4^{2-} = sulfate, SO_3^{2-} = sulfite, NO_3^- = nitrate.

Medium supplements	*Desulfovibrio* Tau1	*Desulfovibrio desulfuricans* DSM 642^T	*Desulfovibrio intestinalis* DSM 11275^T	*Desulfovibrio simplex* DSM 4141^T
Succinate + SO_4^{2-}	-	- [318, 320]	+ [318]	- [317]
DL-Lactate + SO_3^{2-}	+	+ [318, 320]	+ [318]	- [317]
DL-Lactate + NO_3^-	+	+ [318, 320]	- [318]	+ [317]

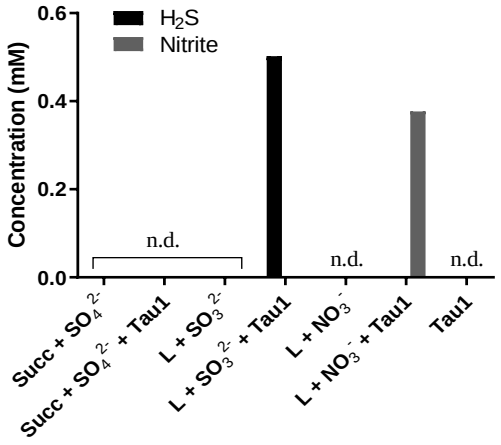

Figure 10: Sulfide and nitrite formation within 48 h by the taurine-converting isolate Tau1 under anoxic conditions with one electron donor and one acceptor (20 mM both) in basal freshwater medium (Appendix, Table A1). H_2S concentration was measured by the methylene blue method and nitrite by the Griess Reagent. Succ = succinate, L = lactate, SO_4^{2-} = sulfate, SO_3^{2-} = sulfite, NO_3^- = nitrate, n.d. = not detected. Data presented as mean (n = 2 - 3).

3.2.3 Human fecal taurine-converting isolate Tau1 was identified as *Desulfovibrio desulfuricans* ATCC 27774

The *16S rRNA* gene sequence of all 13 *Desulfovibrio* isolates was aligned with sequences of the *16S rRNA* gene at subspecies level using BLASTn. All isolates were 99% identical to the subspecies *D. desulfuricans* ATCC 27774 (M34113) (Table 9). Also, their partial *dsrAB* gene sequence was compared and was 100% identical to the subspecies *Desulfovibrio desulfuricans* ATCC 27774 (Table 9).

Furthermore, *D. desulfuricans* ATCC 27774 is capable of utilizing nitrate as TEA and has catalase activity, similar to strain Tau1 [320, 323] (Table 9). However, growth of *D. desulfuricans* ATCC 27774 on succinate and sulfate or DL-lactate and sulfite has not been investigated previously (Table 9).

Table 9: Comparison of sequence identity (*16S rRNA* and partial *dsrAB* gene sequence), growth behavior and catalase activity of *Desulfovibrio* (*D.*) isolates, *D. desulfuricans* ATCC 27774, *D. desulfuricans* DSM 642^T, *D. intestinalis DSM* 11275^T and *D. simplex* DSM 4141^T. Growth on various electron donor-electron acceptor combinations (20 mM each) and catalase activity only investigated for one of the *Desulfovibrio* isolates, namely Tau1. For this purpose, strain Tau1 was incubated for 48 h under anoxic conditions. Growth was monitored and the cultures were tested for H_2S and nitrite formation, using the methylene blue method and the Griess Reagent, respectively (Fig. 10). Catalase activity was determined as described in 2.2.10. Succ = succinate, L = lactate, n.a. = not analyzed.

	16S rRNA		*dsrAB* (partial)		Growth with electron donor + electron acceptor			Catalase activity
	D. desulfuricans ATCC 27774	*D.* spp isolates	*D. desulfuricans* ATCC 27774	*D.* spp isolates	Succ + SO_4^{2-}	L + SO_3^{2-}	L + NO_3^-	
D. spp. *isolate(s)*	99%	100%	100%	100%	-	+	+	+
D. desulfuricans ATCC 27774	100%	99%	100%	100%	n.a.	n.a.	+ [320]	+ [323]
D. desulfuricans DSM 642^T	100%	95 - 97 %	92%	92%	- [318, 320]	+ [318, 320]	+ [318, 320]	- [324]
D. intestinalis DSM 11275^T	97%	98 - 99 %	95%	95%	+ [318]	+ [318]	- [318]	+ [318]
D. simplex DSM 4141^T	97%	96 - 98 %	95%	95%	- [317]	- [317]	+ [317]	n.a.

Based on the results of the *16S rRNA* gene-sequence analysis, the *Desulfovibrio* isolates are phylogenetically closely related to the type strains *D. simplex*, *D. intestinalis* and *D. desulfuricans* or at substrain level to *D. desulfuricans* ATCC 27774. Their partial *dsrAB* gene sequence revealed the highest identity to *D. desulfuricans* ATCC 27774. However, the isolate Tau1 was identical to type strain *D. desulfuricans* DSM 642^T and partially to *D. desulfuricans* ATCC 27774 with respect to the ability to reduce specific electron acceptors in the presence of an electron donor [318, 320]. Catalase activity was similar to that of substrain *D. desulfuricans* ATCC 27774.

3.2.4 The fecal isolate Tau1 converted taurine and isethionate to H_2S

To investigate whether sulfonates other than taurine could serve as an electron acceptor for isolate Tau1, isethionate, TC, cysteate, SQ, DHPS, and 3-sulfolactate were individually tested and compared to the control incubations of Tau1 with taurine, Tau1 without sulfonates or of one sulfonate, without strain Tau1.

Strain Tau1 was able to grow in isethionate reaching a maximal OD_{600} of 0.23 after 48 h (Fig. 11A). This is higher than the maximal OD_{600} of 0.17 observed for taurine after 96 h (Fig. 11A). Isethionate resulted in a decreased doubling time in comparison to taurine, indicating a faster growth on this substrate [3.4 (± 1.0) h vs. 5.2 (± 0.2) h, Table 10]. No increase in OD_{600} was detected during incubation of strain Tau1 with TC, cysteate, SQ, DHPS, or in

the control incubations (Fig. 11A). A slightly increased OD_{600} was detected in incubations of strain Tau1 with 3-sulfolactate (Fig. 11A).

Growth of strain Tau1 was accompanied by black iron sulfide (FeS) precipitation, which interfered with OD_{600} measurements. Therefore, additional CFU/ml were determined over time. With taurine and isethionate cell numbers of strain Tau1 outnumbered those in controls (only Tau1, without sulfonate) by 10^1 CFU/ml (Fig. 11B). CFU/ml of incubations containing strain Tau1 with TC, cysteate, SQ, DHPS or 3-sulfolactate did not differ from the control incubations (data not shown). The time course confirmed that isethionate enabled a better growth than observed for taurine, with the highest CFU/ml reached at 24 h for isethionate and at 96 h for taurine (Fig. 11B). However, the numbers did not reach statistical significance in comparison to the control incubations.

The growth of strain Tau1 with taurine or isethionate led to the depletion of both sulfonates and the simultaneous release of H_2S (Fig. 11C). Degradation of taurine was detected after 24 h of incubation, which is consistent with the increase in OD_{600} (Fig. 11A). Approximately 70% of the taurine was converted to H_2S after 96 h, while the residual 30% of taurine remained undegraded. In the case of isethionate, strain Tau1 released from this sulfonate H_2S directly after inoculation, which parallels the bacterial growth observed (Fig. 11A). Up to 48% of the isethionate was depleted after 72 h (Fig. 11C).

Depletion of SQ, TC, or DHPS was not observed (data not shown). No H_2S was formed in incubations of isolate Tau1 with TC, SQ, DHPS, cysteate, or 3-sulfolactate (data not shown). Strain Tau1 did not convert taurine to isethionate (tested at 72 h of taurine degradation, data not shown). In conclusion, the human fecal isolate Tau1 is a member of the genus *Desulfovibrio*, capable of converting taurine and isethionate to H_2S during anoxic growth.

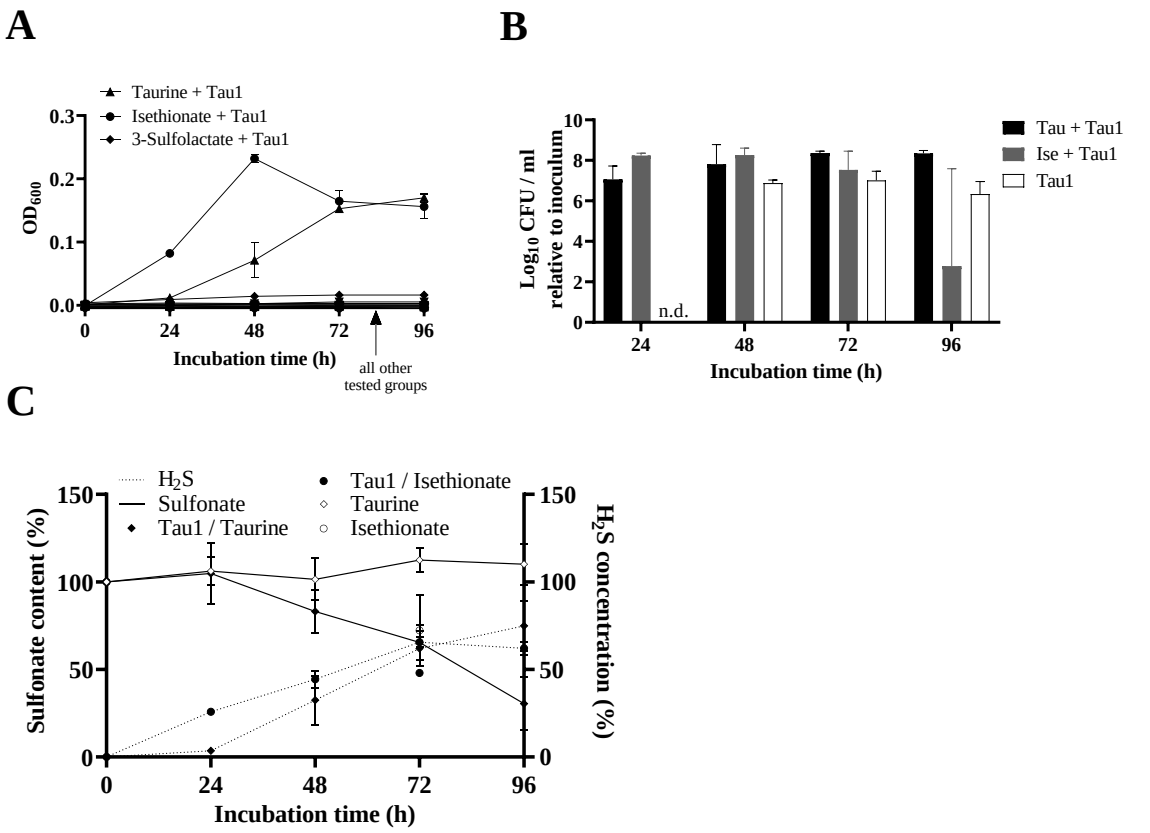

Figure 11: Taurine-converting isolate Tau1 utilized taurine and isethionate (both 20 mM) during anoxic incubation while releasing H_2S. (A) Growth (OD_{600}) during incubation of strain Tau1 with taurine, isethionate, sulfoquinovose (SQ, 4 mM), 2,3-dihydroxypropane-1-sulfonate (DHPS, 4 mM), 3-sulfolactate (4 mM), cysteate (20 mM), taurocholate (20 mM) or without sulfonate. (**B)** Growth of cultures with taurine (Tau + Tau1) or isethionate (Ise + Tau1) compared to growth of only isolate Tau1 without sulfonates (Tau1) based on colony-forming units (CFU). Formed CFU/ml of isolate Tau1 during incubations with TC, cysteate, 3-sulfolactate, SQ, or DHPS were identical with growth of strain Tau1 without sulfonates (data not shown). (**C)** Sulfonate and H_2S concentrations during anoxic incubations of strain Tau1 with taurine or isethionate compared to sulfonate incubation without isolate Tau1. H_2S was measured with the methylene blue method, taurine with the NBD-F assay and isethionate with LC-MS/MS analysis. Data expressed as mean ± SEM (n = 3)**.** n.d. = not detected.

Table 10: Doubling time during incubation of strain Tau1 with taurine or isethionate. Data expressed as mean ± SEM (n = 3)**.**

	Doubling time (h)
Taurine (20 mM) + Tau1	5.2 (± 0.2)
Isethionate (20 mM) + Tau1	3.4 (± 1.0)

3.2.5 *Desulfovibrio simplex* DSM 4141^T utilized the sulfite moiety of taurine

Anoxic growth of *Desulfovibrio* spp. was primarily reported with isethionate and / or cysteate, but not with taurine. Therefore, the ability of *Desulfovibrio* spp. to utilize taurine and to convert it to H_2S was further examined using the type strains of *D. simplex*, *D. intestinalis*, *D. desulfuricans*, and *D. piger*.

From all tested *Desulfovibrio* sp. (*D. simplex*, *D. intestinalis*, *D. desulfuricans*, and *D. piger*), only *D. simplex* utilized taurine as TEA and converted its sulfite moiety to H_2S (Fig. 12, Table 11). The OD_{600} of *D. simplex* increased from 24 h to 96 h to a final OD_{600}

of 0.12 (Fig. 12A). In contrast, the OD_{600} of *D. intestinalis*, *D. desulfuricans*, and *D. piger* cultures did not increase (Fig. 12A). Growth of *D. simplex* was confirmed by the CFU increase within 96 h, with the highest number of 10^8 CFU/ml observed at 72 h (Fig. 12B). *D. intestinalis*, *D. piger*, and *D. desulfuricans* grew under these conditions (Fig. 12B), but did not release H_2S from taurine (Table 11).

On the contrary, *D. simplex* was able to convert taurine to H_2S (Fig. 12C). The initial taurine concentration (20 mM) was continuously reduced between 0 to 96 h with a residual sulfonate content of 74% at 96 h (Fig. 12C). The formation of H_2S from taurine started at 24 h, with a release of 6.5 mM H_2S after 96 h (32.5% of the initial molar taurine concentration, Fig. 12, Table 11).

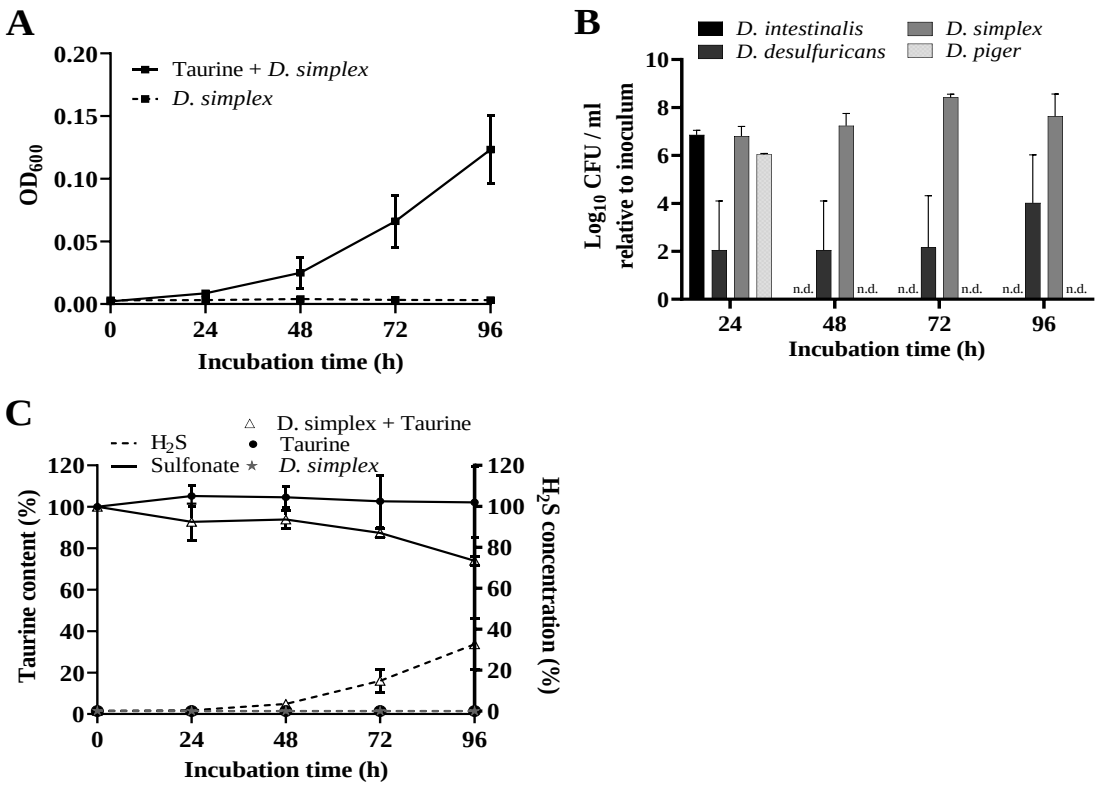

Figure 12: *D. simplex* converted taurine to H_2S under anoxic conditions. (A) Growth (OD_{600}) of *Desulfovibrio* (*D.) simplex* during anoxic incubation in the presence or absence of taurine (20 mM). *D. intestinalis*, *D. desulfuricans*, *D. simplex*, and *D. piger* tested under these conditions did not respond with an increase in OD_{600} (data not shown). (**B)** Growth is based on an increase in colony-forming units (CFU). No CFU were observed in incubations of cultures without taurine (data not shown). n.d. = not detected. (**C)** Taurine and H_2S concentrations measured with the NBD-F assay and the methylene blue method, respectively.

Table 11: H_2S formation (mM) measured with the methylene blue method in anoxic incubations of SRB with taurine (Tau) or sulfate (SO_4^{2-}) (both 20 mM). Control incubations contained only bacteria, taurine or sulfate. Data are presented as mean ± SEM (n = 3).

SRB + TEA or control	Time (h)				
	0	24	48	72	96
D. intestinalis + Tau	0.01 ± 0.00	-0.01 ± 0.00	-0.01 ± 0.00	-0.01 ± 0.00	-0.01 ± 0.00
D. intestinalis + SO_4^{2-}	0.01 ± 0.00	0.24 ± 0.03	1.23 ± 0.97	2.48 ± 2.69	2.43 ± 3.12
D. intestinalis	0.00 ± 0.00	-0.01 ± 0.00	-0.01 ± 0.00	-0.01 ± 0.00	-0.01 ± 0.00
D. desulfuricans + Tau	0.00 ± 0.00	-0.01 ± 0.01	-0.01 ± 0.00	-0.01 ± 0.00	-0.01 ± 0.00
D. desulfuricans + SO_4^{2-}	0.00 ± 0.00	0.16 ± 0.00	0.46 ± 0.09	2.41 ± 0.42	5.26 ± 2.99
D. desulfuricans	0.00 ± 0.00	-0.01 ± 0.00	-0.01 ± 0.00	-0.01 ± 0.00	-0.01 ± 0.00
D. simplex + Tau	0.01 ± 0.00	0.07 ± 0.01	0.69 ± 0.36	2.94 ± 1.12	6.51 ± 2.52
D. simplex + SO_4^{2-}	0.01 ± 0.00	0.12 ± 0.16	0.80 ± 0.23	0.83 ± 0.33	0.67 ± 0.54
D. simplex	0.01 ± 0.00	-0.01 ± 0.00	-0.01 ± 0.00	-0.01 ± 0.00	-0.01 ± 0.00
D. piger + Tau	0.00 ± 0.00	0.03 ± 0.02	0.00 ± 0.00	0.01 ± 0.00	0.01 ± 0.00
D. piger + SO_4^{2-}	0.02 ± 0.00	0.85 ± 0.23	0.08 ± 0.09	0.03 ± 0.02	0.01 ± 0.00
D. piger	0.00 ± 0.00	0.01 ± 0.01	0.00 ± 0.00	0.01 ± 0.00	0.01 ± 0.00
Tau	0.00 ± 0.00	0.00 ± 0.00	0.00 ± 0.00	0.01 ± 0.00	0.01 ± 0.00
SO_4^{2-}	0.00 ± 0.00	0.00 ± 0.00	0.00 ± 0.00	0.01 ± 0.00	0.01 ± 0.00

3.2.6 SQ-converting human fecal isolates were identified as *E. coli*

For the enrichment of SQ-utilizing bacteria, 2% fecal slurries from D1 were incubated in MSM under oxic and anoxic conditions. Control cultures contained fecal slurries only. After three transfers, H_2S formation was detected in the anoxic enrichment culture (Fig. 13), but not in the oxic culture. Thus, isolation of bacteria was done from the anoxic enrichment culture.

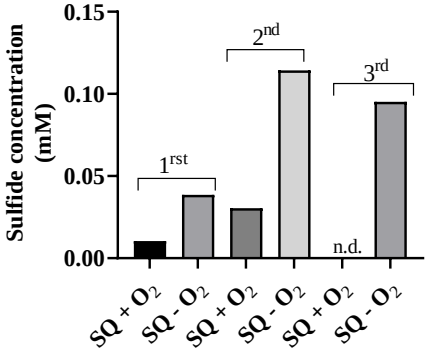

Figure 13: Sulfide concentrations measured by the methylene blue method in anoxic (-O_2) and oxic (+O_2) enrichment subcultures with human fecal slurries from D1 (1%) and SQ (4 mM) during three sequential culture transfers. Data presented as individual value. n.d. = not detected.

A total of five isolates (SQ6, SQ10, SQ11, SQ12, SQ13) were obtained from anoxic cultures after the third transfer. All isolates were characterized as Gram-negative rods (Fig. 14A, isolate SQ6) and identified based on their *16S rRNA* gene sequence as members of the *E. coli* taxonomic group (99% identity with *E. coli, E. albertii, Shigella boydii, S. dysenteriae, S. flexneri, S. sonnei,* 474 - 1040 bp) (Table 12). Alignment of the *16S rRNA* gene sequence of the obtained isolates implied 98 - 100% identity, as well as 99 - 100% identity to the *E. coli* DSM30083^T type strain or to *E. coli* MG1655. The latter is known to degrade SQ to DHPS [251]. RAPD revealed similar patterns of genomic DNA amplicons for the isolates, but a pattern distinct from that of *E. coli* MG1655, indicating strain similarity among the isolates but distinct to the *E. coli* MG1655 (Fig. 14B).

The isolates were further analyzed with PCR with primers specific for *E. coli* K12 strains, *E. coli*, *E. albertii*, and *E. fergusonii*. All isolates were confirmed as *E. coli*, but the PCR band patterns of the isolates were not similar to that of *E. coli* MG1655 (data not shown).

Sulfoquinovosidase (*yihQ*) catalyzes the hydrolysis of SQDG to SQ and has been detected in *E. coli* MG1655 [239]. SQ can be degraded further to DHPS by enzymes encoded in a ten-gene cluster. Herein, *yihS* is responsible for the first step of the sulfoglycolytic reaction, namely the isomerization of SQ to 6-deoxy-6-sulfofructose [249]. Genes encoding these two enzymes (*yihQ* and *yihS*) were present in all isolates (data not shown).

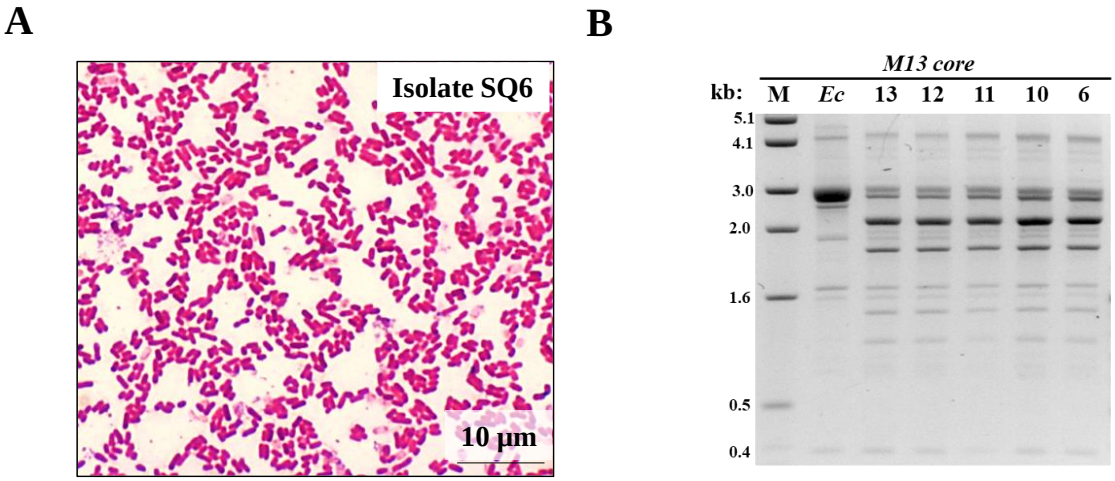

Figure 14: Phenotypic and genotypic identification of sulfoquinovose (SQ)-converting isolates SQ6, SQ10, SQ11, SQ12 and SQ13. (**A)** Gram staining of isolate SQ6. (**B)** RAPD-PCR profiles of isolates SQ6, SQ10, SQ11, SQ12, and SQ13 in comparison to *E. coli* MG1655 (*Ec*) using primer M13-core in a 2% agarose gel in 1 x TAE buffer (Appendix, Table 1A). M = marker.

Table 12: Identification and alignment of SQ-converting isolates SQ6, SQ10, SQ11, SQ12 and SQ13 with *E. coli* DSM30083^T (type strain) and *E. coli* MG1655 (able to degrade SQ to DHPS) based on their *16S rRNA* gene sequence using BLASTn.

16S rRNA	SQ-converting isolates SQ6, SQ10, SQ11, SQ12 and SQ13	*E. coli* taxonomic group	*E. coli* DSM30083^T	*E. coli* strain MG1655
SQ-converting isolates SQ6, SQ10, SQ11, SQ12 and SQ13	98 - 100%	99%	99 - 100%	99 - 100%

3.2.7 SQ utilization by human fecal isolates was dependent on the presence or absence of oxygen

The degradation of SQ to DHPS by *E. coli* under anoxic and oxic conditions has previously been tested [249, 251]. Therefore, SQ conversion by the SQ-converting isolates was compared to that of *E. coli* MG1655 under both conditions. As SQ is a derivative of glucose, growth on the latter was also tested as a reference.

All SQ-converting isolates and *E. coli* MG1655 (Fig. 15A, B), rapidly degraded glucose, no matter whether oxygen was present or not. The isolates depleted glucose completely within 8 h, while *E. coli* MG1655 depleted glucose completely within 22 h, indicating a lower degradation rate for *E. coli* MG1655. Findings are consistent with a higher determined doubling time of 4 h for *E. coli* MG1655 and 2 - 2.5 h for the tested isolates (Table 13). The doubling

time of all bacteria was largely increased when glucose was replaced by SQ and also depended on the presence or absence of oxygen (Table 13). The doubling times were 3 - 8 times higher under oxic conditions and 4 - 25 h times higher under anoxic conditions with SQ than with glucose (Table 13).

Bacterial growth with SQ was accompanied by the conversion of SQ to DHPS (Fig. 15C - H). While the isolates SQ6, SQ11, SQ12 and SQ13 were able to convert SQ to DHPS under oxic and anoxic conditions (Fig. 15C, E-G), strain SQ10 and *E. coli* MG1655 were only able to produce DHPS when oxygen was absent (Fig. 15D, H). Isolates SQ6, SQ11, SQ12 and SQ13 converted SQ to DHPS within 22 - 24 h of anoxic incubation, requiring a longer period of incubation (24 - 48 h) in the presence of oxygen (Fig. 15C, E - G).

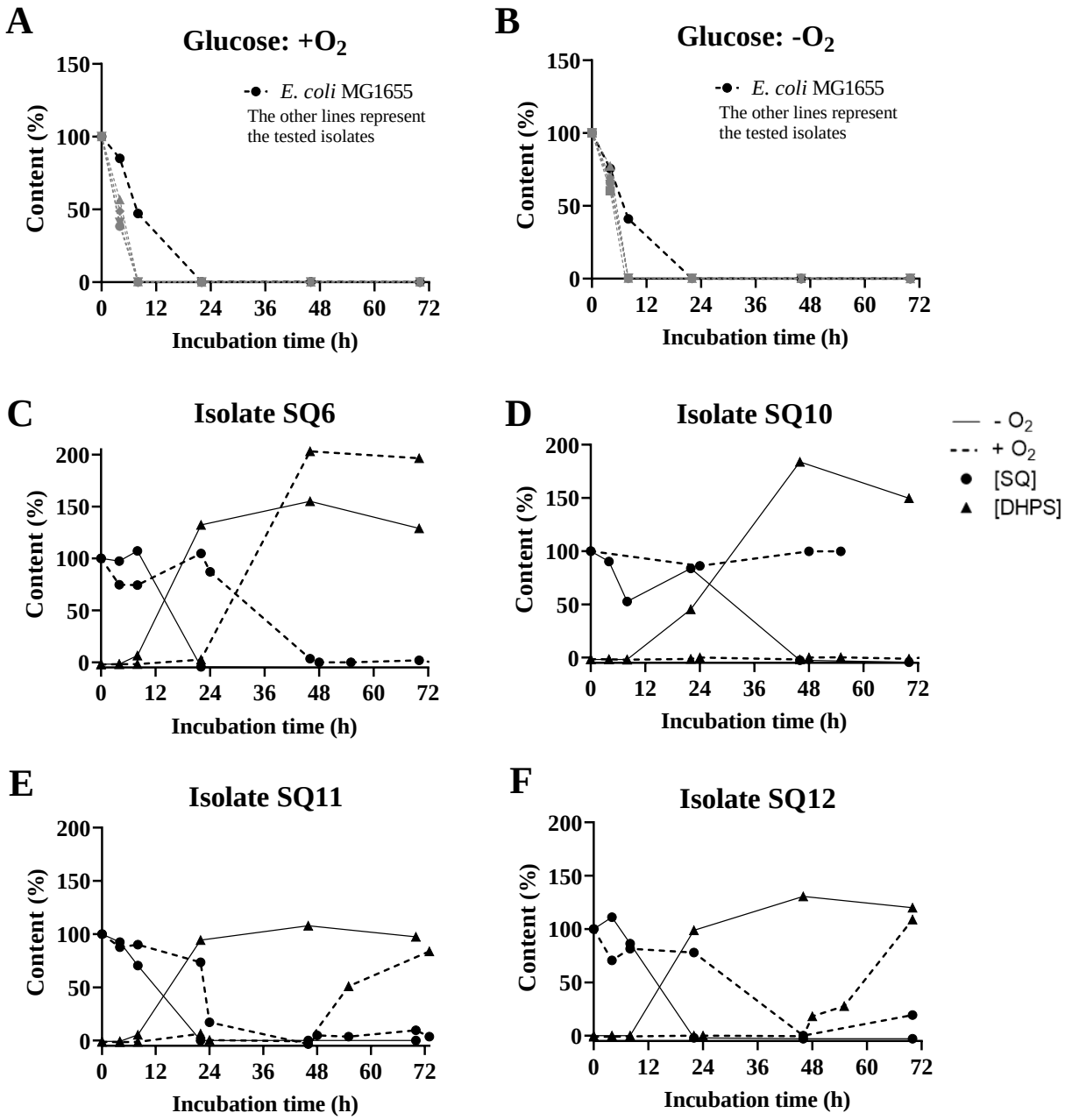

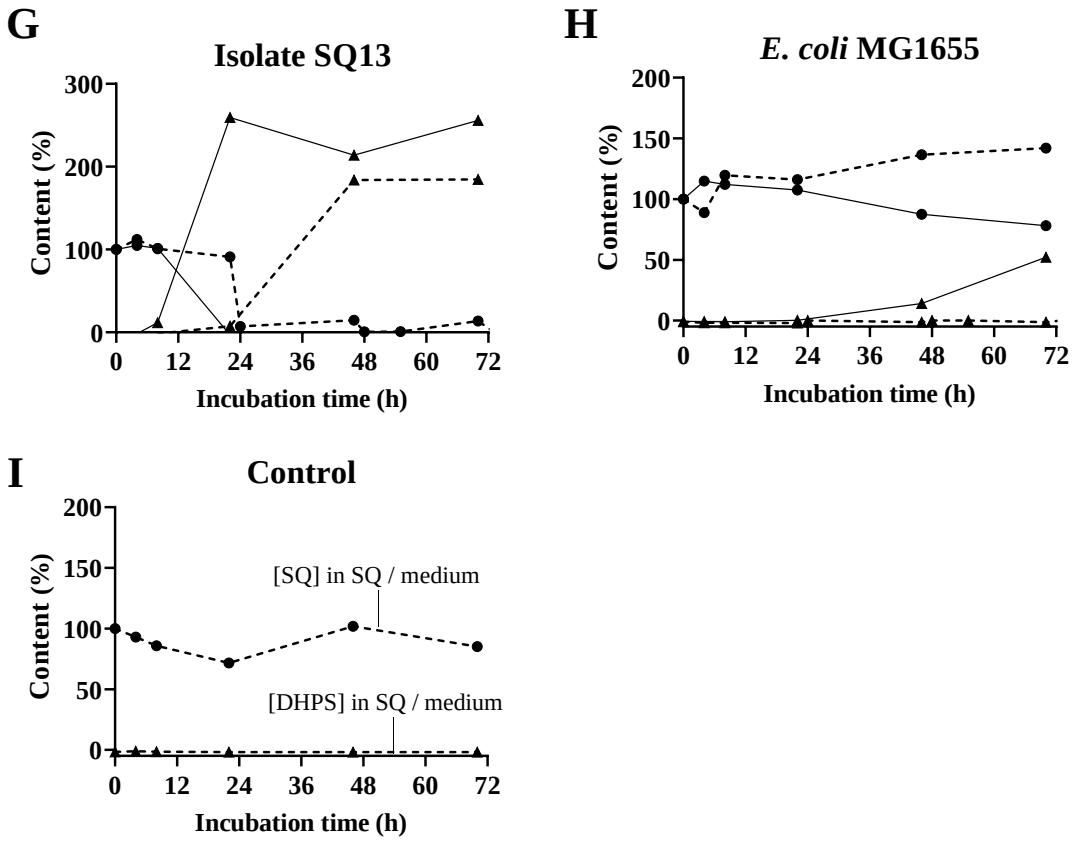

Figure 15: Glucose (4 mM) degradation and conversion of sulfoquinovose (SQ, 4mM) to 2,3-dihydroxypropane-1-sulfonate (DHPS) by *E. coli* isolates (SQ6, SQ10 - SQ13) in comparison to *E. coli* MG1655. (A+B) Glucose concentrations quantified with the DNS method during (**A)** oxic (+ O_2) and (**B)** anoxic (- O_2) incubations of the fecal isolates SQ6, SQ10, SQ11, SQ12, SQ13 or *E. coli* MG1655 with glucose. (**C - I)** SQ and DHPS concentrations measured with LC-MS/MS analysis during oxic (+ O_2) and anoxic (- O_2) incubation of the fecal isolates SQ6, SQ10, SQ11, SQ12, SQ13 or *E. coli* MG1655 with SQ. Control incubation (**I)** contained only SQ. Data presented as mean (n = 1 - 2). n.g. = no growth detected.

Table 13: Growth (doubling time) of isolated *E. coli* strains (SQ6, SQ10 - SQ13) in comparison to *E. coli* MG1655 incubated with glucose (g, 4 mM) or sulfoquinovose (SQ, 4 mM) under oxic (+ O_2) or anoxic (- O_2) conditions. Data presented as mean (n = 1 - 2). n.g. = no growth detected.

Growth conditions	Doubling time (h)	
	+O_2	-O_2
E. coli MG1655 + g	3.8	4.1
SQ6 + g	1.7	2.5
SQ10 + g	1.8	2.6
SQ11 + g	1.9	1.8
SQ12 + g	1.6	2.4
SQ13 + g	1.8	2.5
E. coli MG1655 + SQ	n.g.	51.8
SQ6 + SQ	13.2	8.8
SQ10 + SQ	n.g.	20.0
SQ11 + SQ	16.8	8.8
SQ12 + SQ	14.4	9.5
SQ13 + SQ	15.9	8.9

3.2.8 Human fecal bacteria able to convert isethionate- or 3-sulfolactate were identified as *B. wadsworthia* or *E. coli* respectively

Previous incubation experiments with human fecal slurries and isethionate or 3-sulfolactate had shown that the fecal microbiota of all donors (n = 10) converted both sulfonates to H_2S (Fig. 8). To identify the bacteria responsible for these conversions, human fecal enrichment-cultures (1%) from D10 containing either isethionate or 3-sulfolactate as electron acceptor and both formate and DL-lactate as electron donors were set up.

Five bacterial strains were isolated from the enrichment cultures with isethionate (Ise1 to Ise5) and three from enrichment cultures with 3-sulfolactate (3-SL1 to 3-SL3). Of these, two isethionate- and two 3-sulfolactate-utilizing isolates (Ise2, Ise3, 3-SL1 and 3-SL2) converted the respective sulfonate to H_2S (Fig. 16A). The isolates Ise2 and Ise3 converted 75% of the initial isethionate (20 mM) to H_2S within 48 h (Fig. 16A). The isolates 3-SL1 and 3-SL2 released 42.5% of the initial 3-sulfolactate concentration (4 mM) as H_2S within 48 h (Fig. 16A). All isolates were identified as Gram-negative rods (Fig. 16B, C).

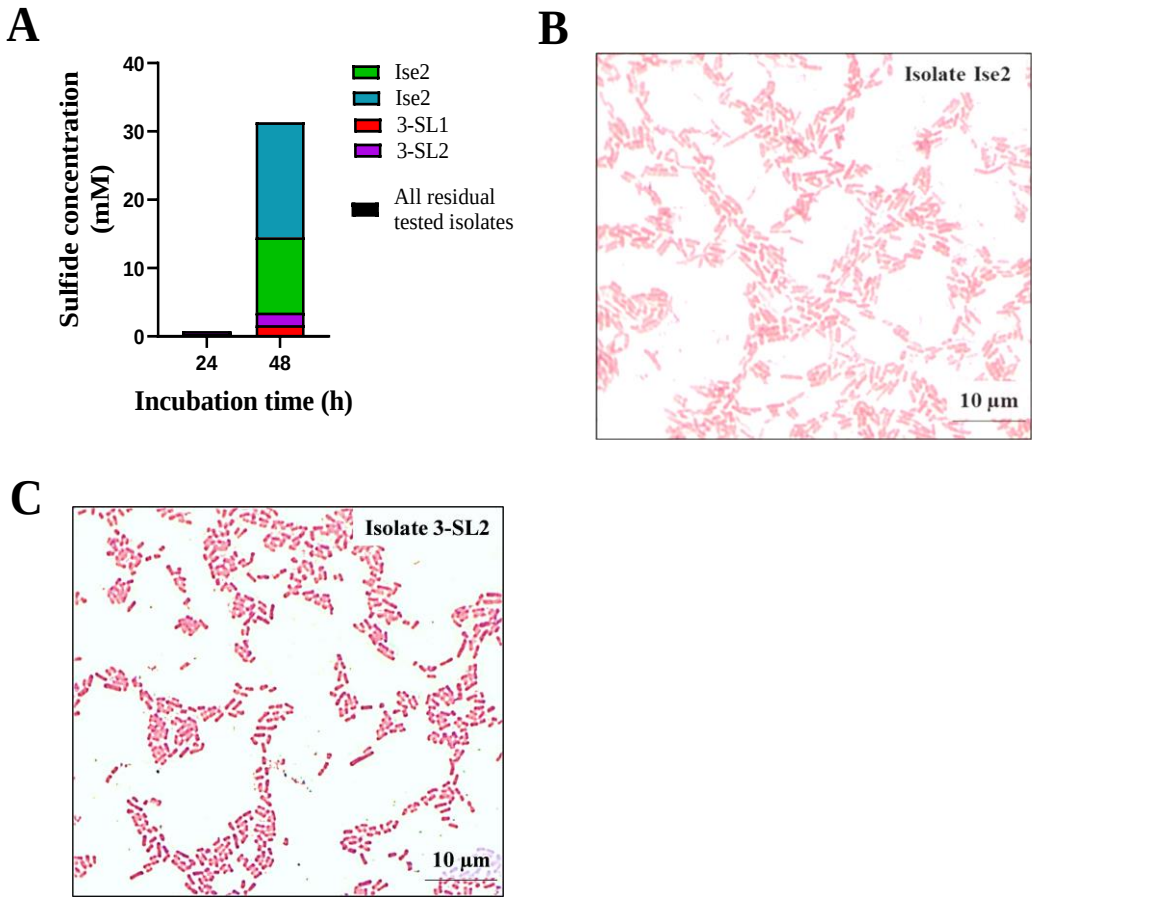

Figure 16: Isethionate- and 3-sulfolactate-utilizing bacteria able to convert both sulfonates to H_2S during anoxic incubation were identified as Gram-negative rods. (A) H_2S concentration in anoxic cultures of isolates Ise1 to Ise5 with isethionate (Ise, 20 mM) or isolates 3-SL1 to 3-SL3 with 3-sulfolactate (3-SL, 4 mM). Ise1 to Ise5 and 3-SL1 to 3-SL3 were isolated from fecal anoxic enrichment cultures growing on isethionate (20 mM) or 3-sulfolactate (4 mM), respectively. Human fecal slurries (1%) from donor 10 were used. **(B)** Gram staining of one isethionate-converting isolate (Ise2) and **(C)** one 3-sulfolactate-converting (3-SL2) isolate. Data are expressed as mean (n = 2).

16S rRNA gene sequencing and alignment with BLASTn identified the isethionate-converting isolates (Ise2 and Ise3) as being identical to each other and to *B. wadsworthia* type CCUG 32349^T (99 - 100% identity, 1329 - 1369 bp) (Table 14A). The ability of *B. wadsworthia* to convert isethionate in this study is in accordance with previous investigations, in which *B. wadsworthia* RZATAU (DSM 11045) and *B. wadsworthia* 3.1.6 converted isethionate to H_2S [8, 136, 312]. The *16S rRNA* gene sequence of *B. wadsworthia* isolates Ise2 and Ise3 was 99% identical to that of *B. wadsworthia* RZATAU (DSM 11045) (Table 14A).

3-Sulfolactate-converting isolates were closely related to the *E. coli* taxonomic group (98 - 100%, isolate 3-SL1: 554 bp, 3-SL2: 1064 bp) (Table 14B). Both isolates were 98 - 99% identical to type strain *E. coli* DSM30083^T and to the SQ-utilizing strain *E. coli* MG1655 (Table 14B). Both isolates were 99% identical to each other and to previously isolated SQ-converting isolates (SQ6, SQ10, SQ11, SQ12 and SQ13) (Table 14B).

Table 14: (A) Identification and alignment of isethionate- and (B) 3-sulfolactate-converting isolates based on their *16S rRNA* gene sequence using BLASTn. *B. wadsworthia* CCUG 32349^T and *E. coli* DSM30083^T are the type strains and *B. wadsworthia* RZATAU (DSM 11045) and *E. coli* MG1655 are known to degrade isethionate to H_2S or SQ to DHPS, respectively [8, 136, 251, 312].

A

16S rRNA	Isethionate-converting isolates Ise2 and Ise3	*B. wadsworthia* type strain CCUG 32349^T	*B. wadsworthia* RZATAU (DSM 11045)
Isethionate-converting isolates Ise2 and Ise3	100%	99 - 100%	99%

B

16S rRNA	3-Sulfolactate converting isolates 3-SL1 and 3-SL2	*E. coli* taxonomic group	*E. coli* DSM30083^T	*E. coli* MG1655	SQ-converting isolates
3-Sulfolactate converting isolates 3-SL1 and 3-SL2	99%	98 - 100%	98 - 99%	98 - 99%	99%

However, RAPD fingerprint patterns of *E. coli* MG1655, isolates SQ6 and 3-SL2 implied strain differences (Fig. 17).

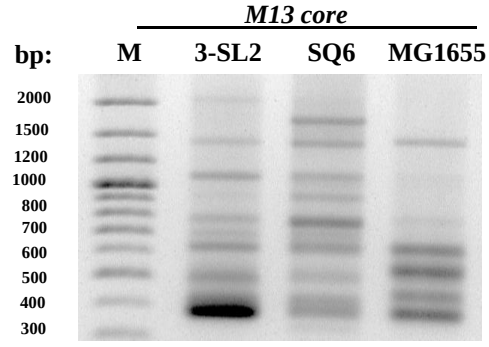

Fig. 17: RAPD-PCR profiles of the isolates 3-SL2, SQ6 and *E. coli* MG1655 using M13-core primer and a 2% agarose gel in 1 x TAE buffer (Appendix, Table A1).

Previous investigations have shown that 3-sulfolactate serves next to DHPS as an intermediate in microbial SQ-to-H_2S degradation (Fig. 2). While from *E. coli* it is well known that the bacterium converts SQ to DHPS, it has never been investigated if *E. coli* is also able to convert 3-sulfolactate or DHPS directly to H_2S [251]. Therefore, the ability of the *E. coli* isolates SQ6 (Fig. 14A), 3-SL2 (Fig. 16C) and *E. coli* MG1655 to convert DHPS or 3-sulfolactate to H_2S was examined.

Growth of all bacteria increased in the presence of 3-sulfolactate and H_2S was simultaneously released (Fig. 18). DHPS did not stimulate the growth of the bacteria, nor the release of H_2S (Fig. 18). *E. coli* MG1655 incubated with 3-sulfolactate had the shortest doubling time (5.4 ± 1.9 h) compared to isolates incubated with 3-sulfolactate (isolate 3-SL2: 6.3 ± 0.01 h and isolate SQ6: 7.4 ± 3.6 h) (Table 15). A slight increase of the OD_{600} was detected for cultures of isolate 3-SL2 incubated without sulfonate: maximally 0.01 within 48 h. This was 15 times lower than the highest OD_{600} observed for isolate 3-SL2 during incubation with 3-sulfolactate (Figure 18).

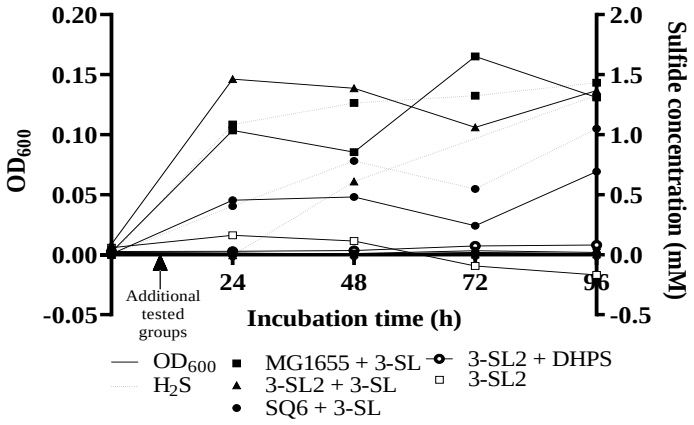

Fig. 18: Growth (OD_{600}) and H_2S formation during anoxic incubation of the isolates 3-SL2, SQ6 or strain *E. coli* MG1655 with 3-sulfolactate (4 mM) or 2,3-dihydroxypropane-1-sulfonate (DHPS, 4 mM) in comparison to cultures without sulfonates. Formate (40 mM) was used as electron donor. The gas phase was N_2/CO_2 (80/20, v/v, %). H_2S was quantified with the methylene blue method. Data are expressed as mean (n = 2).

Table 15: Growth (doubling time) during anoxic incubation of *E. coli* MG1655, the isolate 3-SL2 or the isolate SQ6 with 3-sulfolactate (3-SL, 4 mM). Data are expressed as mean ± SEM (n = 2).

Growth conditions	Doubling time (h)
E. coli MG1655 + 3-SL	5.4 ± 1.9
Isolate 3-SL2 + 3-SL	6.3 ± 0.01
Isolate SQ6 + 3-SL	7.4 ± 3.6

3.2.9 *In vitro* cultures of *B. wadsworthia* converted TC, taurine, isethionate, and DHPS to H_2S

Anoxic respiration of TC, taurine, isethionate, cysteate, and DHPS to H_2S by *B. wadsworthia* has been described earlier [8, 9, 136], which was confirmed in this study (Fig. 19). Growth (OD_{600}) and H_2S formation was detected from 24 h to 96 h during incubation with

TC, isethionate, and taurine (Fig. 19A). A small increase of OD_{600} and H_2S was observed for DHPS when compared to the control incubation without *B. wadsworthia*. While the highest OD_{600} with isethionate was reached at 48 h (OD_{600} = 0.25), the incubation with TC or taurine led to a continuous growth (OD_{600} = 0.30) to 96 h (Fig. 19A). In contrast, growth with DHPS was weaker, with the highest value of 0.005 at 96 h, which is approximately 60 times less than observed for taurine and TC and 50 times less than observed for isethionate. Doubling times of *B. wadsworthia* with TC (5.6 h), taurine (4.8 h) or isethionate (4.2 h) were similar, but 1.8 to 2.5 times higher with DHPS (10.3 h) (Fig. 19C).

TC, taurine, and isethionate (initially 20 mM each), were completely converted to H_2S (Fig. 19A). In contrast, only 1.25% of the initial DHPS (4 mM) was released as H_2S. An incubation time of 120 h of *B. wadsworthia* with DHPS revealed no further increase in H_2S concentration in comparison to after 96 h (data not shown). H_2S release from taurine or isethionate increased continuously to 96 h, while the highest concentration of H_2S released from TC or DHPS was observed at 72 h (Fig. 19A). No growth and release of H_2S were detected within 96 h in cultures containing cysteate, CoM, SQ or 3-sulfolactate (Fig. 19A).

Due to interference of FeS in H_2S-forming cultures with the OD_{600} measurements, bacterial growth was in addition determined based on cell counting using the Thoma chamber. The results confirmed that taurine, isethionate, TC, and DHPS stimulated the growth of *B. wadsworthia*, while cysteate, CoM, SQ or 3-sulfolactate did not do so (Fig. 19B). Since the results for cysteate are in conflict with previous findings, the incubation time for this sulfonate was extended to 207 h. The enumeration of the cells with the counting chamber and the amount of H_2S released, revealed an increase of cells from 48 h (10^6 cells /ml) to 207 h (10^8 cells/ml). Similarly, H_2S was released from cysteate between 80 and 207 h of incubation, with a final concentration of 12 mM at 207 h, indicating a partial conversion (30%) of cysteate to H_2S.

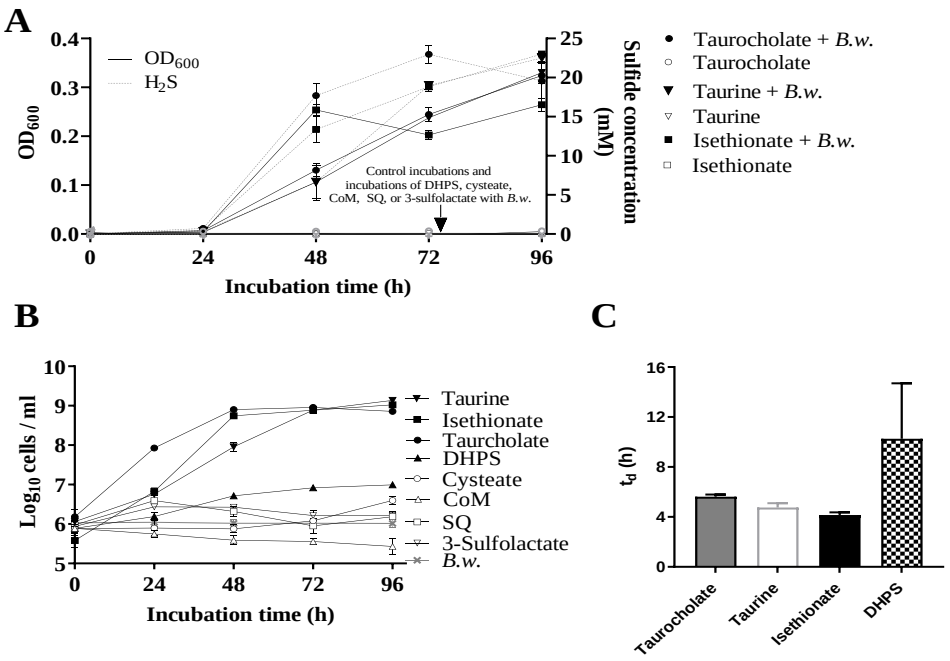

Figure 19: *B. wadsworthia* converted taurocholate, taurine, isethionate and 2,3-dihydroxypropane-1-sulfonate (DHPS) to H_2S during anoxic respiration within 96 h. (A) Growth (OD_{600}) and H_2S formation by *B. wadsworthia* (*B.w.*) exposed to taurocholate, taurine, isethionate (all 20 mM), DHPS, cysteate (20 mM), Coenzyme M (CoM), sulfoquinovose (SQ), or 3-sulfolactate (all 4 mM) under anoxic conditions in comparison to control incubations (each sulfonate without *B. wadsworthia* or *B. wadsworthia* without sulfonate). (**B)** Cell numbers during anoxic incubation with taurocholate, taurine, isethionate, DHPS, cysteate, CoM, SQ, or 3-sulfolactate, determined with the Thoma counting chamber. (**C)** Doubling time (t_d) of incubations of (A). H_2S was quantified with the methylene blue method. Data presented as mean (± SEM).

3.2.10 Anoxic co-culturing of the *E. coli* isolate SQ6 and *B. wadsworthia* led to the conversion of sulfoquinovose to H_2S

A co-culturing model of the gut bacterium *B. wadsworthia* with a member of the *Enterobacteriaceae*, namely *E. rectale* DSM 17629, degrades SQ to H_2S via DHPS under anoxic conditions [325]. Whether a co-culture of another member of the *Enterobacteriaceae*, namely *E. coli* isolate SQ6, and *B. wadsworthia* converts SQ to DHPS was tested in this study (Fig. 20A).

SQ conversion by strain SQ6 has previously been tested in MSM (Appendix, Table A1), whereas DHPS conversion by *B. wadsworthia* has been in a basal medium (Appendix, Table A1). To provide the same growth conditions for both bacteria, the growth of strain SQ6 with SQ in basal medium was tested (Fig. 20B). Strain SQ6 grew in this medium within 24 h, a prerequisite to proceed with the co-culturing experiment.

To ensure that only SQ enabled strain SQ6 and only DHPS enabled *B. wadsworthia g*rowth, the following control incubations were included: 1) incubation of each bacterium with SQ or DHPS, 2) inoculated medium without addition of SQ, and 3) medium containing SQ and DHPS. When strain SQ6 and *B. wadsworthia* were incubated together with SQ, bacterial growth of both strains was enhanced (Fig. 20C). Cell numbers increased to 10^1 cells/µl for both *B. wadsworthia* and isolate SQ6 during co-culture when compared to the control incubations (Fig. 20C). These findings were consistent with the calculated doubling

time: The co-culture had a doubling time of 3.6 ± 0.4 h, while single incubations of strain SQ6 + SQ led to a doubling time of 8.1 ± 0.8 h and of *B. wadsworthia* + DHPS to 15.2 ± 0.5 h (Table 16).

The co-culture converted SQ via DHPS to H_2S (Fig. 20D). SQ was no longer detectable after 24 h even though only 80% of the DHPS was converted (Fig. 20D). The highest DHPS concentration was measured at 24 h and 75% was recovered as H_2S within 72 h (Fig 20D). H_2S formation increased from 1.25% for the incubation of *B. wadsworthia* with DHPS, to 75% for the co-culture with *E. coli* (Fig. 20D).

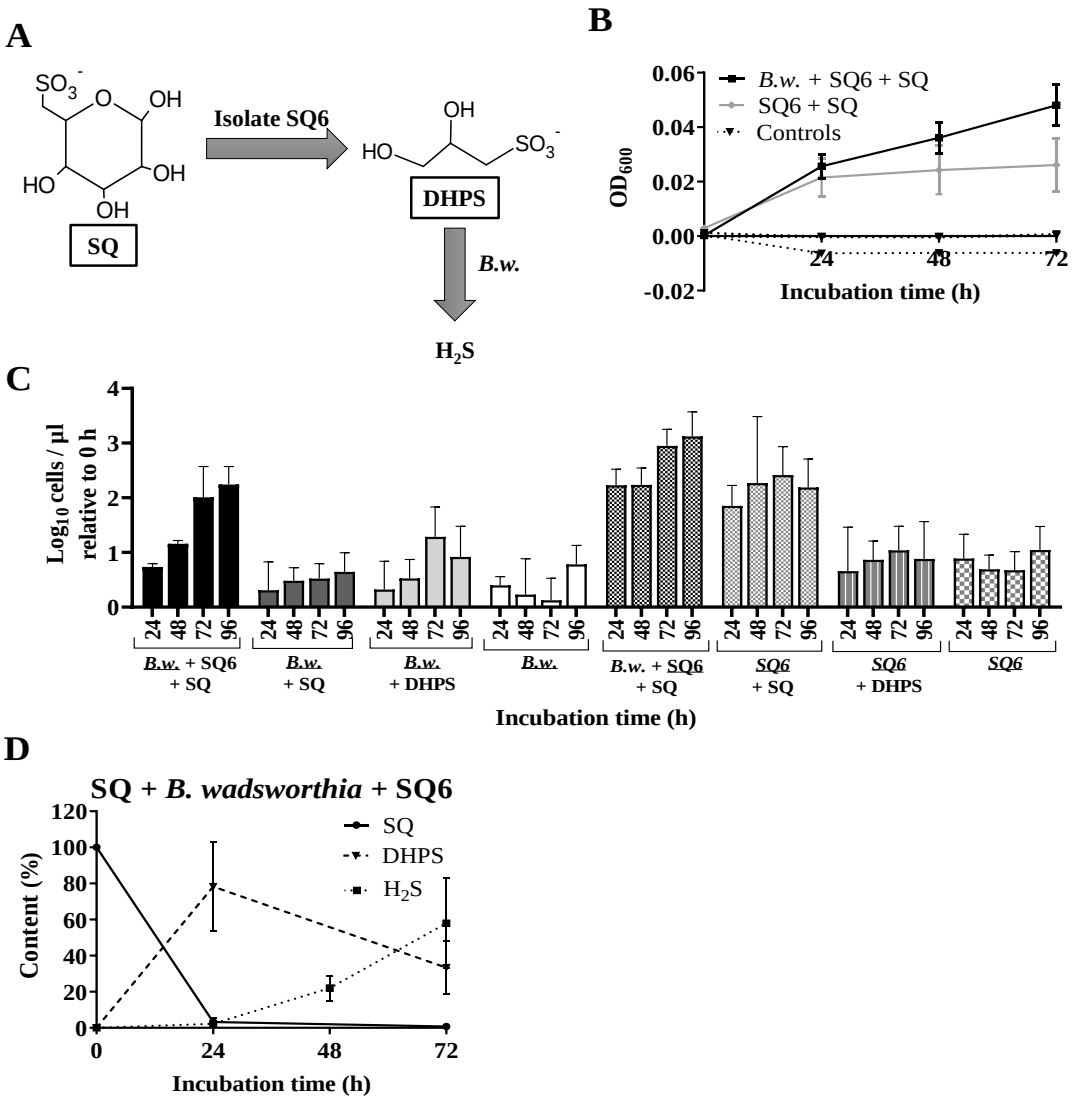

Figure 20: A co-culture of *Bilophila wadsworthia* (*B.w.*) and a fecal *E. coli* isolate completely degraded sulfoquinovose (SQ) to sulfide (H_2S). (A) Scheme of the investigated experiment. (**B)** Growth (OD_{600}) of isolate SQ6 with SQ tested in basal medium (Appendix, Table A1). **(C)** Growth of the SQ-converting isolate SQ6 and *B. wadsworthia* co-cultured for 72 h under anoxic conditions with SQ or 3-dihydroxypropane-1-sulfonate (DHPS) (both 4 mM). Growth was measured with qPCR. Underlined bacteria indicate the cell number of the specific bacterium in this incubation. Included controls were SQ + strain SQ6, SQ + *B. wadsworthia*, DHPS + strain SQ6, DHPS + *B. wadsworthia*, SQ + DHPS or single incubation of strain SQ6 or *B. wadsworthia*. (**D)** Sulfonate and H_2S concentrations measured in the anoxic co-culture experiments. SQ was also degraded during incubation with isolate SQ6, but not during incubation with *B. wadsworthia* or during incubation of SQ without bacterial cultures (data not shown). No H_2S was released when either *B. wadsworthia* or strain SQ6 were cultivated in the absence of any sulfonate. SQ was measured with LC-MS/MS analysis and H_2S with the methylene blue method. Data presented as mean ± SEM (n = 3).

Table 16: Growth (doubling time) of *Bilophila wadsworthia* (*B.w.*) and the *E. coli* isolate SQ6 during anoxic co-culturing with sulfoquinovose (SQ, 4 mM) in comparison to individual incubations with SQ or 2,3-dihydroxypropane-1-sulfonate (DHPS, 4 mM) or SQ (4mM). Data presented as mean ± SEM (n = 3).

Growth conditions	Doubling time (h)
SQ6 + *B.w.* + SQ	3.6 ± 0.4
SQ6 + SQ	8.1 ± 0.8
B.w. + DHPS	15.2 ± 0.5

3.3 Spirulina feeding experiment in conventional mice

Sulfonates serve as sulfite source in the gut and thereby may stimulate the growth of colitogenic bacteria such as *B. wadsworthia* [9]. Knowledge about the fate of dietary sulfonates in the intestinal tract after ingestion and their effect on the gut microbiota composition is scarce. This although sulfonates, such as SQDG are present in salad, spinach or parsley, and therefore part of the daily human nutrition. SQDG are also highly abundant in Spirulina which is used as a nutrition supplement. To investigate whether SQDG enhance the growth of pro-inflammatory bacteria such as *B. wadsworthia*, conventional C57BL/6J mice were fed a semisynthetic diet supplemented with 20% Spirulina (SD) or a semisynthetic control diet (CD) for three weeks. Body-weight development, feed and water intake, macroscopic and histological organ parameters, intestinal inflammation and gut microbiota composition were investigated and related to sulfonate levels in the gastrointestinal tract.

3.3.1 Spirulina diet feeding initially increased body weight and led to fat tissue accumulation, a decreased liver weight and a smaller stomach surface

The body weight of the SD-fed mice was approximately 4% elevated at day two compared to CD-fed mice, but increased in both groups to a similar extent thereafter (Fig. 21A). Similarly, daily food intake from day 0 to day 2 was 30% higher in SD-fed mice than in CD-fed mice, but converged thereafter (Fig. 21B). To illustrate the effect of food intake on the body-weight increase in the first two days of intervention, the ratio of body-weight gain (%) per 1 g consumed diet during this timeframe was determined. This ratio was approximately four times higher in SD-fed compared to CD-fed mice (Fig. 21C), illustrating that food intake is not or not the only reason for the body-weight gain. Other parameters previously associated with body-weight gain that might be affected by the intake of SQDG-containing SD will be discussed below (3.3.6 ff.).

SD-fed mice had a significantly reduced liver weight relative to body weight (CD: 5.92 ± 0.80%; SD: 5.37 ± 0.42%, Fig. 21D) and a reduced stomach surface (CD: 2.14 cm^2 ± 0.53; SD: 1.63 ± 0.32 cm^2, Fig. 21E), while eWAT (1.5 times), sWAT (1.5 times), mWAT (1.5 times) and pWAT (2.5 times) relative to body weight in comparison to CD-fed mice was elevated (Fig. 21F). Shortening of the colon or splenomegaly, which has previously been linked to an infection by *B. wadsworthia* and inflammation [326, 327], was not observed.

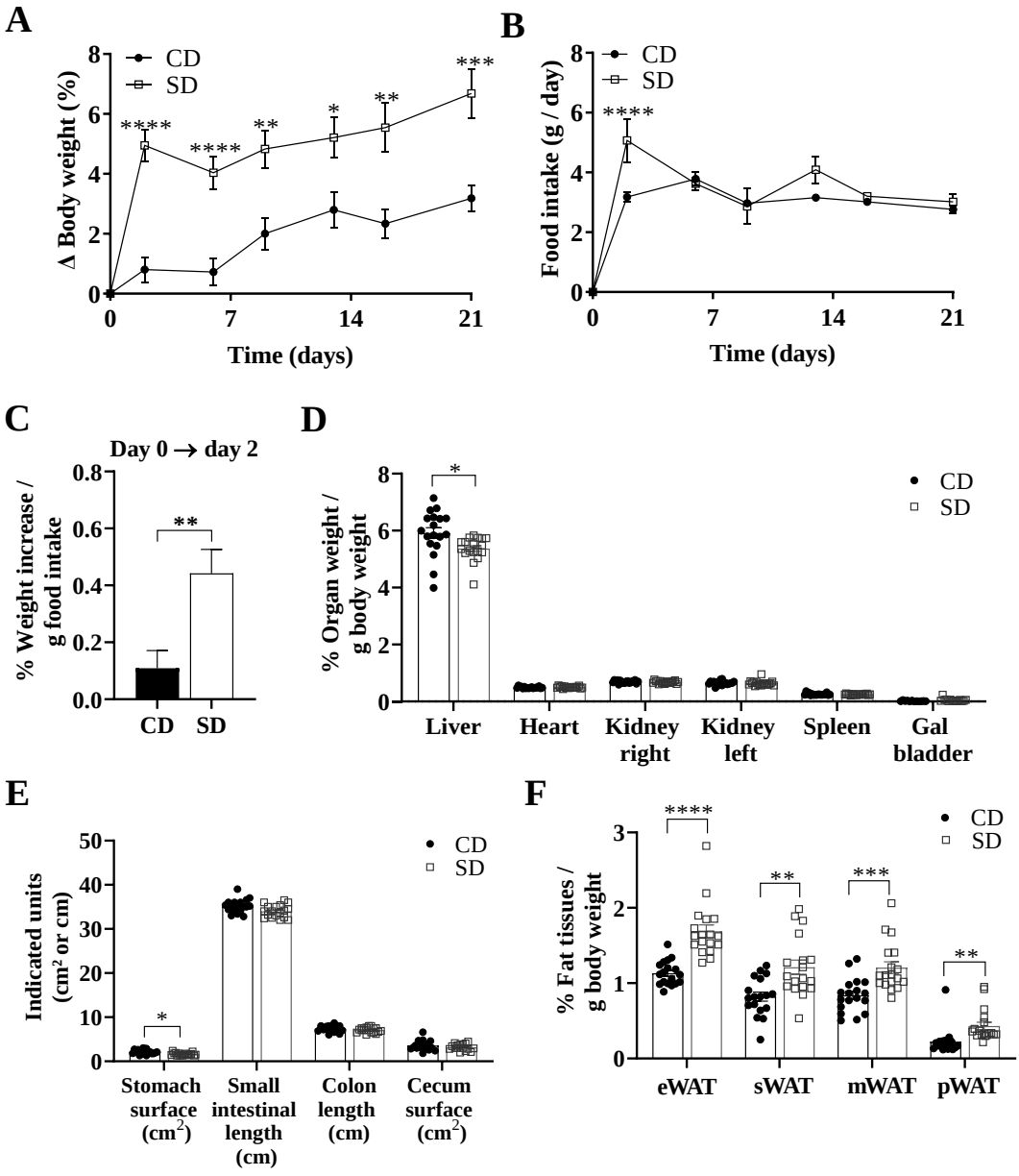

Figure 21: Body-weight increase, liver-weight and stomach surface reduction and fat tissue accumulation in conventional C57BL/6J mice after intake of an SQDG-containing diet. (A) Body-weight development (mean ± SEM, n = 16 - 18), (**B)** time course of food intake, (**C)** ratio of % weight increase per g food intake from day 0 to day 2 (mean ± SEM, n = 17 - 18), and (**D - F)** organ weight, length and size (mean ± SEM, one symbol per mouse) after 3 weeks intake of a semisynthetic diet supplemented with 20% Spirulina of conventional C57BL/6J mice (SD) vs. C57BL/6J mice fed a semisynthetic diet without Spirulina (CD). Stomach and cecum surface were measured by length × width. eWAT = epididymal white adipose tissue, sWAT = subcutaneous white adipose tissue, mWAT = mesenteric white adipose tissue, pWAT = perirenal white adipose tissue. CD vs. SD: **P* < 0.05, ***P* < 0.01, ****P* < 0.001 and *****P* < 0.0001.

3.3.2 SQDG of Spirulina were converted to SQ during small intestinal transit

SQDG were reported to make up 32% of total lipids of Spirulina [328]. Intestinal bioavailability and digestibility of ingested macronutrients encapsulated by a plant cell, such as SQDG, depend on the breakdown of the cell wall. Cell walls are largely made from polysaccharide and glycoproteins, which are often resistant to digestive enzymes of the gastrointestinal tract [329, 330]. Therefore, the microscopic appearance of macronutrients in Spirulina

powder, prepared SD, and fecal samples of mice fed SD (20 days) was compared (Fig. 22A). The microscopic inspection suggests that the preparation and processing of the SD did not lead to a breakdown of the cellular wall of Spirulina. In contrast, the cell integrity after passage through the gastrointestinal tract was diminished, indicating the availability of cellular components from Spirulina such as SQDG for gut bacteria as substrates.

SQ and DHPS in gastrointestinal contents and feces of SD-fed mice were quantified and compared to those of CD-fed mice. After 16 days of intervention, SQ in cecal contents (n = 7/15) and feces (n = 12/12) of mice fed SD was higher than of mice fed CD (Fig. 22B). However, in cecal contents SQ was only observed in seven out of 15 SD-fed mice. Therefore, different cecal SQ concentration between CD- and SD-fed mice did not reach significance. The SQ- and DHPS-concentrations did not differ in stomach, small intestinal, and colonic contents between the two groups, despite of single mice having higher levels (Fig. 22B). This might indicate that SQ is released from SQDG but conversion to DHPS did not occur.

The release of SQ from SQDG seems to predominantly occur in the cecum. The observed differences in sulfonate conversion among individual mice may be due to differences in microbiota composition which will be examined below (3.3.5).

A

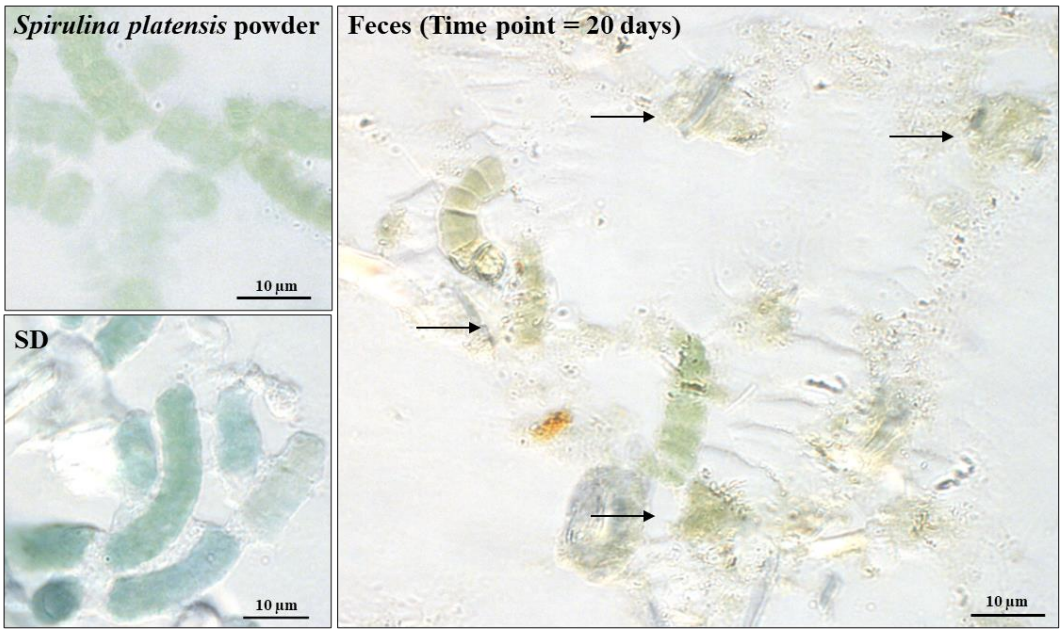

B

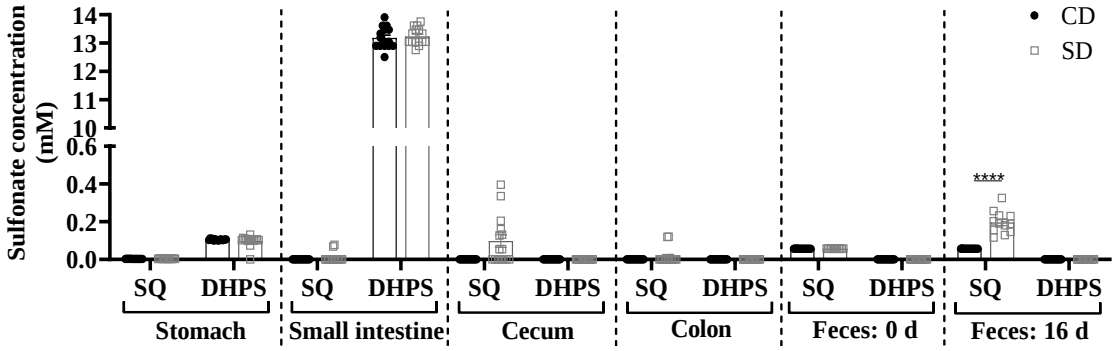

Figure 22: Cell wall breakdown and gastrointestinal release of sulfoquinovose (SQ) in conventional C57BL/6J mice fed a semisynthetic diet supplemented with 20% Spirulina (SD). (A) Representative microscopic images of samples of Spirulina as present in freeze-dried powder, in SD and in murine feces after 20 days (d) of feeding. Samples were examined microscopically at a 100 x magnification. (**B)** SQ and 2,3-dihydroxypropane-1-sulfonate (DHPS) concentrations measured in indicated gastrointestinal contents after 21 d and in feces after 16 d of SD- or semisynthetic control diet (CD)-fed mice with LC-MS/MS analysis (n = 12 - 15, mean ± SEM, one symbol per mouse). Values < LLOQ (detection limit) were set as 0 (SQ: small intestine_CD and colon_CD n = 15 < LLOQ, small intestine_SD and colon_SD, n = 13 < LLOQ, cecum_CD n = 15 < LLOQ, cecum_SD n = 7 < LLOQ. DHPS: stomach_SD n = 1< LLOQ, and small intestine, cecum, colon, feces in both groups all tested samples were < LLOQ). CD- vs. SD-fed mice: ****P < 0.0001.

3.3.3 SQDG-containing diet influenced the expression of SQ- and DHPS-degrading enzymes of bacteria in intestinal contents and tissues.

To investigate whether the elevated SQ levels in cecal contents and feces of SD-fed mice promoted the growth of SQ- and / or DHPS-degrading gut bacteria, gene copies of two bacterial key enzymes involved in the utilization of these sulfonates were analyzed: the isomerase (*yihS*), catalyzing the first step in bacterial SQ degradation, and the *dsrABC*, responsible for the six-electron reduction of SO_3^{2-} to H_2S in the last step of DHPS degradation [9, 249, 251, 331]. The isomerase *yihS* was not present in feces of SD-fed mice and only detected in few CD-fed mice at the beginning of the study and at day six of intervention (Fig. 23A). However, a clear difference in *yihS* abundance was observed in the cecal contents of SD- and

CD-fed mice (Fig. 23C). A reduced gene *yihS* abundance in SD-fed mice indicates a lower SQ degradation, which is consistent with elevated SQ concentrations observed in this part of the gut (3.3.2). *dsrA* abundance in feces of CD-fed mice did not change over time, but decreased in abundance in feces of SD-fed mice until day nine and recovered almost completely until day 16 (Fig. 23B). There were no differences in *dsrA* levels in cecal contents (Fig. 23C).

3.3.4 Spirulina feeding evoked a mild immune response in the ileum

The growth of the colitogenic bacterium *B. wadsworthia* is enhanced by the presence of intestinal sulfonates, inducing colitis [9]. Potential pro-inflammatory effects of the sulfonate-containing SD were analyzed in the intestinal mucosa (Fig. 23D). The pro-inflammatory cytokines interleukin (IL)-6 and tumor necrosis factor (TNF)-α were considered as markers of inflammatory conditions in the intestine. *Il-6* expression was higher in the ileal mucosa of SD-fed mice, but was not affected in jejunal or colon mucosa (Fig. 23D). Similarly, *Tnf-α* was not differently expressed in mucosa in response to the diet, but an increased trend was detected in the ileum (Fig. 23D).

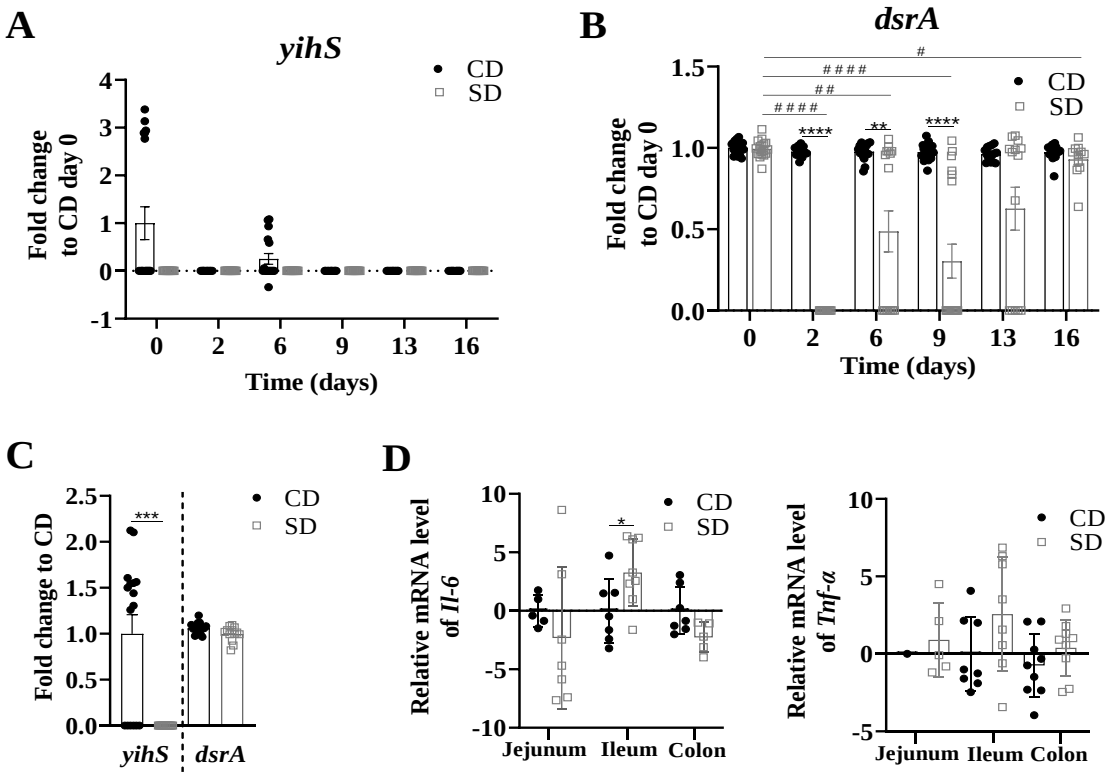

Figure 23: Fold change in the expression of bacterial genes involved in SQ degradation in feces and cecal contents and relative gene expression of inflammatory markers in intestinal mucosa of mice fed a semisynthetic diet supplemented with 20% Spirulina (SD) versus mice fed a semisynthetic control diet (CD) for 21 days. (A, B) Relative fold change of the sulfoquinovose isomerase (*yihS*) and the dissimilatory sulfite reductase subunit A (*dsrA*) in feces or **(C)** in cecal contents. Values were normalized to (CD)-fed mice at day 0. Data presented as mean ± SEM (n = 14 - 18). *: CD versus SD-fed mice for each point in time or tissue; #: SD-fed mice at day 0 versus SD-fed mice at different points in time. (**D)** Gene expression of the inflammatory markers *interleukin* (*Il*)*-6* and *tumor necrosis factor* (*Tnf*)*-α* in intestinal mucosa of CD- vs. SD-fed mice after 21 days of intake. Data presented as mean ± SEM (n = 10). Each dot represents one mouse. Quantified gene-expression levels below the detection limit are not shown. *: CD-fed mice versus SD-fed mice. $*,^{\#}P < 0.05$, $**,^{\#\#}P < 0.01$, $***,^{\#\#\#}P < 0.001$ and $****,^{\#\#\#\#}P < 0.0001$.

3.3.5 The fecal and cecal microbiota diversity were altered due to Spirulina diet

3.3.5.1 Spirulina changed the α- and ß-diversity

α-Diversity, species richness and evenness of murine samples, were estimated using the Shannon-Wiener index, the Simpson index, the OTUs, the richness and the evenness of each sample.

The Shannon-Wiener index describes the evenness and abundance of species (richness) within one sample [332]. The Simpson-index represents the probability of two randomly selected bacterial sequences to belong to the same bacterial species [333, 334]. After 16 days of intervention, the OTUs and the richness were significantly increased in feces of SD-fed mice compared to feces of CD-fed mice (Fig. 24C, D). No differences were detected in the Shannon-Wiener index, the Simpson-index, and the evenness in feces (Fig. 24A, B, E). In cecal contents of SD-fed mice, the OTUs and the richness revealed a significantly increased bacterial α-diversity compared to CD-fed mice (Fig. 24F, G). Also, the evenness was increased (Fig. 24 G).

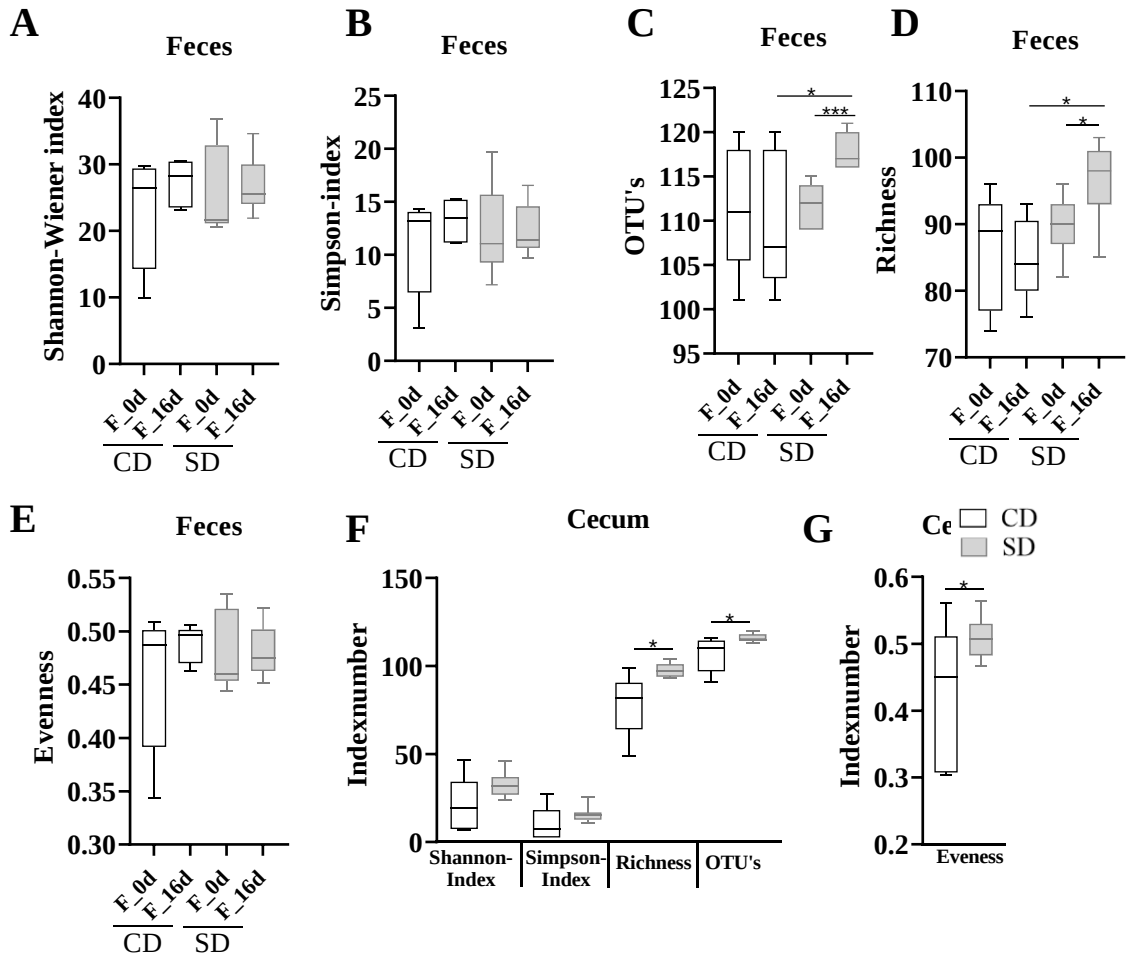

Figure 24: Alpha (α)-diversity, species richness and evenness of fecal (A - E) and cecal (F, G) microbiota of mice fed a semisynthetic diet supplemented with 20% Spirulina (SD) compared to mice fed a semisynthetic control diet (CD). The α -diversity was estimated using the Shannon-Wiener index, the Simpson-index, number of observed species (OTUs), the richness and the evenness of each sample. The Shannon-Wiener index describes the evenness and abundance of species (richness) within one sample. The Simpson-index represents the probability of two randomly selected bacterial sequences to belong to the same bacterial species. F = feces. Diets were given for 21 days. CD vs. SD: * $P < 0.05$ and ***$P < 0.001$; n = 5 - 7 per group.

ß-Diversity describes the spatial differences in microbiota composition among the animals [306]. No differences in the fecal microbiota profile were observed among the mice at the start of the intervention (Fig. 25A). After 16 days, the fecal microbiota profile of SD-fed mice was significantly different compared to baseline (day 0) ($P = 0.001$) (Fig. 25C), while the microbiota composition of CD-fed mice did not change over time (Fig. 25B). Furthermore, microbiota profiles of feces collected at day 16 (Fig. 25D, $P = 0.003$) and cecal contents collected at day 21 (Fig. 25E, $P = 0.002$) of SD-fed mice were significantly different from those of CD-fed mice.

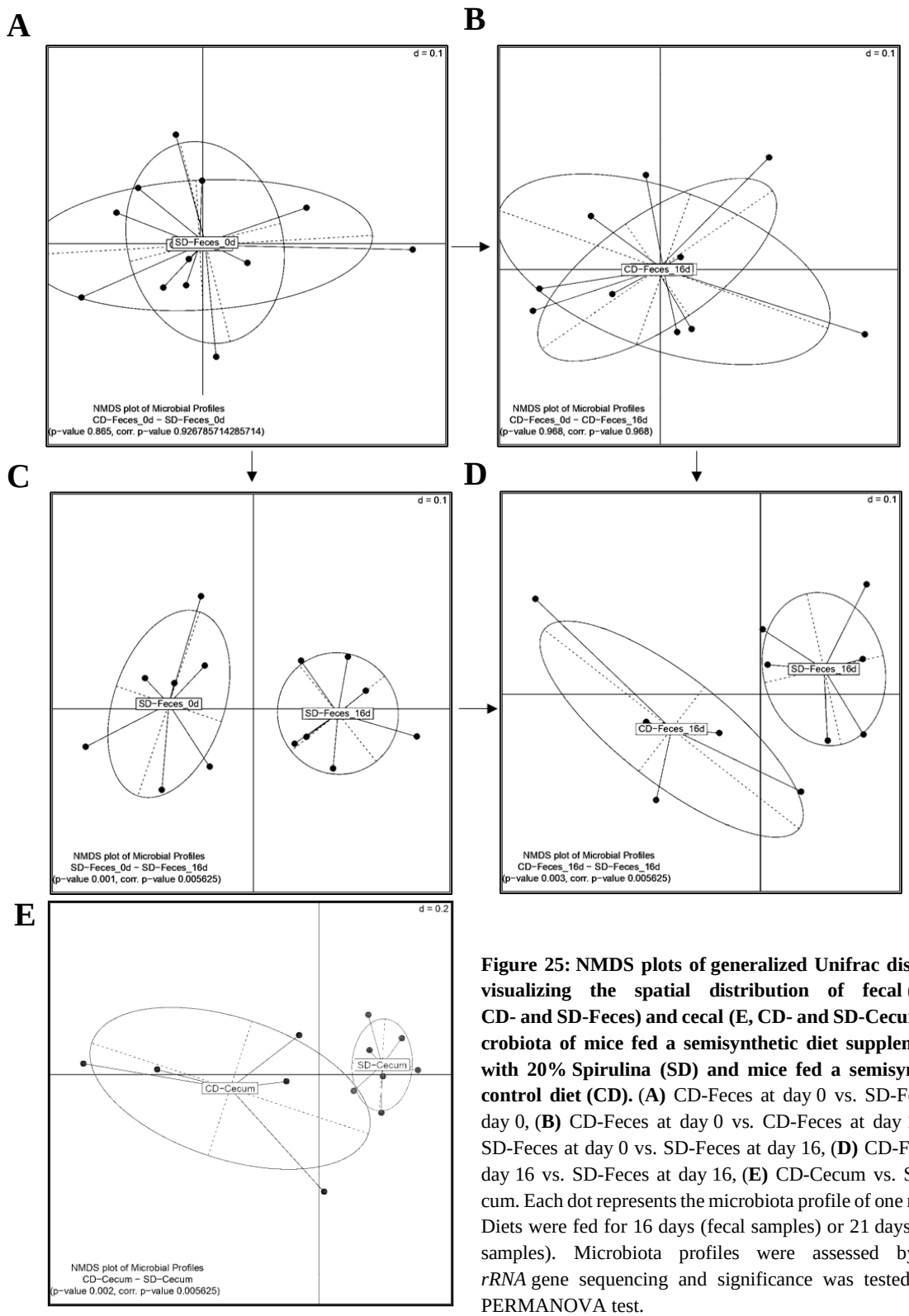

Figure 25: NMDS plots of generalized Unifrac distances visualizing the spatial distribution of fecal (A - D, CD- and SD-Feces) and cecal (E, CD- and SD-Cecum) microbiota of mice fed a semisynthetic diet supplemented with 20% Spirulina (SD) and mice fed a semisynthetic control diet (CD). (**A)** CD-Feces at day 0 vs. SD-Feces at day 0, (**B)** CD-Feces at day 0 vs. CD-Feces at day 16, (**C)** SD-Feces at day 0 vs. SD-Feces at day 16, (**D)** CD-Feces at day 16 vs. SD-Feces at day 16, (**E)** CD-Cecum vs. SD-Cecum. Each dot represents the microbiota profile of one mouse. Diets were fed for 16 days (fecal samples) or 21 days (cecal samples). Microbiota profiles were assessed by *16S rRNA* gene sequencing and significance was tested using PERMANOVA test.

3.3.5.2 Spirulina-containing diet resulted in taxonomic differences

The predominant phyla in feces, before (day 0) and after intervention (day 16), and in cecal contents after 21 days of intervention of all tested subjects were *Bacteroidetes*, *Firmicutes*, *Proteobacteria*, and *Verrucomicrobia* (Fig. 26A - E). The phylum composition in feces of all mice was identical at start of the intervention (Fig. 26A, C). When the mice were fed CD the fecal phylum composition was stable over time (Fig. 26A, B). In mice fed SD, the relative abundance of fecal *Bacteroidetes* increased (Fig. 26B, D: CD-feces_16 d vs. SD-feces_16 d: $P = 0.03$; Fig. 26C, D: SD-feces 0 d vs. SD-feces_16 d: $P < 0.001$). This also applies to cecal contents (Fig. 26E: CD-cecum vs. SD-cecum: $P < 0.001$). In contrast, fecal and cecal *Firmicutes* decreased (Fig. 26B, D: CD-feces_16 d vs. SD-feces_16 d: $P = 0.0027$; Fig. 26C, D: SD-feces 0 d vs. SD-feces_16 d: $P < 0.001$; Fig. 26E: CD-cecum vs. SD-cecum: $P < 0.001$).

The difference in relative abundance of bacterial taxa of the fecal or cecal microbiota in mice receiving CD or SD was determined in order to identify taxonomic differences in response to SQDG-containing diet (Fig. 27, 28). Members of six bacterial families in feces and seven in cecal contents of SD-fed mice were increased in comparison to CD-fed mice (Fig. 27). In feces and cecum these were most notably *Porphyromonadaceae* (feces: $P < 0.0001$; cecum: $P = 0.0001$), *Bacteroidaceae* (feces: $P = 0.0004$; cecum: $P = 0.0005$), *Lactobacillaceae* (feces: $P = 0.0051$; cecum: $P = 0.0298$), and *Rikenellaceae* (feces: $P = 0.0303$; cecum: $P = 0.0177$, Fig. 27). Unclassified *Clostridiales* were significantly increased in feces ($P = 0.0051$, Fig. 27A) and *Prevotellaceae* in cecum ($P = 0.0480$, Fig. 27B). Seven bacterial families were reduced in feces and five in cecal contents of mice fed SD (Fig. 27). In both matrixes, particularly *Erysipelotrichaceae* were decreased (feces: $P = 0.0032$; cecum: $P < 0.0001$, Fig. 27). In addition, SD led to a significant reduced level of *Sutterellaceae* ($P = 0.0480$) in feces (Fig. 27A) and a significant reduction of *Desulfovibrionaceae* in cecal contents ($P = 0.0025$) (Fig. 27B).

At genus level, nine bacterial genera in feces and ten genera in cecal contents were increased in mice fed SD (Fig. 28), particularly *Bacteroides* (both: $P = 0.0025$), *Lactobacillus* (both: $P = 0.0051$), and *Alistipes* (feces: $P = 0.0303$; cecum: $P = 0.0177$). In feces, also the numbers of *Parabacteroides* ($P = 0.0480$) and an unclassified member of the *Clostridiales* ($P = 0.0051$) was significantly increased (Fig. 28A), while in cecum an unclassified member of the *Porphyromonodaceae* ($P = 0.0480$) and *Alloprevotella* ($P = 0.0480$) were significantly increased (Fig. 28B). In mice fed SD, eight bacterial genera were reduced in feces and six in cecal contents (Fig. 28). In both matrixes, *Allobaculum* (feces: $P = 0.0061$; cecum: $P = 0.0480$, Fig. 28) and in fecal samples *Clostridium* IV ($P = 0.0025$) and *Parasutterella* ($P = 0.0480$, Fig. 28A) were significantly reduced, while an unclassified member of the *Lachnospiraceae* ($P = 0.0025$) and of the *Desulfovibrionaceae* ($P = 0.0025$) were significantly decreased in cecal contents (Fig. 28B). *Desulfovibrionaceae*, which *B. wadsworthia* belongs to, were also reduced in feces but this was not statistically significant.

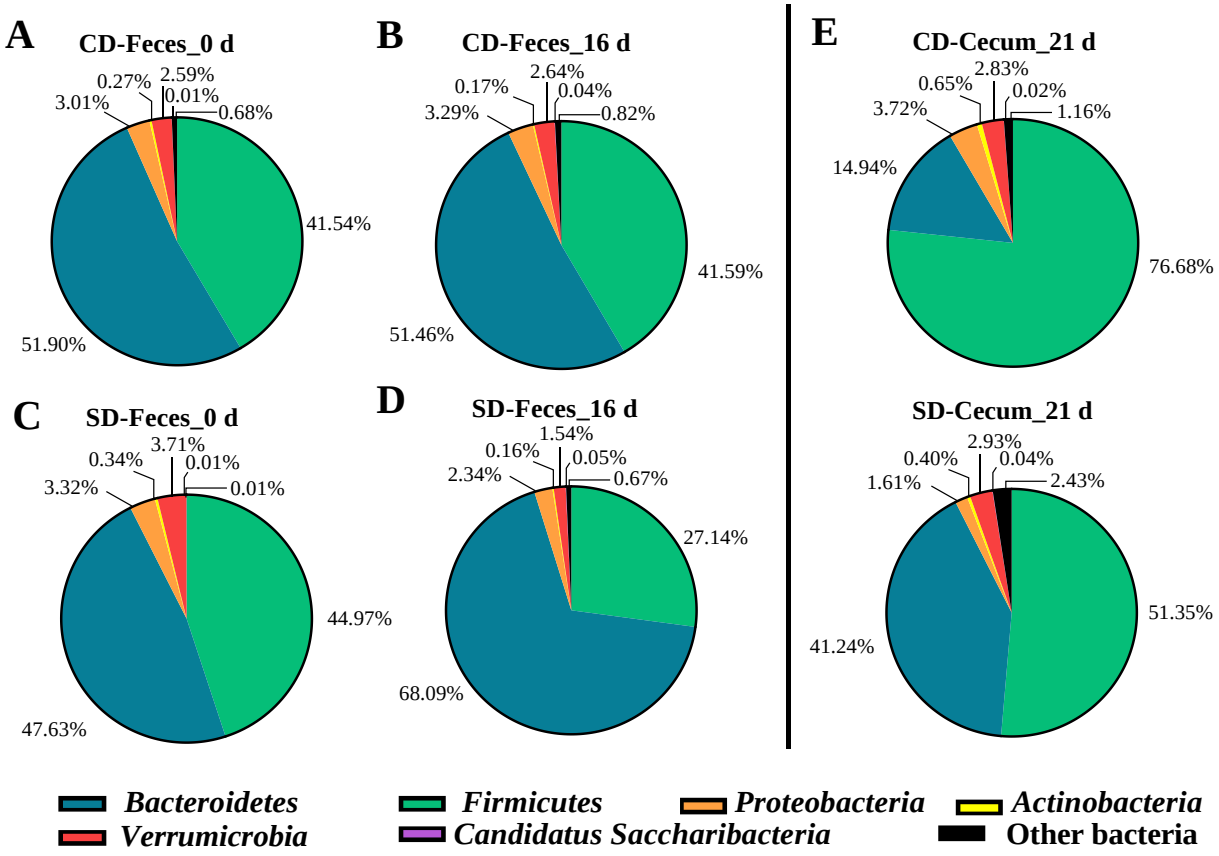

Figure 26: Relative abundance of bacterial phyla in feces (A - D) and cecal contents (E) of mice fed a semisynthetic diet supplemented with 20% Spirulina (SD) and mice fed a semisynthetic control diet (CD) at different times of the experiment. Feces were obtained at day 0 and day 16 of the intervention. Cecal contents were obtained after 21 days of the intervention. n = 5 - 7 per group.

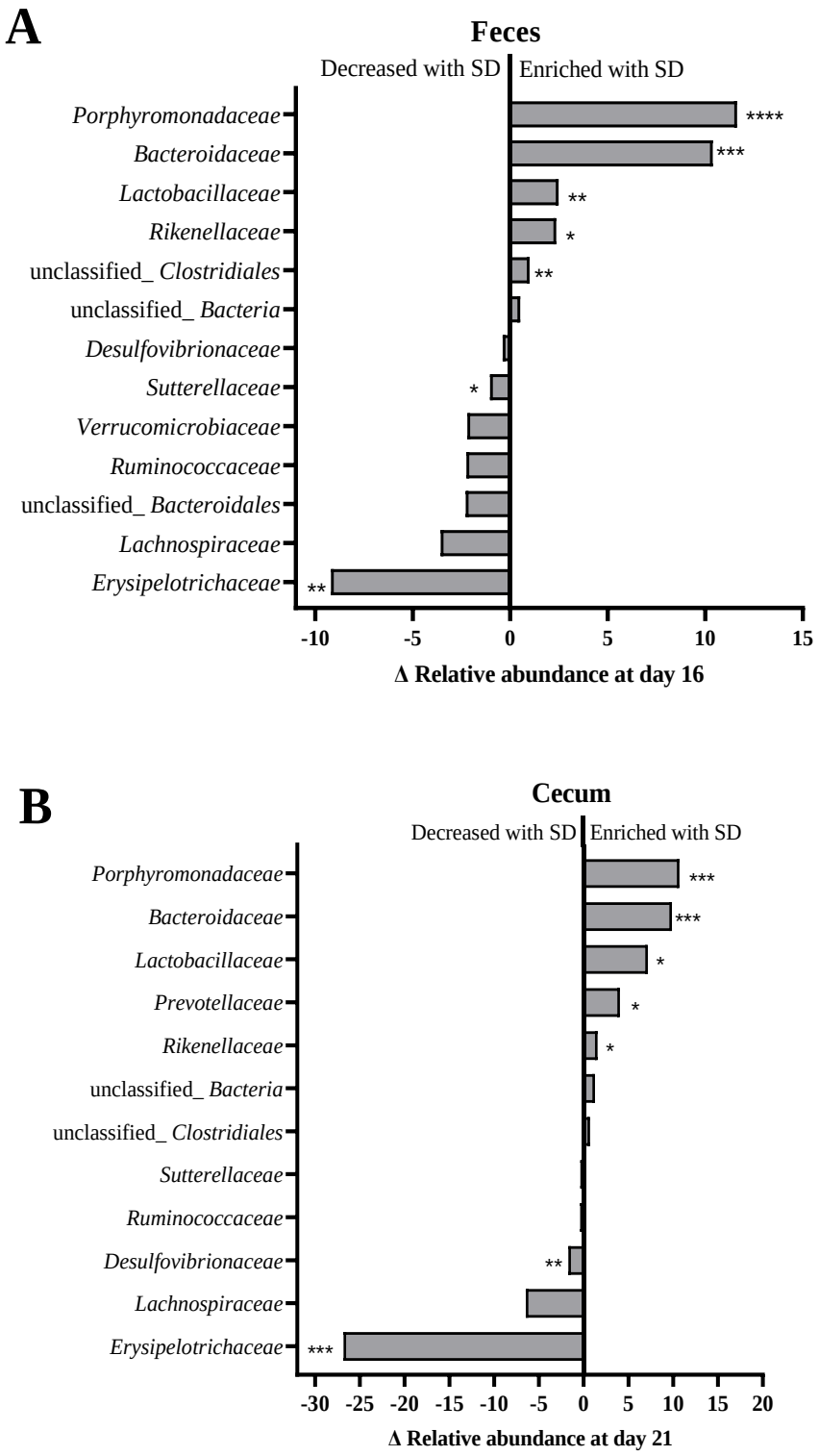

Figure 27: Family-level differences in fecal (A) and cecal (B) microbiota composition between mice fed semisynthetic diet supplemented with 20% Spirulina (SD) and mice fed semisynthetic control diet (CD). Data are presented as mean normalized to CD-fed mice (n = 5 - 7). Fecal samples were collected at day 16 and cecal contents at day 21 of intervention. CD-fed mice vs. SD-fed mice. $^{**}P < 0.01$, $^{***}P < 0.001$ and $^{****}P < 0.0001$.

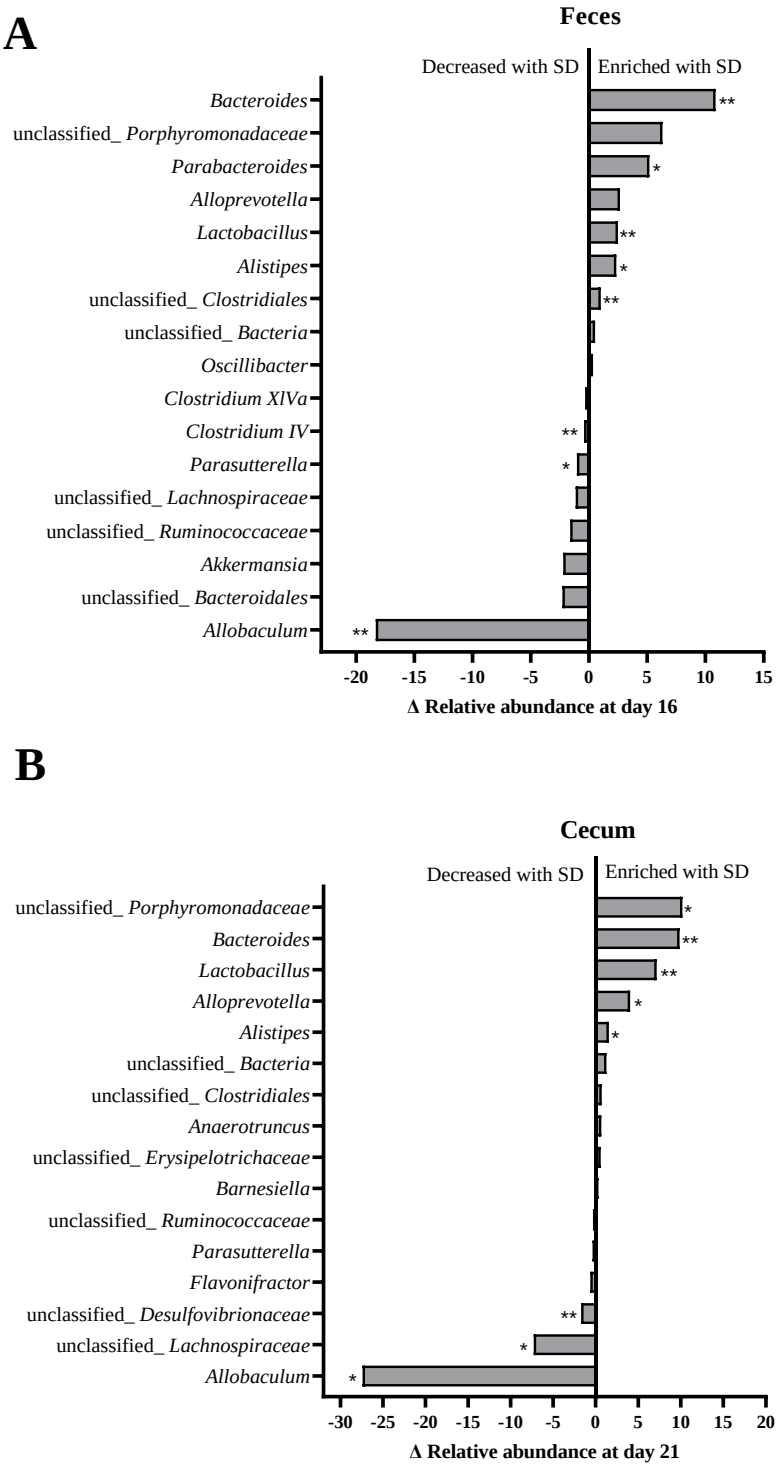

Figure 28: Genus-level differences in fecal (A) and cecal (B) microbiota composition between mice fed semisynthetic diet supplemented with 20% Spirulina (SD) and mice fed semisynthetic control diet (CD). Fecal samples were collected at day 16 and cecal contents at day 21 of intervention. Data are presented as mean normalized to CD-fed mice (n = 5 - 7). CD- versus SD-fed mice. *$P < 0.05$, ***$P < 0.001$ and ****$P < 0.0001$.

3.3.5.3 The Spirulina induced decrease of fecal of *B. wadsworthia* was time-dependent

This study demonstrates that the colitogenic bacterium *B. wadsworthia* degrades DHPS to H_2S and therefore, is important for the complete degradation of SQ. Accordingly, the abundance of *B. wadsworthia* in feces and cecal contents of CD- and SD-fed mice was quantified using qPCR (Fig. 29). SD-feeding reduced the levels of fecal *B. wadsworthia* to 75% from day 0 to day 9, but levels recovered afterwards (Fig. 29A). In cecal samples there were no differences in cell numbers at day 21 (Fig. 29B). Consistently, the cell-number pattern of *B. wadsworthia* in feces of SD-mice over time was similar to the abundance of fecal *dsrA* (Fig. 23B).

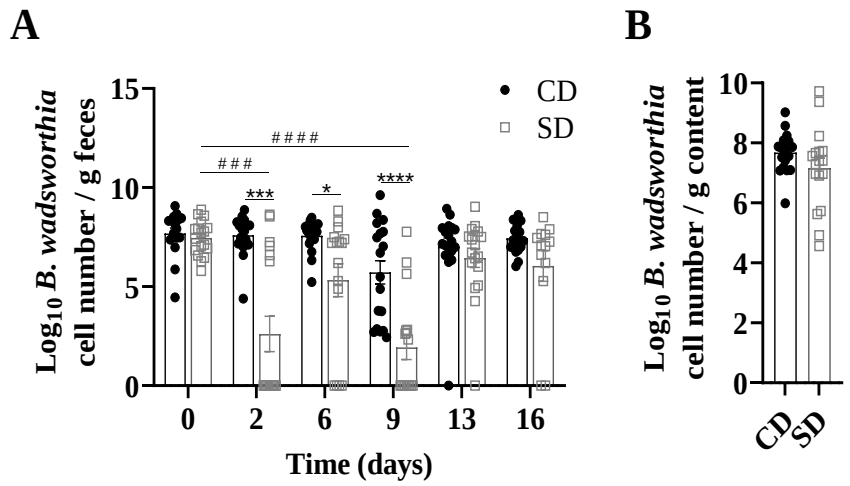

Figure 29: Abundance of *B. wadsworthia* in (A) feces and (B) cecal contents of mice fed semisynthetic diet supplemented with 20% Spirulina (SD) and mice fed semisynthetic control diet (CD). Cell counts were determined with qPCR and data is presented as mean ± SEM. Each dot represents one mouse. *CD- versus SD-fed mice. #SD-fed mice at day 0 versus SD-fed mice at given points in time. $^{*}P < 0.05$, $^{***,\#\#\#}P < 0.001$ and $^{****,\#\#\#\#}P < 0.0001$, n = 18 per group.

3.3.6 Energy intake and food efficiency of SD-fed mice were elevated

In a final step, this study aimed to investigate the increase in body weight observed for mice receiving SD in comparison to CD (3.3.1). Bomb-calorimetry of the diets (CD: 16.9 kJ/g and SD: 17.3 kJ/g; CD: n = 2; SD: n = 1), as well as dietary macronutrient analysis based on the Weender analysis (Table 17) did not reveal major differences in energy and macronutrient content between CD and SD. Energy intake (kJ/day) and food efficiency (mg body weight gain/kJ) of SD-fed mice were compared with those of CD-fed mice (Table 18). Both parameters were higher in SD-fed than in CD-fed mice between day 0 and day 2 (energy intake: 1.7 times higher, food efficiency: 6 times higher). This considerable difference was not observed for the time between day 2 and day 21 (energy intake: 1.1 times higher, food efficiency: 1.3 times lower) (Table 18). The fecal energy contents were similar for both groups (CD: 14.25 ± 0.05 kJ/g and SD: 15.72 ± 0.52 kJ/g; mean ± SEM; n = 4, Table 18).

Analyses revealed that both diets were isocaloric, showed similar macronutrient compositions and that fecal energy contents were similar. Furthermore, energy intake and food efficiency did not differ in between both groups from day 2 and day 21 of intervention. Thus, the differences in energy intake and food efficiency within the first 48 h might be responsible

for the significant weight gain of SD mice, which is consistent with the body-weight gain during the first two days of intervention (3.3.1).

Table 17: Macronutrient composition of control diet (CD) and semisynthetic diet supplemented with 20% Spirulina (SD) according to Weender analysis (also known as proximate analysis). All diet batches used in the animal experiments were analyzed (CD: n = 2; SD: n = 1).

Analyzed macronutrients	Content in CD (%)	Content in SD (%)
Water	10.7	10.8
Raw ash	4.8	5.1
Raw protein	18.3	20.2
Raw fat	4.5	4.4
Raw fiber	1.2	1.5
Nitrogen-free extract	60.7	58.0

Table 18: Biometric parameters of mice fed a semisynthetic diet supplemented with 20% Spirulina (SD) or a semisynthetic control diet (CD) for three weeks. Food efficiency was determined from body-weight gain (mg) per consumed energy (kJ). Energy intake and food efficiency were both determined for the period between day 0 and day 2 as well as between day 2 and day 21 and compared with each other (mean ± SEM, n = 16 - 18). CD- versus SD-fed mice day 0 → day 2: ****$P < 0.0001$ and CD- versus SD-fed mice day 2 → day 21: $^{###}P < 0.001$.

	CD day 0 → day 2	SD day 0 → day 2	CD day 2 → day 21	SD day 2 → day 21
Energy intake (kJ/d)	53.66 ± 2.86	90.77 ± 6.94****	51.91 ± 0.87	58.04 ± 0.99$^{###}$
Food efficiency (mg/kJ)	6.08 ± 3.11	35.98 ± 3.75****	1.64 ± 0.87	1.18 ± 0.70

To elucidate possible causes responsible for the body-weight gain of SD-fed mice, these body parameters potentially linked to obesity were analyzed in the following: blood-glucose level, adipocyte size and number, gene expression of key enzymes linked to the intestinal and hepatic lipid metabolism and transport, hepatic triglyceride concentrations and liver tissue histology.

3.3.7 Spirulina diet feeding did not affect the glucose metabolism

Fat-tissue accumulation and body-weight gain may correlate with increased blood-glucose levels and an impaired glucose tolerance [335]. The glucose transporter type 2 (GLUT2) facilitates the transmembrane glucose transport in many tissues. In liver, the main storage form of glucose is glycogen, biosynthesized by the hepatic glycogen synthase (GYS2). An altered abundance of GLUT2, GYS2 and glycogen is associated with glucose intolerance [337-340].

Plasma-glucose levels of heart blood and of portal vein blood detected in SD-fed and CD-fed mice were similar (Fig. 30A). The intestinal and hepatic *Glut2* mRNA levels in SD mice were not significantly different from those of controls (Fig. 30B). The hepatic gene expression of *Gys2* and the glycogen concentration did not differ between the groups (Fig. 30C, D).

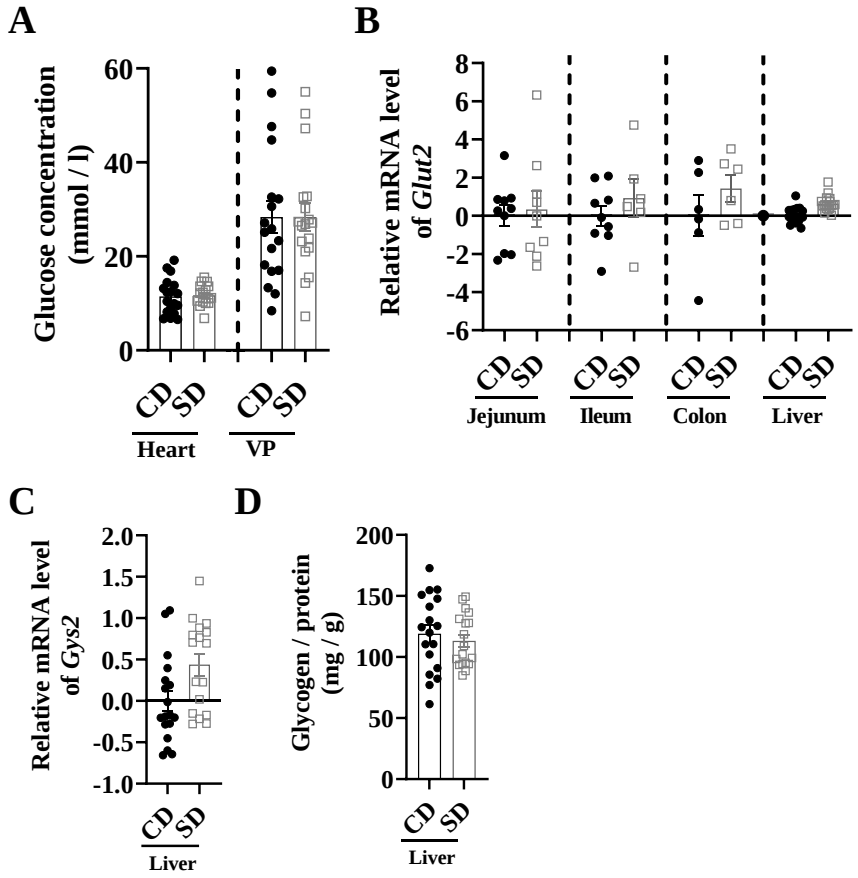

Figure 30: Blood-glucose levels and storage as glycogen of mice fed semisynthetic diet supplemented with 20% Spirulina (SD) and mice fed semisynthetic control diet (CD). (A) Plasma glucose level of heart blood and of blood from the hepatic portal vein (Vena portae hepatis, VP). Data is presented as mean ± SEM (n = 18 per group). **(B)** Gene-expression level of the glucose transporter type 2 (*Glut2*) in intestinal and hepatic tissue (mean ± SEM, n = 6 - 10 per group) and **(C)** of the hepatic glycogen synthase (*Gys2*) (mean ± SEM, n = 17 - 18 per group). **(D)** Hepatic glycogen level (mean ± SEM, n = 18 per group). Each symbol represents one mouse. Samples were obtained after 21 days of intervention.

3.3.8 Spirulina feeding led to hypertrophic obesity

Two forms of obesity correlate with the adipocyte phenotype: namely hypertrophic and hyperplastic obesity [340, 341]. The first type illustrates an increase in adipocyte size in moderate state of obesity and the second an increased adipocyte cell number in a more severe form of obesity [340, 341]. The mean adipocyte area of the mWAT was approximately 90% larger in SD-fed mice than in CD-fed mice (Fig. 31A, B). Due to adipocyte hypertrophy, the adipocyte number per stained slide in SD-fed mice was reduced (ca. 55%) (Fig. 31A, C), indicating a moderate state of obesity.

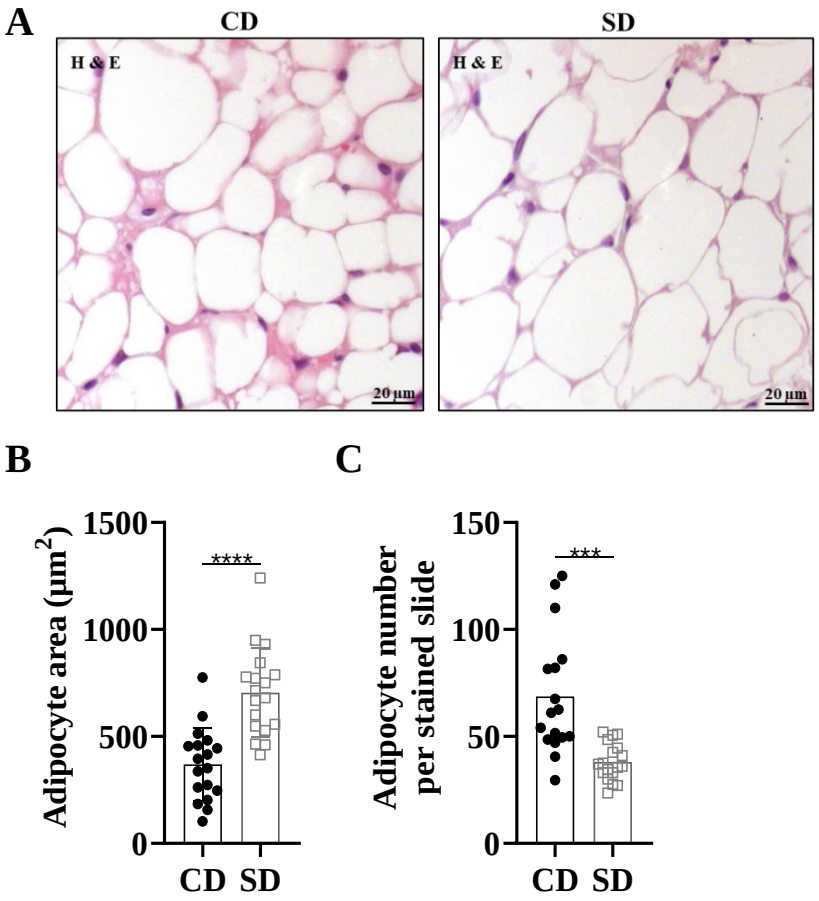

Figure 31: Adipocyte analysis of the mesenteric white adipose tissue (mWAT) of mice fed semisynthetic diet supplemented with 20% Spirulina (SD) and mice fed semisynthetic control diet (CD). (A) Representative images of adipocytes visualized with H&E staining of mWAT. (**B, C)** Adipocyte area and number of the mWAT quantified with ImageJ Plug-in Adiposoft (mean ± SEM, n = 16 - 18 per group). CD- versus SD-fed mice: ***$P < 0.001$ and ****$P < 0.0001$. Samples were obtained after 21 days of intervention. Each symbol represents one mouse.

3.3.9 SD feeding reduced the intracellular lipid availability in jejunal tissue

To further clarify the obesogenic effect of SD, gene expression of key enzymes involved in intestinal lipid metabolism was analyzed (Fig. 32). The selected enzymes are responsible for lipid transport (fatty acid translocase, *Cd36;* fatty acid-binding protein, *Fabp2*), lipid synthesis (fatty acid synthase, *Fasn*), triglycerides synthesis (Acyl-CoA desaturase 1, *Scd1*), lipid catabolism (hormone-sensitive lipase, *Lipe*), and lipid homeostasis (Perilipin 2, *Plin2*).

Mice fed SD displayed lower mRNA levels of *Cd36*, *Scd1* and *Plin2* in jejunal mucosa than CD-fed mice, indicating a reduced cellular uptake and availability of lipids in the SD-fed mice in the jejunum (Fig. 32A). There were no significant differences in the expression of genes related to the intestinal lipid metabolism and transport in ileum and colon, indicating that SD did not affect the lipid metabolism in the distal intestine (Fig. 32B, C).

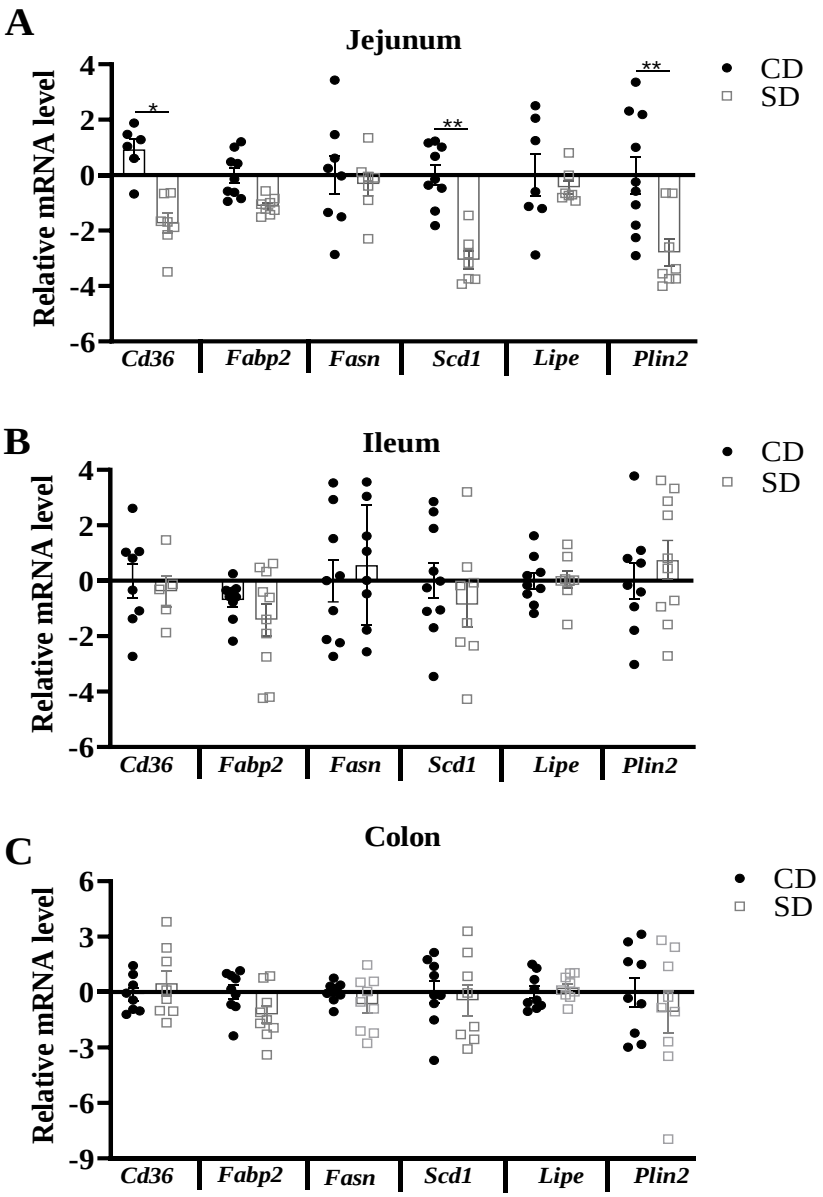

Figure 32: Gene-expression levels of enzymes of the intestinal lipid metabolism in (A) jejunal, (B) ileal and (C) colonic mucosa of mice fed semisynthetic diet supplemented with 20% Spirulina (SD) and mice fed semisynthetic control diet (CD). Data is presented as mean ± SEM, n = 6 - 10 per group. *$P < 0.05$ and **$P < 0.01$. Samples were obtained after 21 days of intervention. Each symbol represents one mouse.

3.3.10 SD reduced gene-expression levels of key enzymes for hepatic lipid uptake and synthesis

The liver has a crucial function in fat metabolism, including lipid uptake, synthesis, storage and consumption [342]. In obesity, hypertrophic adipocytes of white adipose tissue increase in their lipid content over time, resulting in an excess of lipids. Lipids that cannot be stored in the adipose tissue are released into the systemic circulation and deposited in organs such as the liver, which may lead to hepatic formation of lipid droplets and elevated triglyceride levels [342, 343]. Furthermore, hepatic inflammation has previously been linked to obesity [344].

No differences in hepatic tissue histology were detected between SD- and CD-fed mice (Fig. 33). No lipid droplet formation or signs of inflammation, tissue damage, fibrosis or steatosis were observed (Fig. 33). Concentration of triglycerides in the liver did not differ between the groups, while the mRNA level of *Tnf-α* was significantly higher in mice fed SD (Fig. 34A, B).

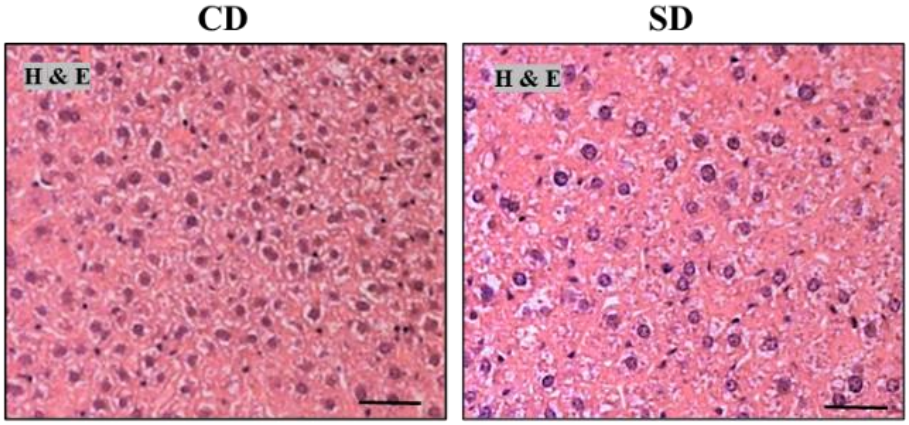

Figure 33: Representative images of hepatic tissue of mice fed semisynthetic diet supplemented with 20% Spirulina (SD) and mice fed semisynthetic control diet (CD). Liver sections were stained with H&E and inspected microscopically at a 400 x magnification. Scale = 10 µM. Samples were obtained after 21 days of intervention.

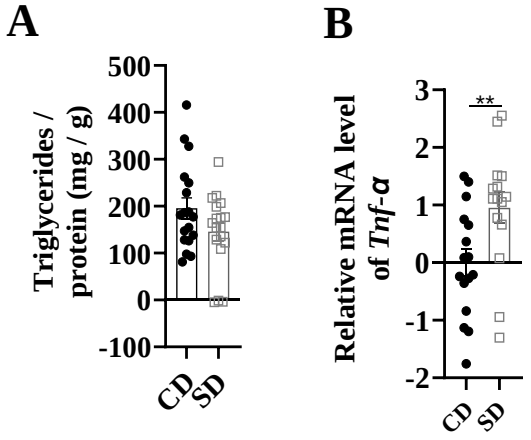

Figure 34: (A) Hepatic triglycerides and (B) gene expression levels of tumor necrosis factor (*Tnf*)-*α* of mice fed semisynthetic diet supplemented with 20% Spirulina (SD) and mice fed semisynthetic control diet (CD). Data are presented as mean ± SEM (n = 15 - 18 per group). Each symbol represents one mouse. Liver was obtained after 21 days of intervention. CD- vs. SD-fed mice: $^{**}P < 0.01$.

To further characterize the weight-gain effects of SD, the gene expression of key enzymes of the hepatic lipid metabolism was analyzed in both groups (Fig. 35). The enzymes chosen are involved in lipid uptake (fatty acid translocase, *Cd36*; very long-chain acyl-CoA synthetase, *Slc27a2;* long-chain fatty acid transport protein 4, *Slc27a4*), cholesterol uptake (fatty acid-binding protein 1, *Fabp1*), lipid synthesis (fatty acid synthase, *Fasn*; elongation of very long chain fatty acids protein 5 and 6, *Elovl5* and *Elovl6*), cholesterol synthesis (3-hydroxy-3-methylglutaryl-coenzyme A reductase, *Hmgcr*), in *de novo* cholesterol and lipid synthesis (ATP-citrate synthase, *Acly*), triglycerides synthesis (acyl-CoA desaturase 1, *Scd1*; diacylglycerol acyltransferase 2, *Dgat2*), lipid catabolism (hormone-sensitive lipase, *Lipe*;

carnitine *O*-palmitoyltransferase 1, *Cpt1a*; peroxisome proliferator-activated receptor alpha, *Pparα*; adiponectin receptor protein 1 and 2, *Adipor1* and *Adipor2*; adiponectin, *Adipoq*), triglycerides hydrolysis (patatin-like phospholipase domain-containing protein 2, *Pnpla2*) and lipid homeostasis (perilipin 5, *Plin5*).

Mice fed SD displayed lower mRNA levels of *Cd36*, *Elovl5* and *Scd1* compared to mice fed CD. In addition, besides *Dgat2*, expression of all other genes responsible for lipid uptake and anabolism, tended to be decreased in SD-fed mice, indicating that hepatic lipid uptake and availability was decreased (Fig. 35A). Gene-expression analysis did not reveal any differences between the groups with regard to lipid catabolism. *Plin5*, responsible for the maintenance of hepatic balance between lipogenesis and lipolysis, was significantly reduced in SD-fed mice. Plin5 deficiency decreases also fatty acid uptake and storage [345].

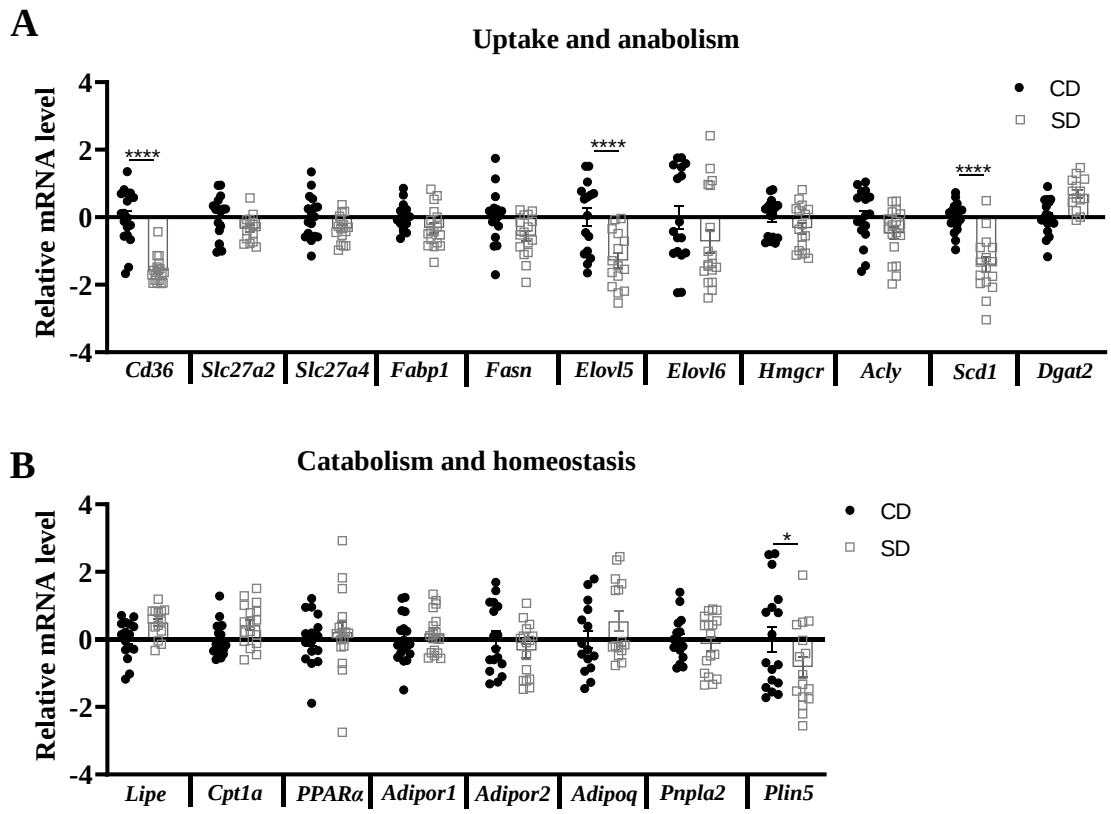

Figure 35: Gene-expression levels of key enzymes of the hepatic lipid metabolism of mice fed semisynthetic diet supplemented with 20% Spirulina (SD) and mice fed semisynthetic control diet (CD). (A) mRNA expression of genes responsible for lipid uptake and synthesis and (**B)** mRNA expression level of genes facilitating lipid degradation and homeostasis in hepatic tissue derived from CD- and SD-fed mice. Samples for analysis were obtained after 21 days of intervention. Each symbol represents one mouse. Data are presented as mean ± SEM (n = 14 - 18 per group). CD vs. SD: **P* < 0.05 and *****P* < 0.0001.

4 DISCUSSION

Knowledge about the microbial dissimilation of sulfonates has increased during the last thirty years (Fig. 2). Sulfonates are present in soil, water, human diet and endogenously within our gut, therefore sulfonate dissimilation by enteric bacteria could be expected [9, 101, 134, 146, 220, 239]. However, most of the studies approaching bacterial sulfonate utilization did not focus on intestinal bacteria, but on environmental bacteria. Information about intestinal sulfonate utilization, especially by human beings, is scarce. In mice, a study of Devkota *et al.* demonstrated that the diet-induced increased availability of TC in the digestive tract stimulates the growth of the sulfite-reducing pathobiont *B. wadsworthia*. The bloom of *B. wadsworthia* was linked to an exacerbated colitis in IL-$10^{-/-}$ mice, which was even more enhanced, when TC was orally applied [9]. H_2S has been recognized as signaling molecule in a wide range of physiological, as well as pathological processes in human beings. It has been linked to IBD and colorectal cancer, but appears to have beneficial health effects as well, such as the prevention of intestinal inflammation, among others [64-69]. *In vitro* experiments demonstrated the ability of *B. wadsworthia* to release H_2S from taurine while utilizing formate as an electron donor [8]. H_2S formation from sulfonates by environmental bacteria is well understood, but knowledge of sulfonate utilization by colitogenic bacteria, other than *B. wadsworthia*, is still missing. In order to investigate the role of sulfonates on intestinal inflammation, this study examined first the ability of the human fecal microbiota to convert sulfonates to H_2S, second the identity of human fecal bacteria that are able to convert sulfonates to H_2S, and third, whether sulfonates are available in the gut after ingestion of a SQDG-rich diet in conventional mice.

4.1 Sulfonate conversion by human gut microbiota

4.1.1 Human gut microbiota converted sulfonates to H_2S with inter-individual differences

Microbial H_2S formation from sulfonates reflects bacterial utilization of the sulfonate-sulfite moiety and is used as an indicator for anoxic sulfonate degradation [8, 139]. The present study revealed that human fecal slurries were able to convert the sulfonates taurine, isethionate, cysteate, 3-sulfolactate, SQ, and DHPS to H_2S during anoxic incubation. This is the first scientific report demonstrating H_2S formation by human fecal slurries from sulfonates other than SQ. In a previous study a mixture of fecal slurries from eight vegetarians was able to convert SQ to the intermediate DHPS and then further to H_2S within 96 h, which is in line with the present study [325]. The ability of human fecal slurries to degrade taurine was only investigated under oxic, not under anoxic conditions [346]. Fecal samples from eight humans were individually cultivated with taurine, but no H_2S was released [346].

Furthermore, the present study is the first one investigating the conversion of sulfonates by human fecal microbiota in a single-batch fermentation systems, allowing to investigate anoxic sulfonate utilization by human fecal bacteria under growth conditions identical to the intestinal environment. H_2S formation could be compared among individuals to make assumptions for the human population. The present study showed inter-individual differences

in sulfonate utilization by human fecal bacteria. Fecal slurries from all tested donors converted taurine, isethionate and 3-sulfolactate to H_2S, while cysteate, SQ and DHPS were only converted by the fecal microbiota from some donors. Fecal microbiota from all donors degraded SQ within 48 h of anoxic incubation, while DHPS and H_2S formation was only observed for fecal slurries from four out of ten donors. This might be explained by inter-individual differences in gut microbiota composition of the tested subjects and might indicate that intestinal sulfonate utilization in the human population differs. Especially intestinal utilization of taurine, isethionate and 3-sulfolactate seems to be more common within the population, while cysteate, SQ and DHPS degradation might be scarcer. Fecal slurries that converted DHPS to H_2S were also able to convert SQ to H_2S. This suggests that DHPS is linked to H_2S formation from SQ, which is in line with previous reports about SQ degradation by human fecal bacteria [325].

The ability of fecal slurries from all donors to degrade taurine, isethionate, and 3-sulfolactate could suggest that bacterial degradation pathways of all three sulfonates are similar to each other. Earlier findings demonstrate that the microbial degradation of taurine and isethionate are linked to each other. Isethionate is a degradation product of taurine, as reported for *B. wadsworthia* or *Clostridium butyricum* BL5262 [8, 119, 136, 146, 147]. However, a connection of both sulfonates to 3-sulfolactate has never been documented before.

Contrary to previous reports that identified isethionate as an intermediate in taurine degradation by *B. wadworthia* this was not confirmed for human fecal slurries in this study [8, 119, 136]. While the present study tested samples after 72 h of incubation for isethionate formation, a previous study reported isethionate formation immediately after inoculation and almost complete exhaustion of isethionate after 48 h of incubation [276]. However, the latter study was published after the experiments described here had been carried out. In future studies, isethionate should be quantified 0 - 48 h after inoculation.

CoM plays a major role in the metabolism of methanogenic archaea, which are common members of the human gut microbiota [196]. In the present study, H_2S formation from CoM was not detected. H_2S formation from CoM by human fecal slurries has never been investigated before. However, previous fermentation experiments using pure cultures of intestinal bacteria such as *B. wadsworthia* or *Desulfovibrio* sp. IC1 had been tested for their ability to convert CoM to H_2S with negative results [8, 161].

4.1.2 Human fecal *Desulfovibrio* spp. converted taurine and isethionate to H_2S

Taurine is after glutamine the second most abundant amino acid in colonic mucosa (2.5 mMol/kg specimen weight) [117]. Gut bacteria, such as *B. wadsworthia*, *Desulfovibrio* sp. RZACYSA and the *Veillonellaceae* 2C, degrade taurine to H_2S under anoxic conditions [9, 137-140]. However, these bacteria were not isolated from the human gut. Most intensively studied *Enterobacteriaceae* so far, represented by seven strains of *E. coli*, were reported to utilize taurine under oxic conditions [153, 194]. The present study confirms the ability of human fecal bacteria to convert taurine to H_2S, but no *E. coli* strains were isolated [8, 136, 137, 139, 140].

One human fecal isolate was identified as *Desulfovibrio* sp., and demonstrated to convert taurine and isethionate to H_2S under anoxic conditions. The sulfonates served as TEA for

anaerobic respiratory growth, while lactate was used as an electron donor. The ability to ferment taurine and / or isethionate by *Desulfovibrio* sp. has previously been described for *D. desulfuricans* DSM 12129, *D.* sp. GRZCYSA, and *D.* sp. RZACYSA. It may be concluded that this ability is quite common for this genus [3, 8, 134, 139, 161, 162, 164]. However, only *D.* sp. RZACYSA was described to convert taurine and isethionate to H_2S, while *D. desulfuricans* DSM 12129 and *D.* sp. GRZCYSA only converted isethionate to H_2S [3, 8, 134, 139, 161, 162, 164]. Even though *Desulfovibrionaceae* are common residents of the human gut, none of the SRB tested previously for this ability were directly isolated from the human gut, but from environmental sources (such as compost soil or lake sediment). Thus, the present study led to the first *Desulfovibrio* spp., directly isolated from human feces, and capable of converting both sulfonates to H_2S, indicating a role of this SRB in the human intestinal sulfonate-sulfur cycle.

These results suggest that the sulfidogenic respiration of taurine beside that is more widespread among *Desulfovibrio* spp. than initially expected. Therefore, various *Desulfovibrio* spp. were tested for their ability to utilize taurine. Indeed, *D. simplex* DSM 4141^T converted taurine to H_2S. Hence, *D. simplex* was identified as another bacterium belonging to *Desulfovibrio* spp. able to utilize taurine and to release H_2S, in addition to the isolated *Desulfovibrio* sp. and *D.* sp. RZACYSA. Further investigations are necessary to fully reveal the function, intestinal niches, and significance of *Desulfovibrio* spp. in the intestinal sulfonate-sulfur cycle.

4.1.3 SQ utilization differed among fecal *E. coli* strains

Microbial SQ utilization involves DHPS and / or 3-sulfolactate as intermediates. While the SQ-EMP sulfoglycolytic pathway in *E. coli* K-12 results in the formation of DHPS, leads the SQ-ED pathway in *Pseudomonas putida* SQ1 to 3-sulfolactate [248, 249]. Similar to *E. coli*, another member of the *Enterobacteriaceae* (*Klebsiella* sp. ABR11), employs the SQ-EMP pathway for the breakdown of SQ, but DHPS is just an intermediate, whereas 3-sulfolactate is the end product [241, 253]. In addition, SQ degradation to DHPS was also demonstrated for a *Citrobacter* sp. strain, also a member of the *Enterobacteriaceae* [251]. Co-culturing models of SQ- and DHPS-degrading gut bacteria, such as of *E. coli* with *Desulfovibrio* sp. DF1 or *E. rectale* with *B. wadsworthia*, degraded SQ to H_2S via the intermediates DHPS and / or 3-sulfolactate [251, 325]. These results suggest that SQ degradation is a common property among *Enterobacteriaceae*, involving DHPS and / or 3-sulfolactate as an intermediate and H_2S as end product.

In the current study, anoxic enrichment cultures on SQ inoculated with human feces led to the isolation of *E. coli* strains. There were no SQ-degrading bacteria isolated from oxic enrichment cultures with SQ, which is somewhat in conflict with the previous isolation of *Klebsiella* sp. ABR11 from sewage sludge on SQ under oxic conditions [347]. Intestinal bacteria other than *E. coli*, able to utilize SQ, could not be isolated from human fecal slurries. In contrast, earlier studies showed the ability of various *Enterobacteriaceae* to utilize SQ, as already described above. However among these, only *E. coli* and *E. rectale* were directly isolated from the human intestinal tract, while *P. putida* SQ1, *Klebsiella* sp. ABR11, *Citrobacter* sp., *Desulfovibrio* sp. and *B. wadsworthia* were obtained from indirect intestinal (sewage sludge) or environmental sources (lake sediment or garden compost) [241, 248, 249,

251, 253, 325]. The current study confirms the ability of human intestinal *E. coli* to utilize SQ under anoxic conditions and might imply that *E. coli* is the main driver for intestinal SQ degradation in human beings.

BLASTn alignment analysis implied a 98 - 100% identity of the obtained fecal *E. coli* isolates (SQ6, SQ10, SQ11, and SQ12) among each other, as well as a 99 - 100% identity to the known SQ-utilizing strain *E. coli* MG1655, indicating identity at species level. However, the ability to convert SQ to DHPS differed among the *E. coli* isolates and *E. coli* MG1655 under oxic and anoxic conditions. *E. coli* MG1655 and isolate SQ10 were not able to degrade SQ under oxic conditions and consequently, no DHPS formation was observed in these cultures. However, intriguingly under anoxic conditions, *E. coli* MG1655 and isolate SQ10 released DHPS from SQ. All other fecal *E. coli* isolates (SQ6, SQ11, SQ12, SQ13) tested were able to degrade SQ to DHPS under both oxic and anoxic conditions. This is in conflict with previous studies that demonstrated both oxic and anoxic SQ degradation for *E. coli* MG1655 [249, 251].

In the currents study, SQ conversion proceeded faster under anoxic conditions (isolates SQ6, SQ11, SQ12, SQ13: 8 - 22 h; SQ10: 22 - 46 h; *E. coli* MG1655: 22 - 72 h) in comparison to oxic conditions (isolates SQ6, SQ11, SQ12, SQ13: 22 - 46 h; SQ10 and *E. coli* MG1655: no SQ degradation). This is in conflict with previous findings [249, 251]. The conversion of SQ to DHPS by *E. coli* MG1655 took 5 - 18 h under oxic conditions, and 12 - 20 h under anoxic conditions [249, 251].

Whether key enzymes of SQ formation and degradation are responsible for the differences in the ability and time course of SQ conversion among the different *E. coli* strains was further investigated in the current study. The bacterial sulfoquinovosidase (YihQ) of *E. coli* MG1655 catalyzes the release of SQ from SQDG [239]. The first step of SQ degradation, which was also detected in *E. coli* MG1655, is the isomerization of SQ to 6-deoxy-6-sulfo-D-fructose catalyzed by SQ isomerase (YihS) [249]. However, in the present study gene expression of *yihQ* and *yihS* was observed in all *E. coli* isolates (SQ6, SQ10, SQ11, SQ12, SQ13) as well as in *E. coli* MG1655. This might indicate that genes other than *yihQ* or *yihS* are responsible for the observed differences in SQ utilization. The sulfoglycolytic pathway is encoded by a ten-gene cluster, including *yihS*. This gene cluster was previously found to be present in > 91% of all commensal *E. coli*, as well as in pathogenic *E. coli* (such as EHEC) and supposed to be part of the core-genome of *E. coli* strains. [249]. While DHAP enters the carbon metabolism for energy conservation, DHPS is excreted and utilized by other bacteria [249]. Sulfoglycolysis is controlled by a transcriptional regulator (CsqR) that inhibits the expression of sulfoglycolytic enzymes when the SQ concentration is low [250]. Therefore, future studies should clarify whether anyone of these genes is responsible for the differences in SQ utilization among *E. coli* strains. Isolation of SQ-utilizing bacteria from a larger number of fecal samples than ten donors might be useful to fully understand the ability and diversity of the gut microbiota to utilize SQ as TAE.

4.1.4 Human fecal *E. coli* strains converted 3-sulfolactate to H_2S

As described above (4.1.3), another intermediate in intestinal microbial SQ degradation besides DHPS might be 3-sulfolactate. Therefore, the ability of *E. coli* to utilize 3-sulfolactate was tested in the present study and compared to their ability to degrade SQ. The fecal *E. coli* isolates (SQ6 and 3-SL2), as well as *E. coli* MG1655 were able to reduce the sulfonate moiety of 3-sulfolactate to H_2S, which had not been reported previously for 3-sulfolactate. Thus, a novel finding of anoxic sulfonate degradation by one of the most intensely studied gut microorganisms is illustrated in this study.

The present study demonstrates a potential link between the microbial conversion of SQ and 3-sulfolactate under anoxic conditions, as both sulfonates were degraded by the same *Enterobacteriaceae* under these conditions. Human fecal slurries from all above tested donors were able to degrade SQ or 3-sulfolactate, as described in 4.1.1. 3-Sulfolactate has been previously demonstrated as an intermediate in microbial SQ degradation, but only under oxic conditions resulting in the release of sulfate as end product. For example, a co-culture of *Pseudomonas putida* SQ1 (DSM 100120) and *Paracoccus pantotrophus* NKNCYSA (DSM 12449) the former first converted SQ to 3-sulfolactate and the latter the sulfonate moiety of 3-sulfolactate subsequently to sulfate [347]. However, the present study might indicate a link between SQ and 3-sulfolactate utilization under an intestinal anoxic environment.

4.1.5 A co-culture of *B. wadsworthia* with *E. coli* enhanced H_2S formation

In this study, a novel co-culturing model is presented, able to degrade SQ via DHPS to H_2S. For the conversion of SQ to DHPS, the SQ-degrading *E. coli* strain SQ6 isolated from human feces in this study was used. This strain probably uses the sulfoglycolytic pathway, as previously described for *E. coli* MG1655 [249]. *B. wadsworthia* (DSM 11045) converted DHPS to H_2S. The described co-culture used in this study is the third example demonstrating SQ degradation via DHPS to H_2S by bacteria complementing those of *E. coli* MG1655 and *Desulfovibrio* sp. strain DF1 or of *E. rectale* DSM17629 and *B. wadsworthia* 3.1.6 [251, 325].

However, the time courses of SQ conversion into DHPS, followed by H_2S release from DHPS differed among these co-cultures. *E. coli* MG1655 degraded SQ within 10 - 22 h, while *E. rectale* degraded SQ within 0 - 144 h, both under anoxic conditions [251, 325]. In the present study, anoxic breakdown of SQ by the *E. coli* isolate SQ6 occurred from 0 - 24 h, which is similar to previous findings for *E. coli* MG1655 [249]. In addition, *E. coli* MG1655 formed DHPS from SQ within 18 - 25 h whereas *E. rectale* DSM17629 did so within 20 - 50 h [251, 325]. In the present study, DHPS formation by the *E. coli* isolate SQ6 proceeded from 0 - 24 h. Finally and in previous studies, *Desulfovibrio* sp. DF1 converted DHPS within 100 - 144 h to H_2S, whereas *B. wadsworthia* 3.1.6 required 18 - 60 h [251, 325]. In the present study, *B. wadsworthia* (DSM 11045) converted DHPS to H_2S within 24 - 27 h.

These results indicate that the conversion of DHPS to H_2S proceeds faster in a co-culture of *E. coli* and *B. wadsworthia* than in a co-culture of *E. coli* MG1655 and *Desulfovibrio* sp. strain DF1 or of *E. rectale* DSM17629 and *B. wadsworthia* 3.1.6. This suggests that the time course of anoxic SQ degradation and, DHPS and H_2S formation depends on the presence of

bacterial strains. This is in line with earlier studies of our research group in which a simplified human intestinal microbiota (SIHUMI) model consortium was co-cultured with *B. wadsworthia* in an SQ-containing medium under anoxic conditions [276, 348]. In this model, H_2S formation was already detected after 3 h [276]. The SIHUMI community contains next to *E. coli* of *Anaerostipes caccae*, *Bacteroides thetaiotaomicron*, *Bifidobacterium longum*, *Blautia producta*, *Clostridium ramosum*, and *Lactobacillus plantarum* [348].

Combinations of bacteria does not only seem to affect the time course of DHPS and H_2S formation and / or degradation during SQ utilization, but also the amount of DHPS and H_2S formed. *E. coli* MG1655 and *E. rectale* converted only 50% of the initially added SQ to DHPS [251, 325], while in the present study 80% of the initially added SQ was recovered as DHPS. Similar observations were made for the H_2S formation. While *Desulfovibrio* sp. DF1 converted 100% of the DHPS, formed from SQ, to H_2S, *B. wadsworthia* 3.1.6 released only 40% of the DHPS as H_2S, which corresponds to 20% of the initial SQ [251, 325]. In the present study, 75% of the DHPS was recovered as H_2S. However, growth conditions and laboratory circumstances of the different co-culturing experiments differ and therefore it might be difficult to compare the ability of sulfonate utilization among the combined bacterial strains.

The present study also revealed that H_2S formation by *B. wadsworthia* increased considerably in the presence of *E. coli*. Incubation of *B. wadsworthia* with DHPS led to a recovery of only 2.5% of the initially added DHPS as H_2S, while co-culturing with the isolated *E. coli* strain SQ6 resulted in approximately 50% recovery as H_2S. Therefore, it can be concluded that the presence of *E. coli* strains in combination with *B. wadsworthia* not only stimulates the onset of H_2S formation as end product of SQ degradation, but also the amount of H_2S produced.

Altogether, sulfonate utilization and conversion to H_2S by the human intestinal microbiota exhibits inter-individual differences, which seems to be dependent on the individual gut microbiota composition. Furthermore, even though *B. wadsworthia* is able to convert sulfonates such as taurine, isethionate and DHPS to H_2S in pure culture, co-culturing with human *Enterobacteriaceae* such as *E. coli* stimulates the release of H_2S, indicating a synergistic effect in the gut environmental sulfonate-sulfur cycle.

4.2 The effects of a SQDG-rich Spirulina supplemented diet in mice

Sulfonates are part of the daily human diet, which contains among others taurine and SQDG. Taurine can be found in meat, fish and life style beverages, and SQDG in thylakoid membranes of chloroplasts in leafy green vegetables, including salad, spinach, and parsley [4, 5, 219, 220]. Intestinal taurine availability determined by the dietary taurine uptake by enterocytes in the small intestinal tract, its synthesis by the liver, and its reabsorption by the kidney [107, 110]. After uptake, taurine is carried via the portal vein to the liver and conjugated with the primary bile acid cholate to form TC [107, 110, 349, 350]. With each ingested lipid-containing diet, TC cycles with glycocholate repeatedly from the gall bladder through the small intestine to the ileal section [114-116, 352] and reaches in small amounts (5%) the distal ileal and the colonic sections undergoing bacterial utilization [114-116, 352]. While

the intestinal availability of taurine is well understood, details of the intestinal availability of SQDG or its degradation products after ingestion are hardly known. So far, only one study demonstrated the fate of SQDG after ingestion, using radioactively labelled [^{35}S]SQDG that was orally administered to guinea pigs. Only 3 h after administration, most of the SQDG (60%) was deacelated and observed as SQG, while only 1 - 5% of the radioactivity was detected as SQDG in the intestinal mucosa. Hence, a stepwise deacelation of SQDG to SQG was assumed to occur in the animal tissues [238]. However, SQ and DHPS were not known to be metabolites of microbial SQDG degradation that time and therefore not included as substrates in this study. To elucidate the effects of SQDG on gut microbiota composition and SQDG degradation, in the present study conventional mice were fed a semisynthetic diet supplemented with Spirulina which is rich in SQDG.

4.2.1 Spirulina reduced the stomach surface in mice

SD led to stomach surface reduction by approximately 25%. The primary function of the stomach is to mix and grind gastric contents and then to release them into the duodenum via the pyloric sphincter [360, 361]. The stomach first empties small particles and liquids, while larger particles are retained in the stomach until the digestive period is over and a fasting state is reached [362-364]. It has been demonstrated that gastric emptying is not only dependent on the size, but also on the density of the particles. The researchers concluded that high-density particles lead to an extended period of gastric emptying and that low-density particles may be homogenously mixed during the gastric digestion state and easily released to the small intestines [364]. It was assumed that the size of the stomach might be dependent on the nature of the food. In the present study, the SD, which contained the SQDG, was more friable than the CD, indicating that gastric digestion of SD may lead to smaller particles in comparison to CD. Gastrointestinal morphology is also dependent on the way how the food is administered, the frequency of dietary intake, and body size and / or shape [365]. Animals with a smaller stomach, eat smaller meals but do so more frequently [360]. In the present study the frequency of the dietary intake by the mice was not analyzed.

4.2.2 Spirulina increased the quantity of intestinal SQ

The lipid fraction of Spirulina contains 11.4 ± 0.71% of SQDG [234-238]. Based on the total lipid fraction of 7.35 ± 0.30% for the Spirulina powder used in the present study, the SQDG content was estimated to be 0.84%. Hence, the SD supplemented with 20% Spirulina contained approximately 170 mg SQDG/100 g diet, and the daily intake of SQDG per mouse was approximately 9 mg.

Spirulina is known as superfood due to its anti-cancer and anti-obesity effects [355-357, 367-371]. Beside lipids, Spirulina is rich in proteins and micronutrients, such as vitamins and minerals, known to have positive effects in the human body [371, 372]. Absorption of the ingested nutrients depends on the bioavailability of these components in the gastrointestinal tract [373, 374]. Bioavailability is determined based on the permeability of the plant-cell wall of Spirulina, digestive enzymes within the gut, and the interaction of the nutrients with each other [374]. To which extent the cell wall has an impact on accessibility and digestion of the intracellular nutrients, depends mainly on the stability of the cell-wall structure after food processing and mastication [375, 376]. Intact cell walls may prevent availability and utilization of intracellular nutrients [377]. In a study with juvenile fish Nile

tilapia (*Oreochromis niloticus*) fed marine microalgae *Nannochloropsis gaditana*, digestibility of protein (16%) and lipids (32%) increased after bead milling of the diet before administration [378]. In addition, pasteurization, freezing or freeze drying increased the bioavailability up to fourfold [378]. To enhance the bioavailability of nutrients contained in Spirulina cells, degradation of the cell wall seems to be essential. There already is considerable knowledge about the bioavailability of intracellular components in Spirulina after ingestion. For example, the bioavailability of iron in Spirulina was compared with that in whole egg, whole wheat and iron sulfate. Iron absorption from Spirulina was lower than that from ferrous sulfate or whole egg, but higher than from whole wheat [379]. A study with Caco-2 cells demonstrated even a 6.5-fold higher cellular ferritin accumulation from Spirulina compared with that from beef meat, indicating a higher bioavailability of iron contained in Spirulina [380]. Spirulina is also known as potential calcium source for human beings. Rats fed a diet supplemented with Spirulina retained a higher serum calcium level compared to rats fed a diet supplemented with milk rich in calcium or calcium carbonate [381]. In view of this high availability of nutrients from Spirulina, it is suggested that Spirulina is an adequate source of a number of important nutrients. This indicates that Spirulina cells are lyzed in the gastrointestinal tract of mammals making also SQDG available for intestinal absorption.

In the present study, the cell wall of Spirulina, which consists of four layers (LI - LIV), was not ruptured during food processing. However, it was demonstrated that the cell-wall integrity in fecal samples after SD-intake was diminished. This suggests a partial break-down of the cell wall of Spirulina in the gastrointestinal tract and release of plant-based nutrients such as SQDG.

As described above (4.2), the fate of SQDG after ingestion has been investigated only once [238]. Despite the ability of the commensal gut bacterium *E. coli*, to convert SQDG *in vitro* to SQ and SQ to DHPS, *in vivo* experiments are missing. Therefore, the degradation of SQDG in relation to SQ and DHPS formation in different sections of the gastrointestinal tract was investigated in the present study. Cecal contents (n = 7/15, 21 days) and feces (n = 12/12, 16 days) of SD-fed mice contained higher levels of SQ than those of CD-fed mice. This supports the assumption that the cell wall was broken down during intestinal passage and that SQDG were available in the gastrointestinal tract. It is assumed that the release of SQ from SQDG in conventional mice predominantly occurred in the cecum, with inter-individual differences. The varieties of SQ formation from SQDG might depend on the presence or absence of bacterial strains within the intestinal tract. Although, *E. coli* seems to be the main player responsible for SQ-utilization within the gut, the ability of SQ utilization among *E. coli* strains differs, as above described (4.1.4). Furthermore, an ovine rumen isolate, *Butyrivibrio* sp. S2, degrades SQDG, but SQ formation was not investigated [382]. Intestinal SQDG degradation in relation to the present intestinal bacteria which may be responsible for the observed inter-individual differences in the utilization of SQDG in this study will be discussed in 4.2.4 to 4.2.6.

In the present study, no SQ was detected in the colonic contents, which suggests that the cecum is not only the main site of SQ release from SQDG, but also of its complete

degradation. However, discrepancies in the observed SQ concentrations in fecal samples, but not in colonic contents, may be due to differences in the point in time of sample collection (namely 16 days versus 21 days of the intervention). No differences in DHPS concentrations were observed throughout the gastrointestinal tract. DHPS was neither observed in the colonic contents nor in feces, which supports the hypothesis that SQ is completely degraded in the cecum.

4.2.3 Spirulina stimulated the gene expression of pro-inflammatory cytokines in ileal sections

SD-fed mice displayed a higher relative expression of *Il-6* and a trend of an increased expression of *Tnf-α* in ileal mucosa. However, expression levels were lower when compared with previous studies [383, 384], indicating a mild inflammation within the ileum. Also, shortening of the colon, an indicator of the severity of acute gastrointestinal inflammation, was not observed [327, 385]. In sum, SD led to a mild activation of the immune system.

Spirulina might have an immuno-stimulatory effect after Ingestion [386], as an aqueous extract of Spirulina increases serum levels of TNF-α, such as in Balb/C female mice [387]. Also, a diet supplemented with 5% Spirulina resulted in an increased gene expression of ileal *Il-6* in C57BL/6J mice [359]. Expression of *Tnf-α* in the cecal mucosa of conventional IL-10$^{-/-}$ mice after intake of SD was elevated as reported in a recent study of our research group [388].

However, most studies report anti-inflammatory and antioxidant effects of Spirulina in the intestine [386]. In rats suffering from colitis induced by trinitrobenzene sulfonic acid, Spirulina reduced the lymphocyte infiltration and the histopathological score [389]. Spirulina supplementation in rats with colitis induced by acetic acid reduced in the severity of diarrhea and bleeding in the colon and inhibited colon shortening. Furthermore, the levels of the cytokines TNF- α and IL-6 in colonic tissue were decreased [390]. The same effects were observed in animal models for ulcerative colitis (UC) induced by dextran sodium sulfate (DSS). In DSS-treated, colitic Wistar rats, hydroalcoholic extracts of Spirulina, which had been administered for 15 days, reduced the TNF- α and IL-6 expression levels in colonic tissue [391]. C57BL/6 mice with DSS-induced colitis daily received aqueous extracts from Spirulina. This reduced the TNF- α expression in colonic tissue, rectal bleeding, diarrhea, colon shortening and had a protective effect on the intestinal barrier as deduced from an elevated expression of colonic Hsp-25, occludin and claudin-4 [392].

In general, Spirulina is considered as a safe nutritional supplement and non-toxic for human beings [393, 394]. It contains functional substances, such as vitamins, phenolics, C-phycocyanins, and essential amino acids, which mediate these anti-inflammatory and other health-promoting effects [395, 396].

Also SQDG are linked to numerous health-promoting effects, such as anti-viral, anti-bacterial and antitumor effects [397, 398]. SQDG purified from the *n*-butanol fraction of the green alga *Caulerpa racemosa* had an antiviral effect against the herpes simplex virus type 2 (50% inhibition at a concentration of 15.6 µg ml^{-1}) and also a moderate inhibition of herpes simplex virus type 1 and Coxsackie virus B3. Furthermore, SQDG reduced the growth of *E. coli* JM109 *in vitro* by inhibiting the activity of its DNA polymerase I, also

indicating an anti-bacterial effect of SQDG [397]. *In vitro* experiments with colon cancer cells (Caco-2 cell line) demonstrated the inhibitory effect of SQDG on tumor cell proliferation within 48 h after administration [399]. Furthermore, the oral application of the SQDG-containing glycolipid fraction to mice reduced the tumor size of an adenocarcinoma in the colon (colon-26 cell line) and suppressed angiogenesis and cell proliferation markers (such as Ki-687) *in vivo* [400]. Interestingly, the SQ-moiety seems to be essential for the anti-cancer activity of SQDG [240].

4.2.4 Spirulina modulated the α- and β-diversity of the cecal and fecal microbiota

Spirulina ameliorates detrimental effects on the gut microbiota composition caused by abnormalities, such as pulmonary fibrosis, or after the intake of a high-fat or a high-fat high-sucrose diet [402-406]. In the present study, feeding Spirulina was linked to an increased α-diversity, an enhanced number of OTUs and a higher richness of bacteria in cecal contents. The bacterial richness of observed species was also increased in feces. The diet further affected the ß-diversity. However, findings of the present study are in conflict with previous studies. 24-month-old C57BL/6J mice fed a 5% Spirulina diet for six weeks had a decreased number of OTUs and a reduced richness in cecal contents, whereas the ß-diversity was not affected [359]. The gut microbiota of C57BL/6J mice fed a low-fat chow diet supplemented with 5% Spirulina for 4 weeks did not undergo changes in microbial α-diversity as deduced from unaltered Shannon's or Simpson's indices [406]. Similarly, administration of a protein-rich diet supplemented with Spirulina (1 or 2 g/kg diet, given *ad libitum*) did not have strong effects on gut microbiota composition in Japanese quail chicks [407]. That these observations do not match the results of the present study might be explained by the differences in amounts of Spirulina supplemented.

In the present study, Spirulina reduced the relative abundance of members of the phylum *Firmicutes*, while that of the phylum *Bacteroidetes* was increased in both cecal contents and feces (Appendix, Table A5). These observations are common to the majority of studies. For example, the relative abundance of intestinal *Firmicutes* in rats fed a high-fat diet supplemented with 3% Spirulina for 14 weeks decreased, while that of *Bacteroidetes* increased [402]. It has to be noted though that most studies that demonstrated an effect of Spirulina on intestinal phyla used pure compounds extracted from Spirulina, including phycocyanin, polysaccharides, or Spirulina ethanolic extracts, not with Spirulina itself [402, 405, 409-411]. For example, C57BL/6 mice, 4 - 6 weeks of age, underwent a single X-ray dose irradiation to induce pulmonary fibrosis. After administration of phycocyanin (50 mg/kg/d), which is a key regulator for photosynthesis in Spirulina, an increase of the relative abundance of intestinal *Bacteroidetes* and a decrease of that of *Firmicutes* was detected [401]. The same effect was observed for mice given polysaccharides (50 - 200 mg per kg body weight per day) extracted from Spirulina for seven days [408]. In contrast, broiler chicks fed a diet supplemented with 0.1% of Spirulina microalgae extract increased the intestinal ratio of *Firmicutes* to *Bacteroidetes*, while a 0.05% supplementation had no effect on this ratio [411]. This may indicate that concentration differences of Spirulina, which is identical to above assumptions, may lead to different effects on the relative abundance of *Firmicutes* and *Bacteroidetes*.

In the present study, the reduction of *Firmicutes* in cecal contents and feces is due to a reduced abundance of the family *Erysipelotrichaceae* and its genus *Allobaculum* (Appendix, Table A5). In addition, *Lachnospiraceae* and *Ruminococcaceae* showed a trend to lower numbers in both matrices (Appendix, Table A5). Genera of the clusters *Clostridium* IV and *Clostridium* XIVa (both belonging to the family *Clostridiaceae*) were reduced in feces, which however was only significant for *Clostridium* IV members (Appendix, Table A5). Findings of the present study are in accordance with previous studies. Rats fed a high-fat diet supplemented with 3% Spirulina showed the reduction in *Firmicutes* due to a reduced number of *Ruminococcaceae* and *Erysipelotrichaceae* [402]. However, the majority of studies that reported similar effects at family level used again only constituents extracted from Spirulina. Phycocyanin in mice reduced the numbers of members of *Lachnospiraceae* (*Lachnoclostridium*), *Erysipelotrichaceae* (*Turicibacter*), *and Clostridiaceae* (*Intestinimonas*) [401]. Spirulina polysaccharides reduced the number of intestinal *Clostridium* and of *Ruminococcaceae* in mice [408]. A reduction of *Lachnospiraceae* and *Ruminococcaceae* was also reported for C57BL/6 mice after oral administration of *Spirulina maxima*-derived pectin and pectin nanoparticles [412].

Other studies also produced results that differ from the observations made in the present study. It has to be noted that the decreased abundance of *Firmicutes* in C57BL/6 mice in response to phycocyanin administration, was mainly due to a reduction of *Erysipelotrichaceae*, whereas *Lachnospiraceae* and *Ruminococcaceae* were increased [403]. The reduction of *Firmicutes* in response to the administration of ethanolic Spirulina extract was mainly due to corresponding changes in *Lachnospiraceae*, *Clostridium* XlVa, and *Allobaculum* (family *Erysipelotrichaceae*), while *Ruminococcaceae* were increased [409, 410].

Despite the Spirulina-induced reduction of the number of *Firmicutes*, which *Lactobacillus* belong to, the number of *Lactobacillus* and the corresponding family *Lactobacillaceae* in feces and cecal contents were enriched (Appendix, Table A5). This is in accordance with earlier findings. For example, feeding C57BL/6J mice a diet containing 5% Spirulina for six weeks, resulted in a 15-fold increase of intestinal *Lactobacillus* [359]. Similarly, in broiler chickens the count of cecal *Lactobacillus* increased linearly with increasing amounts of applied Spirulina (0.25 - 1.0%) [353].

In the present study, the increased number of *Bacteroidetes* was a result of the higher abundance of *Bacteroidaceae*, *Porphyromonadaceae* and *Rikenellaceae* (Appendix, Table A5). In cecal contents, the abundance of the family *Prevotellaceae* and of its genus *Alloprevotella* was also increased (Appendix, Table A5). The effect of Spirulina on *Bacteroidetes* reported in previous studies is highly variable. For example, dry pellets containing 20% Spirulina fed to African catfish (*Clarias gariepinus*) increased the abundance of *Bacteroidaceae* [413]. In contrast, administration of Spirulina microalgae extract (0.05 - 0.1%) to broiler chicks, resulted in a reduction of *Bacteroidetes* due to a decreased abundance of *Bacteroidaceae* [411]. In a study of our research group, the fecal microbiota of IL-$10^{-/-}$ mice fed SD for three weeks were enriched with *Porphyromonadaceae* after 18 days [388].

In conclusion, a semisynthetic diet supplemented with 20% of Spirulina strongly affected the intestinal microbiota composition in conventional mice (Appendix, Table A5). However,

Spirulina contains various bioactive components which makes it difficult to assign the observed effects to specific constituents of Spirulina, such as SQDG. Spirulina-induced changes of the microbiota composition were partially in accordance with previous findings, but most studies were performed with constituents extracted from Spirulina, not with Spirulina itself, which makes it difficult to draw conclusion in comparison to the present study.

4.2.5 Spirulina did not stimulate the growth of SQDG- or SQ-converting bacteria

SQDG can be found in leafy green vegetables, such as spinach and salad. Anoxic SQDG conversion to SQ has been previously described by *E. coli* which in turn can be converted to DHPS by the same bacterium [239, 249, 328]. Other studies demonstrated the ability of a *Citrobacter* strain and *E. rectale* DSM 17629 to form DHPS from SQ [251, 325]. Under oxic conditions, SQ conversion to sulfate, DHPS, or 3-sulfolactate has been demonstrated for various bacteria: 1) Conversion to sulfate by *Agrobacterium* sp. ABR2, 2) conversion via 3-sulfolactate to sulfate by *Pseudomonas putida* DSM 100120, 3) conversion to DHPS by *E. coli* and *Klebsiella oxytoca* DSM 16963, 4) conversion via DHPS to sulfate and 3-sulfolactate by *Klebsiella* sp. ABR11, and 5) conversion to DHPS and 3-sulfolactate by *Rhizobium leguminosarum bv. trifolii* SRDI565 [241, 248, 249, 252, 253, 347].

These SQDG and SQ-utilizing bacteria belong to the following families (and phyla): *Eubacteriaceae* (*Firmicutes*), *Enterobacteriaceae* (*Proteobacteria*), *Rhizobiaceae* (*Proteobacteria*), *Pseudomonadaceae* (*Proteobacteria*), or *Lachnospiraceae* (*Firmicutes*). Feeding a Spirulina diet containing SQDG was postulated to promote the growth of those bacterial strains. However, besides a trend of increased numbers of unclassified *Lachnospiraceae* in cecal contents and of reduced numbers of unclassified *Lachnospiraceae* in feces, unchanged numbers of the other taxa were observed in the present study (Appendix, Table A5). In addition, as indicated above (3.3.5.2), *Firmicutes* and *Proteobacteria* were reduced, rather than enriched (Appendix, Table A5). Therefore, it may be concluded that Spirulina supplementation did not stimulate the growth of SQDG or SQ-converting bacteria in conventional mice.

4.2.6 Sulfonates stimulated the growth of potentially colitogenic bacteria *in vitro*, while Spirulina did not do so *in vivo*

One aim of the present study was to investigate whether sulfonates stimulate the growth of pro-inflammatory gut bacteria such as the pathobiont *B. wadsworthia*. Indeed, in the present study *B. wadsworthia* was isolated from human fecal enrichment cultures using taurine or isethionate as substrates. This also applies to *Desulfovibrio* that was isolated from fecal enrichment cultures on taurine and isethionate.

Desulfovibrio sp. and other SRB have been considered as major risk factor for IBD and they contribute to the formation of the potentially toxic H_2S [417-419]. For example in patients with acute and chronic UC, which is one form of IBD, the counts of colonic *Desulfovibrio* spp. were elevated [414]. In another study, colitic germ-free mice colonized with *D. indonesiensis* displayed an increased cell infiltration in the lamina propria, an enhanced H_2S formation, and an upregulated immune response in the colon [415]. However, SRB are also part of the common gut microbiota and even though H_2S has been linked to IBD, it has also been recognized as a protective agent with anti-inflammatory and cytoprotective functions,

preventing intestinal inflammation [60, 69, 419-422]. Interestingly, both the pro-inflammatory effect of SRB and the toxic effect of H_2S seem to be concentration-dependent. While SRB are common intestinal bacteria with an incidence of approximately 50% in healthy humans, an increased abundance was observed in IBD patients [414, 415, 417]. Similarly, H_2S concentrations higher than 20 or 50 µM are considered to be cytotoxic [70-72].

In the present *in vivo* study, the SQ concentration in cecal contents and feces of SD-fed mice was elevated. But neither the abundance of *B. wadsworthia* nor of the family *Desulfovibrionaceae* were enriched in both matrices. Moreover, the abundance of *B. wadsworthia* was approximately three orders of magnitude reduced in feces until day nine of intervention and recovered afterwards almost completely. In cecum, there were no differences in *B. wadsworthia* numbers in SD-fed versus CD-fed mice. The family *Desulfovibrionaceae* (phylum *Proteobacteria*) had a reduced abundance in cecal contents of SD-fed mice and a reduced trend in feces. Interestingly, not only SRB, but also *B. wadsworthia* belong to the family *Desulfovibrionaceae.* The unchanged abundance of *B. wadsworthia* in cecum, but reduced abundance of cecal *Desulfovibrionaceae* might indicate that *Desulfovibrionaceae* other than *B. wadsworthia* were reduced due to the presence of SQ. The decreased abundance of *Desulfovibrionaceae* is in accordance with previous findings, as daily gavage of Spirulina (1.5 or 3.0 g/kg body weight) lowered the cell number of *Desulfovibrio* spp. in cecal contents of *Balb/c* mice [422]. A reduced number was also observed in cecal contents of a colitis-prone murine animal model ($IL10^{-/-}$) fed SD for three weeks [388]. In contrast, oral gavage of a 95% ethanolic extract of Spirulina (150 mg/kg/day) increased the counts of cecal *Desulfovibrionaceae* after eight weeks of treatment in rats, indicating that intact cells of Spirulina and extracts thereof may have different effects on the intestinal growth of *Desulfovibrionaceae* [410].

Other intestinal bacteria that may be commensal or pathogenic are *E. coli* strains. While adherent-invasive *E. coli* (AIEC) and extraintestinal pathogenic *E. coli* strains (ExPEC) are pathobionts, *E. coli* MG1655 is a commensal gut bacterium. Pathobionts are linked to IBD, while commensal *E. coli* strains are not [423]. Commensal *E. coli* strains able to utilize SQ were also isolated in the present *in vitro* study from human fecal slurries. No pathogenic *E. coli* strain were isolated from enrichment cultures of fecal slurries incubated with sulfonates. However, co-culturing of an isolated commensal *E. coli* strain (SQ6) with *B. wadsworthia* enhanced the growth and the H_2S formation from DHPS of the pathogenic *B. wadsworthia* in comparison to single-cultures of *B. wadsworthia* with DHPS. Co-abundance of commensal *E. coli* with SRB has earlier been linked to an enhanced apoptosis of colon epithelial cells [424]. Whether *E. coli* also enhance the inflammatory characteristics of *B. wadsworthia* is not known yet. Furthermore, no increase in the relative abundance of *Enterobacteriaceae*, to which *E. coli* belong to, after SD intake was observed in conventional mice in the present study (Appendix, Table A5).

Furthermore, IBD is characterized by a lowered bacterial diversity and richness [426-428], which is in contradiction to the present *in vivo* study. But IBD has also been linked to a diminished abundance of *Firmicutes*, which is consistent with the present study (Appendix, Table A5). The reduced relative abundance of *Firmicutes* in IBD was previously described to be a result of decreased populations of butyrate-producing *Clostridiaceae*, such as

members of *Clostridium* clusters IV, XIVa, and XVIII, which was also observed in the present study (Appendix, Table A5) [428]. IBD also correlates with a declined number of *Bacteroidetes* combined with higher numbers of *Proteobacteria* and *Actinobacteria*, as observed in mucosal biopsies of IBD patients compared to those of healthy controls [426]. This is in conflict with the trends observed for *Bacteroides*, *Proteobacteria* and *Actinobacteria* in the present study (Appendix, Table A5).

In sum, while the *in vitro* experiments implied that intestinal sulfonates might stimulate the proliferation of potentially colitogenic bacteria, increased SQ availability in Spirulina-fed conventional mice did not lead to an enrichment of such bacteria in the gut.

4.2.7 Spirulina increased body- and fat-tissue weight in mice

As an unexpected side-effect of the present study, an increased body weight was observed in SD-fed mice in comparison to CD-fed mice. The body weight of the SD-fed mice was approximately 5% increased after two days of intervention when compared to CD-fed mice, but the body-weight gain was not dependent on the amount of ingested food, as the ratio of body-weight increase per 1 g food intake was four times higher in SD-fed mice than in the CD-fed mice. This corresponds to a sixfold higher food efficiency. Afterwards (day two to day 21), the body weight increased by the same rate in both groups and food efficiency was identical. Furthermore, SD led to a 1.5 to 2 times increased weight of eWAT, sWAT, mWAT, and pWAT. However, bomb-calorimetry, as well as the Weender analysis identified both diets as isocaloric and no major differences in the macronutrient composition were detected.

Only a minority of studies reported a weight increase after the intake of Spirulina. Spirulina supplementation led to body-weight gain (averaged 9%) and an elevated body mass index (BMI) in undernourished human immunodeficiency virus (HIV)-positive patients after 12 weeks, who simultaneously received an antiretroviral treatment. However, in the same study Spirulina also resulted in a decrease of fat tissue in these patients [352]. Whether these changes were due to the Spirulina intake or the antiretroviral treatment could not be clarified, because no control group only receiving antiretroviral treatment was included in the study [352]. In another study, up to 1% Spirulina supplementation led to a body-weight increase in broiler chicken after three and five weeks of diet administration [353].

In most studies, Spirulina has been reported to have obesity-preventing effects by reducing body fat and weight. These findings are inconsistent with the results of the present study. For example, 64 obese individuals received twice daily 500 mg Spirulina which significantly reduced the BMI and the appetite [354, 355]. In another study, obese and overweight individuals on a restricted-calorie diet received daily four doses of 500 mg Spirulina. This treatment reduced the body weight, waist circumference, body fat and BMI [356]. However, Spirulina has also been reported to not have an effect on parameters of obesity. Yang *et al.* (2011) fed male and female C57BL/6J mice an American Institute of Nutrition Rodent Diet (AIN-93G and AIN-93M) supplemented with 2.5% or 5% of Spirulina for six months to test the toxicity of the ingested cyanobacteria. The body-weight increase between intervention and control group did not differ [357]. Similar results were obtained with 24-month

old male C57BL/6J mice fed a diet supplemented with 5% Spirulina for six weeks or with Sprague-Dawley rats fed a diet supplemented with 20% Spirulina for one month [358, 359].

In summary, the majority of studies report either a decreased or unchangeg/stable body weight after Spirulina intake, which is in conflict with the present study. It may be concluded that the consumption of SD was not responsible for the weight gain. It may be speculated that SD affected pathways involved in glucose metabolism, lipid uptake and / or lipid synthesis.

4.2.8 Spirulina enhanced the expression of key enzymes for lipid uptake and synthesis

Since obesity and an impaired glucose tolerance are linked to each other [429], the hypothesis that SD-fed mice developed alterations in glucose metabolism, was tested in the present study. No differences in the expression of genes responsible for intestinal and hepatic glucose transport (*Glut2* mRNA level) and hepatic glycogen synthesis (*Gys2* mRNA level) were detected between the groups. Similarly, glucose storage (mg glycogen/g protein), and blood-glucose levels were not affected by SD. It is concluded that SD did not alter the glucose metabolism, which disagrees with previous findings. Studies demonstrated that Spirulina administration has beneficial effects on blood sugar homeostasis. For example daily Spirulina doses of 2 g for two months or 8 g for 3 months administered to diabetes mellitus type 2 patients lowered the blood-glucose levels [430, 431]. Similar effects on blood-glucose levels were reported for diabetic Wistar rats, which were daily gavaged with an aqueous Spirulina solution for four weeks (50 mg/kg/day) [432]. Discrepancies with the present study might be due to differences in the health condition of the previously investigated human subjects and animal models. While earlier studies report results of experiments with diabetic human subjects and animals, the present study performed the experiments with healthy mice.

In the present study, Spirulina-induced fat-tissue accumulation was characterized by an enlarged adipocyte size. This form is considered to be a moderate form of obesity, referred to as hypertrophic obesity, as an increased number of adipocytes was not detected [340, 341]. These results are in contradiction with previous studies, as Spirulina has been linked to anti-obesity effects resulting in a reduction of fat-tissue weight. For example, obese Sprague-Dawley rats fed a high-fat diet and *Spirulina maxima* for four weeks (62 - 250 mg/kg) showed a trend for a reduction of the tissue weights of eWAT, pWAT, and mWAT compared to the control group, which only received the high-fat diet [433]. Interestingly, fat-tissue accumulation decreased relative to an increasing Spirulina concentration [433].

To examine further why previous results regarding the lipid metabolism were in conflict with outcomes of the current study, the lipid metabolism of SD-fed versus CD-fed mice was investigated in detail. In humans, lipid absorption mainly takes place in the jejunum, but there is also evidence that lipid uptake occurs in the ileum with increasing dietary fat load [434]. Accordingly, in mice the ileum is the central site of lipid absorption [435]. In the present study, SD-fed mice displayed a reduced expression of genes responsible for lipid transport (*Cd36* mRNA level), triglyceride synthesis (*Scd1* mRNA level) and lipid homeostasis (*Plin2* mRNA level) in jejunal mucosa, while there were no differences in ileal or

colonic mucosa. In hepatic tissue, Spirulina led to a reduction of *Cd36* and *Scd1* mRNA levels and a lowered expression of genes for lipid synthesis (*Elovl5* mRNA level).

The fatty acid translocase (CD36) facilitates the absorption of long-chain fatty acids and is located in various mammalian tissues such as adipose tissue, liver and the whole gastrointestinal tract [436, 437]. In the gut, CD36 is highly expressed in the small intestine at the apical membrane of enterocytes, which indicates its role in lipid transport across the brush border membrane [438, 439]. There is evidence that *Cd36*-deficiency leads to a diminished intestinal lipid and cholesterol uptake in mice [437, 440]. In humans, *CD36* expression was linked to the liver-fat content [441]. In addition, *Cd36* also correlated with the severity of hepatic steatosis in obese Zucker rats [442]. The Spirulina-induced down-regulation of *Cd36* in jejunum and liver in the present study might indicate that Spirulina intake results in a reduced lipid uptake by enterocytes and hepatocytes.

The acyl-CoA desaturase 1 (SCD1) catalyzes the insertion of double bonds at the delta-9 position in acyl-CoA substrates, such as palmitoyl-CoA and stearoyl-CoA [443]. The enzyme is located at the membrane of the endoplasmic reticulum of hepatocytes and of the intestinal epithelium, next to other mammalian tissues [444-447]. In previous studies, SCD1 has been linked to obesity [446, 447]. Moreover, in gut-specific *Scd1* knockout mice, the desaturase was linked to an increased lipid absorption [446]. Furthermore, liver-specific *Scd1* knockout mice were protected from high-fat diet-induced adiposity [447]. Therefore, SCD1 is suggested to play a pivotal role in lipid biosynthesis and fat accumulation in the body. The reduced gene-expression levels of intestinal and hepatic *Scd1* of SD-fed mice indicates that Spirulina feeding not only diminished lipid uptake, but also lipid anabolism.

Perilipin 2 (PLIN2) enables intracellular lipid storage by coating lipid droplets and therefore is responsible for fat homeostasis [448]. *Plin2* knockout mice show an intestinal lipid uptake and decreased formation of cytoplasmic lipid drops in enterocytes [449]. Furthermore, perilipins have been linked to increased liver-fat content in humans [441]. The lower *Plin2* expression level in the jejunum of SD-fed mice compared to CD-fed mice might be the result of a reduced lipid uptake, which is normally facilitated by CD36.

The elongation of very long chain fatty acids protein 5 (ELOVL5) is involved in microsomal elongation of fatty acids, such as of mono- and polyunsaturated fatty acids, by the addition of two carbon atoms. The function of ELOVL5 in liver metabolism has been described in several studies. As an example, *Elovl5* knockout mice displayed increased liver triglyceride levels and steatosis [450]. This is in agreement with lower liver triglyceride levels in mice with an increased activity of hepatic *Elovl5* [451]. However, some findings of the present study are in conflict with previous results. The Spirulina-induced *Elovl5* reduction in the present study did not correlate with an increased triglyceride concentration in the liver or pathogenic modifications of the liver.

In addition, mRNA levels of further key genes related to hepatic lipid uptake and synthesis tended to be decreased in SD-fed mice. No lipid droplets, signs of fibrosis or steatosis, and no differences in triglyceride levels between SD- and CD-fed mice were observed in the liver.

Taken together, Spirulina intake clearly reduced the expression of *Cd36*, *Scd1*, *Plin2* in jejunal mucosa and of *Cd36*, *Scd1* and *Elovl5* in the liver of conventional mice. These findings indicate that Spirulina affects the expression of genes responsible for the intestinal and hepatic lipid uptake and metabolism. Despite the Spirulina-induced weight gain and fat-tissue accumulation observed in the present study in the early period of the experiment, the gene-expression level of genes involved in intestinal and hepatic intracellular lipid uptake and availability were lowered, which in consideration of the above relationships is difficult to explain. Further investigations on the lipid metabolism at protein level could help to clarify these discrepancies.

5 CONCLUSIONS AND PERSPECTIVES

The gut microbiota has a crucial impact on host health. Diet is the main driver shaping the intestinal microbiota, as diet is the main source of bacterial substrates [35]. Therefore, it is important to unravel the fate of ingested dietary components and how they affect composition and activity of the gut microbiota. In a previous study, the intake of unsaturated fatty acids was associated with a higher release of intestinal TC and a higher abundance of the colitogenic bacterium *B. wadsworthia* [9]. In $IL10^{-/-}$ mice the TC-induced bloom of *B. wadsworthia* led to an exacerbation of colitis. *B. wadsworthia* is able to convert sulfonates such as taurine, present in TC, isethionate, cysteate and DHPS to H_2S which might be linked to IBD [8]. Therefore, this PhD-project aimed to clarify, whether dietary sulfonates or their sulfonated metabolites stimulate the growth of colitogenic bacteria such as *B. wadsworthia* and whether these bacteria convert sulfonates to H_2S.

Human fecal slurries converted several dietary sulfonates to H_2S with inter-individual differences in the ability to form H_2S. Taurine and isethionate-converting isolates from these fecal cultures, able to release H_2S, are potentially pathogenic bacteria (*B. wadsworthia* and *Desulfovibrio* strains). Nevertheless, not only pathogenic human intestinal bacteria are able to utilize sulfonates and to release H_2S, as commensal *E. coli* strains isolated from human fecal slurries in this project were able to convert SQ to DHPS and 3-sulfolactate to H_2S. Presence or absence of such bacteria may explain the inter-individual differences in sulfonate conversion.

The ability to ferment taurine by *Desulfovibrio* strains was previously only described for *D.* sp. RZACYSA isolated from sewage, while isethionate utilization is quite common for this genus [3, 8, 134, 139, 161, 162, 164]. Therefore, the present study led to the first *Desulfovibrio* strain, directly isolated from human feces, and capable of converting taurine and isethionate to H_2S. In addition *D. simplex* DSM 4141^T was identified as another bacterium belonging to *Desulfovibrio* spp. able to utilize taurine and to release H_2S. These results suggest that the sulfidogenic respiration is more widespread among *Desulfovibrio* spp. than initially expected.

The present study describes also the third co-culture model of *E. coli* and *B. wadsworthia* which completely converted SQ via DHPS to H_2S. Previously, two co-culture models were reported to degrade SQ using the same pathway, namely *E. coli* with a *Desulfovibrio* strain or *E. rectale* with *B. wadsworthia* [251, 325]. In this study, H_2S formation by *B. wadsworthia* increased considerably in the presence of *E. coli* (from 2.5 to 50% of the initially added DHPS). Therefore, it can be concluded that the presence of *E. coli* strains in combination with *B. wadsworthia* stimulates the amount of H_2S produced and that co-culturing with human *Enterobacteriaceae* such as *E. coli* stimulates the release of H_2S from pathogens, indicating a synergistic effect in the gut environmental sulfonate-sulfur cycle.

Feeding a low-fat diet supplemented with Spirulina did not affect the relative abundance of potentially colitogenic bacteria such as *B. wadsworthia* and *Desulfovibrionaceae*, but nevertheless was accompanied by a mild inflammation. The abundance of *B. wadsworthia* decreased initially (from day 2 – 9), but recovered afterwards until the end of the intervention in feces, while the number of *Desulfovibrionaceae* in cecum was reduced. However, an extended ingestion of Spirulina might further increase the abundance of *B. wadsworthia* and might lead to a more severe inflammation over time. The Spirulina-containing diet did also not affect the relative abundance of known SQDG- or SQ-converting, as the number of *Enterobacteriaceae* was not affected, but altered the gut microbiota composition and resulted in higher SQ-concentrations in cecal content and feces. Feeding Spirulina was linked to a reduction of *Firmicutes* and an increased number of *Bacteroidetes* in feces and cecum. *Firmicutes* were decreased due to a reduced abundance of the family *Erysipelotrichaceae* and its genus *Allobaculum*, while the increased number of *Bacteroidetes* was a result of the higher abundance of *Bacteroidaceae*, *Porphyromonadaceae* and *Rikenellaceae*. This means that the Spirulina-supplemented diet neither stimulated the growth of potentially colitogenic bacteria nor of previously identified bacteria capable of converting SQDG to SQ. Therefore, gut bacteria other than those already known seem to be responsible for the conversion of SQDG to SQ, probably the enriched *Bacteroidetes* might play a role.

Interestingly, SD feeding was also paralleled by an unexpected fat-tissue accumulation and an increase in body weight. Food intake was not considered as the main cause for the observed body-weight gain. The ratio of body-weight gain (%) per 1 g of consumed diet was four times higher in SD-fed compared to the CD-fed mice indicating differences in food efficiency. However, gene-expression levels of genes involved in the glucose metabolism were not altered and of those involved in lipid uptake and availability were lowered. These findings do not correspond to previous observations [6-8]. It cannot be excluded that gene expression levels did not correspond to the amounts of encoded proteins. For example, post-translational factors can influence the synthesis of proteins. Therefore, determination of protein levels may clarify these discrepancies.

In summary, the conversion of sulfonates by fecal slurries differed considerably among the human donors. *Desulfovibrio* strains and *B. wadsworthia* isolated from human feces were affiliated with taxa known to encompass potential pathogens or commensal gut bacteria. Differences in the conversion of various sulfonates by human fecal slurries might be the result of inter-individual differences in gut microbiota composition. In mice, a diet supplemented with Spirulina did affect the intestinal microbiota composition, but did not alter the abundance of *B. wadsworthia* and *Desulfovibrionaceae*. This indicates that not only these potential colitogenic but also other gut bacteria might utilize sulfonates for growth.

APPENDIX

Table A1: Media and solutions used.

Medium / solution	Components and preparation
Anoxic phosphate buffered saline (aPBS), 1 l	NaCl 8.5 g Na_2HPO_4 0.6 g KH_2PO_4 0.3 g Peptone (Oxoid, Wesel, Germany) 0.1 g Resazurin (Fluka) 1.0 mg Sodium formate (Fluka) (40 mM) Sodium DL-lactate (Sigma-Aldrich) (40 mM) pH 7.0 N_2/CO_2 (80/20, v/v, %) Autoclaved at 121 °C for 15 min Titanium(III) nitrilotriacetate (NTA, 3.18 mM, [271]), sterile filtered (syringe filter, 0.20 µM pore size, Sarstedt) just before inoculation.
NTA	1. NTA (Sigma-Aldrich) 9.6 g in 300 ml anoxic distilled water 2. Add NaOH 40 g/100 ml to reach pH 9.0 3. Add 9.6 ml $TiCl_3$ (Acros Organics, geel, Belgium) 20%; pH was hold > 2.0 with Na_2CO_3 in anoxic distilled water, 8 g/100 ml 4. Add Na_2CO_3 in anoxic distilled water, 8 g/100 ml to reach pH 7.0 5. Volume was filled up to 500 ml with anoxic distilled water 6. Sterile filtered (syringe filter, 0.2 µM pore size, Sarstedt)
Base medium, modified [272]	NH_4Cl 19 mM NaCl 17 mM $MgCl_2$ 2 mM KCl 7 mM $CaCl_2$ 0.3 mM K_2HPO_4 0.1 mM 1,4-Naphtochinon (Sigma-Aldrich) 1.26 µM Resazurin (Fluka) 2 µM Yeast extract (Roth) 3.5 mg/l Selenite-tungstate solution (DSMZ medium 385) 1 ml/l Trace elements solution SL-10 (DSMZ medium 320) 1 ml/l Sodium DL-lactate and / or sodium formate 40 mM pH was adjusted to 7.8; medium was dispersed into Hungate tubes, gas flushed N_2/CO_2 or H_2/CO_2 (80/20, v/v, %), autoclaved (121 °C,15 min) and stored at RT. Prior to inoculation supplementation of: NTA 3.18 mM [271] Seven vitamins solution (DSMZ medium 503) 1 ml/l $NaHCO_3$ (Merck) 0.25%, 120 °C, 15 min One sulfonate 4 mM or 20 mM
Mineral salts medium (MSM), modified [273]	Potassium phosphate salt solution (KPP) 10 mM, pH 7.0 NH_4Cl 20 mM $MgSO_4$ 0.25 mM Trace element solution, modified 500 µl/l HCl (25%, v/v) 200 ml/l $FeCl_2$ 0.719 mM $ZnCl_2$ 0.035 mM $MnCl_2$ 0.015 M H_3BO_3 0.49 mM $CoCl_2$ 0.084 mM $CuCl_2$ 0.0059 mM

	$NiCl_2$ 0.0085 mM Na_2MoO_4 0.12 mM pH was adjusted to 7.2; medium was dispersed into a two-liter flask and autoclaved (121 °C,15 min) and stored at RT.
Freshwater basal medium, modified [195]	NaCl 17 mM NH_4Cl 19 mM $CaCl_2$ 0.3 mM $MgCl_2$ 2 mM K_2HPO_4 0.1 mM Yeast extract 3.5 mM Resazurin 4 µM pH was adjusted to 7.8; medium was dispersed into Hungate tubes, gas flushed N_2, autoclaved (121 °C,15 min) and stored at RT. Prior to inoculation supplementation of: NTA 3.18 mM [271] Seven vitamins solution (DSMZ medium 503) 1 ml/l $FeCl_2$ (Riedel de Häen) 1 mM An electron donor and an electron acceptor
Selenite-tungstate solution (DSMZ medium 385)	NaOH 12.5 mM Na_2SeO_3 11.4 mM Na_2WO_4 12.1 mM
Trace elements solution SL-10 (DSMZ medium 320)	$FeCl_2$ 0.75 M in HCl (25%; 7.7 M; 10.00 ml) $ZnCl_2$ 0.5 mM $MnCl_2$ 0.5 mM H_3BO_3 0.1 mM $CoCl_2$ 0.8 mM $CuCl_2$ 0.01 mM $NiCl_2$ 0.1 mM Na_2MoO_4 0.15 mM
Seven vitamins solution (DSMZ medium 503)	Vitamin B12 (Roth) 0.1 g/L *p*-Aminobenzoic acid (Sigma-Aldrich) 0.08 g/L D(+)-Biotin (Roth) 0.02 g/L Calcium pantothenate (Fluka) 0.1 g/L Nicotinic acid (Roth) 0.2 g/L Pyridoxine hydrochloride (Roth) 0.3 g/L Thiamine-HCl x 2 H_2O (Serva, Heidelberg, Germany) 0.2 g/L Sterile filtered (syringe filter, 0.2 µM pore size, Sarstedt)
HB buffer	Sodium dihydrogen phosphate (Merck) 10 mM EDTA (Roth) 1 mM Polyoxyethylene (10) tridecyl ether (Sigma-Aldrich), 1% v/v pH was adjusted to 7,4 and solution was stored at 4 °C.
MOPS buffer	3-Morpholino-propane-sulfonic acid (Roth) 0.2 M Sodium acetate (Merck) 0.05 M EDTA (Roth) 0.01 M pH was adjusted to 5,5 - 7,0; solution was autoclaved and stored at 4 °C.
TRIS-acetate-EDTA buffer (TAE buffer)	TRIS (Roth) 40 mM Glacial acetic acid (Merck) 20 mM EDTA (Roth) 1 mM pH 8.3
RYU flagella stain [274]	Two parts of the mordant solution Phenol 0.3 M, Tannic acid (Sigma-Aldrich) 0.06 M Aluminum potassium sulfate 0.15 M One part of saturated crystal violet solution (0.3 mM in 95% ethanol). Stain precipitation was eliminated by filtering the RYE stain solution through a filter paper (150 mM, Macherey-Nagel) and a 0.22 µM pore size syringe filter membrane.

Table A2: Sulfonate utilization by bacteria under oxic conditions. N.A. = not analyzed.

	Bacterial species / strain	Source		Sulfonate (sulfonic intermediate)	Sulfur moiety released as	References
OXIC CONDITION	*Acinetobacter* sp. ICD	**Environmentally**	Sediment of a polluted woodland pond	Isethionate	Sulfate	[152]
	Agrobacterium sp. ABR2		Forest leaf mould	SQ	Sulfate	[241, 253]
	Chromohalobacter salexigens DSM 3043^T		Solar salt facility	Taurine	Isethionate	[132]
				3-Sulfolactate	Sulfate and sulfite	[266]
	Cupriavidus necator (*Ralstonia eutropha*) H16 (DSM 428)		Sludge	Taurine, isethionate	Sulfite	[167]
	Cupriavidus pinatubonensis JMP134		Soil	DHPS (3-sulfolactate)	Sulfate	[263]
	Neptuniibacter caesariensis MED92		Seawater	Taurine	Sulfoacetate expected	[123]
	Paracoccus denitrificans PD1222		Soil	Hypotaurine	Sulfite	[452]
	Pseudomonas putida SQ1 (DSM 100120)		Littoral sediment from Lake Constance	SQ (3-sulfolactate)	Sulfate	[248]
	Pseudomonas spp.		Leaf mold	SQ	Unknown product	[241, 253]
	Rhizobium leguminosarum bv. trifolii SRDI565		Roots of the annual clover *Trifolium subterraneum* ssp. *subterraneum*	SQ	DHPS and 3-sulfolactate	[252]
	Rhodococcus sp. RHA1		Gamma-hexachlorocyclohexane-contaminated soil	Taurine	Sulfate and sulfite	[130, 454-456]
	Roseovarius nubinhibens ISM (DSM 15170)		Marine environment	3-Sulfolactate (cysteate), taurine, cysteate	Sulfate	[172]
	Ruegeria pomeroyi DSS-3		Seawater	Genetic presence of taurine, isethionate, cysteate and DHPS degrading genes	Presuming sulfite	[456]
	Roseovarius sp. 217		Marine environment	Taurine	Sulfite	[121]
				Isethionate, cysteate, 3-sulfolactate	Sulfate	
	Silicibacter pomeroyi DSS-3^T (DSM 15171)		Seawater	Taurine	Sulfate expected	[124]
				Cysteate	Sulfate	[129, 190-192]
				3-Sulfolactate (cysteate)	Sulfite	[190]

	Bacterial-ID	Source		Sulfonate (sulfonic intermediate)	Sulfur moiety released as	References
OXIC CONDITION	*Acinetobacter calcoaceticus* SW1 (DSM 16962)	**Potential intestinally**	Wastewater treatment	Taurine	Sulfoacetaldehyde	[457]
	Klebsiella oxytoca TauN1 (= a group of isolates)		Waste water treatment plant	Taurine	Isethionate	[148]
	Klebsiella sp. ABR11		Sewage sludge	SQ (DHPS)	Sulfate and 3-sulfolactate	[241, 253]
	Paracoccus denitrificans NKNIS (DSM 15418)		Communal wastewater treatment plant	Taurine or isethionate	Sulfate and sulfite	[3, 131]
				Cysteate	Sulfopyruvate	
	Pseudomonas putida sp.		Sewage sludge	Taurine, isethionate, cysteate	Sulfite	[157]
	Pseudomonas aeruginosa TAU-5		Manure	Taurine	N.A.	[127]
	Rhodococcus opacus ISO-5		Sludge from sewage treatment plant	Taurine	Sulfate and sulfite	[130, 454-456]
	Acinetobacter radioresistens SH164	**Intestinally or from human beings**	Skin of a patient's forehead	Taurine	Sulfoacetaldehyde	[458]
	Escherichia coli		Human colon	Taurine, cysteate, isethionate	Sulfite	[153-156, 193, 194]
	Escherichia coli K12		Feces of a convalescent diphtheria patient	SQDG	SQ	[239]
				SQ	DHPS	[249]
	Klebsiella aerogenes		Human respiratory, urinary, blood, or gastrointestinal tract	Cysteate, taurine, isethionate	Could not be clarified	[156]
	Pseudomonas sp.		Upper colon from dog	Taurine	Isethionate	[146]
	Serratia marcescens F		From human blood, urinary, wound respiratory tract	Cysteate, taurine and isethionate	Could not be clarified	[156]
	Proteus vulgaris OX19	**N.A.**	N.A.	Cysteate	Sulfate	[182]
	Rhodococcus spp.		N.A.	Taurine, isethionate	Sulfite or sulfate	[158]
	Rhodopseudomonas palustris CGA009		N.A.	Taurine	Sulfoacetate	[459]
	Rhodobacter sphaeroides 2.4.1		N.A.	Taurine	Sulfate expected	[122]

	Bacterial species / strain	Source		Sulfonate (sulfonic intermediate)	Sulfur moiety released as	References
OXIC CONDITION	Co-culture: 1) *Pseudomonas putida* SQ1 (DSM 100120) with 2) *Paracoccus pantotrophus* NKNCYSA (DSM 12449)	**Environmentally and potential intestinally**	1) Littoral sediment from lake Constance 2) Anaerobic digestor of local sewage plant	1) SQ 2) 3-Sulfolactate	1) 3-Sulfolactate 2) Sulfate	[347]
	Co-culture: 1) *Klebsiella oxytoca* TauN1 (DSM 16963) with 2) *Cupriavidus pinatubonensis* JMP134 (DSM 4058)		1) Waste water treatment plant 2) Soil	1) SQ 2) DHPS	1) DHPS 2) Sulfate	[347]

Table A3: Sulfonate utilization by bacteria under anoxic conditions. N.A. = not analyzed.

	Bacterial-ID	Source		Sulfonate (sulfonic intermediate)	Sulfur moiety released as	References
ANOXIC CONDITIONS	*Bacillus krulwichiae* AM31D^T (JCM11691^T)	Environmentally	Soil	Isethionate	Sulfite	[159, 460]
	Citrobacter sp. strain (99% identity with *Citrobacter freundii*)		Garden compost	SQ	DHPS	[251]
	Clostridium chromiireducens (C. pasteurianum) C1		Soil	Taurine or isethionate	Not quantified	[3, 119, 160]
	Clostridium pasteurianum 5 ATCC 6013 (DSM 525^T)		Soil	Cysteate, 3-sulfolactate	Not quantified	[3, 119, 160]
	Clostridium MS-1		Soil	Isethionate, cysteate, 3-sulfolactate	Not quantified	[3, 119, 160]
	Desulfitobacterium dehalogenans DSM 9161		Freshwater pond sediment	Isethionate, cysteate	N.A.	[162]
	Desulfitobacterium sp. PCE 1 (DSM 10344)		Soil	Isethionate or cysteate	N.A.	[162]
	Desulfobacterium autotrophicum DSM 3382		Marine mud	Cysteate	H_2S	[8, 161, 163, 195]
	Desulfomicrobium baculatus DSM 1742		Forest pond	Cysteate, isethionate	N.A.	[8, 161, 163]
	Desulfovibrio desulfuricans IC1 (DSM 12129)		Compost soil	Cysteate, isethionate	H_2S	[8, 161, 162]
	Desulfovibrio desulfuricans ATCC 29577		Tar-sand mixture in waterlogged clay	Isethionate	N.A.	[8, 161, 163]
	Klebsiella sp.		Soil	Cysteate, 3-sulfolactate	Not quantified	[3, 119, 160]
	Marine Microbial Mats		Marine sediments	Taurine, isethionate, cysteate	H_2S	[133]
	Rhodopseudomonas palustris Tau1		Lake sediment	Taurine	Sulfate	[461]
	Rhodobacter sphaeroides Tau3		Lake sediment	Taurine	Sulfate	[461]

	Bacterial-ID	Source		Sulfonate (sulfonic intermediate)	Sulfur moiety released as	References
ANOXIC CONDITIONS	*Alcaligenes* sp. NKNTAU	**Potential intestinally**	Communal sewage work	Taurine	Sulfate	[166]
	Bilophila wadsworthia RZATAU (DSM 11045)		Anaerobic mud, sewage plant	Taurine, isethionate, cysteate or DHPS	H_2S	[8, 137, 139, 140]
	Desulfitobacterium hafniense DSM 10664		Sewage sludge	Isethionate	H_2S	[162]
				3-Sulfolactate	N.A.	[129]
	Desulfonispora thiosulfatigenes DSM 11270^T		Sewage plant	Taurine	Thiosulfate	[76, 164, 215, 216]
	Desulfovibrio sp. GRZCYSA		Sewage and sediment of lake	Isethionate	H_2S	[3, 8, 134, 139, 164]
				Cysteate	H_2S and sulfate	
	Desulfovibrio sp. RZACYSA		Communal sewage works	Taurine, isethionate, cysteate	H_2S	[8, 139]
	Paracoccus pantotrophus NKNCYSA (DSM12449)		Communal wastewater treatment plants	Taurine, isethionate, cysteate (sulfolactate)	Sulfate	[129, 165, 166]
	Paracoccus pantotrophus NKNIS		Communal sewage works	Isethionate	Sulfite and sulfate	[166]
	Bilophila wadsworthia 3.1.6	**Intestinally**	Human gut	Taurine (isethionate)	H_2S	[8, 136]
	Bifidobacterium kashiwanohense PV20-2		Human infant feces	Taurine	Isethionate	[134, 135]
	Butyrivibrio sp. S2		Ovine rumen	SQDG	Fatty acids	[382]
	Clostridium butyricum BL5262		Human gut	Taurine (isethionate)	Sulfite	[119]
	Veillonellaceae 2C		Human feces	Taurine	H_2S	[138]
	Co-culture: 1) *Escherichia coli* K12 with 2) *Desulfovibrio* sp. DF1	**Potentially intestinal and intestinal**	1) Feces of a convalescent diphtheria patient 2) Anaerobic sewage sludge	1) SQ 2) DHPS (3-sulfolactate)	1) DHPS 2) H_2S	[1]
	Co-culture: 1) *Eubacterium rectale* DSM 17629 2) *Bilophila wadsworthia* 3.1.6		1) Human feces 2) Human gut	1) SQ 2) DHPS	1) DHPS 2) H_2S	[325]

Table A4: Used conditions for PCR.

Used conditions		Target (amplicon size in bp)					
		***16S rRNA* (1465), *16S RNA B. wadsworthia* (239)**	**RAPD: M13-core**	***dsrAB* (649)**	***E. coli K12* strains (970), *E. coli* (212), *E. alberti* (393), *E. fergusonii* (575)**	***yihS* (332)**	***yihQ* (2034)**
PCR reaction mixture	Taq buffer (Invitrogen, Karlsruhe, Germany) (µl)	5	5	5	5	5	"Q5 High-Fidelity 2X Master Mix" (New England Biolabs, USA) was used instead with a volume of 25 µl
	$MgCl_2$ (Invitrogen, Karlsruhe, Germany) (mM)	2.5	2.5	1.5	1.5	1.5	
	deoxynucleotide triphosphates (dNTPs, Invitek, Berlin, Germany) (mM)	0.25	0.25	0.25	0.25	0.25	
	Recombinant *Taq* DNA Polymerase (Invitrogen, Karlsruhe, Germany) (U)	2.5	2.5	1	1	1	
	Primer, each (Eurofins Genomics, Ebersberg, Germany) (µM)	0.1	2	0.25	0.2	0.5	0.5
	DNA template (ng)	200	900	500	15	500	50
	End volume (µl)	50	50	50	50	50	50
PCR program peqSTAR Thermocycler (Peqlab, Germany)	Heating lid to (°C)	110	110	110	110	110	110
	Denaturation (°C / minutes)	94 / 4	95 / 5	94 / 3	94 / 3	94 / 3	98 / 0.5
	Number of Cycles	30	30	30	30	35	30
	Denaturation (°C / minutes)	94 / 1	95 / 1	94 / 0.75	94 / 0.75	94 / 1	98 / 0.17
	Annealing (°C / minutes)	55 / 1	50 / 1	53.5 / 0.5	57/ 0.5	57.1 / 0.5	65 / 0.5
	Elongation (°C / minutes)	72 / 1	72 / 1	72 / 1	72 / 1.5	72 / 1	72 / 1
	Final elongation (°C / minutes)	72 / 10	72/ 6	72 / 10	72 / 10	72 / 10	72 / 2
	Stored at (°C)	4	4	4	4	4	4
Gel electrophoresis	Loading buffer	EZ-VISION™ Two DNA dye	EZ-VISION™ One DNA dye	EZ-VISION™ Two DNA dye	EZ-VISION™ One DNA dye	EZ-VISION™ One DNA dye	EZ-VISION™ One DNA dye
	Ladder [GeneRuler 100 bp Plus DNA Ladder (Thermo Fisher Scientific) or 1 kb plus DNA ladder (Invitrogen)]	1 kb	100 bp and 1kb	1 kb	1kb	1kb	1kb
	Agarose gel (%) (Serva, Germany)	1	2	1	2	1	1

Table A5: Difference of bacterial relative abundance in feces (F) and cecal contents (C) after respectively 16 or 21 days of intake of semisynthetic diet supplemented with 20% Spirulina in comparison to semisynthetic control diet in conventional mice. n = 5 - 7 per group. ↑ = increased trend, ↓ = reduced trend, ↑↑ = significantly increased, ↓↓ = significantly reduced, n.d. = not detected. *P < 0.05, **P < 0.01, ***P < 0.001, ****P < 0.001.

Phylum	**Family**	**Genus**
Bacteroidetes ↑↑ (F* + C***)	*Porphyromonadaceae* ↑↑ (F**** + C***)	Unclassified *Porphyromonadaceae* ↑ (F), unclassified *Porphyromonadaceae* ↑↑ (C*) and *Barnesiella* ↑ (C)
	Prevotellaceae ↑↑ (C*)	*Alloprevotella* ↑ (F) and *Alloprevotella* ↑↑ (C*)
	Unclassified *Bacteroidales* ↓ (F)	*Parabacteroides* ↑↑ (F*) and unclassified *Bacteroidales* ↓ (F)
	Rikenellaceae ↑↑ (F* + C*)	*Alistipes* ↑↑ (F* + C*)
	Bacteroidaceae ↑↑ (F*** + C***)	*Bacteroides* ↑↑ (F** + C**)
Firmicutes ↓↓ (F** + C***)	*Lactobacillaceae* ↑↑ (F** + C*)	*Lactobacillus* ↑↑ (F** + C**)
	Unclassified *Clostridiales* ↑↑ (F**) and unclassified *Clostridiales* ↑ (C)	Unclassified *Clostridiales* ↑↑ (F**), unclassified *Clostridiales* ↑ (C), *Clostridium* XIVa ↓ (F), *Clostridium* IV ↓↓ (F**), *Anaerotruncus* ↑ (C) and *Flavonifractor* ↓ (C)
	Erysipelotrichaceae ↓↓ (F** + C***)	*Allobaculum* ↓↓ (F** + C*) and unclassified *Erysipelotrichaceae* ↑ (C)
	Lachnospiraceae ↓ (F + C)	Unclassified *Lachnospiraceae*↓ (F) and unclassified *Lachnospiraceae* ↓↓ (C*)
	Ruminococcaceae ↓ (F + C)	Unclassified Ruminococcaceae ↓ (F + C) and *Oscillibacter* ↑ (F)
Proteobacteria ↓ (F + C)	*Desulfovibrionaceae* ↓ (F) and *Desulfovibrionaceae* ↓↓ (C**)	Unclassified *Desulfovibrionaceae* ↓↓ (C**)
	Sutterellaceae ↓↓ (F*) and *Sutterellaceae* ↓ (C)	*Parasutterella* ↓↓ (F*) and *Parasutterella* ↓ (C)
Verrumicrobia ↓ (F)	*Verrumicrobiaceae* ↓ (F)	*Akkermansia* ↓ (F)
Actinobacteria ↓ (F + C)	n.d.	n.d.

REFERENCES

[1] Kertesz MA. Riding the sulfur cycle - Metabolism of sulfonates and sulfate esters in Gram-negative bacteria (Review). *FEMS Microbiology Reviews* 2000; 24: 135–175.

[2] Seitz AP, Leadbetter ER, Godchaux W. Utilization of sulfonates as sole sulfur source by soil bacteria including *Comamonas acidovorans*. *Arch Microbiol* 1993; 159: 440–444.

[3] Cook AM, Laue H, Junker F. Microbial desulfonation (Review). *FEMS Microbiol Rev* 1998; 22: 399–419.

[4] Stapleton PP, Charles RP, Redmond HP, *et al*. Taurine and human nutrition (Review). *Clinical Nutrition* 1997; 16: 103–108.

[5] Rana SK, Sanders TAB. Taurine concentrations in the diet, plasma, urine and breast milk of vegans compared with omnivores. *Br J Nutr* 1986; 56: 17–27.

[6] Galliard T. Aspects of lipid metabolism in higher plants-I. Identification and quantitative determination of the lipids in potato tubers. *Phytochemistry* 1968; 7: 1907–1914.

[7] Kuriyama I, Musumi K, Yonezawa Y, *et al*. Inhibitory effects of glycolipids fraction from spinach on mammalian DNA polymerase activity and human cancer cell proliferation. *J Nutr Biochem* 2005; 16: 594–601.

[8] Laue H, Denger K, Cook AM. Taurine reduction in anaerobic respiration of *Bilophila wadsworthia* RZATAU. *Appl Environ Microbiol* 1997; 63: 2016–2021.

[9] Devkota S, Wang Y, Musch MW, *et al*. Dietary-fat-induced taurocholic acid promotes pathobiont expansion and colitis in IL10$^{-/-}$ mice. *Nature* 2012; 487: 104–108.

[10] Helander HF, Fändriks L. Surface area of the digestive tract – revisited (Review). *Scand J Gastroenterol* 2014; 49: 681–689.

[11] Vuik F, Dicksved J, Lam SY, *et al*. Composition of the mucosa-associated microbiota along the entire gastrointestinal tract of human individuals. *United Eur Gastroenterol J* 2019; 7: 897–907.

[12] Bengmark S. Ecological control of the gastrointestinal tract. The role of probiotic flora (Review). *Gut* 1998; 42: 2–7.

[13] Cheng LK, O'Grady G, Du P, *et al*. Gastrointestinal system (Review). *WIREs Syst Biol Med* 2010; 2: 65–79.

[14] Groeger S, Meyle J. Oral mucosal epithelial cells (Review). *Front Immunol* 2019; 10: 208.

[15] Furness JB, Rivera LR, Cho HJ, *et al*. The gut as a sensory organ (Review). *Nat Rev Gastroenterol Hepatol* 2013; 10: 729–740.

[16] Sender R, Fuchs S, Milo R. Revised estimates for the number of human and bacteria cells in the body. *PLOS Biol* 2016; 14: e1002533.

[17] Dave M, Higgins PD, Middha S, *et al*. The human gut microbiome: Current knowledge, challenges, and future directions (Review). *Translational Research* 2012; 160: 246–257.

[18] Bäckhed F, Ley RE, Sonnenburg JL, *et al*. Host-bacterial mutualism in the human intestine (Review). *Science* 2005; 307: 1915–1920.

[19] Rinninella E, Raoul P, Cintoni M, *et al*. What is the healthy gut microbiota composition? A changing ecosystem across age, environment, diet, and diseases (Review). *Microorganisms* 2019; 7: 14.

[20] Hugon P, Dufour JC, Colson P, *et al*. A comprehensive repertoire of prokaryotic species identified in human beings (Review). *The Lancet Infectious Diseases* 2015; 15: 1211–1219.

[21] Blaut M, Clavel T. Metabolic diversity of the intestinal microbiota: Implications for health and disease (Review). *J Nutr* 2007; 137: 751S-755S.

[22] Qin J, Li R, Raes J, *et al*. A human gut microbial gene catalogue established by metagenomic sequencing. *Nature* 2010; 464: 59–65.

[23] Arumugam M, Raes J, Pelletier E, *et al*. Enterotypes of the human gut microbiome. *Nature* 2011; 473: 174–180.

[24] Eckburg PB, Bik EM, Bernstein CN, *et al*. Diversity of the human intestinal microbial flora. *Science* 2005; 308: 1635–1638.

[25] Laterza L, Rizzatti G, Gaetani E, *et al*. The gut microbiota and immune system relationship in human graft-versus-host disease (Review). *Mediterr J Hematol Infect Dis* 2016; 8: e2016025.

[26] Nayfach S, Shi ZJ, Seshadri R, *et al*. New insights from uncultivated genomes of the global human gut microbiome. *Nature* 2019; 568: 505–510.

[27] Almeida A, Mitchell AL, Boland M, *et al*. A new genomic blueprint of the human gut microbiota. *Nature* 2019; 568: 499–504.

[28] Gensollen T, Iyer SS, Kasper DL, *et al*. How colonization by microbiota in early life shapes the immune system (Review). *Science* 2016; 352: 539–544.

[29] Cerf-Bensussan N, Gaboriau-Routhiau V. The immune system and the gut microbiota: Friends or foes (Review)? *Nature Reviews Immunology* 2010; 10: 735–744.

[30] Kamada N, Chen GY, Inohara N, *et al*. Control of pathogens and pathobionts by the gut microbiota (Review). *Nature Immunology* 2013; 14: 685–690.

[31] Conlon MA, Bird AR. The impact of diet and lifestyle on gut microbiota and human health (Review). *Nutrients* 2015; 7: 17–44.

[32] Thursby E, Juge N. Introduction to the human gut microbiota (Review). *Biochemical Journal* 2017; 474: 1823–1836.

[33] Goodrich JK, Waters JL, Poole AC, *et al*. Human genetics shape the gut microbiome. *Cell* 2014; 159: 789–799.

[34] Willmann M, Vehreschild MJGT, Biehl LM, *et al.* Distinct impact of antibiotics on the gut microbiome and resistome: A longitudinal multicenter cohort study. *BMC Biol* 2019; 17: 76.

[35] David LA, Maurice CF, Carmody RN, *et al*. Diet rapidly and reproducibly alters the human gut microbiome. *Nature* 2014; 505: 559–563.

[36] Den Besten G, Van Eunen K, Groen AK, *et al*. The role of short-chain fatty acids in the interplay between diet, gut microbiota, and host energy metabolism (Review). *Journal of Lipid Research* 2013; 54: 2325–2340.

[37] Sridharan G V., Choi K, Klemashevich C, *et al*. Prediction and quantification of bioactive microbiota metabolites in the mouse gut. *Nat Commun* 2014; 5: 5492.

[38] Espín JC, González-Sarrías A, Tomás-Barberán FA. The gut microbiota: A key factor in the therapeutic effects of (poly)phenols (Review). *Biochemical Pharmacology* 2017; 139: 82–93.

[39] Loo M. Lifestyle Approaches. In: *Integrative Medicine for Children*. Elsevier, 2009, pp. 37–57.

[40] Parcell S. Sulfur in human nutrition and applications in medicine (Review). *Alternative Medicine Review* 2002; 7: 22–44.

[41] Ingenbleek Y, Kimura H. Nutritional essentiality of sulfur in health and disease (Review). *Nutr Rev* 2013; 71: 413–432.

[42] Hewlings S, Kalman D. Sulfur and human health (Review). *EC Nutr* 2019; 14.9: 785–791.

[43] Townsend DM, Tew KD, Tapiero H. Sulfur containing amino acids and human disease (Review). *Biomedicine and Pharmacotherapy* 2004; 58: 47–55.

[44] Pajares MA, Pérez-Sala D. Mammalian sulfur amino acid metabolism: A nexus between redox regulation, nutrition, epigenetics, and detoxification (Review). *Antioxidants and Redox Signaling* 2018; 29: 408–452.

[45] Jakaria M, Azam S, Haque ME, *et al*. Taurine and its analogs in neurological disorders: Focus on therapeutic potential and molecular mechanisms (Review). *Redox Biol* 2019; 24: 101223.

[46] Mårtensson J, Denneberg T, Lindell Å, *et al*. Sulfur amino acid metabolism in cystinuria: A biochemical and clinical study of patients. *Kidney Int* 1990; 37: 143–149.

[47] Poloni S, Spritzer PM, Mendes RH, *et al*. Leptin concentrations and SCD-1 indices in classical homocystinuria: Evidence for the role of sulfur amino acids in the regulation of lipid metabolism. *Clin Chim Acta* 2017; 473: 82–88.

[48] Carbonero F, Benefiel AC, Alizadeh-Ghamsari AH, *et al*. Microbial pathways in colonic sulfur metabolism and links with health and disease (Review). *Front Physiol* 2012; 3: 448.

[49] Vairavamurthy A, Zhou W, Eglinton T, *et al*. Sulfonates: A novel class of organic sulfur compounds in marine sediments. *Geochim Cosmochim Acta* 1994; 58: 4681–4687.

[50] Christl SU, Gibson GR, Cummings JH. Role of dietary sulphate in the regulation of methanogenesis in the human large intestine. *Gut* 1992; 33: 1234–1238.

[51] Lewis S, Cochrane S. Alteration of sulfate and hydrogen metabolism in the human colon by changing intestinal transit rate. *Am J Gastroenterol* 2007; 102: 624–633.

[52] Peck HD. Enzymatic basis for assimilatory and dissimilatory sulfate reduction. *J Bacteriol* 1961; 82: 933–939.

[53] Brahmacharimayum B, Mohanty MP, Ghosh PK. Theoretical and practical aspects of biological sulfate reduction: A review (Review). *Glob NEST JournalGlobal NEST Int J* 2019; 21: 222–244.

[54] Teigen LM, Geng Z, Sadowsky MJ, *et al*. Dietary factors in sulfur metabolism and pathogenesis of ulcerative colitis (Review). *Nutrients* 2019; 11: 931.

[55] Keller KL, Rapp-Giles BJ, Semkiw ES, *et al*. New model for electron flow for sulfate reduction in *Desulfovibrio alaskensis* G20. *Appl Environ Microbiol* 2014; 80: 855–868.

[56] Carbonero F, Gaskins HR. Sulfate-reducing bacteria in the human gut microbiome. In: *Encyclopedia of Metagenomics*. Springer US, 2015, pp. 617–619.

[57] Rey FE, Gonzalez MD, Cheng J, *et al*. Metabolic niche of a prominent sulfate-reducing human gut bacterium. *Proc Natl Acad Sci U S A* 2013; 110: 13582–13587.

[58] Kuever J, Rainey FA, Widdel F. *Bergey's Manual of Systematic Bacteriology*. Second Edi. 2005.

[59] Rowan FE, Docherty NG, Coffey JC, *et al*. Sulphate-reducing bacteria and hydrogen sulphide in the aetiology of ulcerative colitis (Review). *British Journal of Surgery* 2009; 96: 151–158.

[60] Nava GM, Carbonero F, Croix JA, *et al*. Abundance and diversity of mucosa-associated hydrogenotrophic microbes in the healthy human colon. *ISME J*. 2012; 6: 57–70.

[61] Baron EJ, Summanen P, Downes J, *et al*. *Bilophila wadsworthia*, gen. nov. and sp. nov., a unique Gram-negative anaerobic rod recovered from appendicitis specimens and human faeces. *J Gen Microbiol* 1989; 135: 3405–3411.

[62] Finegold S, Summanen P, Hunt Gerardo S, *et al*. Clinical importance of *Bilophila wadsworthia* (Review). *European Journal of Clinical Microbiology & Infectious Diseases* 1992; 11: 1058–1063.

[63] Sifri CD, Madoff LC. Appendicitis. In: *Mandell, Douglas, and Bennett's Principles*

and Practice of Infectious Diseases. Elsevier Inc., 2014, pp. 982-985.e1.

[64] Figliuolo VR, Coutinho-Silva R, Coutinho CMLM. Contribution of sulfate-reducing bacteria to homeostasis disruption during intestinal inflammation (Review). *Life Sci* 2018; 215: 145–151.

[65] Kang F, Nie J, Yang Z, *et al*. Role of hydrogen sulfide mediated autophagy related genes in intestinal function injury of sepsis (Review). *Zhonghua wei zhong bing ji jiu yi xue* 2020; 32: 118–120.

[66] Wu D, Wang H, Teng T, *et al*. Hydrogen sulfide and autophagy: A double edged sword (Review). *Pharmacological Research* 2018; 131: 120–127.

[67] Libiad M, Vitvitsky V, Bostelaar T, *et al*. Hydrogen sulfide perturbs mitochondrial bioenergetics and triggers metabolic reprogramming in colon cells. *J Biol Chem* 2019; 294: 12077–12090.

[68] Hale VL, Jeraldo P, Mundy M, *et al*. Synthesis of multi-omic data and community metabolic models reveals insights into the role of hydrogen sulfide in colon cancer. *Methods* 2018; 149: 59–68.

[69] Qin M, Long F, Wu W, *et al*. Hydrogen sulfide protects against DSS-induced colitis by inhibiting NLRP3 inflammasome. *Free Radic Biol Med* 2019; 137: 99–109.

[70] Mimoun S, Andriamihaja M, Chaumontet C, *et al*. Detoxification of H_2S by differentiated colonic epithelial cells: Implication of the sulfide oxidizing unit and of the cell respiratory capacity. *Antioxidants and Redox Signaling* 2012; 17: 1–10.

[71] Lagoutte E, Mimoun S, Andriamihaja M, *et al*. Oxidation of hydrogen sulfide remains a priority in mammalian cells and causes reverse electron transfer in colonocytes. *Biochim Biophys Acta - Bioenerg* 2010; 1797: 1500–1511.

[72] Li X, Bazer FW, Gao H, *et al*. Amino acids and gaseous signaling (Review). *Amino Acids* 2009; 37: 65–78.

[73] Schwitzguébe JP, Aubert S, Grosse W, *et al*. Sulphonated aromatic pollutants: Limits of microbial degradability and potential of phytoremediation (Review). *Environmental Science and Pollution Research* 2002; 9: 62–72.

[74] Kertesz MA, Cook AM, Leisinger T. Microbial metabolism of sulfurand phosphorus-containing xenobiotics (Review). *FEMS Microbiol Rev* 1994; 15: 195–215.

[75] Stalmams M, Belanger SE, Sabaliunas D. Understanding the environmental safety of surfactants: A historic perspective. In: *Handb Cleaning/Decontamination of Surfaces* 2007; 2: 625–654.

[76] Denger K, Ruff J, Rein U, *et al*. Sulphoacetaldehyde sulpho-lyase (EC 4.4.1.12) from *Desulfonispora thiosulfatigenes*: Purification, properties and primary sequence. *Biochem J* 2001; 357: 581–586.

[77] Musio R. Applications of 33S NMR Spectroscopy. In: *Annual Reports on NMR Spectroscopy*. Academic Press, 2009, pp. 1–88.

[78] De la Rosa J, Stipanuk MH. Evidence for a rate-limiting role of cysteinesulfinate decarboxylase activity in taurine biosynthesis *in vivo*. *Comp Biochem Physiol -- Part B Biochem* 1985; 81: 565–571.

[79] Lourenço R, Camilo ME. Taurine: a conditionally essential amino acid in humans? An overview in health and disease (Review). *Nutr Hosp* 2002; 17: 262–70.

[80] Foos TM, Wu JY. The role of taurine in the central nervous system and the modulation of intracellular calcium homeostasis (Review). *Neurochem Res* 2002; 27: 21–26.

[81] Timbrell JA, Seabra V, Waterfield CJ. The *in vivo* and *in vitro* protective properties of taurine (Review). *General Pharmacology* 1995; 26: 453–462.

[82] Lambert IH, Hansen DB. Regulation of taurine transport systems by protein kinase CK2 in mammalian cells (Review). *Cellular Physiology and Biochemistry* 2011; 28: 1099–1110.

[83] Tang XW, Hsu CC, Schloss J V., *et al*. Protein phosphorylation and taurine biosynthesis *in vivo* and *in vitro*. *J Neurosci* 1997; 17: 6947–6951.

[84] Jacobsen JG, Smith LH. Biochemistry and physiology of taurine and taurine derivatives (Review). *Physiological reviews* 1968; 48: 424–511.

[85] Sturman JA, Rassin DK, Gaull GE. Taurine in development (Review). *Life Sci* 1997; 21:1-22.

[86] Hayes KC, Sturman JA. Taurine in metabolism (Review). Annual review of nutrition 1981; 1: 401–425.

[87] Sole MJ, Jeejeebhoy KN. Conditioned nutritional requirements and the pathogenesis and treatment of myocardial failure (Review). *Current Opinion in Clinical Nutrition and Metabolic Care* 2000; 3: 417–424.

[88] Rigo J, Senterre J. Is taurine essential for the neonates? *Biol Neonate* 1977; 32: 73–76.

[89] Zelikovic I, Chesney RW, Friedman AL, *et al*. Taurine depletion in very low birth weight infants receiving prolonged total parenteral nutrition: Role of renal immaturity. *J Pediatr* 1990; 116: 301–306.

[90] Lima L. Taurine and its trophic effects in the retina (Review). *Neurochem Res* 1999; 24: 1333–1338.

[91] Devreker F, Van Den Bergh M, Biramane J, *et al*. Effects of taurine on human embryo development *in vitro*. *Hum Reprod* 1999; 14: 2350–2356.

[92] Niittynen L, Nurminen ML, Korpela R, *et al*. Role of arginine, taurine and homocysteine in cardiovascular diseases (Review). *Annals of Medicine* 1999; 31: 318–326.

[93] Howard D, Thompson DF. Taurine: An essential amino acid to prevent cholestasis in neonates? *Ann Pharmacother* 1992; 26: 1390–1392.

[94] Teitelbaum DH, Tracy T. Parenteral nutrition-associated cholestasis (Review).

Semin Pediatr Surg 2001; 10: 72–80.

[95] Sunami Y, Tazuma S, Kajiyama G. Gallbladder dysfunction enhances physical density but not biochemical metastability of biliary vesicles. *Dig Dis Sci* 2000; 45: 2382–2391.

[96] El Agouza IM, Eissa SS, El Houseini MM, *et al*. Taurine: A novel tumor marker for enhanced detection of breast cancer among female patients. *Angiogenesis* 2011; 14: 321–330.

[97] Stipanuk MH, Londono M, Lee JI, *et al*. Enzymes and metabolites of cysteine metabolism in nonhepatic tissues of rats show little response to changes in dietary protein or sulfur amino acid levels. *J Nutr* 2002; 132: 3369–3378.

[98] Hirschberger LL, Daval S, Stover PJ, *et al*. Murine cysteine dioxygenase gene: structural organization, tissue-specific expression and promoter identification. *Gene* 2001; 277: 153–161.

[99] Hu JM, Ikemura R, Chang KT, et al. Expression of cysteine sulfinate decarboxylase mRNA in rat mammary gland. *J Vet Med Sci* 2000; 62: 829–834.

[100] Tappaz M, Almarghini K, Do K. Cysteine sulfinate decarboxylase in brain: identification, characterization and immunocytochemical location in astrocytes (Review). *Advances in Experimental Medicine and Biology*. Springer, Boston, MA, 1994, pp. 257–268.

[101] Salze GP, Davis DA. Taurine: A critical nutrient for future fish feeds (Review). *Aquaculture* 2015; 437: 215–229.

[102] Wang X, He G, Mai K, *et al*. Differential regulation of taurine biosynthesis in rainbow trout and Japanese flounder. *Sci Rep* 2016; 6: 21231.

[103] Agnello G, Chang LL, Lamb CM, *et al*. Discovery of a substrate selectivity motif in amino acid decarboxylases unveils a taurine biosynthesis pathway in prokaryotes. *ACS Chem Biol* 2013; 8: 2264–2271.

[104] Birdsall TC. Therapeutic applications of taurine (Review). *Altern Med Rev* 1998; 3: 128–36.

[105] Wójcik OP, Koenig KL, Zeleniuch-Jacquotte A, *et al*. The potential protective effects of taurine on coronary heart disease (Review). *Atherosclerosis* 2010; 208: 19–25.

[106] Vitvitsky V, Garg SK, Banerjee R. Taurine biosynthesis by neurons and astrocytes. *J Biol Chem* 2011; 286: 32002–32010.

[107] Tappaz ML. Taurine biosynthetic enzymes and taurine transporter: molecular identification and regulations (Review). *Neurochemical Research* 2004; 29: 83–96.

[108] Ripps H, Shen W. Review: taurine: a ‘very essential’ amino acid (Review). *Mol Vis* 2012; 18: 2673–2686.

[109] Laidlaw SA, Shultz TD, Cecchino JT, *et al*. Plasma and urine taurine levels in vegans. *Am J Clin Nutr* 1988; 47: 660–663.

[110] O'Flaherty L, Stapleton PP, Remond HP, *et al*. Intestinal taurine transport: a review. *Eur J Clin Invest* 1997; 27: 873–880.

[111] Anderson CMH, Howard A, Walters JRF, *et al*. Taurine uptake across the human intestinal brush-border membrane is via two transporters: H^+-coupled PAT1 (SLC36A1) and Na^+- and Cl^--dependent TauT (SLC6A6). *J Physiol* 2009; 587: 731–744.

[112] Chen Z, Fei Y-J, Anderson CMH, *et al*. Structure, function and immunolocalization of a proton-coupled amino acid transporter (hPAT1) in the human intestinal cell line Caco-2. *Journal of Physiology* 2003; 546: 349–361.

[113] Ramamoorthy S, Leibach FH, Mahesh VB, *et al*. Functional characterization and chromosomal localization of a cloned taurine transporter from human placenta. *Biochem J* 1994; 300: 893–900.

[114] Dawson PA, Karpen SJ. Intestinal transport and metabolism of bile acids (Review). *J Lipid Res* 2015; 56: 1085–1099.

[115] Ridlon JM, Wolf PG, Gaskins HR. Taurocholic acid metabolism by gut microbes and colon cancer (Review). *Gut Microbes* 2016; 7: 201–215.

[116] Hofmann AF. The continuing importance of bile acids in liver and intestinal disease (Review). *Archives of Internal Medicine* 1999; 159: 2647–2658.

[117] Ahlman B, Leijonmarck CE, Lind C, *et al*. Free amino acids in biopsy specimens from the human colonic mucosa. *J Surg Res* 1993; 55: 647–653.

[118] Holmes AJ, Chew YV, Colakoglu F, *et al*. Diet-microbiome interactions in health are controlled by intestinal nitrogen source constraints. *Cell Metab* 2017; 25: 140–151.

[119] Xing M, Wei Y, Hua G, *et al.* A gene cluster for taurine sulfur assimilation in an anaerobic human gut bacterium. *Biochem J* 2019; 476: 2271–2279.

[120] Ghandforoush-Sattari M, Mashayekhi S, Krishna C V, *et al*. Pharmacokinetics of oral taurine in healthy volunteers. *J Amin Acids* 2010; 2010: 346237.

[121] Baldock MI, Denger K, Smits THM, *et al*. *Roseovarius* sp. strain 217: aerobic taurine dissimilation via acetate kinase and acetate-CoA ligase. *FEMS Microbiol Lett* 2007; 271: 202–206.

[122] Denger K, Smits THM, Cook AM. Genome-enabled analysis of the utilization of taurine as sole source of carbon or of nitrogen by *Rhodobacter sphaeroides* 2.4.1. *Microbiology* 2006; 152: 3197–3206.

[123] Krejčík Z, Denger K, Weinitschke S, *et al*. Sulfoacetate released during the assimilation of taurine-nitrogen by *Neptuniibacter caesariensis*: Purification of sulfoacetaldehyde dehydrogenase. *Arch Microbiol* 2008; 190: 159–168.

[124] Gorzynska AK, Denger K, Cook AM, *et al.* Inducible transcription of genes involved in taurine uptake and dissimilation by *Silicibacter pomeroyi* DSS-3T. *Arch Microbiol* 2006; 185: 402–406.

[125] Wiethaus J, Schubert B, Pfänder Y, *et al.* The GntR-like regulator TauR activates expression of taurine utilization genes in *Rhodobacter capsulatus*. *J Bacteriol* 2008; 190: 487–493.

[126] Masepohl B, Führer F, Klipp W. Genetic analysis of a *Rhodobacter capsulatus* gene region involved in utilization of taurine as a sulfur source. *FEMS Microbiol Lett* 2001; 205: 105–111.

[127] Shimamoto G, Berk RS. Catabolism of taurine in *Pseudomonas aeruginosa*. *BBA - Enzymol* 1979; 569: 287–292.

[128] Kondo H, Kagotani K, Oshima M, *et al*. Purification and some properties of taurine dehydrogenase from a bacterium. *J Biochem* 1973; 73: 1269–1278.

[129] Rein U, Gueta R, Denger K, *et al*. Dissimilation of cysteate via 3-sulfolactate sulfo-lyase and a sulfate exporter in *Paracoccus pantotrophus* NKNCYSA. *Microbiology* 2005; 151: 737–747.

[130] Ruff J, Denger K, Cook AM. Sulphoacetaldehyde acetyltransferase yields acetyl phosphate: purification from *Alcaligenes defragrans* and gene clusters in taurine degradation. *Biochem J* 2003; 369: 275–285.

[131] Brüggemann C, Denger K, Cook AM, *et al*. Enzymes and genes of taurine and isethionate dissimilation in *Paracoccus denitrificans*. *Microbiology* 2004; 150: 805–816.

[132] Krejčík Z, Hollemeyer K, Smits THM, *et al*. Isethionate formation from taurine in *Chromohalobacter salexigens*: purification of sulfoacetaldehyde reductase. *Microbiology* 2010; 156: 1547–1555.

[133] Visscher PT, Gritzer RF, Leadbetter ER. Low-molecular-weight sulfonates, a major substrate for sulfate reducers in marine microbial mats. *Appl Environ Microbiol* 1999; 65: 3272–3278.

[134] Zhou Y, Wei Y, Nanjaraj Urs AN, *et al*. Identification and characterization of a new sulfoacetaldehyde reductase from the human gut bacterium *Bifidobacterium kashiwanohense*. *Biosci Rep* 2019; 39: BSR20190715.

[135] Li M, Wei Y, Yin J, *et al*. Biochemical and structural investigation of taurine:2-oxoglutarate aminotransferase from *Bifidobacterium kashiwanohense*. *Biochem J* 2019; 476: 1605–1619.

[136] Peck SC, Denger K, Burrichter A, *et al*. A glycyl radical enzyme enables hydrogen sulfide production by the human intestinal bacterium *Bilophila wadsworthia*. *Proc Natl Acad Sci USA* 2019; 116: 3171–3176.

[137] Laue H, Friedrich M, Ruff J, *et al*. Dissimilatory sulfite reductase (Desulfoviridin) of the taurine-degrading, non-sulfate-reducing bacterium *Bilophila wadsworthia* RZATAU contains a fused DsrB-DsrD subunit. *J Bacteriol* 2001; 183: 1727–1733.

[138] Feng Y, Stams AJM, de Vos WM, *et al.* Enrichment of sulfidogenic bacteria from the human intestinal tract. *FEMS Microbiol Lett* 2017; 364: 7.

[139] Laue H, Denger K, Cook AM. Fermentation of cysteate by a sulfate-reducing

bacterium. *Archives of Mircobiology* 1997; 3: 210–214.

[140] Liu J, Wei Y, Lin L, *et al*. Two radical-dependent mechanisms for anaerobic degradation of the globally abundant organosulfur compound dihydroxypropanesulfonate. *Proc Natl Acad Sci* 2020; 117: 202003434.

[141] Barrow KD, Karsten U, King RJ. Isethionic acid from the marine red alga Ceramium flaccidum. *Phytochemistry* 1993; 34: 1429–1430.

[142] Hellio C, Simon-Colin C, Clare AS, *et al*. Isethionic acid and floridoside isolated from the red alga, Grateloupia turuturu, inhibit settlement of Balanus amphitrite cyprid larvae. *Biofouling* 2004; 20: 139–145.

[143] Holst PB, Nielsen SE, Anthoni U, *et al*. Isethionate in certain red algae. *J Appl Phycol* 1994; 6: 443–446.

[144] Jacobsen JG, Collins LL, Smith LH. Urinary excretion of isethionic acid in man. *Nature* 1967; 214: 1247–1248.

[145] Kumpulainen E, Pesonen I, Lähdesmäki P. Exchange of isethionate between blood and tissues in adult and 7-day-old mice. *Acta Physiol Scand* 1982; 114: 419–423.

[146] Fellman JH, Roth ES, Avedovech NA, *et al*. The metabolism of taurine to isethionate. *Arch Biochem Biophys* 1980; 204: 560–567.

[147] Fellman JH, Roth ES, Avedovech NA, *et al*. Mammalian hypotaurine aminotransferase: isethionate is not a product. *Life Sci* 1980; 27: 1999–2004.

[148] Von Rekowski KS, Denger K, Cook AM. Isethionate as a product from taurine during nitrogen-limited growth of *Klebsiella oxytoca* TauN1. *Arch Microbiol* 2005; 183: 325–330.

[149] Sun JZ, Parr JW, Erickson MCE. Solubilization of sodium cocoyl isethionate. Journal of Cosmetic Science 2003; 54: 559–568.

[150] Fernández-Ferreiro A, Varela MS, Gil-Martínez M, *et al*. *In vitro* evaluation of the ophthalmic toxicity profile of chlorhexidine and propamidine isethionate eye drops. *J Ocul Pharmacol Ther* 2017; 33: 202-209.

[151] Delobel P. Rhabdomyolysis associated with pentamidine isethionate therapy for American cutaneous leishmaniasis (Review). *J Antimicrob Chemother* 2003; 51: 1319–1320.

[152] King JE, Jaouhari R, Quinn JP. The role of sulfoacetaldehyde sulfo-lyase in the mineralization of isethionate by an environmental *Acinetobacter* isolate. *Microbiology* 1997; 143: 2339–2343.

[153] Van der Ploeg JR, Weiss MA, Saller E, *et al*. Identification of sulfate starvation-regulated genes in *Escherichia coli*: A gene cluster involved in the utilization of taurine as a sulfur source. *J Bacteriol* 1996; 178: 5438–5446.

[154] Eichhorn E, Van Der Ploeg JR, Kertesz MA, *et al*. Characterization of α-ketoglutarate-dependent taurine dioxygenase from *Escherichia coli*. *J Biol Chem* 1997; 272: 23031–23036.

[155] Uria-Nickelsen MR, Leadbetter ER, Godchaux W. Sulfonate-sulfur utilization involves a portion of the assimilatory sulfate reduction pathway in *Escherichia coli*. *FEMS Microbiol Lett* 1994; 123: 43–8.

[156] Uria-Nickelsen MR, Leadbetter ER, Godchaux W. Sulphonate utilization by enteric bacteria. *J Gen Microbiol* 1993; 139: 203–208.

[157] Kahnert A, Vermeij P, Wietek C, *et al*. The ssu locus plays a key role in organosulfur metabolism in *Pseudomonas putida* S-313. *J Bacteriol* 2000; 182: 2869–2878.

[158] Chien C-C, Leadbetter ER, Godchaux W. *Rhodococcus* spp. utilize taurine (2-aminoethanesulfonate) as sole source of carbon, energy, nitrogen and sulfur for aerobic respiratory growth. *FEMS Microbiol Lett* 1999; 176: 333–337.

[159] Tong Y, Wei Y, Hu Y, *et al*. A pathway for isethionate dissimilation in *Bacillus krulwichiae*. *Appl Environ Microbiol* 2019; 85: e00793-19.

[160] Chien CC, Leadbetter ER, Godchaux W. Taurine-sulfur assimilation and taurine-pyruvate aminotransferase activity in anaerobic bacteria. *Appl Environ Microbiol* 1997; 63: 3021–3024.

[161] Lie TJ, Pitta T, Leadbetter ER, *et al*. Sulfonates: novel electron accepters in anaerobic respiration. *Arch Microbiol* 1996; 166: 204–210.

[162] Lie TJ, Godchaux W, Leadbetter ER. Sulfonates as terminal electron acceptors for growth of sulfite-reducing bacteria (*Desulfitobacterium* spp.) and sulfate-reducing bacteria: effects of inhibitors of sulfidogenesis. *Appl Environ Microbiol* 1999; 65: 4611–4617.

[163] Lie TJ, Leadbetter JR, Leadbetter ER. Metabolism of sulfonic acids and other organosulfur compounds by sulfate-reducing bacteria. *Geomicrobiol J* 1998; 15: 135–149.

[164] Denger K, Stackebrandt E, Cook AM. *Desulfonispora thiosulfatigenes* gen. nov., sp. nov., a taurine-fermenting, thiosulfate-producing anaerobic bacterium. *Int J Syst Bacteriol* 1999; 49: 1599–1603.

[165] Mikosch C, Denger K, Schäfer EM, *et al*. Anaerobic oxidations of cysteate: degradation via L-cysteate:2-oxoglutarate aminotransferase in *Paracoccus pantotrophus*. *Microbiology* 1999; 145: 1153–1160.

[166] Denger K, Laue H, Cook AM. Anaerobic taurine oxidation: A novel reaction by a nitrate-reducing *Alcaligenes* sp. *Microbiology* 1997; 143: 1919–1924.

[167] Weinitschke S, Denger K, Cook AM, *et al*. The DUF81 protein TauE in *Cupriavidus necator* H16, a sulfite exporter in the metabolism of C2 sulfonates. *Microbiol* 2007; 153: 3055–3060.

[168] Consden R, Gordon AH, Martin AJ. The identification of amino-acids derived from cystine in chemically modified wool. *Biochem J* 1946; 40: 580-582.2.

[169] Huxtable RJ. Physiological actions of taurine (Review). *Physiological Reviews* 1992; 72: 101–164.

[170] Koshikawa T, Nakashio S, Kusuyama K. Presence of cysteic acid in the sporangium and in metabolic pathway during sporulation of *Bacillus subtilis* NRRL B558. *J Gen Microbiol* 1981; 124: 415–423.

[171] Fischer FG, Brander J. Eine Analyse der Gespinste der Kreuzspinne. *Hoppe Seylers Z Physiol Chem* 1960; 320: 92–102.

[172] Denger K, Mayer J, Buhmann M, *et al*. Bifurcated degradative pathway of 3-sulfolactate in *Roseovarius nubinhibens* ISM via sulfoacetaldehyde acetyltransferase and (S)-cysteate sulfolyase. *J Bacteriol* 2009; 191: 5648–5656.

[173] Girard A, Robin P, Jacquot R. Effects of an alimentary overload of methionine on the plasma concentration of free amino acids and certain of their derivatives. Study on growing rats. *C R Acad Hebd Seances Acad Sci D* 1968; 266: 2160–3.

[174] Gejyo F, Ito G, Kinoshita Y. Identification of N-monoacetylcystine in uremic plasma. *Clin Sci* 1981; 60: 331–334.

[175] Ida S, Kuriyama K. Simultaneous determination of cysteine sulfinic acid and cysteic acid in rat brain by high-performance liquid chromatography. *Anal Biochem* 1983; 130: 95–101.

[176] Do KQ, Mattenberger M, Streit P, *et al*. *In vitro* release of endogenous excitatory sulfur-containing amino acids from various rat brain regions. *J Neurochem* 1986; 46: 779–786.

[177] Wilson DF, Pastuszko A. Transport of cysteate by synaptosomes isolated from rat brain: evidence that it utilizes the same transporter as aspartate, glutamate, and cysteine sulfinate. *J Neurochem* 2006; 47: 1091–1097.

[178] Tolosa EA, Chepurnova NK, Khomutov RM, *et al*. Reactions catalysed by cysteine lyase from the yolk sac of chicken embryo. *BBA - Enzymol* 1969; 171: 369–371.

[179] Martin WG, Sass NL, Hill L, *et al*. The synthesis of taurine from sulfate IV. An alternate pathway for taurine synthesis by the rat. *Proc Soc Exp Biol Med* 1972; 141: 632–633.

[180] Boström H, Åqvist S, Faurholt C. Utilization of S^{35}-labelled sodium sulphate in the synthesis of chondroitin sulphuric acid, taurine, methionine and cystine. *Acta Chem Scand* 1952; 6: 1557–1559.

[181] Ibanez ML, Lindstrom ES. Metabolism of sulfate by the chromatophore of *Rhodospirillum*. *J Bacteriol* 1962; 84: 451–455.

[182] Karney EB, Singer TP. The oxidation of cysteinesulfinic and cysteic acids in *Proteus vulgaris*. *BBA - Biochim Biophys Acta* 1953; 11: 270–275.

[183] Seltmann G, Voigt W. Verwertung anorganischer Schwefelquellen durch *Staphylococcus aureus*-Stämme. *Z Allg Mikrobiol* 1977; 17: 437–450.

[184] Anderson GH, Ashley DVM, Jones JD. Utilization of L-methionine sulfoxide, L-methionine sulfone and cysteic acid by the weanling rat. *J Nutr* 1976; 106: 1108–14.

[185] Pieniazek D, Rakowska M, Kunachowicz H. The participation of methionine and

cysteine in the formation of bonds resistant to the action of proteolytic enzymes in heated casein. *Br J Nutr* 1975; 34: 163–173.

[186] Chang KC, Marshall HF, Satterlee LD. Sulfur amino acid stability. Hydrogen peroxide treatment of casein, egg white, and soy isolate. *J Food Sci* 1982; 47: 1181–1183.

[187] Weinstein CL, Griffith OW. Cysteinesulfonate and beta-sulfopyruvate metabolism. Partitioning between decarboxylation, transamination, and reduction pathways. *J Biol Chem* 1988; 263: 3735–43.

[188] Stapley EO, Starkey RL. Decomposition of cysteic acid and taurine by soil micro-organisms (Review). *J Gen Microbiol* 1970; 64: 77–84.

[189] Gritzer RF. Sulfonate metabolism by some aerobic and anaerobic bacteria. *Doctoral Dissertation* 2004.

[190] Denger K, Smits THM, Cook AM. L-cysteate sulpho-lyase, a widespread pyridoxal 5′-phosphate-coupled desulphonative enzyme purified from *Silicibacter pomeroyi* DSS-3T. *Biochem J* 2006; 394: 657–664.

[191] González JM, Covert JS, Whitman WB, *et al*. *Silicibacter pomeroyi* sp. nov. and *Roseovarius nubinhibens* sp. nov., dimethylsulfoniopropionate-demethylating bacteria from marine environments. *Int J Syst Evol Microbiol* 2003; 53: 1261–1269.

[192] Moran MA, Buchan A, González JM, *et al*. Genome sequence of *Silicibacter pomeroyi* reveals adaptations to the marine environment. *Nature* 2004; 432: 910–913.

[193] Eichhorn E, Van Der Ploeg JR, Leisinger T. Deletion analysis of the *Escherichia coli* taurine and alkanesulfonate transport systems. *J Bacteriol* 2000; 182: 2687–2795.

[194] Eichhorn E, Leisinger T. *Escherichia coli* utilizes methanesulfonate and L-cysteate as sole sulfur sources for growth. *FEMS Microbiol Lett* 2006; 205: 271–275.

[195] Widdel F, Bak F. Gram-negative mesophilic sulfate reducing bacteria. In: *The Prokaryotes*. Springer New York, 1992, pp. 3352–3378.

[196] Shokes JE, Duin EC, Bauer C, *et al*. Direct interaction of coenzyme M with the active-site Fe-S cluster of heterodisulfide reductase. *FEBS Lett* 2005; 579: 1741–1744.

[197] Huynh HTT, Nkamga VD, Drancourt M, *et al*. Genetic variants of dental plaque *Methanobrevibacter oralis*. *Eur J Clin Microbiol Infect Dis* 2015; 34: 1097–1101.

[198] Nguyen-Hieu T, Khelaifia S, Aboudharam G, *et al*. Methanogenic archaea in subgingival sites: A review. *APMIS* 2013; 121: 467–477.

[199] Wilson M. *The human microbiota in health and disease: an ecological and community-based approach*. 2019; 1.

[200] Miller TL, Wolin MJ. Enumeration of *Methanobrevibacter smithii* in human feces. *Arch Microbiol* 1982; 131: 14–18.

[201] Belay N, Mukhopadhyay B, Conway de Macario E, *et al*. Methanogenic bacteria in human vaginal samples. *J Clin Microbiol* 1990; 28: 1666–1668.

[202] Koskinen K, Pausan MR, Perras AK, *et al*. First insights into the diverse human archaeome: specific detection of Archaea in the gastrointestinal tract, lung, and nose and on skin. *MBio* 2017; 8: 1–17.

[203] Pochart P, Lémann F, Flourié B, *et al.* Pyxigraphic sampling to enumerate methanogens and anaerobes in the right colon of healthy humans. *Gastroenterology* 1993; 105: 1281–1285.

[204] Mathur R, Kim G, Morales W, *et al*. Intestinal *Methanobrevibacter smithii* but not total bacteria is related to diet-induced weight gain in rats. *Obesity* 2013; 21: 748–754.

[205] Pimentel M, Mayer AG, Park S, *et al.* Methane production during lactulose breath test is associated with gastrointestinal disease presentation. *Dig Dis Sci* 2003; 48: 86–92.

[206] Peled Y, Weinberg D, Hallak A, *et al*. Factors affecting methane production in humans. Gastrointestinal diseases and alterations of colonic flora. *Dig Dis Sci* 1987; 32: 267–271.

[207] Mihajlovski A, Doré J, Levenez F, *et al*. Molecular evaluation of the human gut methanogenic archaeal microbiota reveals an age-associated increase of the diversity. *Environ Microbiol Rep* 2010; 2: 272–280.

[208] Paul K, Nonoh JO, Mikulski L, *et al*. Methanoplasmatales, thermoplasmatales-related archaea in termite guts and other environments, are the seventh order of methanogens. *Appl Environ Microbiol* 2012; 78: 8245–8253.

[209] Zhang H, DiBaise JK, Zuccolo A, *et al.* Human gut microbiota in obesity and after gastric bypass. *Proc Natl Acad Sci U S A* 2009; 106: 2365–2370.

[210] Armougom F, Henry M, Vialettes B, *et al.* Monitoring bacterial community of human gut microbiota reveals an increase in *Lactobacillus* in obese patients and *Methanogens* in anorexic patients. *PLoS One* 2009; 4: e7125.

[211] Graham DE, Taylor SM, Wolf RZ, *et al*. Convergent evolution of coenzyme M biosynthesis in the *Methanosarcinales*: cysteate synthase evolved from an ancestral threonine synthase. *Biochem J* 2009; 424: 467–478.

[212] Graupner M, Xu H, White RH. Identification of an archaeal 2-hydroxy acid dehydrogenase catalyzing reactions involved in coenzyme biosynthesis in methanoarchaea. *J Bacteriol* 2000; 182: 3688–3692.

[213] Helgadóttir S, Rosas-Sandoval G, Söll D, *et al*. Biosynthesis of phosphoserine in the *Methanococcales*. *J Bacteriol* 2007; 189: 575–582.

[214] Graupner M, Xu H, White RH. Identification of the gene encoding sulfopyruvate decarboxylase, an enzyme involved in biosynthesis of coenzyme M. *J Bacteriol* 2000; 182: 4862–4867.

[215] Denger K, Laue H, Cook AM. Thiosulfate as a metabolic product: the bacterial

fermentation of taurine. *Arch Microbiol* 1997; 168: 297–301.

[216] Lie TJ, Clawson ML, Godchaux W, *et al.* Sulfidogenesis from 2-aminoethanesulfonate (taurine) fermentation by a morphologically unusual sulfate-reducing bacterium, *Desulforhopalus singaporensis* sp. nov. *Appl Environ Microbiol* 1999; 65: 3328–3334.

[217] Benson AA, Daniel H, Wiser R. A sulfolipid in plants. *Proc Natl Acad Sci* 1959; 45: 1582–1587.

[218] Benson AA. The plant sulfolipid (Review). *Adv Lipid Res* 1963; 1: 387–394.

[219] Harwood JL, Nicholls RG. The plant sulpholipid-- a major component of the sulphur cycle (Review). *Biochem Soc Trans* 1979; 7: 440–447.

[220] Goddard-Borger ED, Williams SJ. Sulfoquinovose in the biosphere: Occurrence, metabolism and functions (Review). *Biochemical Journal* 2017; 474: 827–849.

[221] Van Mooy BAS, Rocap G, Fredricks HF, *et al*. Sulfolipids dramatically decrease phosphorus demand by picocyanobacteria in oligotrophic marine environments. *Proc Natl Acad Sci U S A* 2006; 103: 8607–8612.

[222] Radunz A. Über das Sulfochinovosyl-diacylglycerin aus höheren Pflanzen, Algen und Purpurbakterien (Review). *Hoppe Seylers Z Physiol Chem* 1969; 350: 411–417.

[223] Sato N, Wada H. Lipid biosynthesis and its regulation in cyanobacteria (Review). *Lipids in Photosynthesis* 2009; 157–177.

[224] Mizusawa N, Wada H. The role of lipids in photosystem II (Review). *Biochimica et Biophysica Acta - Bioenergetics* 2012; 1817: 194–208.

[225] Shimojima M. Biosynthesis and functions of the plant sulfolipid (Review). *Progress in Lipid Research* 2011; 50: 234–239.

[226] Haines TH. Sulfolipids and halosulfolipids. In: *Lipids and Biomembranes of Eukaryotic Microorganisms* 1973; 197–232.

[227] Yongmanitchai W, Ward OP. Positional distribution of fatty acids, and molecular species of polar lipids, in the diatom *Phaeodactylum tricornutum*. *J Gen Microbiol* 1993; 139: 465–472.

[228] Anesi A, Obertegger U, Hansen G, *et al*. Comparative analysis of membrane lipids in psychrophilic and mesophilic freshwater dinoflagellates. *Front Plant Sci* 2016; 7: 524.

[229] Sanda S, Leustek T, Theisen MJ, *et al.* Recombinant *Arabidopsis* SQD1 converts UDP-glucose and sulfite to the sulfolipid head group precursor UDP-sulfoquinovose *in vitro*. *J Biol Chem* 2001; 276: 3941–3946.

[230] Yu B, Xu C, Benning C. *Arabidopsis* disrupted in SQD2 encoding sulfolipid synthase is impaired in phosphate-limited growth. *Proc Natl Acad Sci U S A* 2002; 99: 5732–5737.

[231] Benning C, Somerville CR. Identification of an operon involved in sulfolipid biosynthesis in *Rhodobacter sphaeroides*. *J Bacteriol* 1992; 174: 6479–6487.

[232] Galliard T. Aspects of lipid metabolism in higher plants-II. The identification and quantitative analysis of lipids from the pulp of pre- and post-climacteric apples. *Phytochemistry* 1968; 7: 1915–1922.

[233] Hudson BJF, Karis IG. The lipids of the alga *Spirulina*. *J Sci Food Agric* 1974; 25: 759–763.

[234] Mata TM, Martins AA, Oliveira O, *et al*. Lipid content and productivity of *Arthrospira platensis* and *Chlorella vulgaris* under mixotrophic conditions and salinity stress. *Chem Eng Trans* 2016; 49: 187–192.

[235] El Baky HHA, El Baroty GS, Mostafa EM. Optimization growth of *Spirulina* (*Arthrospira*) *platensis* in photobioreactor under varied nitrogen concentration for maximized biomass, carotenoids and lipid contents. *Recent Pat Food Nutr Agric* 2018; 11: 40–48.

[236] Ridine Albert, Ridine Wague, Mbaïguinam, *et al*. Changes in the physico-chemical properties of *Spirulina platensis* from three production sites in Chad. *Journal of Animal and Plant Sciences* 2012; 13: 1811-1822.

[237] Xue C, Hu Y, Saito H, *et al*. Molecular species composition of glycolipids from *Sprirulina platensis*. *Food Chem* 2002; 77: 9–13.

[238] Gupta SD, Sastry PS. Metabolism of the plant sulfolipid-sulfoquinovosyl-diacylglycerol: Degradation in animal tissues. *Arch Biochem Biophys* 1987; 259: 510–519.

[239] Speciale G, Jin Y, Davies GJ, *et al*. YihQ is a sulfoquinovosidase that cleaves sulfoquinovosyl diacylglyceride sulfolipids. *Nat Chem Biol* 2016; 12: 215–217.

[240] Sacoman JL, Badish LN, Sharkey TD, *et al*. The metabolic and biochemical impact of glucose 6-sulfonate (sulfoquinovose), a dietary sugar, on carbohydrate metabolism. *Carbohydr Res* 2012; 362: 21–29.

[241] Roy AB, Hewlins MJE, Ellis AJ, *et al*. Glycolytic breakdown of sulfoquinovose in bacteria: A missing link in the sulfur cycle. *Appl Environ Microbiol* 2003; 69: 6434–6441.

[242] Daniel H, Miyano M, Mumma RO, *et al*. The plant sulfolipid. Identification of 6-sulfo-quinovose. *J Am Chem Soc* 1961; 83: 1765–1766.

[243] Zähringer U, Moll H, Hettmann T, *et al*. Cytochrome b558/566 from the archaeon *Sulfolobus acidocaldarius* has a unique Asn-linked highly branched hexasaccharide chain cotaining 6-sulfoquinovose. *Eur J Biochem* 2000; 267: 4144–4149.

[244] Peyfoon E, Meyer B, Hitchen PG, *et al*. The S-layer glycoprotein of the crenarchaeote *Sulfolobus acidocaldarius* is glycosylated at multiple sites with chitobiose-linked N-glycans. *Archaea* 2010; 2010: 754101.

[245] Palmieri G, Balestrieri M, Peter-Katalinić J, *et al*. Surface-exposed glycoproteins of hyperthermophilic *Sulfolobus solfataricus* P2 show a common N- glycosylation profile. *J Proteome Res* 2013; 12: 2779–2790.

[246] Vinogradov E, Deschatelets L, Lamoureux M, *et al*. Cell surface glycoproteins from

Thermoplasma acidophilum are modified with an N-linked glycan containing 6-C-sulfofucose. *Glycobiology* 2012; 22: 1256–1267.

[247] Okazaki Y, Shimojima M, Sawada Y, *et al*. A chloroplastic UDP-Glucose pyrophosphorylase from *Arabidopsis* is the committed enzyme for the first step of sulfolipid biosynthesis. *Plant Cell* 2009; 21: 892–909.

[248] Felux AK, Spiteller D, Klebensberger J, *et al*. Entner-Doudoroff pathway for sulfoquinovose degradation in *Pseudomonas putida* SQ1. *Proc Natl Acad Sci U S A* 2015; 112: E4298–E4305.

[249] Denger K, Weiss M, Felux AK, *et al*. Sulphoglycolysis in *Escherichia coli* K-12 closes a gap in the biogeochemical sulphur cycle. *Nature* 2014; 507: 114–117.

[250] Shimada T, Yamamoto K, Nakano M, *et al*. Regulatory role of CsqR (YihW) in transcription of the genes for catabolism of the anionic sugar sulfoquinovose (SQ) in *Escherichia coli* K-12. *Microbiol (United Kingdom)* 2019; 165: 78–89.

[251] Burrichter A, Denger K, Franchini P, *et al*. Anaerobic degradation of the plant sugar sulfoquinovose concomitant with H_2S production: *Escherichia coli* K-12 and *Desulfovibrio* sp. strain DF1 as co-culture model. *Front Microbiol* 2018; 9: 2792.

[252] Li J, Epa R, Scott N, *et al*. A sulfoglycolytic Entner-Doudoroff pathway in *Rhizobium leguminosarum bv. trifolii* SRDI565. *Appl Environ Microbiol* 2020; 86: e00750-20.

[253] Roy AB, Ellis AJ, White GF, *et al*. Microbial degradation of the plant sulpholipid. *Biochemical Society Transactions* 2000; 28: 781–783.

[254] Busby WF, Benson AA. Sulfonic acid metabolism in the diatom *Navicula pelliculosa*. *Plant Cell Physiol* 1973; 14: 1123–1132.

[255] Busby WF. Sulfopropanedial and cysteinolic acid in the diatom. *BBA - Gen Subj* 1966; 121: 160–161.

[256] Durham BP, Sharma S, Luo H, *et al*. Cryptic carbon and sulfur cycling between surface ocean plankton. *Proc Natl Acad Sci U S A* 2015; 112: 453–457.

[257] Iglesias MJ, Soengas R, Probert I, *et al*. NMR characterization and evaluation of antibacterial and antiobiofilm activity of organic extracts from stationary phase batch cultures of five marine microalgae (Dunaliella sp., D. salina, Chaetoceros calcitrans, C. gracilis and Tisochrysis lutea). *Phytochemistry* 2019; 164: 192–205.

[258] Götz F, Longnecker K, Kido Soule MC, *et al*. Targeted metabolomics reveals proline as a major osmolyte in the chemolithoautotroph *Sulfurimonas denitrificans*. *Microbiologyopen* 2018; 7: e00586.

[259] Meyer BH, Zolghadr B, Peyfoon E, *et al*. Sulfoquinovose synthase - an important enzyme in the N-glycosylation pathway of *Sulfolobus acidocaldarius*. *Mol Microbiol* 2011; 82: 1150–1163.

[260] Van Mooy BAS, Fredricks HF, Pedler BE, *et al*. Phytoplankton in the ocean use non-phosphorus lipids in response to phosphorus scarcity. *Nature* 2009; 458: 69–72.

[261] Bonsen PP, Spudich JA, Nelson DL, *et al*. Biochemical studies of bacterial sporulation and germination. XII. A sulfonic acid as a major sulfur compound of *Bacillus subtilis* spores. *J Bacteriol* 1969; 98: 62–68.

[262] White RH. Intermediates in the biosynthesis of coenzyme M (2-Mercaptoethanesulfonic Acid). *Biochemistry* 1986; 25: 5304–5308.

[263] Mayer J, Huhn T, Habeck M, *et al*. 2,3-Dihydroxypropane-1-sulfonate degraded by *Cupriavidus pinatubonensis* JMP134: purification of dihydroxypropanesulfonate 3-dehydrogenase. *Microbiology* 2010; 156: 1556–1564.

[264] Cook AM, Denger K, Smits THM. Dissimilation of C3-sulfonates (Review). *Archives of Microbiology* 2006; 185: 83–90.

[265] Irimia A, Madern D, Zaccaï G, *et al*. Methanoarchaeal sulfolactate dehydrogenase: prototype of a new family of NADH-dependent enzymes. *EMBO J* 2004; 23: 1234–1244.

[266] Denger K, Cook AM. Racemase activity effected by two dehydrogenases in sulfolactate degradation by *Chromohalobacter salexigens*: purification of (S)-sulfolactate dehydrogenase. *Microbiology* 2010; 156: 967–974.

[267] Rosa LT, Bianconi ME, Thomas GH, *et al*. Tripartite ATP-independent periplasmic (TRAP) transporters and tripartite tricarboxylate transporters (TTT): From uptake to pathogenicity (Review). *Front Cell Infect Microbiol* 2018; 8: 33.

[268] Hungate RE. A roll tube method for cultivation of strict anaerobes (Review). *Methods Microbiol* 1969; 3: 117–132.

[269] Bryant MP. Commentary on the Hungate technique for culture of anaerobic bacteria (Review). *Am J Clin Nutr* 1972; 25: 1324–1328.

[270] Moore WEC. Techniques for routine culture of fastidious anaerobes (Review). *Int J Syst Bacteriol* 1966; 16: 173–190.

[271] Moench TT, Zeikus JG. An improved preparation method for a titanium(III) media reductant. *J Microbiol Methods* 1983; 1: 199–202.

[272] Da Silva SM, Venceslau SS, Fernandes CLV, *et al*. Hydrogen as an energy source for the human pathogen *Bilophila wadsworthia*. *Antonie van Leeuwenhoek* 2008; 93: 381–390.

[273] Thurnheer T, Kohler T, Cook AM, *et al.* Orthanilic acid and analogues as carbon sources for bacteria: growth physiology and enzymic desulphonation. *J Gen Microbiol* 1986; 132: 1215–1220.

[274] Heimbrook ME, Wang WLL, Campbell G. Staining bacterial flagella easily. *J Clin Microbiol* 1989; 27: 2612–2615.

[275] Naghili H, Tajik H, Mardani K, *et al.* Validation of drop plate technique for bacterial enumeration by parametric and nonparametric tests. *Vet Res forum* 2013; 4: 179–83.

[276] Haange SB, Groeger N, Froment J, *et al.* Multiplexed quantitative assessment of the

fate of taurine and sulfoquinovose in the intestinal microbiome. *Metabolites* 2020; 10: 1–16.

[277] Ihaka R, Gentleman R. R: A Language for data analysis and graphics (Review). *J Comput Graph Stat* 1996; 5: 299–314.

[278] Sturgeon RJ. Monosaccharides. In: *Methods in Plant Biochemistry*. Academic Press, 1990, pp. 1–37.

[279] Bernfeld P. Amylases α and β. *Methods Enzymol* 1955; 1: 149–158.

[280] Miller GL. Use of dinitrosalicylic acid reagent for determination of reducing sugar. *Anal Chem* 1959; 31: 426–428.

[281] Wang X, Chi D, Su G, *et al*. Determination of taurine in biological samples by high-performance liquid chromatography using 4-fluoro-7-nitrobenzofurazan as a derivatizing agent. *Biomed Environ Sci* 2011; 24: 537–542.

[282] Eneroth P. Thin-layer chromatography of bile acids. *J Lipid Res* 1963; 4: 11–16.

[283] Cline JD. Spectrophotometric determination of hydrogen sulfide in natural waters. *Limnol Oceanogr* 1969; 14: 454–458.

[284] Cassella RJ, De Oliveira LG, Santelli RE. On line dissolution of ZnS for sulfide determination in stabilized water samples with zinc acetate, using spectrophotometry by methylene blue method. *Spectrosc Lett* 1999; 32: 469–484.

[285] Strocchi A, Furne JK, Levitt MD. A modification of the methylene blue method to measure bacterial sulfide production in feces. *J Microbiol Methods* 1992; 15: 75–82.

[286] Reese BK, Finneran DW, Mills HJ, *et al.* Examination and refinement of the determination of aqueous hydrogen sulfide by the methylene blue method (Review). *Aquat Geochemistry* 2011; 17: 567–582.

[287] Kageyama A, Benno Y, Nakase T. Phylogenetic evidence for the transfer of *Eubacterium lentum* to the genus *Eggerthella* as *Eggerthella* lenta gen. nov., comb. nov. *Int J Syst Bacteriol* 1999; 49: 1725–1732.

[288] Doud MS, Light M, Gonzalez G, *et al.* Combination of *16S rRNA* variable regions provides a detailed analysis of bacterial community dynamics in the lungs of cystic fibrosis patients. *Hum Genomics* 2010; 4: 147–169.

[289] Doud M, Zeng E, Schneper L, *et al.* Approaches to analyse dynamic microbial communities such as those seen in cystic fibrosis lung (Review). *Hum Genomics* 2009; 3: 246–256.

[290] Lee STM, Davy SK, Tang SL, *et al*. Mucus sugar content shapes the bacterial community structure in thermally stressed *Acropora muricata*. *Front Microbiol* 2016; 7: 371.

[291] Nübel U, Engelen B, Felsre A, *et al.* Sequence heterogeneities of genes encoding *16S rRNAs* in *Paenibacillus polymyxa* detected by temperature gradient gel electrophoresis. *J Bacteriol* 1996; 178: 5636–5643.

[292] Shen W, Wolf PG, Carbonero F, *et al.* Intestinal and systemic inflammatory

responses are positively associated with sulfidogenic bacteria abundance in high-fat–fed male C57BL/6J mice. *J Nutr* 2014; 144: 1181–1187.

[293] Birch M, Denning DW, Law D. Rapid genotyping of *Escherichia coli* O157 isolates by random amplification of polymorphic DNA. *Eur J Clin Microbiol Infect Dis* 1996; 15: 297–302.

[294] Kuhnert P, Nicolet J, Frey J. Rapid and accurate identification of *Escherichia coli* K-12 strains. *Appl Environ Microbiol* 1995; 61: 4135–4139.

[295] Lindsey RL, Garcia-Toledo L, Fasulo D, *et al.* Multiplex polymerase chain reaction for identification of *Escherichia coli*, *Escherichia albertii* and *Escherichia fergusonii*. 2017; 140: 1–4.

[296] Baldwin J, Collins B, Wolf PG, *et al.* Table grape consumption reduces adiposity and markers of hepatic lipogenesis and alters gut microbiota in butter fat-fed mice. *J Nutr Biochem* 2016; 27: 123–135.

[297] Williams JGK, Kubelik AR, Livak KJ, *et al*. DNA polymorphisms amplified by arbitrary primers are useful as genetic markers. *Nucleic Acids Res* 1990; 18: 6531–6535.

[298] Altschul SF, Gish W, Miller W, *et al*. Basic local alignment search tool. *J Mol Biol* 1990; 215: 403–410.

[299] Lagkouvardos I, Kläring K, Heinzmann SS, *et al.* Gut metabolites and bacterial community networks during a pilot intervention study with flaxseeds in healthy adult men. *Mol Nutr Food Res* 2015; 59: 1614–1628.

[300] Lagkouvardos I, Joseph D, Kapfhammer M, *et al*. IMNGS: A comprehensive open resource of processed *16S rRNA* microbial profiles for ecology and diversity studies. *Sci Reports 2016 61* 2016; 6: 1–9.

[301] Lagkouvardos I, Fischer S, Kumar N, *et al*. Rhea: a transparent and modular R pipeline for microbial profiling based on 16S rRNA gene amplicons. *PeerJ* 2017; 5: e2836.

[302] Whittaker RH. Evolution and measurement of species diversity (Review). *Taxon* 1972; 21: 213–251.

[303] Thukral AK. A review on measurement of alpha diversity in biology (Review). *Agric Res J* 2017; 54: 1.

[304] Chen J, Bittinger K, Charlson ES, *et al*. Associating microbiome composition with environmental covariates using generalized UniFrac distances. *Bioinformatics* 2012; 28: 2106–2113.

[305] Minchin PR. An evaluation of the relative robustness of techniques for ecological ordination. *Vegetatio* 1987; 69: 89–107.

[306] Whittaker RH. Vegetation of the Siskiyou Mountains, Oregon and California. *Ecol Monogr* 1960; 30: 279–338.

[307] Lowry OH, Rosebrough NJ, Farr AL, *et al.* Protein measurement with the folin

phenol reagent. *J Biol Chem* 1951; 193: 265–75.

[308] Chomzynski P. Single-step method of RNA isolation by acid guanidinium thiocyanate–phenol–chloroform extraction. *Anal Biochem* 1987; 162: 156–159.

[309] Pfaffl MW. A new mathematical model for relative quantification in real-time RT-PCR. *Nucleic Acids Res* 2001; 29: 2002–2007.

[310] Motulsky HJ, Brown RE. Detecting outliers when fitting data with nonlinear regression - a new method based on robust nonlinear regression and the false discovery rate. *BMC Bioinformatics* 2006; 7: 123.

[311] Xing M, Wei Y, Zhou Y, *et al*. Radical-mediated C-S bond cleavage in C2 sulfonate degradation by anaerobic bacteria. *Nat Commun* 2019; 10: 1–11.

[312] Laue H, Cook AM. Biochemical and molecular characterization of taurine:pyruvate aminotransferase from the anaerobe *Bilophila wadsworthia*. *Eur J Biochem* 2000; 267: 6841–6848.

[313] Shi X, Gao G, Tian J, *et al*. Symbiosis of sulfate-reducing bacteria and methanogenic archaea in sewer systems. *Environ Int* 2020; 143: 105923.

[314] Wagner M, Roger AJ, Flax JL, *et al.* Phylogeny of dissimilatory sulfite reductases supports an early origin of sulfate respiration. *J Bacteriol* 1998; 180: 2975–2982.

[315] Postgate JR, Campbell LL. Classification of *Desulfovibrio* species, the nonsporulating sulfate-reducing bacteria. *Bacteriological reviews* 1966; 30: 732–738.

[316] Cypionka H. Oxygen respiration by *Desulfovibrio* species (Review). *Annual Review of Microbiology* 2000; 54: 827–848.

[317] Zellner G, Messner P, Kneifel H, *et al*. *Desulfovibrio* simplex spec. nov., a new sulfate-reducing bacterium from a sour whey digester. *Arch Microbiol* 1989; 152: 329–334.

[318] Fröhlich J, Sass H, Babenzien H-D, *et al*. Isolation of *Desulfovibrio intestinalis* sp. nov. from the hindgut of the lower termite Mastotermes darwiniensis. *Can J Microbiol* 1999; 45: 145–152.

[319] Brauman A, Koenig JF, Dutreix J, *et al*. Characterization of two sulfate-reducing bacteria from the gut of the soil-feeding termite, Cubitermes speciosus. *Antonie Van Leeuwenhoek* 1990; 58: 271–275.

[320] Devereux R, He SH, Doyle CL, *et al*. Diversity and origin of *Desulfovibrio* species: phylogenetic definition of a family. *J Bacteriol* 1990; 172: 3609–3619.

[321] Schwartz W. Postgate, J.R., the sulfate-reducing bacteria (Review). *J Basic Microbiol* 1985; 25: 202–202.

[322] Dilling W, Cypionka H. Aerobic respiration in sulfate-reducing bacteria. *FEMS Microbiol Lett* 1990; 71: 123–127.

[323] Lobo SAL, Melo AMP, Carita JN, *et al*. The anaerobe *Desulfovibrio desulfuricans* ATCC 27774 grows at nearly atmospheric oxygen levels. *FEBS Lett* 2007; 581:

433–436.

[324] Warren YA, Citron DM, Merriam CV, *et al*. Biochemical differentiation and comparison of *Desulfovibrio* species and other phenotypically similar genera. *J Clin Microbiol* 2005; 43: 4041–4045.

[325] Hanson BT, Kits KD, Löffler J, *et al*. Sulfoquinovose is a select nutrient of prominent bacteria and a source of hydrogen sulfide in the human gut. *ISME J* 2021; 15: 2779-2791.

[326] Feng Z, Long W, Hao B, *et al*. A human stool-derived *Bilophila wadsworthia* strain caused systemic inflammation in specific-pathogen-free mice. *Gut Pathog* 2017; 9: 59.

[327] Fierer J, Okamoto S, Banerjee A, *et al*. Diarrhea and colitis in mice require the *Salmonella* pathogenicity island 2-encoded secretion function but not SifA or Spv effectors. *Infect Immun* 2012; 80: 3360–3370.

[328] Tropis M, Bardou F, Bersch B, *et al*. Composition and phase behaviour of polar lipids isolated from *Spirulina maxima* cells grown in a perdeuterated medium. *Biochim Biophys Acta - Biomembr* 1996; 1284: 196–202.

[329] Gerken HG, Donohoe B, Knoshaug EP. Enzymatic cell wall degradation of *Chlorella vulgaris* and other microalgae for biofuels production. *Planta* 2013; 237: 239–253.

[330] Waldron KW, Parker ML, Smith AC. Plant cell walls and food quality (Review). *Compr Rev Food Sci Food Saf* 2003; 2: 128–146.

[331] Crane BR, Getzoff ED. The relationship between structure and function for the sulfite reductases (Review). *Curr Opin Struct Biol* 1996; 6: 744–756.

[332] Spellerberg IF. Shannon-Wiener Index (Review). In: *Encyclopedia of Ecology, Five-Volume Set*. Elsevier Inc., 2008, pp. 3249–3252.

[333] Simpson EH. Measurement of diversity (Review). *Nature* 1949; 163: 688.

[334] McCarthy BC, Magurran AE. Measuring biological diversity (Review). *J Torrey Bot Soc* 2004; 131: 277.

[335] Fujioka S, Matsuzawa Y, Tokunaga K, *et al*. Contribution of intra-abdominal fat accumulation to the impairment of glucose and lipid metabolism in human obesity. *Metabolism* 1987; 36: 54–59.

[336] Seino Y, Yamamoto T, Koh G. Insulin and glucose transporter gene expression in obesity and diabetes. *Proc Soc Exp Biol Med* 1992; 200: 210–213.

[337] Ait-Omar A, Monteiro-Sepulveda M, Poitou C, *et al*. GLUT2 accumulation in enterocyte apical and intracellular membranes: a study in morbidly obese human subjects and ob/ob and high fat-fed mice. *Diabetes* 2011; 60: 2598–2607.

[338] Chen C, Williams PF, Caterson ID. Liver and peripheral tissue glycogen metabolism in obese mice: effect of a mixed meal. *Am J Physiol - Endocrinol Metab* 1993; 265: E743-51.

[339] Seo E, Kang H, Choi H, *et al*. Reactive oxygen species-induced changes in glucose and lipid metabolism contribute to the accumulation of cholesterol in the liver during aging. *Aging Cell* 2019; 18: e12895.

[340] Khan T, Muise ES, Iyengar P, *et al*. Metabolic dysregulation and adipose tissue fibrosis: role of collagen VI. *Mol Cell Biol* 2009; 29: 1575–1591.

[341] Björntorp P, Sjöström L. Number and size of adipose tissue fat cells in relation to metabolism in human obesity. *Metabolism* 1971; 20: 703–713.

[342] Gluchowski NL, Becuwe M, Walther TC, *et al*. Lipid droplets and liver disease: from basic biology to clinical implications (Review). *Nature Reviews Gastroenterology and Hepatology* 2017; 14: 343–355.

[343] Van Dam AD, Boon MR, Berbée JFP, *et al*. Targeting white, brown and perivascular adipose tissue in atherosclerosis development (Review). *Eur J Pharmacol* 2017; 816: 82–92.

[344] Sun B, Karin M. Obesity, inflammation, and liver cancer (Review). *Journal of Hepatology* 2012; 56: 704–713.

[345] Montgomery MK, Watt MJ, Keenan SN, *et al.* Perilipin 5 deletion in hepatocytes remodels lipid metabolism and causes hepatic insulin resistance in mice. *Diabetes* 2019; 68: 543–555.

[346] Sasaki K, Sasaki D, Okai N, *et al.* Taurine does not affect the composition, diversity, or metabolism of human colonic microbiota simulated in a single-batch fermentation system. *PLoS One* 2017; 12: e0180991.

[347] Denger K, Huhn T, Hollemeyer K, *et al.* Sulfoquinovose degraded by pure cultures of bacteria with release of C 3-organosulfonates: complete degradation in two-member communities. *FEMS Microbiol Lett* 2012; 328: 39–45.

[348] Becker N, Kunath J, Loh G, *et al*. Human intestinal microbiota: Characterization of a simplified and stable gnotobiotic rat model. *Gut Microbes* 2011; 2: 25–33.

[349] Danielsson H. Present status of research on catabolism and excretion of cholesterol. *Advances in lipid research* 1963; 1: 335–385.

[350] Sjövall J. Dietary glycine and taurine on bile acid conjugation in man. *Proc Soc Exp Biol Med* 1959; 100: 676–678.

[351] Kumar RS, Brannigan JA, Prabhune AA, *et al*. Structural and functional analysis of a conjugated bile salt hydrolase from *Bifidobacterium longum* reveals an evolutionary relationship with penicillin V acylase. *J Biol Chem* 2006; 281: 32516–32525.

[352] Azabji-Kenfack M, Dikosso SE, Loni EG, *et al*. Potential of *Spirulina platensis* as a nutritional supplement in malnourished HIV-infected adults in sub-saharan Africa: a randomised, single-blind study. *Nutr Metab Insights* 2011; 4: 29–37.

[353] Park JH, Lee SI, Kim IH. Effect of dietary *Spirulina* (*Arthrospira*) *platensis* on the growth performance, antioxidant enzyme activity, nutrient digestibility, cecal microflora, excreta noxious gas emission, and breast meat quality of broiler

chickens. *Poult Sci* 2018; 97: 2451–2459.

[354] Dinicolantonio JJ, Bhat AG, Okeefe J. Effects of Spirulina on weight loss and blood lipids: A review (Review). *Open Hear* 2020; 7: e001003.

[355] Zeinalian R, Farhangi MA, Shariat A, *et al*. The effects of *Spirulina platensis* on anthropometric indices, appetite, lipid profile and serum vascular endothelial growth factor (VEGF) in obese individuals: a randomized double blinded placebo controlled trial. *BMC Complement Altern Med* 2017; 17: 225.

[356] Yousefi R, Mottaghi A, Saidpour A. *Spirulina platensis* effectively ameliorates anthropometric measurements and obesity-related metabolic disorders in obese or overweight healthy individuals: a randomized controlled trial. *Complement Ther Med* 2018; 40: 106–112.

[357] Yang Y, Park Y, Cassada DA, *et al. In vitro* and *in vivo* safety assessment of edible blue-green algae, Nostoc commune var. sphaeroides Kützing and *Spirulina plantensis*. *Food Chem Toxicol* 2011; 49: 1560–1564.

[358] Bigagli E, Cinci L, Niccolai A, *et al*. Safety evaluations and lipid-lowering activity of an *Arthrospira platensis* enriched diet: a 1-month study in rats. *Food Res Int* 2017; 102: 380–386.

[359] Neyrinck AM, Taminiau B, Walgrave H, *et al.* Spirulina protects against hepatic inflammation in aging: An effect related to the modulation of the gut microbiota? *Nutrients* 2017; 9: 633.

[360] Sutton SC. Companion animal physiology and dosage form performance (Review). *Adv Drug Deliv Rev* 2004; 56: 1383–1398.

[361] Brown BP, Schulze-Delrieu K, Schrier JE, *et al.* The configuration of the human gastroduodenal junction in the separate emptying of liquids and solids. *Gastroenterology* 1993; 105: 433–440.

[362] Szurszewski JH. A migrating electric complex of canine small intestine. *Am J Physiol* 1969; 217: 1757–1763.

[363] Kumar D, Wingate DL. *An illustrated guide to gastrointestinal motility*. 1993.

[364] Tuleu C, Andrieux C, Boy P, *et al.* Gastrointestinal transit of pellets in rats: Effect of size and density. *Int J Pharm* 1999; 180: 123–131.

[365] Kararli TT. Comparison of the gastrointestinal anatomy, physiology, and biochemistry of humans and commonly used laboratory animals (Review). *Biopharmaceutics & Drug Disposition* 1995; 16: 351–380.

[366] Hirahashi T, Matsumoto M, Hazeki K, *et al*. Activation of the human innate immune system by Spirulina: augmentation of interferon production and NK cytotoxicity by oral administration of hot water extract of *Spirulina platensis*. *Int Immunopharmacol* 2002; 2: 423–434.

[367] Mao TK, Van De Water J, Gershwin ME. Effects of a Spirulina-based dietary supplement on cytokine production from allergic rhinitis patients. *J Med Food* 2005; 8: 27–30.

[368] Khan Z, Bhadouria P, Bisen P. Nutritional and therapeutic potential of Spirulina (Review). *Curr Pharm Biotechnol* 2005; 6: 373–379.

[369] Basha OM, Hafez RA, El-Ayouty YM, *et al.* C-Phycocyanin inhibits cell proliferation and may induce apoptosis in human HepG2 cells. *Egypt J Immunol* 2008; 15: 161–167.

[370] Narmadha T V, Sivakami V, Ravikumar M, *et al.* Effect of Spirulina on lipid profile of hyperlipidemics. *World J Nucl Sci Technol* 2012; 2: 19–22.

[371] Borowitzka M. Micro-algae as sources of fine chemicals (Review). *Microbiol Sci* 1986; 3: 372–5.

[372] Liestianty D, Rodianawati I, Arfah RA, *et al.* Nutritional analysis of *Spirulina* sp to promote as superfood candidate. *IOP Conference Series: Materials Science and Engineering* 2019; 509: 012031.

[373] Nguyen P, Grajeda R, Melgar P, *et al.* Effect of zinc on efficacy of iron supplementation in improving iron and zinc status in women. *J Nutr Metab* 2012; 2012: 216179.

[374] Jafari SM, McClements DJ. Nanotechnology approaches for increasing nutrient bioavailability (Review). *Advances in Food and Nutrition Research* 2017; 81: 1-30.

[375] Capuano E. The behavior of dietary fiber in the gastrointestinal tract determines its physiological effect (Review). *Crit Rev Food Sci Nutr* 2017; 57: 3543–3564.

[376] Grundy MML, Edwards CH, Mackie AR, *et al*. Re-evaluation of the mechanisms of dietary fibre and implications for macronutrient bioaccessibility, digestion and postprandial metabolism (Review). *Br J Nutr* 2016; 116: 816–833.

[377] Holland C, Ryden P, Edwards CH, *et al.* Plant cell walls: Impact on nutrient bioaccessibility and digestibility (Review). *Foods* 2020; 9: 201.

[378] Teuling E, Wierenga PA, Agboola JO, *et al.* Cell wall disruption increases bioavailability of Nannochloropsis gaditana nutrients for juvenile Nile tilapia (Oreochromis niloticus). *Aquaculture* 2019; 499: 269–282.

[379] Kapoor R, Mehta U. Iron status and growth of rats fed different dietary iron sources. *Plant Foods Hum Nutr* 1993; 44: 29–34.

[380] Puyfoulhoux G, Rouanet J-M, Besançon P, *et al.* Iron availability from iron-fortified Spirulina by an *in vitro* digestion/Caco-2 cell culture model. 2001; 49: 1625–9.

[381] Ekantari N, Harmayani E, Pranoto Y, *et al.* Calcium of *Spirulina platensis* has higher bioavailability than those of calcium carbonate and high-calcium milk in sprague dawley rats fed with vitamin D-deficient diet. *Pakistan J Nutr* 2017; 16: 179–186.

[382] Hazlewood G, Dawson RMC. Characteristics of a lipolytic and fatty acid-requiring *Butyrivibrio* sp. isolated from the ovine rumen. *J Gen Microbiol* 1979; 112: 15–27.

[383] Ganesh BP, Klopfleisch R, Loh G, *et al*. Commensal *Akkermansia muciniphila* exacerbates gut inflammation in *Salmonella Typhimurium*-infected gnotobiotic

mice. *PLoS One* 2013; 8: 74963.

[384] Ring C, Klopfleisch R, Dahlke K, *et al*. *Akkermansia muciniphila* strain ATCC BAA-835 does not promote short-term intestinal inflammation in gnotobiotic interleukin-10-deficient mice. *Gut Microbes* 2019; 10: 188–203.

[385] Oh SY, Cho KA, Kang JL, *et al*. Comparison of experimental mouse models of inflammatory bowel disease. *Int J Mol Med* 2014; 33: 333–340.

[386] Finamore A, Palmery M, Bensehaila S, *et al*. Antioxidant, immunomodulating, and microbial-modulating activities of the sustainable and ecofriendly Spirulina (Review). *Oxid Med Cell Longev* 2017; 2017: 3247528.

[387] Shokri Hojjatollah, Khosravi Ali Reza, Taghavi Mehdi. Efficacy of *Spirulina platensis* on immune functions in cancer mice with systemic candidiasis. *Journal of Mycology Research* 2014; 1: 7-13.

[388] Burkhardt W, Rausch T, Klopfleisch R, *et al*. Impact of dietary sulfolipid-derived sulfoquinovose on gut microbiota composition and inflammatory status of colitis-prone interleukin-10-deficient mice. *Int J Med Microbiol* 2021; 311: 151494.

[389] Coskun ZK, Kerem M, Gurbuz N, *et al.* The study of biochemical and histopathological effects of Spirulina in rats with TNBS-induced colitis. *Bratisl Lek Listy* 2011; 112: 235-243.

[390] Abdel-Daim MM, Farouk SM, Madkour FF, *et al*. Anti-inflammatory and immunomodulatory effects of *Spirulina platensis* in comparison to *Dunaliella salina* in acetic acid-induced rat experimental colitis. *Immunopharmacol Immunotoxicol* 2015; 37: 126–139.

[391] Morsy MA, Gupta S, Nair AB, *et al.* Protective effect of *Spirulina platensis* extract against dextran-sulfate-sodium-induced ulcerative colitis in rats. *Nutrients* 2019; 11: 2309.

[392] Guo W, Zhu S, Feng G, *et al.* Microalgae aqueous extracts exert intestinal protective effects in Caco-2 cells and dextran sodium sulphate-induced mouse colitis. *Food and Function* 2020; 11: 1098–1109.

[393] Marles RJ, Barrett ML, Barnes J, *et al*. United states pharmacopeia safety evaluation of Spirulina (Review). *Crit Rev Food Sci Nutr* 2011; 51: 593–604.

[394] Riccio G, De Luca D, Lauritano C. Monogalactosyldiacylglycerol and sulfolipid synthesis in microalgae. *Mar Drugs* 2020; 18: 237.

[395] Riss J, Décordé K, Sutra T, *et al*. Phycobiliprotein C-phycocyanin from *Spirulina platensis* is powerfully responsible for reducing oxidative stress and NADPH oxidase expression induced by an atherogenic diet in hamsters. *J Agric Food Chem* 2007; 55: 7962–7967.

[396] Machu L, Misurcova L, Ambrozova JV, *et al*. Phenolic content and antioxidant capacity in algal food products. *Molecules* 2015; 20: 1118–1133.

[397] Furukawa T, Nishida M, Hada T, *et al.* Inhibitory effect of sulfoquinovosyl diacylglycerol on prokaryotic DNA polymerase I activity and cell growth of

Escherichia coli. *J Oleo Sci* 2007; 56: 43–47.

[398] Wang H, Li YL, Shen WZ, *et al*. Antiviral activity of a sulfoquinovosyl-diacylglycerol (SQDG) compound isolated from the green alga Caulerpa racemosa. *Bot Mar* 2007; 50: 185–190.

[399] Hossain Z, Kurihara H, Hosokawa M, *et al*. Growth inhibition and induction of differentiation and apoptosis mediated by sodium butyrate in Caco-2 cells with algal glycolipids. *Vitr Cell Dev Biol - Anim* 2005; 41: 154–159.

[400] Maeda N, Kokai Y, Ohtani S, *et al*. Anti-tumor effect of orally administered spinach glycolipid fraction on implanted cancer cells, colon-26, in mice. *Lipids* 2008; 43: 741–748.

[401] Li W, Lu L, Liu B, *et al*. Effects of phycocyanin on pulmonary and gut microbiota in a radiation-induced pulmonary fibrosis model. *Biomed Pharmacother* 2020; 132: 110826.

[402] Yu T, Wang Y, Chen X, *et al*. *Spirulina platensis* alleviates chronic inflammation with modulation of gut microbiota and intestinal permeability in rats fed a high-fat diet. *J Cell Mol Med* 2020; 24: 8603–8613.

[403] Xie Y, Li W, Lu C, *et al*. The effects of phycocyanin on bleomycin-induced pulmonary fibrosis and the intestinal microbiota in C57BL/6 mice. *Appl Microbiol Biotechnol* 2019; 103: 8559–8569.

[404] Wan X zhi, Li T tian, Zhong R ting, *et al*. Anti-diabetic activity of PUFAs-rich extracts of Chlorella pyrenoidosa and *Spirulina platensis* in rats. *Food Chem Toxicol* 2019; 128: 233–239.

[405] Guo W, Zhu S, Li S, *et al*. Microalgae polysaccharides ameliorates obesity in association with modulation of lipid metabolism and gut microbiota in high-fat-diet fed C57BL/6 mice. *Int J Biol Macromol* 2021; 182: 1371–1383.

[406] Rasmussen HE, Martínez I, Lee JY, *et al.* Alteration of the gastrointestinal microbiota of mice by edible blue-green algae. *J Appl Microbiol* 2009; 107: 1108–1118.

[407] Yusuf M, Hassan M, MM, Abdel-Daim M, *et al.* Value added by *Spirulina platensis* in two different diets on growth performance, gut microbiota, and meat quality of Japanese quails. *Vet world* 2016; 9: 1287–1293.

[408] Ma H, Xiong H, Zhu X, *et al.* Polysaccharide from *Spirulina platensis* ameliorates diphenoxylate-induced constipation symptoms in mice. *Int J Biol Macromol* 2019; 133: 1090–1101.

[409] Li TT, Tong AJ, Liu YY, *et al*. Polyunsaturated fatty acids from microalgae *Spirulina platensis* modulates lipid metabolism disorders and gut microbiota in high-fat diet rats. *Food Chem Toxicol* 2019; 131: 110558.

[410] Li TT, Liu YY, Wan XZ, *et al.* Regulatory efficacy of the polyunsaturated fatty acids from microalgae *Spirulina platensis* on lipid metabolism and gut microbiota in high-fat diet rats. *Int J Mol Sci* 2018; 19: 3075.

[411] Chang C-WT, Takemoto JY, Chang P-E, *et al*. Effects of mesobiliverdin IXα-enriched microalgae feed on gut health and microbiota of broilers. *Front Vet Sci* 2020; 7: 586813.

[412] Chandrarathna HPSU, Liyanage TD, Edirisinghe SL, *et al*. Marine microalgae, *Spirulina maxima*-derived modified pectin and modified pectin nanoparticles modulate the gut microbiota and trigger immune responses in Mice. *Mar Drugs* 2020; 18: 175.

[413] Rosenau S, Oertel E, Mott AC, *et al.* The effect of a total fishmeal replacement by *Arthrospira platensis* on the microbiome of African catfish (Clarias gariepinus). *Life* 2021; 11: 558.

[414] Rowan F, Docherty NG, Murphy M, *et al*. *Desulfovibrio* bacterial species are increased in ulcerative colitis. *Dis Colon Rectum* 2010; 53: 1530–1536.

[415] Figliuolo VR, Dos Santos LMD, Abalo A, *et al*. Sulfate-reducing bacteria stimulate gut immune responses and contribute to inflammation in experimental colitis. *Life Sci* 2017; 189: 29–38.

[416] Gibson GR, Macfarlane S, Macfarlane GT. Metabolic interactions involving sulphate-reducing and methanogenic bacteria in the human large intestine. *FEMS Microbiol Ecol* 1993; 12: 117–125.

[417] Gibson GR, Cummings JH, Macfarlane GT. Growth and activities of sulphate-reducing bacteria in gut contents of healthy subjects and patients with ulcerative colitis. *FEMS Microbiol Lett* 1991; 86: 103–111.

[418] Cummings JH, Macfarlane GT, Macfarlane S. Intestinal bacteria and ulcerative colitis (Review). *Issues Intest Microbiol* 2003; 4: 9–20.

[419] Kushkevych I, Dordević D, Kollár P. Analysis of physiological parameters of *Desulfovibrio* strains from individuals with colitis. *Open Life Sci* 2018; 13: 481–488.

[420] Stewart J, Chadwick V, Murray A. Carriage, quantification, and predominance of methanogens and sulfate-reducing bacteria in faecal samples. *Lett Appl Microbiol* 2006; 43: 58–63.

[421] Hansen EE, Lozupone CA, Rey FE, *et al*. Pan-genome of the dominant human gut-associated archaeon, *Methanobrevibacter smithii*, studied in twins. *Proc Natl Acad Sci* 2011; 108: 4599–4606.

[422] Hu J, Li Y, Pakpour S, *et al*. Dose effects of orally administered Spirulina suspension on colonic microbiota in healthy mice. *Front Cell Infect Microbiol* 2019; 9: 243.

[423] Kaper JB, Nataro JP, Mobley HLT. Pathogenic *Escherichia coli* (Review). *Nat Rev Microbiol 2004 22* 2004; 2: 123–140.

[424] Coutinho CMLM, Coutinho-Silva R, Zinkevich V, *et al*. Sulphate-reducing bacteria from ulcerative colitis patients induce apoptosis of gastrointestinal epithelial cells. *Microb Pathog* 2017; 112: 126–134.

[425] Knoll RL, Forslund K, Kultima JR, *et al.* Gut microbiota differs between children with inflammatory bowel disease and healthy siblings in taxonomic and functional composition: a metagenomic analysis. *Am J Physiol - Gastrointest Liver Physiol* 2017; 312: G327–G339.

[426] Frank DN, Amand AL St., Feldman RA, *et al.* Molecular-phylogenetic characterization of microbial community imbalances in human inflammatory bowel diseases. *Proc Natl Acad Sci U S A* 2007; 104: 13780.

[427] Gevers D, Kugathasan S, Denson L, *et al.* The treatment-naive microbiome in new-onset Crohn's disease. *Cell Host Microbe* 2014; 15: 382–392.

[428] Atarashi K, Tanoue T, Oshima K, *et al*. Treg induction by a rationally selected mixture of *Clostridia* strains from the human microbiota. *Nat 2013 5007461* 2013; 500: 232–236.

[429] Seltzer HS, Allen EW, Herron AL, *et al*. Insulin secretion in response to glycemic stimulus: relation of delayed initial release to carbohydrate intolerance in mild diabetes mellitus. *J Clin Invest* 1967; 46: 323–335.

[430] Parikh P, Mani U, Iyer U. Role of Spirulina in the control of glycemia and lipidemia in type 2 diabetes mellitus. *J Med Food* 2001; 4: 193–199.

[431] Lee EH, Park J-E, Choi Y-J, *et al.* A randomized study to establish the effects of Spirulina in type 2 diabetes mellitus patients. *Nutr Res Pract* 2008; 2: 295.

[432] Guldas M, Ziyanok-Demirtas S, Sahan Y, *et al*. Antioxidant and anti-diabetic properties of *Spirulina platensis* produced in Turkey. *Food Sci Technol* 2021; 41: 615–625.

[433] Heo MG, Choung SY. Anti-obesity effects of *Spirulina maxima* in high-fat diet induced obese rats via the activation of AMPK pathway and SIRT1. *Food Funct* 2018; 9: 4906–4915.

[434] Booth C, Alldis D, Read A. Studies on the site of fat absorption: 2 fat balances after resection of varying amounts of the small intestine in man. *Gut* 1961; 2: 168–174.

[435] Berdanier CD. The gastrointestinal system and metabolism (Review). *Lab Mouse* 2004; 245–259.

[436] Chen M, Yang Y, Braunstein E, *et al.* Gut expression and regulation of FAT/CD36: possible role in fatty acid transport in rat enterocytes. *Am J Physiol Endocrinol Metab* 2001; 281: E916-23.

[437] Nassir F, Wilson B, Han X, *et al*. CD36 is important for fatty acid and cholesterol uptake by the proximal but not distal intestine. *J Biol Chem* 2007; 282: 19493–19501.

[438] Chevrot M, Martin C, Passilly-Degrace P, *et al.* Role of CD36 in oral and postoral sensing of lipids (Review). *Handb Exp Pharmacol* 2012; 209: 295–307.

[439] Poirier H, Degrace P, Niot I, *et al.* Localization and regulation of the putative membrane fatty-acid transporter (FAT) in the small intestine. Comparison with fatty acid-binding proteins (FABP). *Eur J Biochem* 1996; 238: 368–373.

[440] Drover V, Ajmal M, Nassir F, *et al*. CD36 deficiency impairs intestinal lipid secretion and clearance of chylomicrons from the blood. *J Clin Invest* 2005; 115: 1290–1297.

[441] Greco D, Kotronen A, Westerbacka J, *et al.* Gene expression in human NAFLD. *Am J Physiol Gastrointest Liver Physiol* 2008; 294: G1281-7.

[442] Buqué X, Martínez M, Cano A, *et al*. A subset of dysregulated metabolic and survival genes is associated with severity of hepatic steatosis in obese Zucker rats. *J Lipid Res* 2010; 51: 500–513.

[443] Miyazaki M, Ntambi J. Role of stearoyl-coenzyme A desaturase in lipid metabolism (Review). *Prostaglandins Leukot Essent Fatty Acids* 2003; 68: 113–121.

[444] Miyazaki M, Jacobson MJ, Man WC, *et al*. Identification and characterization of murine SCD4, a novel heart-specific stearoyl-CoA desaturase isoform regulated by leptin and dietary factors. *J Biol Chem* 2003; 278: 33904–33911.

[445] Lundåsen T, Pedrelli M, Bjørndal B, *et al*. The PPAR pan-agonist tetradecylthioacetic acid promotes redistribution of plasma cholesterol towards large HDL. *PLoS One* 2020; 15: e0229322.

[446] Burchat N, Akal T, Zalma B, *et al*. Spatio-nutritional regulation of intestinal desaturases. *FASEB J* 2020; 34: 1–1.

[447] Miyazaki M, Flowers M, Sampath H, *et al.* Hepatic stearoyl-CoA desaturase-1 deficiency protects mice from carbohydrate-induced adiposity and hepatic steatosis. *Cell Metab* 2007; 6: 484–496.

[448] Wolins N, Brasaemle D, Bickel P. A proposed model of fat packaging by exchangeable lipid droplet proteins. *FEBS Lett* 2006; 580: 5484–5491.

[449] Frank DN, Bales ES, Monks J, *et al.* Perilipin-2 modulates lipid absorption and microbiome responses in the mouse intestine (Review). *PLoS One* 2015; 10: e0131944.

[450] Moon Y, Hammer R, Horton J. Deletion of ELOVL5 leads to fatty liver through activation of SREBP-1c in mice. *J Lipid Res* 2009; 50: 412–423.

[451] Tripathy S, Lytle K, Stevens R, *et al.* Fatty acid elongase-5 (Elovl5) regulates hepatic triglyceride catabolism in obese C57BL/6J mice. *J Lipid Res* 2014; 55: 1448–1464.

[452] Felux AK, Denger K, Weiss M, *et al*. *Paracoccus denitrificans* PD1222 utilizes hypotaurine via transamination followed by spontaneous desulfination to yield acetaldehyde and, finally, acetate for growth. *J Bacteriol* 2013; 195: 2921–2930.

[453] Denger K, Ruff J, Schleheck D, *et al*. Rhodococcus opacus expresses the *xsc* gene to utilize taurine as a carbon source or as a nitrogen source but not as a sulfur source. *Microbiology* 2004; 150: 1859–1867.

[454] Cook AM, Denger K. Dissimilation of the C2 sulfonates (Review). *Archives of Microbiology* 2002; 179: 1–6.

[455] Schleheck D, Lechner M, Schönenberger R, *et al*. Desulfonation and degradation of the disulfodiphenylethercarboxylates from linear alkyldiphenyletherdisulfonate surfactants. *Appl Environ Microbiol* 2003; 69: 938–944.

[456] Landa M, Burns AS, Durham BP, *et al*. Sulfur metabolites that facilitate oceanic phytoplankton–bacteria carbon flux. *ISME J* 2019; 13: 2536–2550.

[457] Weinitschke S, Styp von Rekowski K, Denger K, *et al*. Sulfoacetaldehyde is excreted quantitatively by *Acinetobacter calcoaceticus* SW1 during growth with taurine as sole source of nitrogen. *Microbiology* 2005; 151: 1285–1290.

[458] Krejcík Z, Schleheck D, Hollemeyer K, *et al*. A five-gene cluster involved in utilization of taurine-nitrogen and excretion of sulfoacetaldehyde by *Acinetobacter radioresistens* SH164. *Arch Microbiol* 2012; 194: 857–863.

[459] Denger K, Weinitschke S, Hollemeyer K, *et al*. Sulfoacetate generated by *Rhodopseudomonas palustris* from taurine. *Arch Microbiol* 2004; 182: 254–258.

[460] Yumoto I, Yamaga S, Sogabe Y, *et al*. *Bacillus krulwichiae* sp. nov., a halotolerant obligate alkaliphile that utilizes benzoate and m-hydroxybenzoate. *Int J Syst Evol Microbiol* 2003; 53: 1531–1536.

[461] Novak RT, Gritzer RT, Leadbetter ER, *et al*. Phototrophic utilization of taurine by the purple nonsulfur bacteria *Rhodopseudomonas palustris* and *Rhodobacter sphaeroides*. *Microbiology* 2004; 150: 1881–1891.

ACKNOWLEDGEMENT

I would like to take this opportunity to thank all those who have supported me during my doctoral studies and who have contributed significantly to the development of this dissertation.

Zuallererst möchte ich mich bei Prof. Dr. Michael Blaut für die Möglichkeit bedanken, an diesem interessanten Forschungsprojekt in der Abteilung „Gastrointestinale Mikrobiologie“ des Deutschen Instituts für Ernährungsforschung zu arbeiten. Des Weiteren möchte ich mich bei Prof. Blaut, Dr. Annett Braune und Dr. Wiebke Burkhardt für ihre Unterstützung und die kritischen Diskussionen bedanken, die mir geholfen haben, mich weiter zu verbessern. Mein Dank gilt auch Prof. Dr. Michael Blaut, Dr. Annett Braune und Dr. Sören Ocvirk für die Zeit, die sie sich für das kritische Lesen dieser Arbeit genommen haben.

Ich bedanke mich bei allen Gutachtern für ihre Bereitschaft zur Übernahme der Gutachtertätigkeit und allen Teilnehmenden der Prüfungskommission. Mein besonderer Dank geht an Anke Gühler und Sabine Schmidt für die wissenschaftliche und nicht-wissenschaftliche Unterstützung im Labor und die großzügige Hilfsbereitschaft. Bei der Gruppe von Prof. Martin von Bergen vom Helmholtz-Zentrum Umweltforschung - UFZ in Leipzig möchte ich mich für die massenspektrometrische Analysen der Sulfonate bedanken. Speziell bedanke ich mich bei Dr. Ulrike Rolle-Kampczyk, Dr. Sven Haange, Dr. Katharina Fritz, Dr. Jean Froment, Olivia Pleßow und Nicole Groeger für die Unterstützung zur Etablierung der Sulfonatanalysen. Bedanken möchte ich mich außerdem bei Dr. Klaus Neuhaus von der Technische Universität München ZIEL (Institute for Food & Health Core Facility Mikrobiom / NGS, Freising) für die Sequenzierung der murinen Darminhalten.

Dank gilt auch meinen Praktikanten und Bachelorstudierenden Nora Mindermann, Christoph Horlebein, Markus Hermanowski und Katharina Burger für ihr Interesse an dem Thema und die tolle Zusammenarbeit. Ich bedanke mich weiterhin bei allen Mitarbeiter:innen der Abteilung für das angenehme und freundliche Arbeitsklima, die Hilfsbereitschaft und für ihr stets offenes Ohr bei fachlichen Fragen. Vielen Dank für die schöne Zeit!

Für die finanzielle Unterstützung, die dieses PhD-Projekt möglich gemacht hat, danke ich der Deutschen Forschungsgesellschaft. Ebenfalls danke ich Prof. Dr. Susanne Klaus und den Kolleg:innen der EST für Ihre Unterstützung bei fachlichen Fragen und die Erlaubnis zur Mitbenutzung ihrer Geräte.

Ein besonderer Dank gilt meiner Familie, die immer für mich da ist und mich bei meinem Vorhaben unterstützt hat. Auch wenn oft hunderte Kilometer zwischen uns lagen, hattet ihr immer ein offenes Ohr für mich. I also deeply appreciate the support of my friends. Thank you for your positive attitude and thoughts!

Vielen Dank - Heel veel bedankt - Thank you!

LIST OF ORIGINAL COMMUNICATIONS

Full length articles

Haange SB, Groeger N, Froment J, et al. Multiplexed quantitative assessment of the fate of taurine and sulfoquinovose in the intestinal microbiome. Metabolites 2020; 10: 1–16.

Burkhardt W, Rausch T, Klopfleisch R, *et al*. Impact of dietary sulfolipid-derived sulfoquinovose on gut microbiota composition and inflammatory status of colitis-prone interleukin-10-deficient mice. *Int J Med Microbiol* 2021; 311: 151494.

Scientific events

Rausch T, Burkhardt W, Braune A, and Blaut M (2017) Identification of human gut bacteria utilizing dietary sulfonates. 10th Seeon Conference "Microbiota, Probiotics and Host", July 7th - 9th 2017, Monastery Seeon, Germany (Poster presentation).

Rausch T, Burkhardt W, Braune A, and Blaut M (2018) Conversion of sulfonates by human intestinal microbiota. 11th Seeon Conference "Microbiota, Probiotics and Host", July 6th - 8th 2018, Monastery Seeon, Germany (Oral presentation).

Rausch T, Burkhardt W, Froment J, Fritz K, Rolle-Kampczyk U, von Bergen M, Blaut M, and Braune A (2019) Dietary sulfonates are efficiently converted by the human gut microbiota. 71st "Annual Conference of the German Society for Hygiene and Microbiology (DGHM)", February 25th - 27th 2019, georg-August University in Göttingen, Germany (Poster presentation).

Rausch T, Burkhardt W, Haange S, Froment J, Fritz K, Rolle-Kampczyk U, von Bergen M, Blaut M, and Braune A. (2019) Inter-individual differences in conversion of dietary sulfonates by the human gut microbiota. "The First Stellenbosch University African Microbiome Workshop and Symposium", November 28th - 30th 2019, Wallenberg Research and Conference Centre, STIAS, Stellenbosch University, South Africa (Poster Presentation).

DECLARATION OF ACADEMIC HONESTY

I hereby declare that my thesis entitled “Role of intestinal bacteria in the conversion of dietary sulfonates” is my own original work and has not previously, in part or in its entirety, been submitted at any university for a degree. Information derived from published work of others has been stated in the text and a list of references is given in the bibliography.

Potsdam, 12.03.2022

_____

Theresa Rausch